FUZZY LOGIC BASED CONTROL FOR MEMBRANE OXYGENATOR IN BLOOD PURIFICATION PROCESS

HANY HAZFIZA BINTI MANAP

FACULTY OF ENGINEERING
UNIVERSITY OF MALAYA
KUALA LUMPUR

2020

FUZZY LOGIC BASED CONTROL FOR MEMBRANE OXYGENATOR IN BLOOD PURIFICATION PROCESS

HANY HAZFIZA BINTI MANAP

THESIS SUBMITTED IN FULFILMENT OF THE REQUIREMENTS FOR THE DEGREE OF DOCTOR OF PHILOSOPHY

FACULTY OF ENGINEERING
UNIVERSITY OF MALAYA
KUALA LUMPUR

2020

UNIVERSITY OF MALAYA

ORIGINAL LITERARY WORK DECLARATION

Name of Candidate: HANY HAZFIZA BINTI MANAP

Matric No: KHA140110 (17005180/2)

Name of Degree: Doctor of Philosophy (PhD)

Title of Thesis:

Fuzzy Logic Based Control For Membrane Oxygenator In Blood Purification Process

Field of Study: Biomedical Engineering (Engineering and Engineering Trades)

I do solemnly and sincerely declare that:

(1) I am the sole author/writer of this work;

(2) This Work is original;

(3) Any use of any work in which copyright exists was done by way of fair dealing and for permitted purposes and any excerpt or extract from, or reference to or reproduction of any copyright work has been disclosed expressly and sufficiently and the title of the work and its authorship have been acknowledged in this Work;

(4) I do not have any actual knowledge nor do I ought reasonably to know that the making of this work constitutes an infringement of any copyright work;

(5) I hereby assign all and every rights in the copyright to this Work to the University of Malaya ("UM"), who henceforth shall be owner of the copyright in this Work and that any reproduction or use in any form or by any means whatsoever is prohibited without the written consent of UM having been first had and obtained;

(6) I am fully aware that if in the course of making this work, I have infringed any copyright whether intentionally or otherwise, I may be subject to legal action or any other action as may be determined by UM.

Candidate's Signature Date:

Subscribed and solemnly declared before,

Witness's Signature Date:

Name:

Designation:

FUZZY LOGIC BASED CONTROL FOR MEMBRANE OXYGENATOR IN BLOOD PURIFICATION PROCESS

ABSTRACT

Membrane oxygenator in Extracorporeal Life Support (ECLS) is commonly used as a main component in Cardiopulmonary Bypass (CPB), Extracorporeal Membrane Oxygenator (ECMO) and Extracorporeal Carbon Dioxide Removal ($ECCO_2R$). In this study, the focus is on Carbon Dioxide (CO_2) gas exchange process in membrane oxygenator, which the CO_2 is automatically controlled by adjusting sweep gas flow rate that entering the membrane oxygenator in achieving the desired pCO_2 required by the particular patients. This automatic control action is controlled by the implementation of three controllers, Proportional-Integral-Derivative (PID) that is tuned by Ziegler-Nichols continuous cycling method, Fuzzy Logic Controller (FLC) and Fuzzy-PID controllers. This study is conducted in two stages: simulation and experimental work for two tasks, namely setpoint tracking and disturbance rejection. For evaluation of setpoint tracking, desired setpoint of arterial partial carbon dioxide (pCO_2) is set at 40 mmHg at the beginning of the process, and been increased by 5% to 42 mmHg at the middle of the process, and been adjusted back to 40 mmHg at the end of the process. For disturbance rejection, an external disturbance is applied to the process plant (in membrane oxygenator) by a sudden shutoff of mass flow controller (MFC) to stop the sweep gas flow rate until 0 L/min at the middle of process. All the simulation works are done using level-2 S-Function in MATLAB/SIMULINK environment. An application of NI-USB 6009 DAQ in corporation with MATLAB/SIMULINK environment is used for both pCO_2 sensors and mass flow controller as an actuator to control sweep gas flow rate in the experimental work. Fuzzy-PID recorded the best performance in both setpoint tracking and disturbance rejection tasks during simulation. The control performance become worst with loss of control action in experimental setting using similar PID and FLC parameters/rules, due to some assumptions

and defined parameters in mathematical modelling that are differ than actual parameters used in experimental work. Re-tune process is conducted to calculate newly parameter for PID and rule for FLC and Fuzzy-PID. The proposed controllers then able to automatically control CO_2 gas transfer in membrane oxygenator according to the desired setpoint. As a conclusion, all the controllers produce a good ability to automatically control CO_2 removal from membrane oxygenator for both tasks, with Fuzzy-PID outshines the other controllers, PID and FLC. This can be seen from the lowest performance indices and the time taken to achieve the setpoint for Fuzzy-PID is lower by 21.15% compared to PID and 65.25% lower compared to FLC during setpoint tracking task. For disturbance task, Fuzzy-PID also recorded the fastest time to adapt with the disturbance, which 89.33% and 51.52% faster than PID and FLC, respectively. Hence, this in-vitro bench set-up has great potential to be further extended study.

Keywords: Membrane oxygenator, CO_2 gas exchange, Proportional-Integral-Derivative (PID), Fuzzy Logic Controller (FLC), Fuzzy-PID.

ABSTRAK

Oksigenator membran dalam sistem Sokongan Hayat Luar Badan (ECLS) biasanya digunakan sebagai komponen utama dalam Proses Pintasan Kardiopulmonari (CPB), Oksigenator Membran Luar Badan ECMO) dan Sistem Penyingkiran Karbon Dioksida di Luar Badan ($ECCO_2R$). Dalam kajian ini, tumpuan diberikan kepada proses pertukaran gas karbon dioksida (CO_2) dalam oksigenator membran, di mana CO_2 dikawal secara automatik dengan menyesuaikan kadar aliran gas sapuan yang memasuki oksigenator membran bagi mencapai pCO_2 yang dikehendaki oleh pesakit tertentu. Tindakan pengendalian automatik ini dikawal melalui pelaksanaan tiga pengawal, iaitu Berkadaran-Kamiran-Terbitan (PID) yang disesuaikan dengan kaedah kitaran berterusan Ziegler-Nichols, Pengawal Logik Kabur (FLC) dan Pengawal Fuzzy-PID. Proses kawalan ini kemudian dijalankan menerusi dua tahap, iaitu kerja simulasi dan eksperimen. Ia juga digunakan untuk mengawal CO_2 dalam dua tugas, iaitu penjejakan titik sasaran dan penyingkiran gangguan beban. Untuk penjejakan titik sasaran, sasaran karbon dioksida separa (pCO_2) arteri yang dikehendaki ditetapkan pada 40 mmHg pada permulaan proses, dan ditingkatkan sebanyak 5% hingga 42 mmHg di tengah-tengah proses, dan diselaraskan kembali ke 40 mmHg pada akhir proses. Untuk penyingkiran gangguan, gangguan luaran diperkenalkan pada loji proses (dalam oksigenator membran) dengan pengawal aliran jisim (MFC) dihentikan secara tiba-tiba untuk menghentikan kadar aliran gas sapu sehingga 0 L/min di tengah-tengah proses. Semua kerja-kerja simulasi dilakukan menggunakan perisian MATLAB / SIMULINK level-2, sementara itu, untuk kerja eksperimen, aplikasi dan peranti NI-USB 6009 DAQ digunakan untuk kedua-dua sensor pCO_2 dan pengawal aliran jisim sebagai pelaksana untuk mengawal kadar aliran gas sapuan. Semasa simulasi, semua pengawal mempamerkan tindakan kawalan yang memuaskan, di mana Fuzzy-PID merekodkan prestasi yang luar biasa dalam kedua-dua tugas penjejakan titik yang disasarkan dan tugas penyingkiran gangguan beban. Malangnya, apabila parameter PID dan

FLC yang sama digunakan dalam kerja-kerja ujikaji, prestasi kawalan menjadi paling teruk dengan kehilangan tindakan kawalan. Ini mungkin disebabkan oleh beberapa andaian dan parameter yang ditentukan dalam pemodelan matematik yang berbeza dari parameter sebenar yang digunakan dalam ujikaji. Oleh itu, proses talaan semula dijalankan untuk mengira parameter baru yang sesuai untuk PID, FLC dan Fuzzy-PID. Dengan tetapan baru ini, keseluruhan pengawal dapat mengawal pemindahan gas CO_2 secara automatik dalam oksigenator membran mengikut titik sasaran yang dikehendaki. Apabila parameter PID yang sama dan peraturan FLC digunakan untuk pemodelan matematik (simulasi), prestasi yang memuaskan juga diperolehi untuk kedua-dua penjejakan titik sasaran dan penyingkiran gangguan beban. Untuk menyimpulkan kajian ini, semua pengawal menghasilkan keupayaan kawalan yang baik untuk mengawal CO_2 secara automatik dari oksigenator membran untuk kedua-dua tugasan, dengan pengawal Fuzzy-PID lebih menyerlah berbanding dari dua lagi pengawal, PID dan FLC. Ini boleh dilihat daripada index perncapaian terendah oleh Duzzy-PID dan masa yang diambil untuk mencapai titik sasaran, di mana lebih rendah sebanyak 21.15% berbanding PID dan lebih rendah sebanyak 65.25% berbanding FLC semasa tugas penjejakan titik sasaran. Dalam tugas penyingkiran gangguan, Fuzzy-PID juga merekodkan masa terpantas untuk beradaptasi dengan gangguan, dimana ia mencatatkan 89.33% lebih pantas daripada PID dan 51.52% daripada FLC. Oleh itu, ujian in-vitro ini mempunyai potensi besar untuk diperluaskan di masa hadapan.

Kata kunci: oksigenator membran, pertukaran gas karbon dioksida, Berkadaran-Kamiran-Terbitan (PID), Pengawal Logik Kabur (FLC), Pengawal Fuzzy-PID.

ACKNOWLEDGEMENTS

Firstly, I would like to dedicate a very special thanks to my supervisors, Ir. Dr. Ahmad Khairi bin Abdul Wahab and Dr. Fathiah binti Mohamed Zuki for their useful guidance, insightful comments, and considerable encouragements to me in completing this thesis. Also, thanks for your consideration to every problems and obstacles that I ever had during my years as a postgraduate student. Next, I would like to acknowledge University of Malaya for providing me with financial aid through Skim Biasiswa Universiti Malaya (SBUM). I wish to acknowledge University of Malaya Research Grant (UMRG), No: RP015-2012G, and also the Postgraduate Research Grant (PPP), No: PG022-2015B, Department of Biomedical Engineering, University of Malaya, Malaysia.

Also, I would like to thank my first mentor in research, Prof Nooritawati Md Tahir for all you have taught me in this area. Starting from the opportunity and guidance that you gave me as your research assistant, I start to realise that research is my passion and continue with it until today.

To my husband, Afiq Faisal bin Abu Kassim, thank you so much for your unconditional support and also the cooperation that you gave me, especially towards the end of my postgraduate study. To my children, Akif Nuruddin bin Afiq Faisal, Ali Hyder bin Afiq Faisal and Aimi Khalisa binti Afiq Faisal, thank you for your invaluable support during my PhD work. Last but not least, thanks to all of my family members, my family in-law and my friends. Each of you can share in this accomplishment, for without your support it would not have been possible.

TABLE OF CONTENTS

LIST OF FIGURES

LIST OF TABLES

LIST OF SYMBOLS AND ABBREVIATIONS

ANOVA	:	Analysis of Variance
ARDS	:	Acute Respiratory Distress Syndrome
AV	:	Arteriovenous
CA	:	Carbonic Anhydrase
CFD	:	Computational Fluid Dynamic
COPD	:	Chronic Obstructive Pulmonary Disease
COVID-19	:	Coronavirus 2019
CPB	:	Cardiopulmonary Bypass
$ECCO_2R$	:	Extracorporeal Carbon Dioxide Removal
ECLS	:	Extracorporeal Life Support
ECMO	:	Extracorporeal Membrane Oxygenator
ELSO	:	Extracorporeal Life Support Organization
FDA	:	Food and Drug Administration
FLC	:	Fuzzy Logic Controller
g	:	Gas
HCO_3^-	:	Bicarbonate
HFM	:	Hollow Fibre Membrane
IAE	:	Integral Absolute Error
ICU	:	Intensive Care Unit
iLA	:	Interventional Lung Assist Device
ISE	:	Integral Squared Error
ITAE	:	Integral Time Absolute Error
K_{cr}	:	Critical gain
K_d	:	Derivative gain
K_i	:	Integral gain
K_p	:	Proportional gain
MFC	:	Mass Flow Controller
MSE	:	Mean Squared Error
NIV	:	Non-Invasive Ventilation
O_2	:	Oxygen
PCO_2	:	Partial Pressure of Carbon Dioxide
pH	:	Potential of Hydrogen
PID	:	Proportional–Integral–Derivative
pl	:	Plasma
PMP	:	Polymethylpentene
pO_2	:	Partial Pressure of Oxygen
rbc	:	Red Blood Cell
R-ED	:	Respiratory Electrolysis
s	:	Second (time)
SISO	:	Single-In-Single-Out

SpO_2	:	Saturation of Oxygen
SPSS	:	Statistical Package for the Social Sciences
SPSS	:	Statistical Package for Sosial Sciences
UMMC	:	University Malaya Medical Centre
VV	:	Veno-venous
Q_b	:	Blood flow rate
Q_g	:	Sweep gas flow rate

LIST OF APPENDICES

CHAPTER 1: INTRODUCTION

1.1 Research background

Over the last decade, the use of Extracorporeal Life Support (ECLS) is increasing proportionally with the improvement in its design, which make this machine become smaller, less invasive and easier to use. A huge leap in membrane technology, which evolved from the bubble oxygenator in 1970's until the recent innovation of membrane oxygenator made from polymethylpentene (PMP) has resulted in a massive improvement in gas exchange process with great reduction in oxygenator failure rate.

This research is mainly focus on the proposed automated control system of carbon dioxide (CO_2) transfer in the membrane oxygenator. To develop an automated control system, part of human system, where this automated control will be implemented, which is the human circulatory system must be completely understood beforehand, in addition to the proposed mechanism of the controller itself.

1.2 Problem statement

During membrane oxygenator operation, the sweep gas adjustment is a must, since CO_2 clearance is highly dependent on the sweep gas flow rate (Chung et al., 2014; Duncan, 2001). The importance of manipulating the sweep gas by adjusting its flow rate was highlighted by Richard et al. (2014) and Extracorporeal Life Support Organization (ELSO) (2013), where sweep gas rate should be carefully adjusted in order to give a partial pressure of CO_2 (pCO_2) between 35-45 mm Hg. In the current clinical practice, the O_2 gas that flows to the oxygenator is still manually adjusted until the optimum partial pressure (O_2 and CO_2) in the arterial blood is achieved. This manual adjustment is performed by a perfusionist. The perfusionist are required to manually and constantly observe, interpret and process the data to optimize the

whole process. These tasks demand their high commitment to achieve required accuracy, alertness and experience (Boschetti et al., 2002). Thus, it has great potential for human errors, which can lead to serious damage to tissue and nervous cell.

To relieve the operator from the high load task of manual control, an automatic control loop of this process is proposed. This is done using these three basic principles as follows:

i. Installation of on-line pCO_2 sensors at inlet and outlet of the membrane oxygenator.
ii. Automation of the sweep gas flow rate by adding an actuator to it so that it can be driven electronically, which is mass flow controller in this study.
iii. Development of controllers (in this case a PID controller, FLC and Fuzzy-PID controller), and its connection to the online pCO_2 measurement (as in (i)) and the automatic mass flow controller (as in (ii)).

1.3 Research questions

From the problem statements mentioned previously, there are five research questions that rises, which must be answered in order to complete the study:

1. What is the most appropriate mathematical modelling that can describe CO_2 gas transfer in hollow fibre membrane oxygenator?

2. Can the mathematical model in (1) be simulated in MATLAB/SIMULINK environment and what is the determinant factor of CO_2 removal from hollow fibre membrane oxygenator during extracorporeal life support? What is the best controller to be used for this purpose?

3. Can this automated control be developed based on this simulation work for online implementation in experimental work?

4. Can the in-vitro gas exchange module developed in this study able to be used for automation of CO_2 gas exchange and is it possible to apply automatic controller in this experimental set-up by using the same control strategies developed during simulation work?

5. What is the best controller to be used for this purpose and is the simulation and experimental results agreeing each other?

1.4 Objectives of the study

The aim of this study is to design and develop an automated control of CO_2 gas transfer in hollow fibre membrane oxygenator system by implementing advanced controllers for sweep gas flow rate adjustment based on the feedback from pCO_2 measurement. In order to achieve this aim, there are five objectives that will be accomplished, which are:

1. To identify the most suitable mathematical modelling and demonstrated CO_2 gas exchange in hollow fibre membrane. This mathematical model will be implemented using level-2 s-function MATLAB/SIMULINK environment.

2. To implement PID, FLC and Fuzzy-PID controllers in simulation work for controlling the rate of CO_2 elimination from a hollow fibre membrane oxygenator during extracorporeal life support by manipulating sweep gas flow rate. This simulation work will be done using the mathematical model identified in (1). All the controllers will be

employed separately to see their individual performance, follows by the comparison of the three controllers in controlling the process variable.

3. To develop an experimental setup for extracorporeal life support using hollow fibre membrane oxygenator as process plant, which in-vitro gas exchange module in bench top laboratory setup.

4. To employ experimental work on newly developed in-vitro gas exchange module and prove the concept of automation for CO_2 gas exchange in hollow fibre membrane oxygenator by manipulating sweep gas flow rate using the same controllers and control strategies implemented in (2). This experimental work will be performed separately for each controller.

5. To compare the performance between different controllers, namely PID, FLC and Fuzzy-PID for both simulations (as in (2)) and experimental works (as in (4)) in terms of qualitative and quantitative analysis.

1.5 Significant of the study

The encouraging performance of automatic control will be escalated in this study by introducing Fuzzy-PID controller to automatically control CO_2 gas transfer rate in membrane oxygenator. Fuzzy-PID is a fusion between PID controller and FLC, which selected due to its self-tuning ability and on-line adaptation to nonlinear, time varying, and uncertain system. This controller also is an improvement to conventional PID controller that has some drawbacks, which cannot automatically adjust its P, I and D gains according to the system's changes, since it has no knowledge about the process plant. PID is linear and symmetric type of controller; hence its performance is varying in non-linear system (Visek et al. 2014). CO_2 gas transfer in

membrane oxygenator is highly non-linear, due to the chemical binding of O_2 and CO_2 that exist within the blood. Thus, to improve its performance, it is a good idea to fusion it with another decision-maker controller that is robust in classifying the system's state, which is FLC. By applying this strategy, Fuzzy-PID controller is expected to perform better compared when PID controller and FLC used alone.

Sweep gas flow rate in this study will be controlled by three types of control strategies, namely PID (Proportional–Integral–Derivative), FLC (Fuzzy Logic Controller) and the fusion of PID and FLC, Fuzzy-PID controller. To this date, there are no study reported yet on the application of Fuzzy-PID as the controller that solely focus on CO_2 removal control strategy in membrane oxygenator. This is due to the scope of this study, which is to dedicate this control strategy for $ECCO_2R$ system. $ECCO_2R$ system is typically used when the primary purpose of the operator is to remove CO_2 with little or no expectation in providing significant amount of extracorporeal oxygenation.(Brodie, 2018) Thus, it is differs from the common oxygenation control strategy for the application in ECMO system that mainly focus on O_2 control, which can be found redundantly in the literatures (Brendle et al., 2017; Hexamer et al., 2004; Kopp et al., 2016; Misgeld et al. 2012; Misgeld, Werner et al. 2005; Walter et al., 2009b; Walter et al., 2010b). In addition, different approaches in control strategy, which are the application of mass flow controllers (Aalborg GFC17) as the actuator and the application of toggle switch to produce disturbance also make this study outstanding compared to the others, since most of the previous studies used stepper motor that coupled with electronic valve (Conway et al., 2019) and anaesthesia gas monitor (Brendle et al., 2017; Brendle et al., 2017; Walter et al., 2009a) to control the gas supply to the process plant.

In this proposed automated control, rate of O_2 and CO_2 diffusion are carefully adjusted so that normal range of pO_2 and pCO_2 are maintained to provide the safe extracorporeal circulation. With the introduction of automated control for oxygenator, patient's safety can be significantly ensured by having fast and precise control reference tracking on optimum setpoint and a good disturbance rejection, in maintaining the normal range of blood gas value during treatments (Dhinakaran & Lincon, 2014). In conjunction to our proposed improved strategies, a detailed study on the automatic control of pCO_2 level in oxygenator was conducted due to its high potential in producing the significant contribution to this field (Manap & Abdul Wahab, 2016).

1.6 Scope and limitation

The scope of this study involved CO_2 gas exchange and control of CO_2 gas removal from membrane oxygenator, through in-vitro gas exchange module in a bench setup. This study will cover the control process of CO_2 gas exchange in a hollow fibre membrane oxygenator to implement an automated control strategy for $ECCO_2R$ system. $ECCO_2R$ system is typically used when the primary purpose of the operator is to remove CO_2 with little or no expectation in providing significant amount of extracorporeal oxygenation (Brodie, 2018). This method of extracorporeal support is similar with veno-venous Extracorporeal Membrane Oxygenation (ECMO) system, but it uses smaller intravenous access catheter.

Since the word 'in-vitro' means 'process that performed outside the living system', it gives clear indication that this study only involved blood sample that has been circulated within the gas exchange module and do not involved any living animal/human.

Due to the 'in-vitro' typed experiment is being considered in this work; the limitation of this study is the usage of human blood during blood purification process in order to mimics the real

operation of membrane oxygenator in on the patients. As a solution, bovine blood will be employed due to its ease of availability and it is a very good substitute for human blood (Vaslef et al. 1994; Wickramasinghe et al. 2005).

The other limitation of this study is regarding the published literatures that are very limited, since there are not many studies that are focusing on CO_2 removal, while abundance of studies carried on the control process of O_2 gas exchange in Extracorporeal Life Support (ECLS) Thus, the practical practice knowledge on CO_2 removal process control is quite limited. To deals with this limitation, a thorough literature reviews also are performed on the studies regarding pO_2 control in ECLS in order to determine the appropriate methodology for this study.

1.7 Thesis outline

Chapter 1 provides overall description of the project itself along with the brief outline of each chapters in this thesis. All the research elements such as problem statement, research questions, objectives, significance, scope and limitation of this study are stated in here.

Chapter 2 reviews the work done by other researchers related to the membrane oxygenator and its practice to the patients with respiratory deficiency. The whole literatures are divided into four main parts. Summary of the major agreements and disagreements, and the stand where this thesis sits are stated in this chapter.

Chapter 3 explains the mathematical modelling and simulation of the CO_2 gas transfer in the membrane oxygenator. The effect of sweep gas flowrate to the CO_2 gas transfer rate also are simulated, including the statistical analysis to prove the significance of the changes made in the sweep gas flowrate to the CO_2 transfer rate in the membrane oxygenator.

Chapter 4 highlights the methodology, results and discussions of the findings from the simulation study, as the extended of the work in Chapter 3. Unlike Chapter 3, which only focuses in the mathematical modelling of CO_2 gas exchange in membrane oxygenator, this chapter highlights all the simulation studies on automated control process for the three types of the proposed controllers, namely the PID, FLC and Fuzzy-PID.

Chapter 5 elaborates further the methodology, results and discussion on the experimental results for the whole study. The experimental results are analysed and the performance of each controller are evaluated.

Chapter 6 deals with the conclusions of the project as a whole. Recommendations for possible future developments are also stated here.

CHAPTER 2: LITERATURE REVIEW

2.0. Introduction

The main objective of this study is to design and develop an automated control of membrane oxygenator for CO_2 gas exchange by implementing advanced control strategies in sweep gas flow rate adjustment based on the feedback from carbon dioxide partial pressure (pCO_2) measurement. In order to achieve this aim, reviews of published literatures have been conducted thoroughly within many aspects. This effort mainly regarding the usage of membrane oxygenator and its efficiency to support in respiratory failures; gas exchange process in an oxygenator for O_2 and CO_2 and the influence of the sweep gas flow rate to CO_2 removal rate in the oxygenator itself. Finally, the current investigations on the automated control applications that involved membrane oxygenator in extracorporeal life support strategy.

2.1. The human blood circulatory system

The human blood circulatory system can be systematically described as a continuous single closed circuit, which consisted of two separated sub-circuits: pulmonary (lung) and systemic (body) circulation, connected by the heart (Applegate, 2006). Figure 2.1 shows the interconnection between pulmonary circulation, which connected in series with systemic circulation and separated by the heart that acts as the natural blood pump.

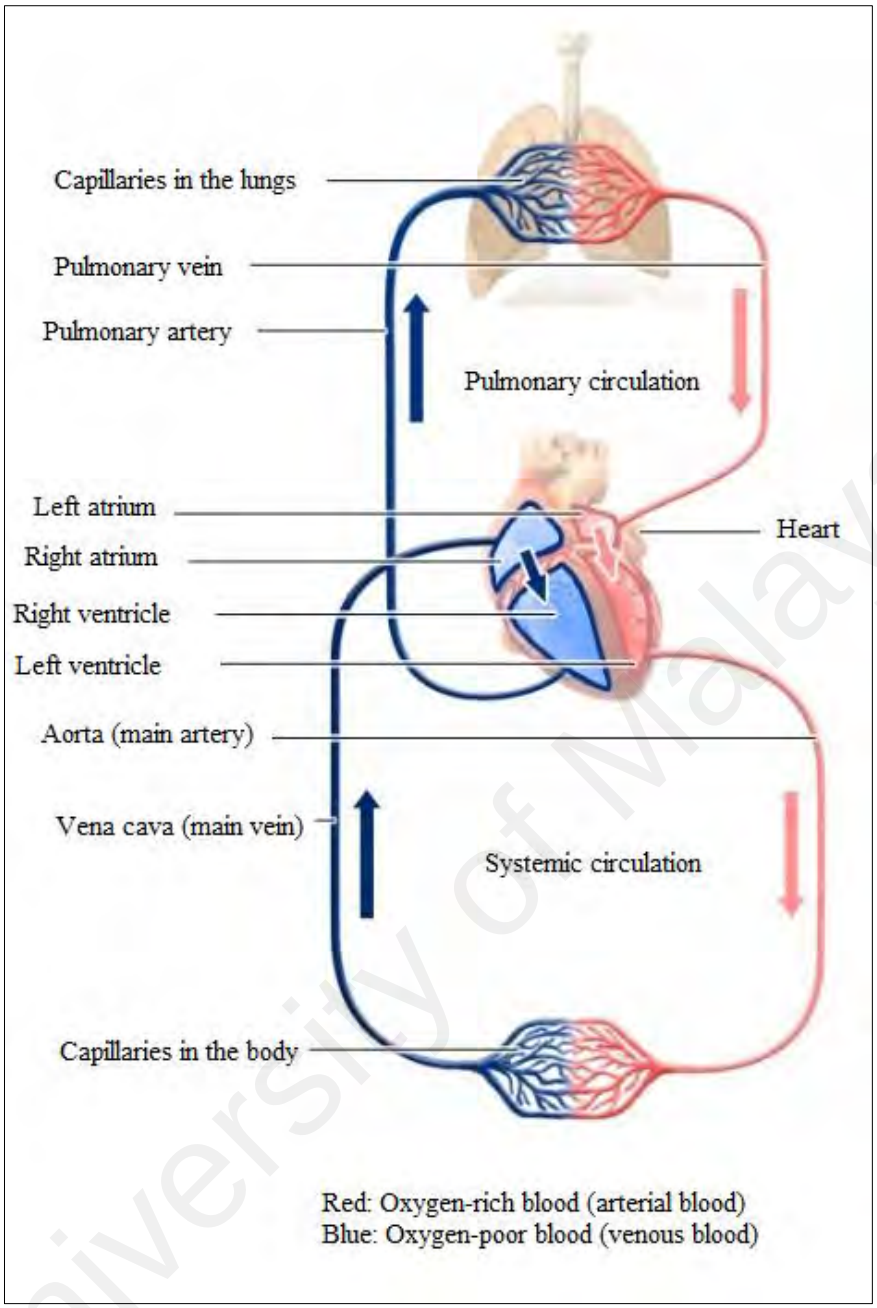

Figure 2.1. O_2 and CO_2 circulation in human body (Applegate, 2006).

The systemic circulation goes from left ventricle to the right atrium, passes the different organ areas, such as the brain and muscle. Meanwhile, in the pulmonary circulation, blood is pumped by the right ventricle to the left atrium, passing through the right pulmonary artery, capillaries in lungs and pulmonary veins. There, gas exchange between O_2 and CO_2 occurs. This

cardiovascular arrangement maintains an adequate blood flow for optimum perfusion of the organs and all of the tissues in human body, to ensure:

1. O_2 delivery.
2. CO_2 removal.
3. Nutrients delivery (glucose, amino acids, etc).
4. Hydrogen ions removal and maintains proper concentration of other ions.
5. Transportation of vital hormones and other specific substances.
6. Body heats maintenance.

There are two types of respirations occur in human circulatory system, as illustrated in Figure 2.2, which are:

i. *External respiratory*

External respiratory referred to the exchange of O_2 and CO_2 between the air in the lungs and blood in its surrounding capillaries, which occurs in pulmonary circulation. There, O_2 will diffuses from lung's alveoli into the blood, while CO_2 diffuses from the blood into the air of the alveoli via respiratory membrane. The rate of this gas exchange across respiratory membrane is based on few factors, such as membrane's surface area, membrane's thickness, gas solubility and concentration gradient of the gas between two sides of the membrane (Applegate, 2006). Based on these factors, membrane oxygenator is used in this study. Thus, membrane's surface area, thickness and gas solubility will be assumed as constant at all cases of studies (for the simulation works, similar surface area, membrane thickness and gas solubility are used as the parameter in the mathematical modelling. Meanwhile, in the experimental work, same oxygenator and same gas type and percentage is used for all case of study), while concentration gradient is

deviated accordingly to the change of sweep gas flow rate, in order to control the rate of CO_2 gas exchange.

ii. Internal respiratory

Unlike the external respiratory, internal respiratory that occurs in systemic circulatory is the gas exchange process between the tissue cells and the blood in tissue capillaries. After external respiration (O_2 diffuse into the blood while CO_2 diffuses out from the blood), blood returns to the left sides of the hearts and pumped to the tissue capillaries. At this point, blood has higher O_2 concentration and lower CO_2 concentration than the body tissue cells. The lower of O_2 content and higher CO_2 content in body tissue cells is due to the metabolism process, since tissue cells consume O_2 and produce CO_2 in this process. Again, this concentration gradients that exist will drive the O_2 from tissue capillaries to the tissue cells, and CO_2 from the tissue cells into the capillaries. This process is a reverse process of internal respiratory that occurs in the lungs. In simpler word, O_2 is gained and CO_2 is removed in the pulmonary circulation, while O_2 is consumed and CO_2 is produced in systemic circulation. For this reason, during simulation works (in Chapters 3 and 4), 46 mmHg will be used as the initial pCO_2 that enters the process plant, which is membrane oxygenator, while for experimental study, in the design of in-vitro gas exchange module, two membrane oxygenators are used, which is referred as oxygenation part (automated control of membrane oxygenation will takes place here) and de-oxygenation part (another membrane oxygenator is used to remove O_2 and to add CO_2, which its pCO_2 will be monitored by pCO_2 sensor as 46 mmHg). The de-oxygenated part will be discussed later in Section 5.12 of Chapter 5. This approach is planned to mimics both pulmonary and systemic circulation, in order to make this study as close as possible to the human respiratory system. The value of

46 mmHg is selected to be the initial pCO_2 value, since the normal pCO_2 in arterial blood is between 40 mmHg to 45 mmHg. Hence, initial pCO_2 is selected above the normal range to simulated patients with respiratory disease, since operation of membrane oxygenator in Extracorporeal Life Support (ECLS) system is implemented on the patient with respiratory disease.

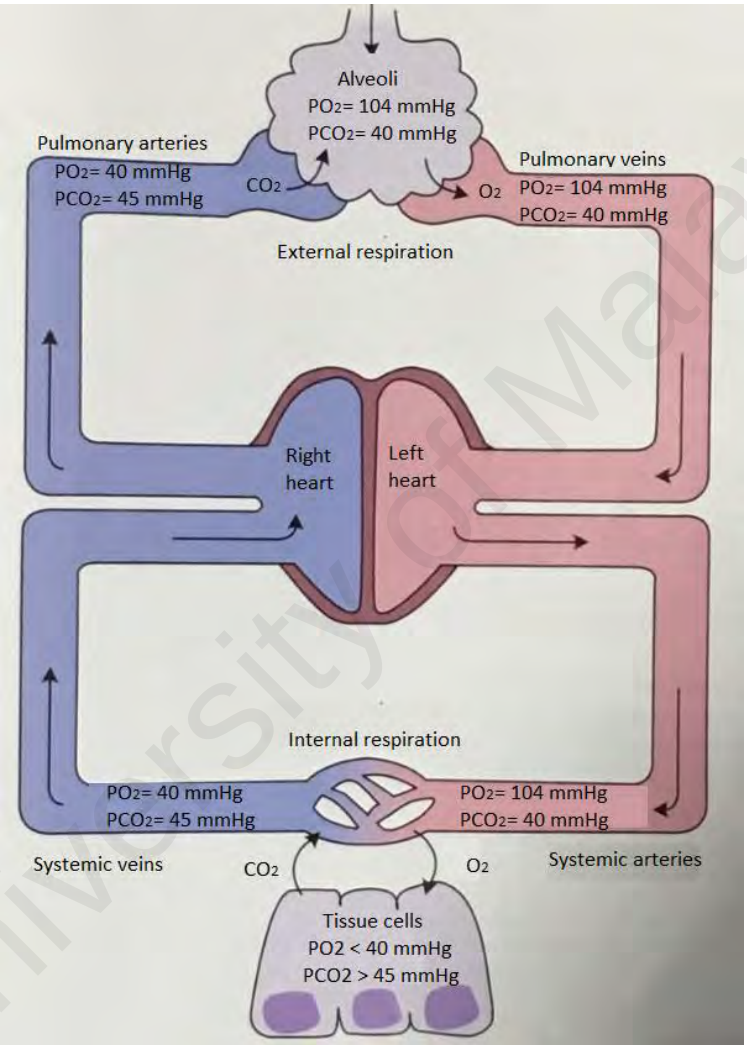

Figure 2.2. External and internal respiration (Applegate, 2006).

2.1.1. Transport of blood-gas and acid-base management.

As explained in the previous section, gas exchange occurs during pulmonary circulation. During respiration, gas exchange occurs primarily via diffusion, which driven by concentration gradient. Concentration gradient causes the gas molecules been transferred from high

concentration region to low concentration region. This is the principle of gas exchange in the lungs.

Pulmonary ventilation occurs through inhalation that brings air into the lungs. This gas mixture primarily consists of nitrogen (78.6%), oxygen (20.9%), water vapour (0.5%) and CO_2 (0.04%) (Molnar & Gair, 2013). From this percentage, it can be seen that the air that enters the lungs will have higher concentration of oxygen and lower concentration of CO_2.

On the other hand, venous blood that is entering the lungs contains low oxygen concentration and higher CO_2 concentration. This concentration gradient (between inhaled air and venous blood) allows gas exchange process in lungs, where the O_2 from the inhaled air is diffuses into venous blood, whilst CO_2 from venous blood is diffused out to the inhales air across the alveoli. As the result of gas exchange, blood that leaving lungs contain higher oxygen concentration and low CO_2 concentration. This blood then is referred as 'arterial blood' and this term will be used in this whole thesis.

2.1.1.1. Oxygen transport in human body

After diffusion of O_2 from alveolus to capillary, it dissolves in the blood plasma, with 3% remains in the plasma as dissolved gas, while the rest diffuse from plasma to the red blood cell, to form a compound called oxyhemoglobin (Applegate, 2006). The reaction between O_2 and haemoglobin that occurs in lungs is called loading, as shown in Figure 2.3(a). Here, the pO_2 is high. Since the bond between O_2 and haemoglobin are unstable and reversible, when the blood reached the tissue capillaries (where pO_2 is low), the bond breaks and O_2 is released to the tissue. This is then called as unloading process and it is illustrated in Figure 2.3(b).

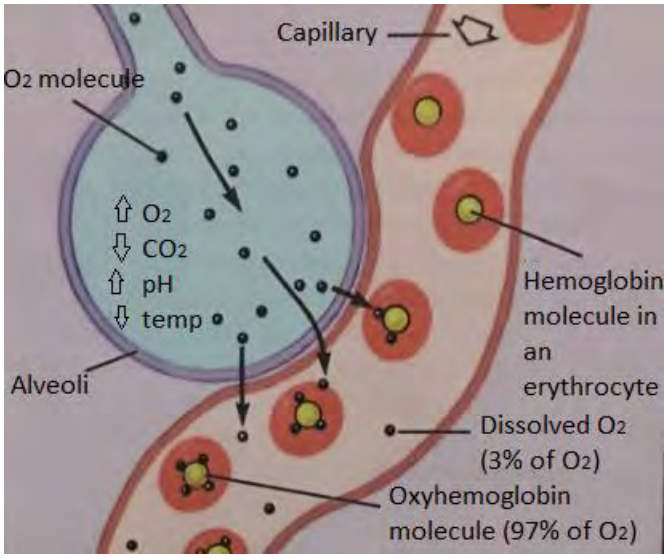

(a)

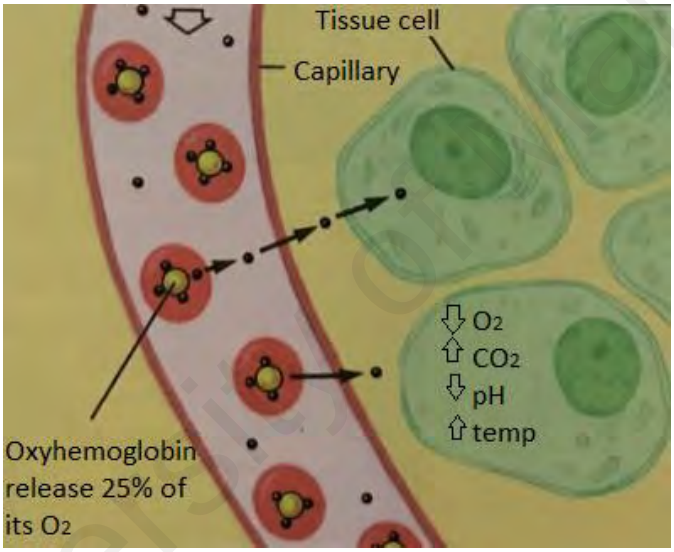

(b)

Figure 2.3: (a) loading and (b) unloading process of O_2. Adapted from (Applegate, 2006).

Cell uses O_2 for metabolism. From this process, CO_2 and heat are produced as by-product of the metabolism. The CO_2 then reacts with water to form carbonic acid, which make the cellular environment more acidic. For this reason, the respiratory process must be carried out continuously for any living organism. Otherwise, if the process is disturbed or obstructed by any factor, such as respiratory disease or lung injury, an alternative method for respiratory process must be applied to the respective patients to avoid complications and organ failures.

2.1.1.2. Carbon dioxide transport in human body

In resting condition, an approximately 250 mL/min of CO_2 is produced by an adult healthy man, subjected to the metabolic activity, caloric intake and core body temperature. CO_2 is generated in the mitochondria as by-product of cellular metabolism. Through a series of partial pressure gradient, CO_2 then passes via cytoplasm and extracellular fluid until it reaches venous blood stream. From venous blood stream, CO_2 is transferred to the lung's alveoli, where the ventilation occurs and then released to the outer ambient.

In the human blood, CO_2 presents in three different forms, which are as dissolved CO_2 in the plasma, bound as bicarbonate and bound as carbamate when combines with haemoglobin (Geers & Gros, 2000). According to Arthurs and Sudhakar (Arthurs & Sudhakar, 2005), in arterial blood, partial pressure of CO_2 that bounded as bicarbonate is 90%, while dissolved CO_2 and carbamate are only 5% each. On the other hand, 70% of CO_2 is transported as bicarbonate in venous blood, with 23% of carbamate form and 7% of dissolved CO_2 (as in Figure 2.4).

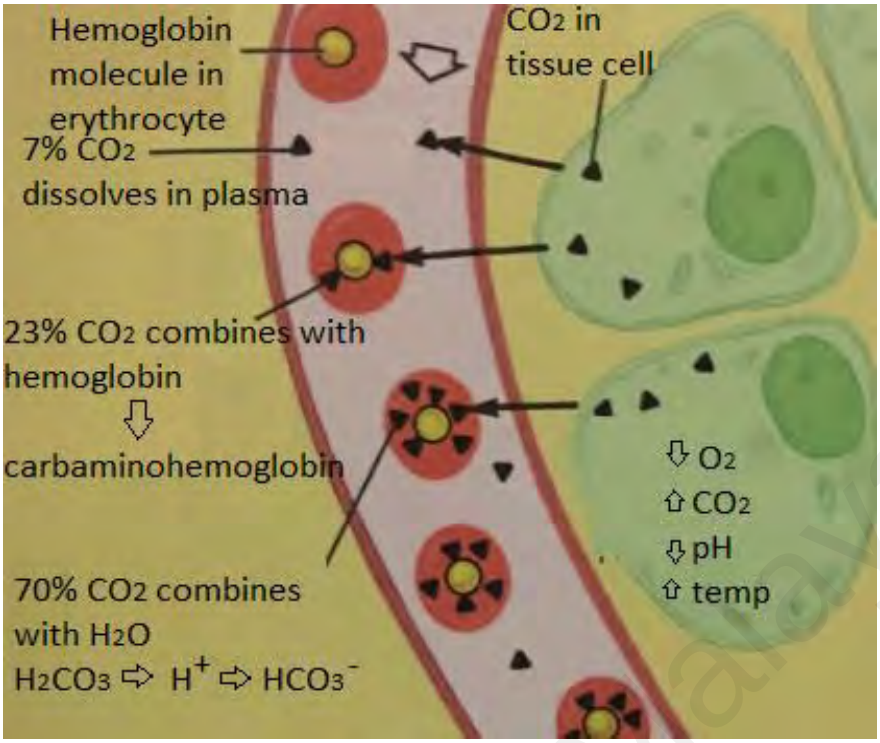

(a)

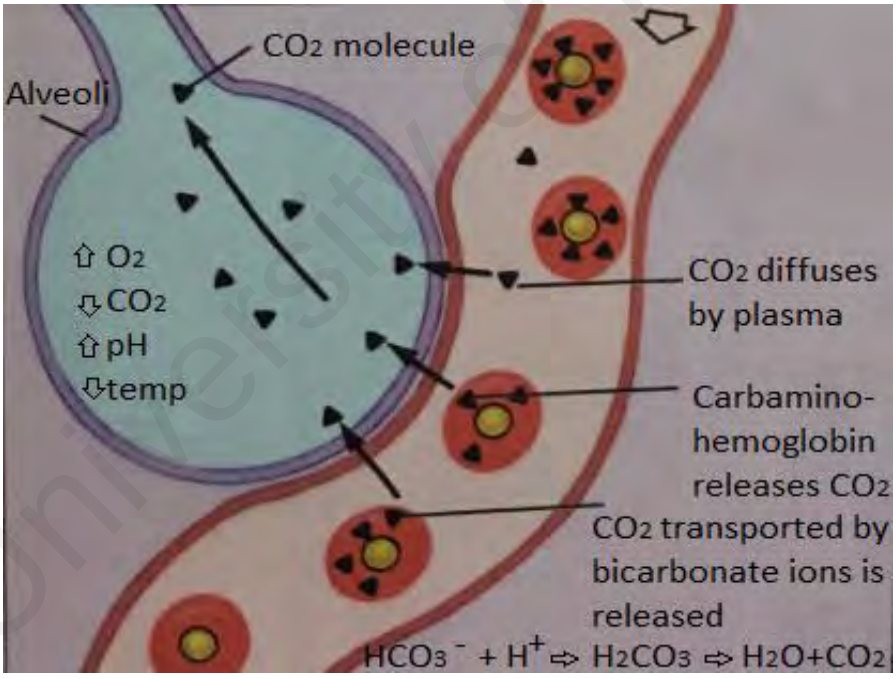

(b)

Figure 2.4: CO_2 transport. (a) CO_2 diffuses from tissue cells into blood for transport, (b) CO_2 is release from blood component and diffused into alveoli. Adapted from (Applegate, 2006).

For both arterial and venous blood, most of the CO_2 is transported in the form of bicarbonate ions. CO_2 that diffuses into the red blood cell combines with water and form carbonic acid. There, an enzyme inside the red blood cells called Carbonic Anhydrase (CA), speeds up this reaction. Thus, the CO_2 that is contained within bicarbonate ions can be written as:

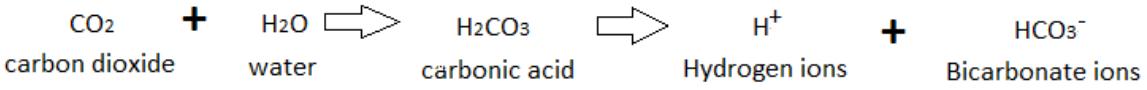

[2.1]

An increase in CO_2 levels on blood elevates numbers of hydrogen ions, resulting in the reduction of pH. Conversely, a decrease in CO_2 levels in the blood will results in a reduction of hydrogen ions that increase the pH and cause the blood to be more alkaline. This relationship signifies that the proper control of CO_2 levels in blood is extremely important in human respiratory system. During the implantation of artificial lung to patients, CO_2 level is among the main parameter to be monitored closely to avoid any fatality to the patients. All of this highlights the importance of this study and its significant contribution to the development of artificial lungs technology.

The concept of gas exchange across membrane for respiratory purpose in membrane oxygenator is inspired from the mechanism of alveolus in the lung. The difference between both membrane oxygenator as artificial lung and alveolus as a unit of gas exchange in human lung is depicted in Figure 2.5. As we can see from the figure, the gas exchange in human lung (native lung) is across the respiratory membrane, while gas exchange in membrane oxygenator (artificial lung) is across the membrane (made of polypropylene as used in this study). The same principle of gas exchange (based to the concentration gradient exist between venous blood and sweep gas) is applied for both native and artificial lung (membrane oxygenator).

This is due to the main purpose of the membrane oxygenator implementation on patients itself, which acts as temporary replacement for native lung, in order to provide support to patient's respiration, by allowing gas exchange across its membrane.

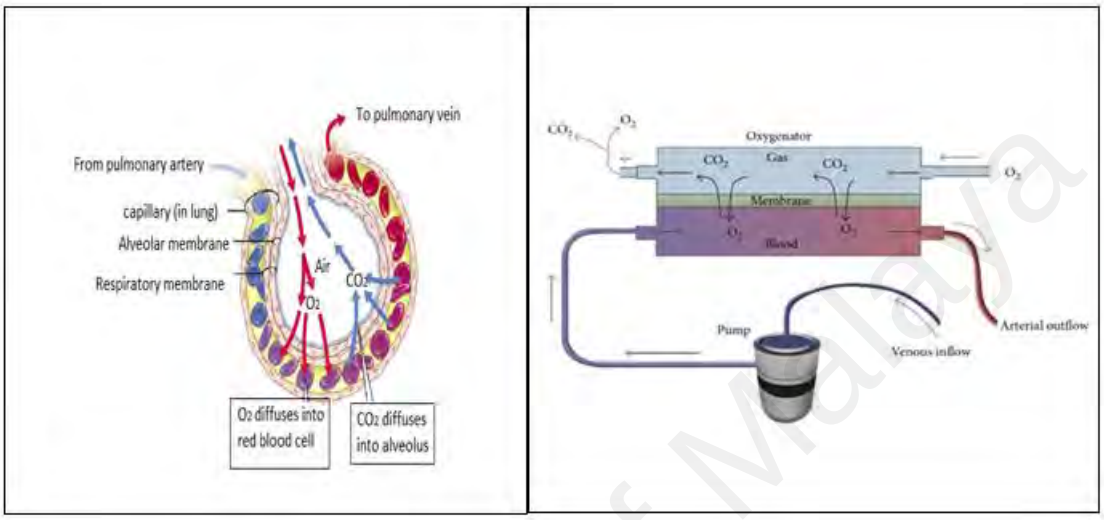

Figure 2.5: Difference between gas exchange in lung and in membrane oxygenator applied in this study. Adapted from (Cove et al. , 2012).

2.1.1.3. Acid-base management

In respiratory system, acid-base balance is defined as the regulations in hydrogen ions (H^+) concentrations, which may vary from $>10^{-14}$ up to 10^0 equivalents per litre (Misgeld, 2007). This hydrogen ions (H^+) is represented by the pH values, which defined as the negative decadic logarithm:

$$\text{pH} = \log \frac{1}{[H^+]} = -\log[H^+] \qquad [2.2]$$

From the above equation, a low pH value is indication of high concentration of hydrogen ion, which is called acidosis. Conversely, a high pH values means a low concentration of hydrogen ion, a state that referred as alkalosis. Both states (acidosis and alkalosis) can cause fatality, if it is below 6.8 or above 8.0 pH values, respectively for a long time. Table 2.1 shows the nominal arterial blood gas values.

Table 2.1: Nominal arterial blood gas value for adult human (Singh et al., 2013).

Value	Components	Normal range
pH	Acidity/alkalinity	7.35-7.45
pCO_2	Partial pressure of CO_2 in arterial blood	35-45 mmHg
pO_2	Partial pressure of O_2 in arterial blood	90-100 mmHg
HCO_3-	Bicarbonate in blood	22-26mEq/Litre

2.2. Extracorporeal Life Support System (ECLS)

Respiratory failure is characterized by inadequate gas exchange process in human body due to dysfunctionality of one or more vital organs that is important in respiratory system. There are several diseases that can lead to respiratory failure, such as Acute Respiratory Distress Syndrome (ARDS), Chronic Obstructive Pulmonary Disease (COPD), asthma and more. To cope up with these fatal diseases, different treatments have been employed to reduce the mortality rate of patients with respiratory failure, including Non-Invasive Ventilation (NIV) (Ambrosino et al., 1995; Confalonieri et al., 1996; Manap & Abdul Wahab, 2016; Plant et al., 2009), endotracheal intubation (Drolet et al., 2000; Zimmerman et al., 1993), mechanical ventilation (Luksza et al. 1986; Serpa Neto et al. 2014; Zimmerman et al., 1993), and also Extracorporeal Life Support System (ECLS). The term 'ECLS' itself encompasses a spectrum of temporary mechanical support, which provide support for the failing lung, heart or both (Finney, 2014). Thus, the most common modalities of ECLS includes Cardiopulmonary Bypass (CPB), Extracorporeal Membrane Oxygenation (ECMO), Interventional Lung Assist Device (iLA® Novalung®) and Extracorporeal CO_2 Removal ($ECCO_2R$). During the implementation of this life support, pathophysiologic processes are allowed to heal or resolves, either by medical/surgical intervention, by transplantation, or even by spontaneous means (Skinner et al., 2006).

Due to this circumstance, it must be ensured that the pathophysiologic processes must be reversible before applying the ECLS system. Even though ECLS is the most sophisticated method in dealing with respiratory failure, it usually implemented as a salvage therapy, where it is used only when the other respiratory procedures such as NIV, endotracheal intubation and mechanical ventilation failed (Fica et al., 2012; Lobaz & Carey, 2011; Pego-Fernandes et al., 2012). Hence, it is only applied on patients with pre-treatment predicted mortality threshold reaching above 80-90% (Chauhan & Subin, 2011). In simpler words, it is an option that only needs to be considered as the last resort to treat the related diseases.

2.2.1. Use of oxygenator in extracorporeal life support for respiratory failure

Membrane oxygenator is an essential component in ECLS strategy, such as ECMO, CPB (also known as heart lung machine) and ECCO$_2$R system. Generally, ECLS strategies works based on the principle of gas exchange to support patients' respiratory cycle, based on four objectives (Chauhan & Subin, 2011):

(i) To remove CO_2 and blood oxygenation.
(ii) To improve delivery of tissue oxygen (O_2).
(iii) To maintain normal physiologic metabolic.
(iv) To allow lung to rest with or without cardiac offloading.

While sharing common principle and objectives, there are some differences between them, due to their purpose, limitation and ventilation strategy. The difference between ECMO and CPB are described as in Table 2.2:

Table 2.2: Differences between Extracorporeal Membrane Oxygenator and Cardiopulmonary Bypass (Punjabi & Taylor, 2013).

ECMO	CPB
The purpose of ECMO is to allow time for intrinsic recovery of patient's heart and lungs.	The purpose of CPB is for lung support during different types of cardiac surgical procedure
Usually implemented using cervical cannulation, which can be conducted under local anaesthesia	Frequently implemented by transthoracic cannulation, which can be conducted under general anaesthesia.
Can be used for longer-term support, ranged between 3-10 days	Only used for short term support, due to its purpose (measured in hours)
ECMO has both cannulation which are arteriovenous (AV) and veno-venous (VV)	Only venous and arterial cannulation

From Table 2.2, CPB is used to provide support during cardiac surgical, while ECMO and $ECCO_2R$ is implemented to support patient with respiratory failure. Even though ECMO and $ECCO_2R$ share a common goal, which is to maintain adequate oxygen uptake and eliminate CO_2 from patients with respiratory failure, there are many differences between both inventions. The main difference between ECMO and $ECCO_2R$ is regarding its principle, where ECMO is invented for CO_2 removal and delivery of tissue oxygen, while $ECCO_2R$ operates solely to remove CO_2. Hence, $ECCO_2R$ only requires low-flow blood rate (around 0.2-2.0 L/min) to clear CO_2 that metabolised by patients with small cannula dimension (8-29 French) through its more compact system (Del Sorbo et al., 2014). On the other hand, in ECMO operation, high-flow blood flow (2.0 L/min) and larger cannula dimension (16-31 French) are needed, which make it more sophisticated and demand highly experienced medical team to operate. A precise

distinction between these terms (ECMO and $ECCO_2R$) is generally difficult to figure out, and they are distinguished by the purpose of its application, either to provide primarily oxygenation or removal of CO_2 (Brodie, 2018).

There are several evidences reported regarding significant and contribution of ECMO in extracorporeal technology. At early stage, ECMO was introduced with the first adult patient survived (J. D. Hill et al., 1972) and successful use in new born respiratory failure case (Bartlett et al., 1976). Then, ECMO was employed in severe Acute Respiratory Distress Syndrome (ARDS) cases with high rate of survivors (Chiu et al., 2015; Linden et al., 2009; Roch et al., 2014), patients with ARDS due to Influenza A (H1N1) pneumonia (Chan et al., 2010; Pappalardo et al., 2013) and as a bridge to lung transplantation and graft recovery (Bittner et al., 2012; Javidfar et al., 2012; Toyoda et al., 2013).

The implementation of ECMO also brings significant contribution during the latest pandemic of Coronovirus 2019 (COVID-19) disease. Zhan et al. (Zhan et al., 2020) in their first case of COVID-19 successfully treated by ECMO in Xinyang City, China revealed that this treatment was able to treat 54-year-old man COVID-19 patient. Prior to ECMO intervention, patient's oxygen saturation declined to only 81% while his chest x-ray showed high patchy shadows in both lungs. No complication was reported for this case and the patient was discharged after 29 days of treatment. Li et al. (Li et al., 2020) then applied ECMO on 8 patients suffered from severe hypoxia resulting from COVID-19 with all the precaution steps taken, as seen in figure 2.6. They reported 50% mortality after being treated with ECMO for 3 hours to 47 days. In the United States of America, Jacobs et al. (Jacobs et al., 2020) employed ECMO for 32 patients with confirmed COVID-19 and recorded 10 death due to this life-threatening disease. The ECMO implementation is emerging day by day in reported widely across the world (N. Chen

et al., 2020; Guan et al., 2020; Huang et al., 2020; Wang et al., 2020; Yang et al., 2020; Zhou et al., 2020).

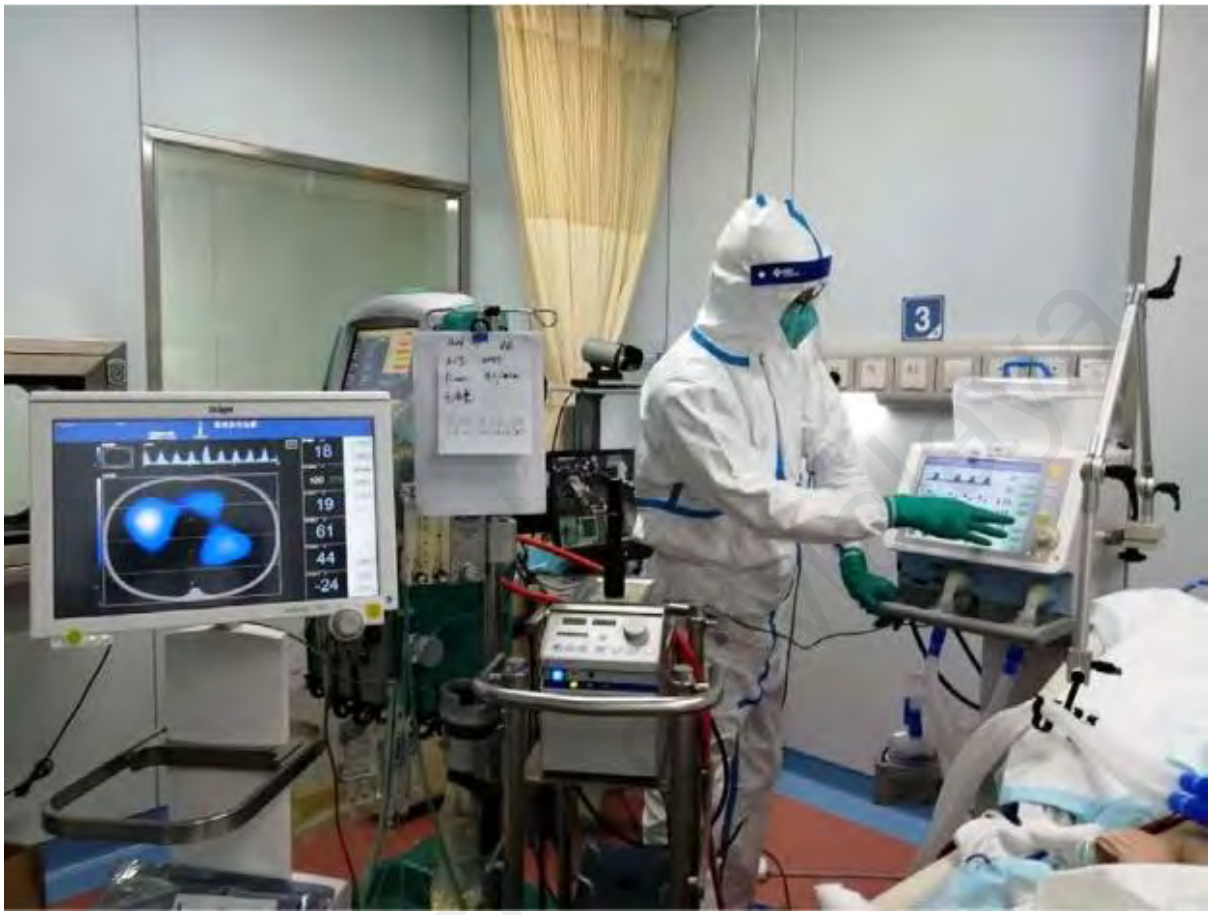

Figure 2.6: Patient with COVID-19 is supported with ECMO and mechanical ventilation support (Li et al., 2020).

Instead of its great contributions in treatment of patients with severe, life-threatening respiratory dysfunction, ECMO has its weakness too. One of the restrictions of this extracorporeal technology is, it requires highly specialised centre due to its complexity, invasiveness and high cost (Kluge et al., 2012). This experience was reported by (Fuehner et al., 2012), where interdisplinary team was required to implement ECMO, which composed of thoracic surgeon, critical care expert and transplant pulmonologist. In addition, patient that qualifies for this procedure and ECMO procedure that will be employed on that particular patient must be selected carefully to reduce ECMO-related complications (Bermudez et al.,

2011). Since the application of ECMO to the patients is considered highly sophisticated, there are several ECMO-related complications that arise from this procedure. Some of them are bleeding and bloodstream infection (Aubron et al., 2013; Bittner et al., 2012; Muller et al., 2009), cardiac arrest after air embolism (Fuehner et al., 2012), sepsis (Bittner et al., 2012), deep venous thrombosis at cannulation site (Javidfar et al., 2012), neurological complications such as intracranial hemorrhage and cerebral infraction (Hervey-Jumper et al., 2011) and also multi organ dysfunction with renal failure (Chen et al. 2014; Fuehner et al., 2012).

Frequent episodes of adverse event and mechanical complication associated with ECMO therapy open a wide opportunity for $ECCO_2R$ to be introduced as an alternative method in extracorporeal life support technology (Lund & Federspiel, 2013). Hence, in this study, the improvement and development work of membrane oxygenator will be done by considering its normal operation in $ECCO_2R$ system. This study will solely focus in removing CO_2 from venous blood using Hollow Fibre Membrane (HFM) oxygenator with concept of automated control.

2.2.2. Principles of gas exchange in membrane oxygenator during $ECCO_2R$ implementation and its components

$ECCO_2R$ is designed to remove CO_2 from blood in order to allow lung to 'rest'. The approach is quite similar with ECMO, but it only requires substantially lower blood flow in order to provide an effective and minimally invasive extracorporeal therapy. Basically, $ECCO_2R$ comprised of drainage cannula, which located in a large central vein, pump (for VV bypass circuit), a membrane lung and a return cannula (Cove et al., 2012). In normal operation, blood is pumped through membrane lung and CO_2 is removed from membrane lung by diffusion. The placement of these three essential components is demonstrated in Figure 2.7.

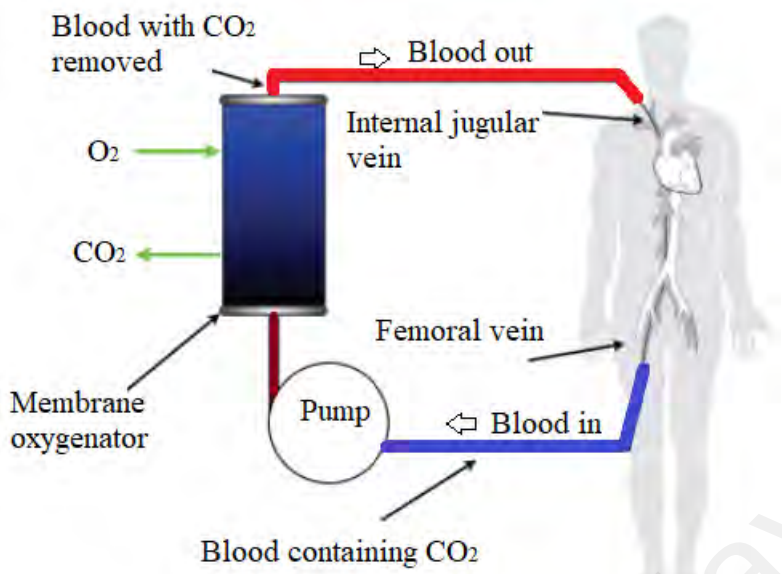

Figure 2.7: Placement of basic component in ECCO$_2$R (Cove et al., 2012).

There are two types of configurations of ECCO$_2$R, which are arteriovenous (AV) and veno-venous (VV) (Baker et al., 2012). In AV ECCO$_2$R, both artery and vein (commonly femoral artery and vein) are cannulated. For this purpose, imaging method such as ultrasound may be use to assist in assessing the diameter of artery. Arterial blood then flows through membrane lung (for gas exchange) and is returned to the body via the veins ((NICE), 2011). AV ECCO$_2$R is a simpler method in ECCO$_2$R since membrane lung is connected from arterial to venous, thus eliminate the needs of pump and associated tubing in the circuit (Federspiel & Svitek, 2004). In contrast, VV ECCO$_2$R involves venous cannulation. Two venous catheters are used for the cannulation, either single access via double lumen catheter or dual access system. Since venous blood accelerates in low flow, VV circuit is driven by a low-flow pump. Apart of its difference in pumping system, both AV and VV systems still need the continuous infusion of heparin in order to minimize the risk of thrombus formation ((NICE), 2011). The ECCO$_2$R related complication among the patients also differs according to the ECCO$_2$R types. Common complication that involves AV ECCO$_2$R are limb ischaemia, compartment syndrome, cannula thrombosis and bleeding during cannulation, while typical complications that occur following

from VV ECCO$_2$R procedure are cannula thrombosis, thrombosis of exchange membrane and pump malfunction (Baker et al., 2012).

As shown in Figure 2.8, the main component in ECCO$_2$R are the inflow cannula, a pump, a membrane oxygenator and an outflow cannula (Chung et al., 2014), and the most vital component is membrane oxygenator. Gas exchange occurs in the oxygenator, where the blood is exposed to the sweep gas (commonly O_2) which then oxygenates and removes CO_2 as illustrated in previous Figure 2.7. This process takes over the lung's function, thus the oxygenator is also known as artificial lung.

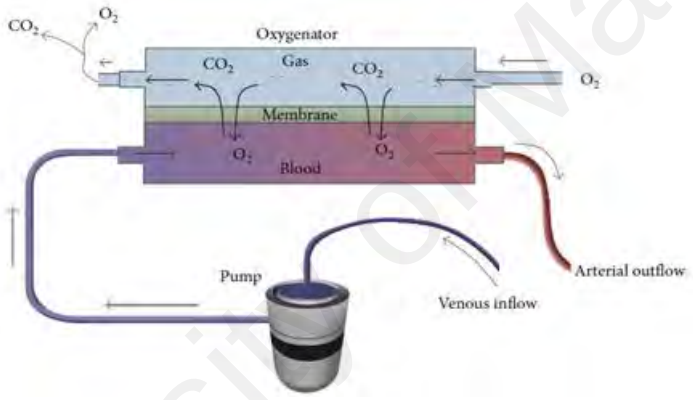

Figure 2.8: Blood circulation to oxygenator and gas exchange inside oxygenator (Chung et al., 2014).

In oxygenator, CO_2 removal occurs due to presence of diffusion gradient in blood and sweep gas. Sweep gas (either O_2 or normal room air) is circulated through hollow fibre, while blood is accelerating outside the fibre. Here, CO_2 concentration in blood is higher than CO_2 concentration in sweep gas. Thus, CO_2 in blood will diffuse across the membrane into sweep gas and the diffused CO_2 then is exhausted from the cartridge. The schematic diagram on basic membrane oxygenator principle is shown in Figure 2.9. In clinical practices, there are several types of commercial membrane oxygenator that are available, which are Quadrox, iLA membrane ventilator, Hilite, Affinity NT and much more.

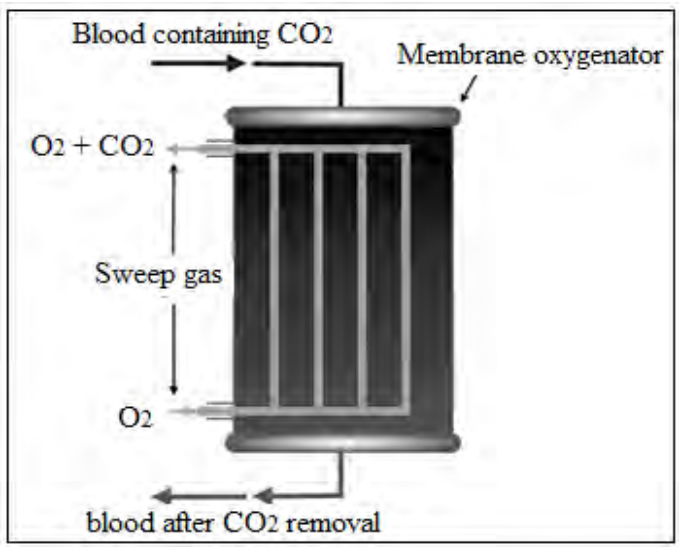

Figure 2.9: Diagram showing the basic principle of a membrane lung. Adapted from (Cove et al., 2012).

2.2.3. The clinical experience of ECCO$_2$R system

The application of ECCO$_2$R in treating respiratory failure had been widely used in the past. There are a few common types of ECCO$_2$R that are available in the market today, namely the Interventional lung assist (iLA), DECAP/ DECAPSMART system and Hemolung Respiratory Assist System. The iLA is an Arteriovenous (AV) ECCO$_2$R that do not comprise any pump system, while DECAP/DECAPSMART and Hemolung is a Veno-venous (VV) ECCO$_2$R, which consist of pump as a part of their circuit setup.

2.2.3.1. Interventional Lung Assist (iLA)

Interventional lung assist (iLA) by Novalung (Hechingen, Germany) is the most popular commercial AV ECCO$_2$R in the market today. The iLA is a low-gradient device that driven based on patients' cardiac output and do not requires external pump at all. Hence, adequate mean arterial blood pressure is compulsory and strictly cannot be applied on patients with low cardiac output or cardiogenic shock (Matheis, 2003). During its early introduction, iLA can only functions effectively (with favourable hemodynamic and ability to remove CO_2 as the

indicators) for 1-6 days, due to the rupture of its hydrophobic surface (Walles, 2007). This occurrence cause plasma leaking thus interfering the gas exchange and increase the risk of infections (Cove et al., 2012). To improve this limited lifetime issue, a new diffusion membrane that can resist plasma leakage was introduced in 2003. It is known as polymethylpentene (PMP) and acts as separation layer between blood and gas phase (Walles, 2007). The efficiency of PMP as fibre gas exchanger in both oxygen and CO_2 exchange was demonstrated by Toomasian et al. (2005). In iLA system, PMP fibres are stacked together into a complex configuration of hollow fibres, to ensure the maximum gas exchange. During gas exchange, ventilating gas (commonly O_2) is running inside these fibres, while blood flows through its exterior surface. In addition, PMP membrane surface that is in contact with blood is coated with heparin to enhance biocompatibility and non-thrombogenic properties. The typical placement of iLA setup during CO_2 removal was shown in Figure 2.10.

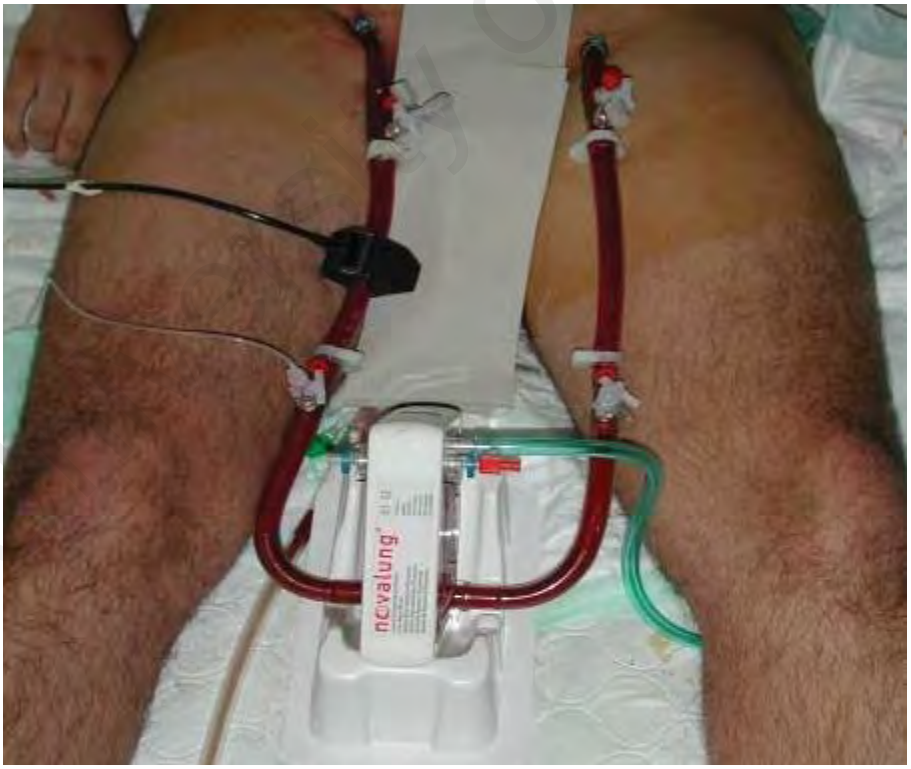

Figure 2.10: iLA placement during CO_2 removal procedure (Muller et al., 2009).

The iLA has been successfully used in several respiratory failure cases, such as Chronic Obstructive Pulmonary Disease (COPD), ARDS, asthma and also as a bridge to lung transplantation. Bein et al. (Bein et al., 2006) conducted a retrospective study to evaluate the effectiveness and incidence of complication of iLA, and the participants were 90 patients with ARDS which treated with iLA for 24 hours. Cannula walls used was extremely thin to minimize resistance to flow and to reduce complication risk (13-21 French for arterial and 19-21 French for venous, which the exact diameter was determined by cannulated vessel and required shunt flow). Surprisingly, 37 out of 90 patients involved survived with hospital treatment, and the non-survivors were 53 patients, which contributed to mortality rate of 58.8%. The study also reported that CO_2 removal rate after 2 hours of iLA initiation was 141 mL/min at iLA flow rate of 2.2 L/min. In fact, this procedure also suffered from some complications (24.4% patients involved), which majority of the patients experienced ischemia of a lower limb after arterial cannulation. However, by considering its low mortality rate, iLA was deemed for the successful in treating patients ARDS. The commencement of iLA among severe ARDS patients also reported by Muller et al. (2009), where pCO_2 of pronounced hypercapnia patients were significantly fell from 66.7 mmHg to 35.8 mmHg after 24 hours. In conjunction with pCO_2 reduction, blood pH also rose to 7.41, compared with pH 7.24 before iLA implantation.

In addition to ARDS, treatment of iLA also was implemented among the patients with acute life-threatening asthma. According to a case report of a 40 years old woman with known asthma that documented by Lobaz and Carey (2011), beneficial effect of iLA was shown immediately by that patient. On admission to the hospital, her blood pH was 7.32, pCO_2 4.45 kPa and partial pressure O_2 (pO_2) was 24.5 kPA. With this condition, she was treated with nebulised salbutamol and ipratropium, IV hydrocortisone, aminophylline infusion, magnesium sulphate boluses, coamoxiclav and clarithromycin, and admitted to the high dependency unit. Unfortunately, her condition was worsening with arterial blood gases recorded at pH 7.23,

pCO_2 7.9 kPa and pO_2 29.2 kPa. Then, this patient was treated with non-invasive ventilation (NIV) using a BIPAP hood, where she was poorly tolerated and lastly been transferred to intensive care unit (ICU). Since the attempt of NIV procedure on this patient was unsuccessful, ECMO was used in this case. Using ECMO, patient's condition was improved to 13.5 kPa, with pH 7.07 and pO_2 22 kPa. Since this device was never been used despite of patient's instable clinical state, ECMO procedure was cancelled and the patient was referred to the medical team for $ECCO_2R$ using iLA by Novalung. After initiation of iLA, its beneficial effects were seen immediately. CO_2 level was reduced to 6.4 kPA at iLA blood flow rate 1.5 L/min and the patient was heamodynamically more stable after 45 minutes. Full conventional medical therapy for bronchospasm was resumed with iLA and lung protective ventilation strategy for the next 4 days, until the improvement of lung was seen. The patients then were transferred to the ward from ICU on day 13 and approved for hospital discharge after 16 days. From this case report, in can be observed that iLA by Novalung capable to prevent patient deterioration and death, by allowing time for protective lung ventilation strategy until the effect of severe broncophasm to the patient was reversed. The advantage of pumpless $ECCO_2R$ technique of iLA in dealing with life-threatening asthma also was documented also by Elliot et al. (2007) in two case reports, which reporting the successfulness of iLA in preventing respiratory acidosis among asthma patients.

In 2012, a study reported the clinical study regarding feasibility, effectiveness and safety of partial $ECCO_2R$ by using iLA from Novalung among COPD patients (Kluge et al., 2012). 21 patients with acute hypercapnic respiratory failure (majority due to COPD) were treated by iLA, while 21 matched control patients were selected for conventional invasive mechanical ventilation since the patients were not responding to non-invasive ventilation. As the results, 90% of the patients that treated by iLA did not require intubation. Compared with matched

control group, this iLA group of patients also showed a shorted hospital length of stay with improved median pCO_2 level and pH within 24 hours. However, there were some limitations and side effects of iLA highlighted. To operate iLA effectively, cardiac index should be greater than 3 l/min.m^2 and mean arterial pressure should exceed 70 mmHg in order to allow for the circulatory tolerance of an artificial arterio-venous shunt of up to 25% of cardiac output. The other limitation is the arterial cannulation that can lead to vascular complication in the early period of iLA introduction. If large cannulas (17-19 French) were used, lower limb ischaemia from arterial cannulation were frequently occurred. In contrast, smaller arterial cannulas had reduced the complication percentage. Two major complications that are related to iLA also observed in this study, which both related to local bleeding. Instead of its complication, iLA was proven as a method to cope with case of patients with acute hypercapnic respiratory failure.

Due to its simplicity, ease of use and pumpless system, iLA was implanted as an alternative treatment option in two US soldier in Iraq with acute pulmonary failure, resulted from blast exposure and gunshot injury (Zimmermann et al., 2007). Both soldiers suffered from hypercapnia and iLA was chosen to be used in the Baghdad hospital, which lack of sophisticated medical device before they were transported to hospital in Germany for further treatment. After iLA implantation, oxygen percentage had significantly increased and CO_2 removal also improved. This successful suggested the feasibility of iLA in treating injured soldiers.

2.2.3.2. Low-flow veno-venous DECAP

Low-flow veno-venous DECAP (Hemodec, Italy) or the Decapsmart (Medica, Italy) was invented solely to remove CO_2 using decapneizator as its main component (Gramaticopolo et al., 2010). The Decapneizator acts as membrane oxygenator for CO_2 removal, which can be

implemented by itself or in conjunction with continuous renal replacement therapy (CRRT) for the patients with respiratory and renal failure. In a single use, the system is known as DECAP (Figure 2.11) and DECAPSMART in case of combination with CRRT (Figure 2.12). The association of membrane oxygenator with CRRT as a respiratory and renal support is an advantage of this commercial system as compared to iLA and Hemolung.

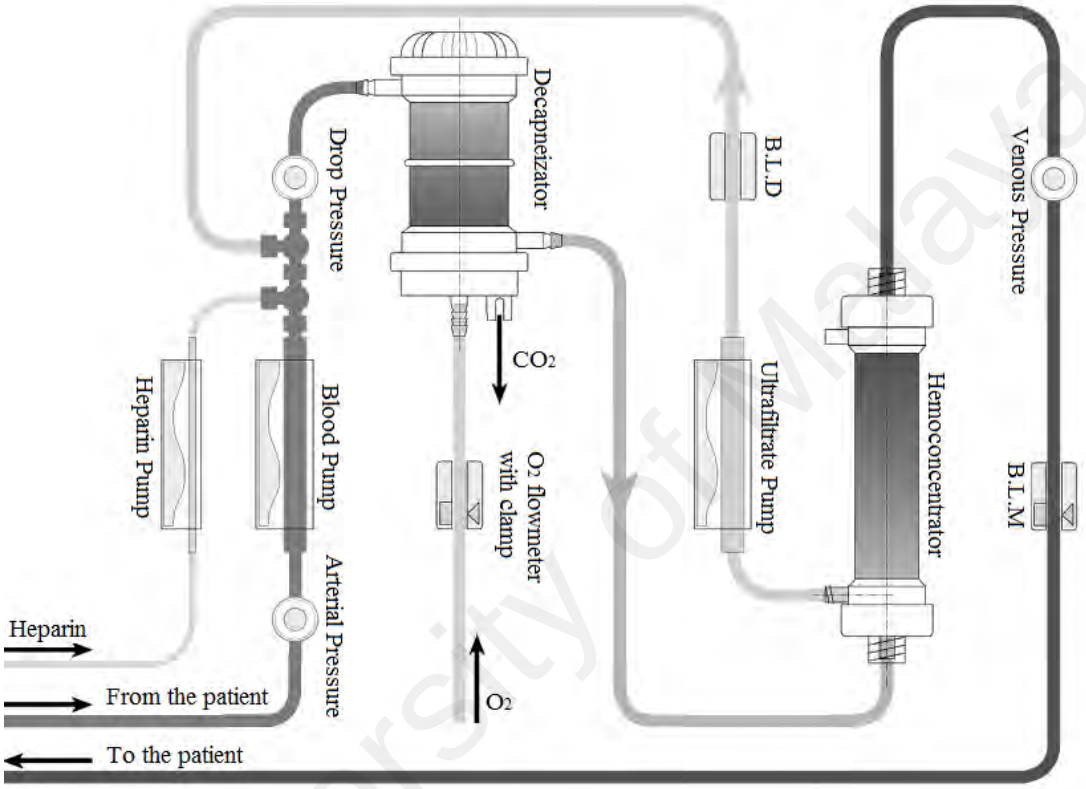

Figure 2.11: Circuit of low-flow veno-venous DECAP (Gramaticopolo et al., 2010)

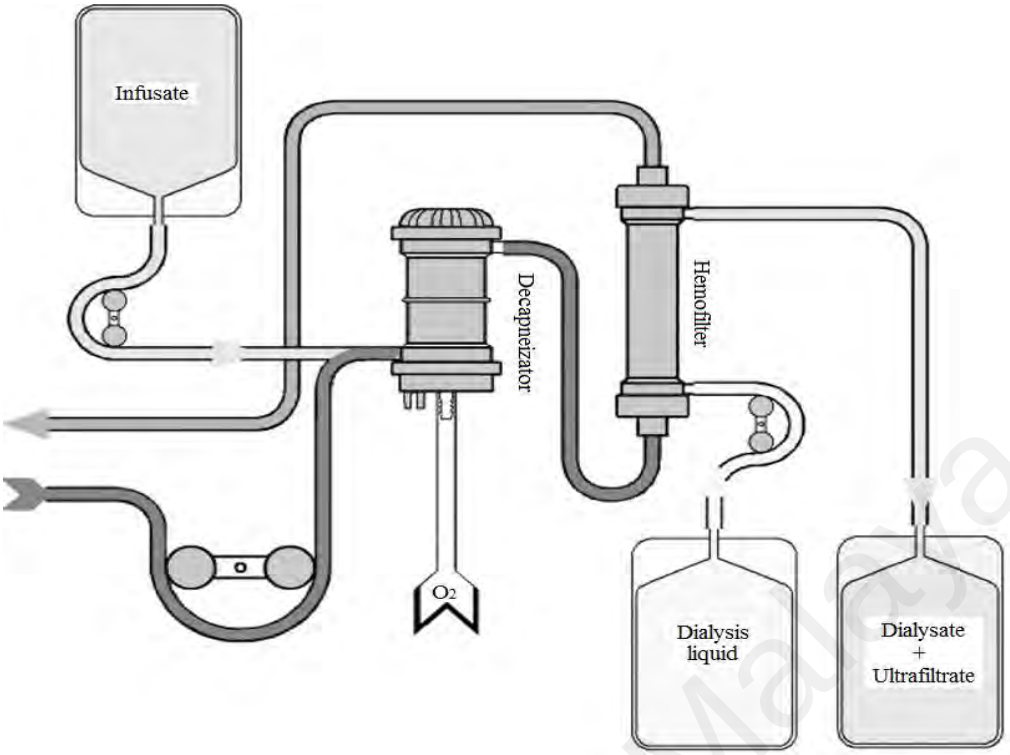

Figure 2.12: Low-flow veno-venous DECAP circuit in combination with CRRT circuit (DECAPSMART) (Gramaticopolo et al., 2010)

As shown in Figure 2.11, common DECAP/DECAPSMART circuit comprised of modified neonatal oxygenator that located in series with polysulfone hemofilter (1.35 m^2) and two roller pumps (the first roller pump to accelerate blood flow to the oxygenator ad hemofilter, while the second roller pump functions to recirculates the ultrafiltrate to the inflow of the oxygenator).

The application of DECAP/DECAPSMART in respiratory and renal failure is reported widely. Since DECAP can permit the achievement of low tidal volume (V_T), it was selected by Terragni et al. (2009) in treatment of 32 patients with ARDS. In this study, low V_T strategy was used on the patients with $V_T \leq 6$ ml/kg and plateau pressure $\leq$30 cm H_2O, according to ARDS Net Protocol. In case of hypercapnia, patients were subjected to bicarbonate infusion up to 20 mEq/h, while DECAP was initiated only if the pH remained $\leq$7.25. System used in this study was DECAP membrane lung and hemofilter that associated in series. No patient-related

complication occurred, while only 8 case of mechanical were observed. As the result, $V_T <$ 6ml/kg was effectively enhancing lung protection, whereas the selected $ECCO_2R$ technique had efficiently treated respiratory acidosis due to low V_T. The same system was implemented by Forster et al. (2013) in 10 ventilated critically ill patients ARDS and Acute Kidney Injury (AKI), before they came with the conclusion that CO_2 elimination via this system was safe and tolerable.

In 2010, Gramaticopolo and his colleague also advocated the efficiency of DECAP/DECAPSMART in their case report on a 41-year-old Caucasian man that suffered from multiorgan failure, including jaundice, acute kidney injury and respiratory failure (Gramaticopolo et al., 2010). At the beginning, ventilation strategy was employed to the patient. After 3 days, a moderate hypercapnic acidosis was present with high CO_2 value and unacceptably high ventilator pressure. After 12-hour cycle of treatment, renal functions had shown an improvement, tolerable value of protective ventilation was achieved and pH value increased up to pH 7.41. Eventually, this patient was deemed for hospital discharge after 2 weeks.

DECAP system consist of neonatal membrane lung was used (without association with CRRT) by Iacovazzi et al. (2012). In their case report, a 69-year-old man that previously submitted to left pneumonectomy and diagnosed a single right upper lung lobe lesion was considered to receive intraoperative apnea therapy. In this therapy, patient's oxygenation was preserved through apneic oxygenation with continuous positive air-way pressure (CPAP) of 5 cmH_2O and inspiratory oxygen fraction (FiO_2) of 1. At the same time, DECAP system was employed to prevent respiratory acidosis. The apnea period lasts for 13 minutes without any complication. The pCO_2 measurement was maintained in the range of 38.5-41.7 mmHg, while pH ranges between 7.36-7.40. Thus, this case report suggested that the association of CO_2 removal therapy

and apneic oxygenation was an effective solution to manage anesthesiological situation, which required moderate apnea periods.

2.2.3.3. Hemolung

Hemolung (Alung Technologies, USA) is designed using the same technique to renal dialysis, but in this device, oxygenator and centrifugal pump are fused together as one unit. The main component of Hemolung RAS system is a cartridge, controller assembly and double-lumen cathether. Cartridge contains a cylindrical bundle of siloxane and heparin-coated hollow fibre membrane (HFM). These siloxanes and HFM then are located around a spinning core, so that they can simultaneously accelerate blood flow (centrifugally) around the cartridge. At this time, sweep gas, which contains either air or oxygen is drawn by vacuum pump to produce negative pressure through fibre lumens. This allows CO_2 elimination from the blood into oxygen sweep gas (Wearden et al., 2012). The negative pressure of sweep gas is a safety feature that can prevent air-embolism in the event of membrane leakage. Figure 2.13 shows a typical Hemolung system.

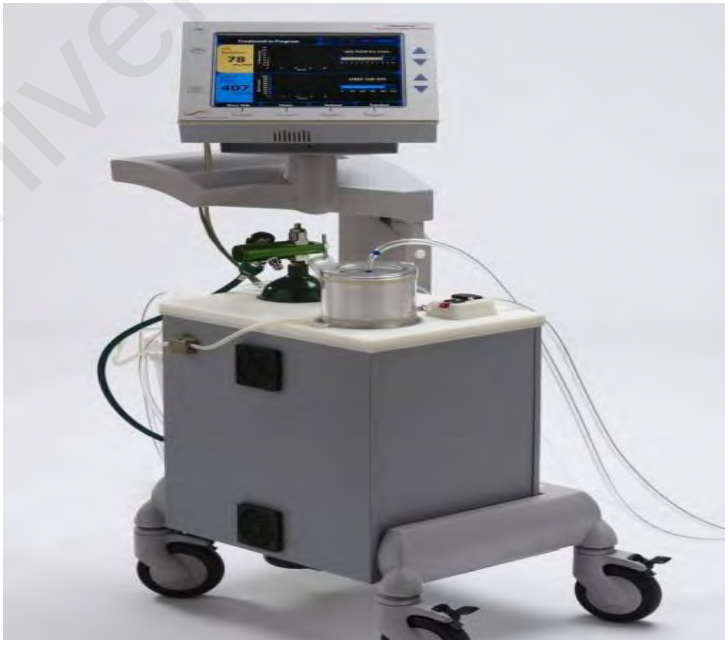

Figure 2.13: Hemolung system (Batchinsky et al., 2010)

The reliable performances of Hemolung $ECCO_2R$ were reported in many cases, such as in patients with COPD. Studies by Burki et al. (2013) on three groups of patients aged 21 to 80 year old with COPD and hypercapnic respiratory failure shown a significant decrease in pCO_2 in group 1 (patients that require intubation and invasive positive pressure ventilation) and group 2 (patients that require non-invasive positive pressure ventilation who had failed two weaning attempts) within 1 hour of implantation, from 78.9 mmHg to 65.9 mmHg, whereas pH increased to pH 7.34 from pH 7.28. In group 3 (patients who already on invasive mechanical ventilation) pCO_2 and pH also had decreased with constant ventilator setting, even the reading was not precisely accessed due to ventilator setting adjustments. In conjunction, mortality rate was reduced to 35% and none of these deaths could be attributed with $ECCO_2R$.

In a clinical summary provided by Bonin et al. (2013), a 50-year-old man severe COPD was failed in non-invasive ventilation attempt. Consequently, patient's pCO_2 increased up to 85 mmHg with pH less than 7.3. At this stage, intubation became crucially needs, but it cannot be adopted due to pneumothorax. Hence, $ECCO_2R$ therapy by Hemolung was considered. After the initiation of $ECCO_2R$, pCO_2 was in the range of 60 to 55 mmHg while pH was maintained between 7.34-7.40. This is another successful case on Hemolung reported, in addition to a case report by Cole et al. [65].

In addition to clinical trial on human, the reliability of Hemolung also been demonstrated to animals, such as sheeps (Wearden et al., 2012) and Yorkshire pigs (Batchinsky et al., 2010). Both studies recorded the safety and effective performance of Hemolung without any significant risk of adverse reactions. A consistence achievement on clinically relevant percentage of CO_2 removal by Hemolung $ECCO_2R$ device were proven and agreed in these studies.

The good performance of $ECCO_2R$ draws positive good attention for development approach in maximizing CO_2 removal rate. Investigations on the improvement of $ECCO_2R$ design are actively conducted in various aspects, such as blood acidification (Zanella et al., 2009), the designation of intravascular oxygenator (IVOX) (Mortensen, 1992) followed by its improvement on gas exchange performance (Federspiel et al., 1997; Mihelc et al., 2009; W. Tao et al., 1994), combination of membrane lung $ECCO_2R$ with ultrafiltration method (V. Scaravilli et al., 2014) and surface modification of hollow fibres membrane (Arazawa et al., 2015; Arazawa et al., 2012; Kaar et al., 2007; Kimmel et al., 2013). In this study, improvement work will be dedicated to the development of automatic control of membrane oxygenator in $ECCO_2R$, due to its bright potential to contribute significantly in this field.

2.3. Improvement strategy in $ECCO_2R$ for CO_2 removal purpose

There are various strategies from various disciplines that have been conducted in enhancing CO_2 removal in membrane oxygenator, such as using biocatalytic concept, regional electrodialysis and automated control approaches.

Firstly, in order to facilitate the removal of CO_2, the biocatalytic concept on the membrane oxygenators is fully utilized. In commercial use, duration for $ECCO_2R$ implementation is too long, ranged from 2-30 days. This may cause $ECCO_2R$-related complications and discomfort to the patients. In some case, membrane gas exchanger required changing after several hours, as occurred in case reported by Elliot (Elliot et al., 2007). To overcome this constraint, a new initiation was introduced by applying biocatalytic concept in $ECCO_2R$ design. This novel approach used immobilized carbonic anhydrase (CA) to facilitate the conversion of bicarbonate to CO_2 in hollow fibre membrane, which can shorten the duration of $ECCO_2R$ while improving CO_2 transfer efficiency (Oh et al., 2010). Idea of facilitated transport of CO_2 across membrane that was grafted with CA enzyme was initially described by Broun and co-worker in 1970

(Broun, Selegny, Minh, & Thomas, 1970). This idea was supported by strong evidences that explained the ability of CA in catalysing hydration of CO_2 (Berg et al., 2002; Chegwidden et al., 2013; Geers & Gros, 2000; Gilmour, 2010; Rhoades & Bell, 2009; Supuran & De Simone, 2015; Uchikawa & Zeebe, 2012), where:

$$CO_2 + H_2O \xleftrightarrow{CA} HCO_3^- + H^+ \quad [2.3]$$

The two species in equation [2.3] is interconvertible. CA can be the best candidate for $ECCO_2R$ improvement due to high content of bicarbonate ion that exists in blood transportation. In human blood, CO_2 presents in three different forms, which are as dissolved CO_2, bound as bicarbonate and bound as carbamate (Geers & Gros, 2000). According to Arthurs and Sudhakar (Arthurs & Sudhakar, 2005), in arterial blood, partial pressure of CO_2 that bounded as bicarbonate is 90%, while dissolved CO_2 and carbamate are only 5% each. On the other hand, 60% of CO_2 is transported as bicarbonate in venous blood, with 30% of carbamate form and 10% of dissolved CO_2. Based on equation [2.3], due to high portion of bicarbonate ion present in blood, it can be a great opportunity to use CA in accelerating the conversion of bicarbonate ion to CO_2 directly at the outer membrane surface. Consequently, more CO_2 can be eliminated from the blood to sweep gas (commonly oxygen) that is flow inside the membrane by passive diffusion. This will increase the efficiency of CO_2 removal in $ECCO_2R$ system.

There are several ways to manipulate CA enzyme for biocatalyzing approach, such as contained liquid membrane (Bao et al., 2004; Carroll et al., 1992; Cowan et al. 2003; Trachtenberg et al., 2009) and enzyme immobilization (Sahoo et al. 2012; Vinoba, et al., 2012; Zhang et al. 2010). However, for extracorporeal CO_2 removal purpose, research was focused on CA immobilization in facilitating $ECCO_2R$ operation (Arazawa et al., 2015; Arazawa et al., 2012; Kaar et al., 2007; Kimmel et al., 2013; Salley et al., 1990). Enzyme immobilization is

more preferable in medical use since the enzyme can be reused, thus lengthens the enzyme's lifespan (Yong et al., 2015). Immobilization also results in thermal stability (Kanbar & Ozdemir, 2010) and high hemocompatibility properties (Oh et al., 2010), which are the important factors in dealing with human blood.

In 1990, Salley et al. (Salley et al., 1990) proposed a method of CA immobilization by encapsulating this enzyme in 5-20 μm cellulose nitrate microcapsules. These microcapsules then were immobilized onto 0.1 m^2 silicon rubber membrane that acts as an interface for CO_2 diffusion from blood to the air (sweep gas). As a result, 60% higher CO_2 removal rate (4.14 mL/min) was reported for membrane that was treated with CA, compared with 2.58 mL/min removal rate in case of untreated membrane.

As an alternative approach, Kaar et al. (Kaar et al., 2007) develop bioactive hollow fibre membrane using covalent immobilization of CA enzyme. In this work, hollow fibre membrane was treated with plasma modification before been activated by cyanogen bromide (CNBr). The CNBr activated hollow fibre membranes then were incubated with CA in sodium carbonate buffer for immobilization. Consequently, bioactive hollow fibre membrane capable to remove CO_2 from sodium bicarbonate solution more effective compared to unmodified membrane, where CA addition to the bioactive hollow fibre membrane contributed to the highest performance with approximately 9.5 ml/min/m^2 removal rate. As an extended work, Oh et al. (Oh et al., 2010) then investigated the effect of CA immobilization work by Kaar et al. (Kaar et al., 2007) and advocated its successfulness in enhancing hamocompatibity and gas exchange rate.

Research on CA immobilization for $ECCO_2R$ improvement also carried out by Arazawa et al. (Arazawa et al., 2012), where the biocatalyst membrane was prepared in a similar way with Kaar et al. (Kaar et al., 2007). Those membranes then were inserted into gas exchange module

to evaluate its performance in removing CO_2 from blood. By comparing the removal rate, gas exchange module with bioactive hollow fibre membrane outshines the unmodified module with 108 mL/min/m^2 removal rate, rather than 79 mL/min/m^2 as in unmodified module. Kimmel et al. (Kimmel et al., 2013) then explored the use of glutaraldehyde activated chitosan for CA immobilization purpose. They also reported the improvement of CO_2 removal efficiency and optimum hemocompatibility properties of the membrane surface.

In the most recent study, Arazawa and his colleague (Arazawa et al., 2015) extended their work by mixing dilute sulphur dioxide in oxygen sweep gas in order to create the acidic environment within the diffusional boundary layer adjacent to the hollow fibre membrane surface, which was previously immobilized by CA. This work was inspired by blood acidification study that reported by Zanella et al. (Zanella et al., 2009), and concluded that dilute acidic sweep gas has great potential in increasing CO_2 removal rate when used in combination with biocatalytic hollow fibre membrane.

The second strategy on $ECCO_2R$ modification is to utilise the R-ED technique. R-ED is a novel approach of regional blood acidification that apply electrodialysis cell in $ECCO_2R$ setup in order to acidify the blood without any exogenous acid (Zanella et al., 2015). Basically, it is a combination of hemofilter, membrane lung and electrodialysis unit. In electrodialysis unit, two hemodifiltrate were formed from electrolysis process (since electrodialysis process shifted chloride ion between hemofiltrate flows), which is acidic hemofiltrate (rich in chloride) and alkaline hemofiltrate (poor in chloride) (Zanella et al., 2015). Acidic hemofiltrate functions to acidify blood that entering membrane lung, thus enhancing CO_2 removal in this component. The significance effects of regional extracorporeal blood acidification to $ECCO_2R$ performance was previously documented in various research reports (Zanella et al., 2014; Zanella et al., 2014; Zanella et al., 2009). On the other hand, alkaline hemofiltrate was re-infused into

extracorporeal circuit, which functions to restore the blood's sodium chloride content and sustain the electrolyte equilibrium (Zanella et al., 2015).

The first successful in-vivo application of electrodialysis was reported by Zanella et al. (Zanella et al., 2015). By using R-ED technique, this investigation group managed to remove CO_2 from blood of healthy swine with rate of 112 ± 6 mL/min, whilst only 64.5 ± 5 mL/min CO_2 removal rate was obtained using the conventional $ECCO_2R$ system. As for adverse effect, no hemolysis presence was detected and pH of mixed venous blood was also maintained within the normal physiological range.

In addition to in-vivo study, Zanella et al. (Zanella et al., 2016) also performed an in-vitro study for $ECCO_2R$ by R-ED technique, which uses polyelectrolytic carbonated solution as blood substitute. In this in-vitro experiment, focus was given to the effect of raising the electrodialysis current on the amount of CO_2 sequestrated by membrane lung (VCO_2), concentration of sodium (Na^+) and potassium (K^+), as well of calcium concentration on hemofiltrate circuit. Rising of electrodialysis current through electrodialysis cell increased VCO_2 up to 238%, while significant increment of chloride concentration was observed as electrodialysis current increased from 0 to 8A. In contrast, no significant changes were recorded for Na^+ and K^+ concentrations for the same parameter.

The successful outcome of R-ED study could be the benchmark for the other researchers to explore more on this novel technique. In addition, the possibility of fusion between CA immobilized membrane lung and R-ED technique also could be investigated for further improvement of $ECCO_2R$ technology.

Finally, the last improvement strategy in CO_2 removal is to be discussed here, which is the selected approach in this study. The automatic control approach for CO_2 removal rate in

membrane oxygenator is proposed. The investigation of automatic control for membrane oxygenator was not widely conducted. In fact, currently, there is no investigation reported for auto-control of membrane oxygenator in $ECCO_2R$ system. To deal with this limited source of literature, a review on the research works that involve automatic control in another ECLS strategy such as CPB and ECMO was performed and described in this section. Since these two devices (CPB and ECMO) also employed membrane oxygenator in their circuit, the procedure that reported for both devices can be inspired to be used in current $ECCO_2R$ system developed in this study.

2.4. Automatic control of gas transfer in membrane oxygenator

In this study, an auto-tuning control system will be implemented in controlling CO_2 gas transfer in membrane oxygenator. Sweep gas flow rate will be controlled by three types of control strategies, namely PID (proportional–integral–derivative), FLC (fuzzy logic controller) and the fusion of PID and FLC, which will be addressed in this study as Fuzzy-PID. For control input values, the measurement of CO_2 partial pressure (pCO_21 and pCO_22) at the inlet and outlet of oxygenator are used, while output for the controllers is the mass flow controller to control the flow rate of oxygen that entering the oxygenator.

The implementation of automated control in ECLS is numerous. In 2004, Hexamer and his colleague (Hexamer, Misgeld, Prenger-Berninghoff, Schutt, et al., 2004) reported their work on automatic control of blood gas parameter in CPB. Prior to the simulation of control system, they developed a process model for gas transfer by taking into account the chemical binding of O_2 and CO_2 within the blood. After process simulation in MATLAB/SIMULINK environment, PI-controller was implemented to control pO_2 and pCO_2 in the blood that leave the oxygenator. Even though a limited performance of this controller was obtained, this controller showed some robustness with regard to process uncertainty of this highly non-linear model.

As an improvement strategy to their previous work (Hexamer et al., 2004), Misgeld et al. (2005) then added another two controllers, namely H∞ and General Predictive Controller (GPC) in their real time using dSPACE environment. PI and H∞ controller was robustly tuned for automatic control of blood flow during extracorporeal circulation, while GPC showed less compensation to non-linearity of the developed model.

Again, for their later work that was published in 2010, Misgeld, Werner and Hexamer (Misgeld et al., 2010) improved their automatic control strategy for in-vitro evaluation. They used gas blender that made up of electronic valve, so that PI controller that acts as the automatic controller generated command signal to this gas blender to adjust oxygen fraction (to control pO_2) and total gas flowrate (to control pCO_2). The disturbance also was introduced to the process plant by changing the arterial blood flow, which means the change in arterial partial blood gas pressure. The controllers showed robust stability and good performance in maintaining the setpoint and to reject the applied disturbance.

Apart of the implementation of auto-control membrane oxygenator in CPB, the development of self-regulated system for membrane oxygenator also was performed to membrane oxygenator for ECMO system. Dhinakaran and Lincon (2014) studied and developed an auto tuning control for ECMO by simultaneously control both O_2 and CO_2 in arterial blood. To control partial pressure of O_2, O_2 fraction of nitrogen was used as control input values, while gas flow to the oxygenator was selected to control partial pressure of CO_2. In addition, blood gas analyser and gas blender play a role as feedback control. As the result, these authors had successfully recognized step response of FiO_2 and the ratio of the input setpoint to the output flow of O_2 partial pressure. In conjunction to their previous work, the same authors (Dhinakaran & Lincon) extended their study by testing PID controller in simulation, and

proved that this PID controller was able to tolerate with the uncertainty of both O_2 and CO_2 gas exchange. It also had good performance by showing the robust stability.

Kopp et al. (Kopp et al., 2016) then described a cascaded control system, which referred as SmartECLA, which maintained both SpO_2 and pCO_2 in six female pigs. To demonstrate the reliable function and efficacy of this automatically controlled SmartECLA, PI controller with gain scheduling was selected as control approach to set sweep gas flow and O_2 fraction of the electronic gas mixer. They concluded the efficiency of their method, where 98% of SpO_2 readings were recorded at least 90%, while pCO_2 value that was measured by blood gas analyser was between 30.9 to 42.7 mmHg.

Unlike the other study that used measurement of pO_2 and pCO_2 as input of the controller, Brendle et al. (Brendle et al., 2017) came with different approach of in-vivo evaluation, which was the application of gas transfer rate to control O_2 and CO_2 on ECMO therapy. The proposed system introduced 2 Single-In-Single-Out (SISO) H∞ controller, which set O_2 gas transfer rate using O_2 fraction of sweep gas, and CO_2 gas transfer rate using sweep gas flow in a fully anesthetized pig. These authors proved the feasibility and sufficient response time for their method of study.

In addition to PI, GPC, H∞ and PID controller, there are many more controllers that used to control gas transfer in ECLS, such as FLC. Conway et al. (Conway et al., 2019) in the latest reported study that related to this topic implemented FLC system to control O_2 and pCO_2 gas exchange in membrane oxygenator in the development of their auto-regulatory ECMO control system. This was an in-vivo study on 4 healthy hybrid sheep (ovine). This research team controlled pO_2 by appropriately changed the blood flow and pCO_2 using sweep gas flow, which comprised of 100% O_2. The results revealed that FLC controller was successfully control the

oxygenation with 90% and above SpO_2 reading, while 66.7% of pCO_2 measurements were around the setpoint (40 mmHg), with average error of 1.10 mmHg.

The outshine performance of FLC in ECLS was advocated in various studies (G. Hatzakis et al., 2001; Hatzakis & Davis, 2002; Nemoto et al., 1999). This indicate its high potential to be employed to achieve the goal of in this recent study, due to its natural representation of the subjective human notion in medical decision making (Nemoto et al., 1999).

To this date, there are no study reported yet on the application of Fuzzy-PID as the controller that mainly focus on CO_2 removal control strategy in membrane oxygenator. This is due to the scope of this study, which is to implement this control strategy for $ECCO_2R$ system. $ECCO_2R$ system is typically used when the primary purpose of the operator is to remove CO_2 with little or no expectation in providing significant amount of extracorporeal oxygenation (Brodie, 2018), unlike the common oxygenation control strategy for the application in ECMO system that mainly focus on O_2 control, which can be found redundantly in the literatures (Brendle et al., 2017; Hexamer et al., 2004; Kopp et al., 2016; Misgeld et al., 2012; Misgeld et al., 2010; Walter et al., 2009b; Walter et al., 2010b). The execution of experimental work in this study also improved from the previous study, such as the use of mass flow controller to manipulate sweep gas flow rate and the use of NI USB 6009 in data acquisition.

All of these are the elements of novelty of this study, which may provide the new reference to the other researchers that sharing the same interest, as its significant contribution to this field of study.

2.5. Factor determinant of CO_2 removal in membrane oxygenator

The relationship of CO_2 exchange with sweep gas flow rate in membrane oxygenator was described by Duncan (2001) and also by Chung et al. (2014). These authors concluded that

CO_2 elimination in membrane oxygenator is dependent on sweep gas rate, while O_2 uptake is influenced by fraction of oxygen in sweep gas rate and blood flow rate. This theory also was proven by numerical simulation that been conducted by Turri and Yanagihara (2011a).

For experimental evidence of this relationship, Federspiel and Hattler (1996) performed an investigation that a real test using commercial oxygenator and proved that sweep gas flow rate had strong relationship with CO_2 gas exchange process. To validate this finding, Hout et al. (2000a) used two commercial blood oxygenators in an in-vitro test loop system and concluded that CO_2 exchange is highly dependent on sweep gas flow rate. This result can be seen in Figure 2.14.

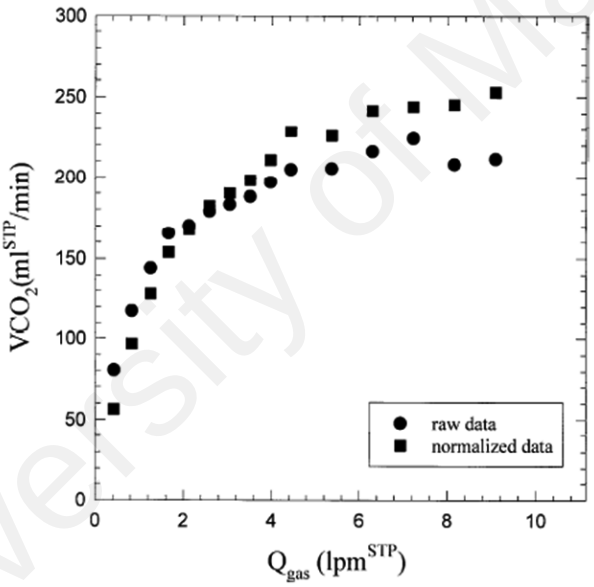

Figure 2.14: CO_2 exchange rate (VCO_2) as a function of the sweep gas flow rate (Q_{gas}) (Hout et al., 2000a).

Due to this theory, Richard et al. (2014) and Extracorporeal Life Support Organization (ELSO) (2013) suggested a guideline during implementing membrane oxygenator in ECLS strategy, which sweep gas rate should be carefully adjusted in order to give a partial pressure of pCO_2 between 30-40 mm Hg.

In the different approach, Sun et al. (Sun et al., 2018) conducted a single pass in-vitro bench model test using fresh-heparinized slaughterhouse blood to evaluate the ability of CO_2 removal in 4 different commercial membrane oxygenators (Terumo Capiox RX 05, Marquet Quadrox-iD Padiatric, Medos Hilite 2400 and Novalung iLA). They concluded that amount of CO_2 removed at any blood flow is dependent on the CO_2 inlet and sweep gas flow. Since the approach of these authors was quite similar with the one conducted in this study (almost similar in terms of in-vitro bench model, same bovine blood sample, same membrane oxygenator), these findings strengthen the hypothesis of this study, which sweep gas flow rate is major determinant of CO_2 removal.

This strong relationship shows how crucial the adjustment of sweep gas flow rate in membrane oxygenator during $ECCO_2R$ operation is, which support the idea of implementing an automated sweep gas flow rate adjustment using feedback control system. Thus, the desired and optimal pCO_2 for an $ECCO_2R$ system could be achieved. Through this improvement work, it is hoped that the human error due to extreme workload of the perfusionist can be reduced and $ECCO_2R$ system can remove CO_2 efficiently from blood by utilising an automatic sweep gas flow rate control.

2.6. Use of Mathematical Model to predict gas transfer rates in membrane oxygenator and experimental value

In order to develop a membrane oxygenator, the first step is to understand the gas exchange process that occurs in the membrane oxygenator during extracorporeal life support. Hence, construction of a mathematical model that can simulate the gas exchange process seems suited this particular purpose.

Mathematical models have been widely implemented in biomedical engineering field to provide an explicit framework for understanding a biological system. In context of membrane oxygenator, mathematical model was used to explain O_2 and CO_2 diffusion in membrane oxygenator, since it involved blood. Blood can be classified as a shear thinning non-Newtonian fluid, since it shows both viscous and elastic properties (Taskin et al. 2010). When these unique properties of blood were understood, it is much easier for a researcher to determine mass transfer coefficient for a mathematical model in order to theoretically predict O_2 and CO_2 transfer in an oxygenator. This prediction then can be used for optimizing the final design for the best membrane oxygenator system. Using computer-assisted method by means of process simulation, cost for trial-and-error manufacturing and testing for multiple produced prototype design can be minimized (Vaslef et al., 1994).

The theoretical idea of O_2 and CO_2 diffusion in membrane oxygenator was previously analysed and experimentally determined by Weissman and Mockros (1967; 1969) by considering the reaction between oxygen and hemoglobin. Analysis of O_2 transfer rate was calculated and also the improvement in O_2 transfer rate for different configuration of oxygenator. Based on the analysis, it was concluded that tubular oxygenator is practical for this purpose.

In agreement to Weissman and Mockros (1969), Mockros and Leonard (1985) extended their study for a compact cross-flow tubular oxygenators to determine partial pressure of O_2 in both their prediction oxygenation performance and their experimental measurement. By incorporating oxygen-haemoglobin reaction, which exists in the blood, the governing differential equation for the O_2 partial pressure elevation in blood, with respect to the distance along the oxygenator is as follows:

$$\frac{dP}{dx} = a\ \frac{P_b - P}{[1+\lambda\,(P)]^{2/3}} \qquad [2.4]$$

In which,

$$a = \left(\frac{4}{p}\left(\frac{(1-p)}{d}\right)^{(1+m)}\left(\frac{A_f \eta}{Q\rho}\right)^{m}\frac{\phi}{(\upsilon/D)^{2/3}}\right) \quad [2.5]$$

In equations [2.4] and [2.5], P is the partial pressure of O_2 in blood, x is the distance of the oxygenator from inlet to the outlet, P_b is the partial pressure of O_2 on gas side, p is the porosity of the fibre unit, d is the external diameter of the tube, Q is the blood flow rate, ρ is the density of the blood, m and φ are constants that depend upon the porosity and tube arrangement, υ is the kinematic viscosity of the blood, D is the diffusivity of O_2 in blood, A_f is the gross frontal area of the tube stack and η is the absolute viscosity of blood. From equation [2.4], λ is proportional to the slope of oxyhemoglobin dissociation curve. Thus, using Hill's equation to describe the curve, $\lambda\ (P)$ can be determined as:

$$\lambda\ (P) = \frac{1.34}{k}\ C_{Hb}\ \frac{n}{P_{50}}\left(\frac{P}{P_{50}}\right)^{n-1}\frac{1}{[1+(P/P_{50})^{n}]^2} \quad [2.6]$$

Where, C_{Hb} is haemoglobin concentration, k is the O_2 solubility in whole blood, n and P_{50} is the Hill equation parameters, which n is differs based on blood species (2.85 for bovine blood, 2.7 for human blood), while P_{50} depends on pH and temperature of the blood.

For the experimental measurement, blood oxygenator namely '*Miniprime'* was employed, which consist of a bundle of micro porous polypropylene that wound around a core. The results reported proved that the theoretical performance that been predicted by the above model was quite similar with the experimental values by blood oxygenator in terms of inlet and outlet saturation values. These researchers also suggested that the most efficient design for artificial lungs is in the cross-flow configuration. The equation that derived from this study also becomes the reference for the other researchers (Svitek & Federspiel, 2008; Vaslef et al., 1994) in their investigations.

Inspired by the hallmark work by Mockros and Leonard (1985), Vaslef et. al (1994) developed their own mathematical model to predict O_2 transfer too, but in an advanced method. In this study, some constants (α and β) in equation [2.7] were pre-determined using water test, so that the constant values then were used to predict the O_2 exchange rate. This group of researchers came out with a first order ordinary differential equation (ODE), which:

$$\frac{dP}{dx} = \frac{4\alpha}{\rho}\left(\frac{1-\rho}{d}\right)^{2-\beta}\left(\frac{A_f v}{Q_b}\right)^{1-\beta}\left(\frac{D}{v}\right)^{2/3}\frac{(P_b - P)}{[1+\lambda(P)]^{2/3}} \quad [2.7]$$

From equation [2.7], *dP/dx* is the gradient of O_2 partial pressure at location *x* along the blood path, *ρ* is oxygenator porosity, *d* is the outer diameter of individual fibre, P_b is partial pressure, A_f is gross fontal area of blood path, *v* is the kinematic viscosity of blood and Q_b is blood flow rate. *D*, *v* and *λ(P)* are blood properties, while *α, β* are the constant for oxygenator properties that will be found in the water test. In this test, water was used in their in-vitro experiment setup just to find the α and β constant, while during real experiment, bovine blood was used.

Once the constant values *α* and *β* are known, equation [2.7] was solved to predict the O_2 transfer rate of bovine blood. Next, an experiment for O_2 exchange was conducted using three commercial HFM oxygenators, namely Sarns Membrane Oxygenator, Sarns Turbo Oxygenator and Bentley Univox, which each of them comprised of different geometries. This experimental result was compared with the predicted O_2 transfer rate calculated from equation [2.7]. The observation proved that the predicted O_2 transfer rate was closed to measured values.

Analogous to Mockros model (1985), Svitek and Federspiel (2008) developed a mathematical model that able to predict CO_2 removal exchange rate in HFM oxygenator. This study was quite differed from the previous work, where CO_2 was considered, instead of O_2 as in the

previous works. Their works began with the construction of concentration profile for both CO_2 and O_2 with the fibre bundle. The equation of first order ODE that derived by these authors (Svitek & Federspiel) for the change of gas partial pressure as the function of distance into the fibre bundle is:

$$\frac{dP}{dr} = \frac{2\pi k a_v L}{Q\lambda} \ \Delta P \qquad [2.8]$$

Where P is partial pressure, a_v is the surface area per volume of fibre bundle, L is the bundle thickness, Q is the flowrate of blood through the fibre bundle, r is the radial coordinate. In equation [2.8], λ is an effective solubility that incorporate both the dissolved gas and both are chemically bound, which:

$$\lambda_{CO2} = \frac{\partial C_{CO2}}{\partial\, CO2} = qt\, P_{co2}^{t-1} \qquad [2.9]$$

$$\lambda_{O2} = \alpha_{O2} + C_T \frac{dS_{O2}}{dP_{O2}} \qquad [2.10]$$

In equation [2.9] and [2.10], constants q and t represent regression parameter with values of 0.128 and 0.369, respectively. α_{O2} then stands for solubility of oxygen in blood, C_T is the maximum capacity of bound O_2 in blood, by assuming for 100% haemoglobin saturation (S_{O2}).

In addition, the mass transfer coefficient which is denoted by letter '*k*' in equation [2.8] also was derived from an analogous heat transfer correlation for flow perpendicular to a bundle of tubes, and the final mass transfer coefficient for both CO_2 and O_2 are:

$$k_{CO2} = a\alpha_{CO2} d_h^{b-1} \left(\frac{Q}{2\pi r L}\right)^b \left(D_{CO2} + \frac{D_{HCO3}}{\alpha_{CO2}}\right)^{2/3} \overline{\lambda CO_2} \left(1 + \frac{1}{\alpha_{CO2}} \overline{\lambda CO_2}\right)^{1/3} v^{1/3-b} \qquad [2.11]$$

$$k_{O2} = a\alpha_{O2} d_h^{b-1} \left(\frac{Q}{2\pi r L}\right)^b D_{O2}^{2/3} \left(1 + \frac{C_T}{\alpha_{O2}}\right)^{1/3} v^{1/3-b} \qquad [2.12]$$

In both equations, a and b are the coefficients that depend on the geometry of the fibre bundle, which has been experimentally determined in the water test, d_h is the hydraulic diameter characteristic of the fibre bed packing, $\overline{\lambda CO_2}$ is the constant slope of the CO_2 dissociation curve,

D_{CO2} is the diffusivity of CO_2 in blood, D_{HCO3} is the diffusivity of HCO_3 in blood and v is the kinematic viscosity in water.

The concentration profile in equation [2.8] then was used to determine total gas exchange for blood oxygenator, $\dot{V}$ by substituting it to the equation:

$$\dot{V} = Q_b \Delta C \qquad [2.13]$$

In equation [2.13], Q_b is the blood flow rate, while ΔC is the concentration change of O_2 or CO_2 between the inlet and outlet of the membrane oxygenator.

As the experimental setup, an experimental module of membrane oxygenator was fabricated in order to compare the theoretical prediction of CO_2 from previously constructed mathematical modelling (as in equation [2.8] until [2.13]) with the experimental measurement that obtained from their self-fabricated membrane oxygenator.

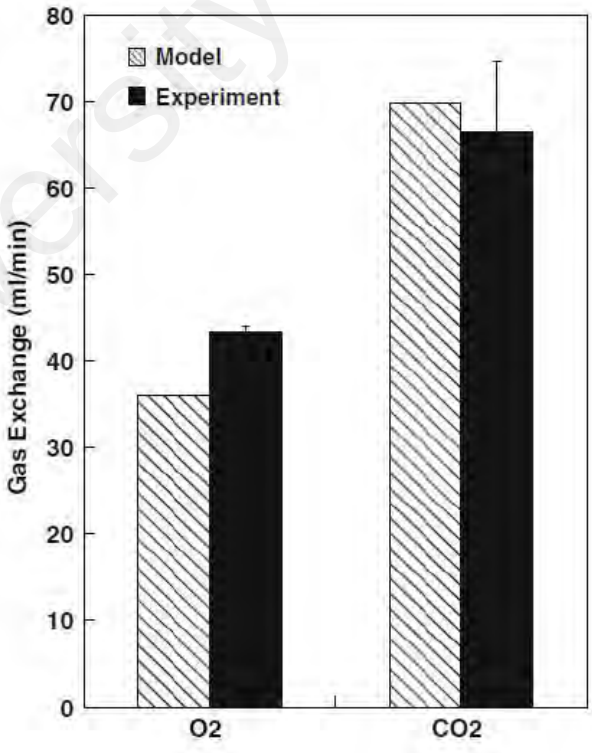

Figure 2.15: Comparison of experimental (filled bars) and predicted (dashed bars) O_2 and CO_2 transfer in oxygenator module (Svitek & Federspiel, 2008).

Based on the results reported by these authors (Svitek & Federspiel), it was clearly shown in Figure 2.15 that the difference between predicted CO_2 exchange rates (using mathematical model) and measured experimental data did not much, which varies in the range of 6% to 9% accordingly to the blood flow rate. This observation thus validates the mathematical model that was developed in the reported study.

Mathematical modelling also could be used to determine the best design for membrane oxygenator. For example, Matsuda and Sakai (2000) investigated the effect of number of tied hollow fibre on blood flow in terms of friction factor and mass transfer coefficient. They found an inverse proportional relationship between numbers of tied hollow fibre on O_2 transfer rate, due to effectiveness of blood contact to the membrane. Relationship between Sherwood number and Reynolds number for different numbers of tied hollow fibre then proved that single hollow fibre is the most effective design for optimum O_2 transfer rate. An optimum structure parameter for membrane oxygenator was also been figured out in this study.

Tabesh et al. (2012) then used a theoretical model to evaluate the design of HFM oxygenator in terms of geometric data, configuration properties and design specification for 6 commercial oxygenators. Vaslef et al. (1994) also used the computer method to validate their prototype device of implantable artificial lung in order to reduce the cost for trial-and-error manufacturing. The same method also been implemented by Hormes et al. (2011) who employed Computational Fluid Dynamic (CFD) model to predict O_2 and CO_2 within HFM oxygenator. Using the commercial software Ansys CFX 11 (Ansys Inc., USA), these authors developed a numerical model and compared the simulation with the experiment data. It is reported that the predicted mass flow rate for CFD simulation was closely related with the experimental data.

As an advanced works in numeric analysis and designing of membrane oxygenator, Turri and Yanagihara (Turri & Yanagihara, 2011a) developed a two-dimensional computer-assisted numeric simulator, which takes account for blood buffering capacity. The functions of this numeric simulator were to predict O_2 and CO_2 mass exchange in HFM, study the effect of blood base excess and also the effect of sweep gas flow rate to gas mass exchange. In addition to their successful in predicting O_2 and CO_2 mass exchange as compared with the experimental value, the researchers also concluded there was no effect of blood base excess on CO_2 mass exchange rate. For the effect of sweep gas flowrate, it was reported that only CO_2 exchange rate was affected by the sweep gas flow rate, whilst O_2 exchange rate shows no significant increasing as the sweep gas flow rate increased. This observation was agreed with the theory by Chung et al. (2014), where the CO_2 removal in an oxygenator is depends on sweep gas flow rate, while oxygen intake is affected by fraction of delivered oxygen and blood flow rate.

2.7. Sensor for pCO_2 measurement,

In this study, two flow-through pCO_2 sensors, Model GS-136-COFT from Lazar Research Laboratories, United States of America were used for pCO_2 measurement. This pCO_2 sensor are a complete potentiometric cell that contains two elements, which are silver/silver chloride (Ag/AgCl) reference and a pH measurement element. Both elements are cased within a thermoplastic body, with the chloride ion-containing electrolyte, and are isolated from the sample by a PTFE membrane. The parts of this sensor are depicted in Figure 2.16, which the figure is taken from its user manual.

During measurement, CO_2 in the sample solution will diffuse through the PTFE membrane, and dissolves further into the fill solution found between the membrane and internal pH membrane. Here, the CO_2 is converted to bicarbonate and hydrogen ions. The pH will change

proportionally with the concentration of dissolved CO_2 gas in the sample solution. This diffusion of CO_2 gas then continues until an equal partial pressure of CO_2 is achieved between the sample and thin film.

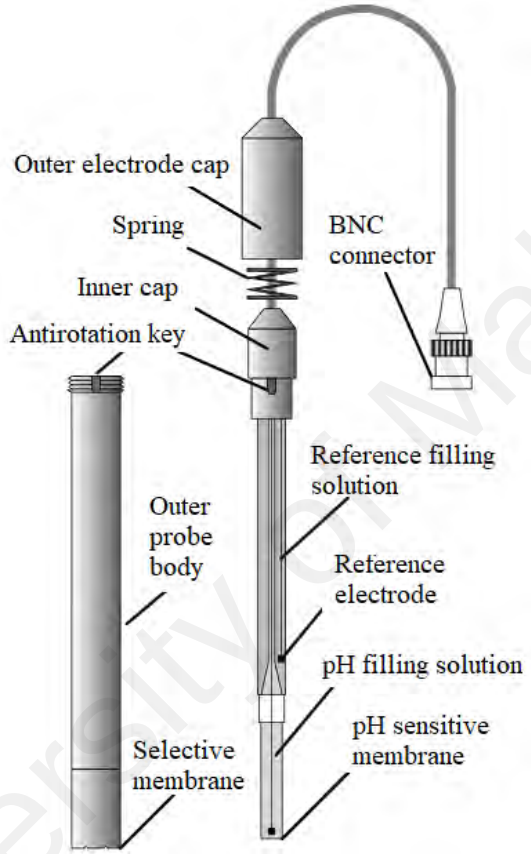

Figure 2.16: pCO_2 sensor and its parts.

The implementation of this sensor for pCO_2 measurement in blood are numerous. In 2008, Findlay et al. (Findlay et al., 2008) used this sensor to setup microcosm with specific temperature and pCO_2 level. Bian et al. (Bian et al. 2013) then employed this sensor for measuring tissue pCO_2 on vastus medialis muscle of rats after been exposed to sustained hemorrhagic shock, followed by the same application of this sensor in their extension work in 2015 (Bian & Chang, 2015).

2.8. Summary

In this chapter, the review of the literature was conducted, starting from the proven of $ECCO_2R$ efficiency and safety, the proof of relationship between CO_2 exchange and sweep gas flow rate, current investigations of automatic control in ECLS strategy and mathematical modelling of O_2 and CO_2 exchange in membrane oxygenator. In order to control CO_2 exchange in membrane oxygenator, knowledge regarding the static and dynamic behaviour of the underlying process must be fully understood. This will be done by developing a modelling that describes the behaviour of CO_2 gas exchange in membrane oxygenator in the next chapter.

CHAPTER 3: MATHEMATICAL MODELLING AND CARBON DIOXIDE GAS TRANSFER IN MEMBRANE OXYGENATOR

3.0. Introduction

In this chapter, a mathematical modelling of CO_2 gas exchange in membrane oxygenator is described in details. This mathematical modelling will be used to simulate the gas transfer process, factor determinant of arterial pCO_2 during ECLS and its relationship between manipulated and process variable.

3.1. Methodology

Total flow rate of sweep gas that enters the membrane oxygenator was previously proven as the determinant factor for pCO_2 exchange in oxygenator either by simulation studies (Turri & Yanagihara, 2011a), in vitro (Federspiel & Hattler, 1996; Hout et al., 2000b) or even in vivo studies (Karabulut et al., 2002; Park et al., 2016; Schmidt et al., 2013). Thus, in this study, sweep gas flow rate was used as the output of the controller, while pCO_2 value that leave the oxygenator is taken as the process output. This closed loop control system is designed to automatically adjust the sweep gas flow rate by considering the response of pCO_2 measurement to the previous change of this manipulated variable (Tehrani, 2012). In short, this present control system is dedicated to prevent both excessive and insufficient removal of CO_2 during extracorporeal circulation through membrane oxygenator by adjusting sweep gas flow rate in a robust and safely manner.

3.1.1. Modelling of CO_2 transfer and open-loop control

Mathematical modelling is the description of behaviour of dynamic system, which embodies either scientific principles or empirical observation or even both, related to the system in interest. By using mathematical modelling, the simulation of any process is possible, so that the researchers are able to explore the intrinsic behaviour of the said system in economical and safe manner, especially when the system or process is inaccessible or even non-existent yet (for the case of new design) (Klee & Allen, 2007).

Basically, the modelling of CO_2 gas transfer process in this study is adopted from the mathematical model that been developed by Hexamer and Werner (Hexamer & Werner, 2003a), which is the reformulated model by Hill et al. (Hill et al., 1973a, 1973b).

The modelling method for blood-gas exchange is compartmental modelling in this study and is based on the volume accounting equations of the compartment's gas (g), plasma (pl) and red blood cells (rbc). Figure 3.1 shows a mixing chamber, as a generic compartment, with diffusion occurs along the oxygenator membrane. The equation that describes the component *i* is:

$$V_{mc}\frac{d\,[C]_i}{dt} = \dot{Q}_{b,in}[C]_{i,in} - \dot{Q}_{b,out}[C]_{i,out} + D_i\left(P_{i,ext} - P_i\right) + R_i \qquad [3.1]$$

Where $d[C]_i$ denotes the concentration of component *'i'*, V_{mc} denotes the volume of the compartment/mixing chamber, $\dot{Q}_{b,in}, \dot{Q}_{b,out}$ represent flow rates of blood (in and out) and $[C]_{i,in}, [C]_{i,out}$ are the concentration of component *i* at inflow and outflow (inflow concentrations of components correspond to venous conditions in the membrane oxygenator). at inflow and outflow of the compartment. On the other hand, D_i is the bulk diffusion capacity over the membrane oxygenator, which its mass transfer is driven by gradient of partial pressure, $Pi_{,ext}$-P_i. Finally, R_i then stands for gain/loss of the substrate due to chemical reactions. For the

equations below, equation similar to equation [3.1] will be ordered in gas, O_2 and CO_2 (and related) equations, also perfect mixing of components will be assumed, i.e. $[C]_{i,out} = [C]_i$.

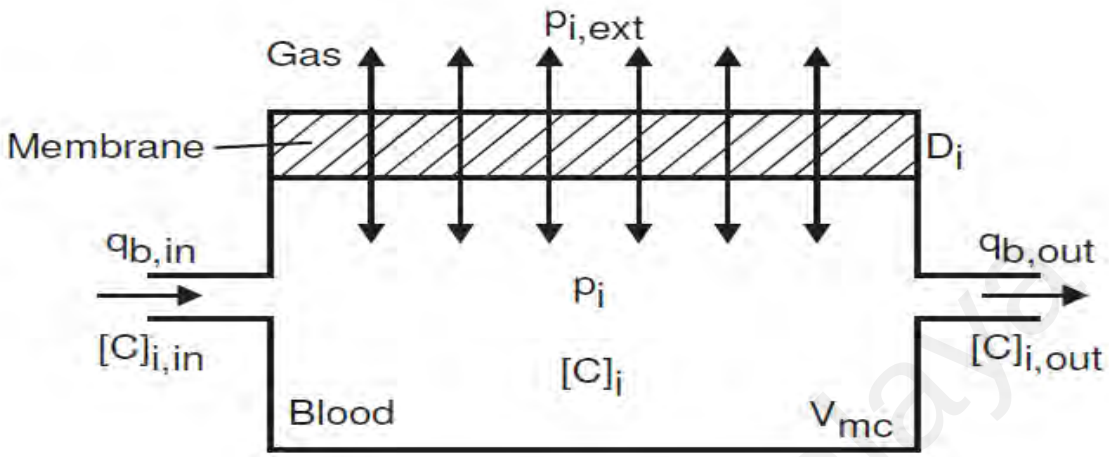

Figure 3.1: The generic model (Hexamer & Werner, 2003b).

i. Gas Compartment

Two components are distinguished in the gas compartment, which are oxygen (O_2) and carbon dioxide (CO_2). The gas fraction - partial pressure dependency (Henry's law) is written as (Misgeld, 2007; Walter et al., 2012; Walter et al., 2016; Walter et al., 2010; Walter et al., 2009a; Walter et al., 2010b):

$$p_{O2,g} = p_{bar} \cdot F_{O2} \quad [3.2]$$

$$p_{CO2,g} = p_{bar} \cdot F_{CO2} \quad [3.3]$$

where $pO_{2,g}$ and $pCO_{2,g}$ are the gas partial pressures, P_{bar} is the atmospheric pressure and lastly, Fi_{O2} and Fi_{CO2} are the mixing fractions of the respective gases. With the assumption $q_{g,in} = q_{g,out} = q_q$ and equation [3.2] and [3.3], the gas compartment describing equations are:

$$V_g \frac{F_{O2}}{dt} = \dot{Q}_g(F_{O2,in} - F_{O2}) - D_{O2}(pO_{2_g} - pO_{2_b}) \quad [3.4]$$

$$V_g \frac{F_{CO2}}{dt} = \dot{Q}_g(F_{CO2,in} - F_{CO2}) - D_{CO2}(pCO_{2_g} - pCO_{2_b}) \quad [3.5]$$

There are two important assumptions are made for gas compartment (Misgeld, 2007):

1. F_{CO2} in equation [3.2] is zero (since there is no CO_2 is used in sweep gas).
2. There is perfect mixing condition in gas compartment ($F_{O2,in} = F_{O2}\ and\ F_{CO2,in} = F_{CO2}$). The perfect mixing is assumed, since the gas that flows inside the gas compartment is 100% oxygen. Hence, the fraction of O_2 that in the compartment is the same as O_2 fraction that entering in the compartment.

By substituting [3.2] and [3.3] into [3.4] and [3.5], the equations can be rearranged as:

$$V_g \frac{dpO2_g}{dt} = \dot{Q}_g \left(pO_{2_{g,in}} - pO_{2_g}\right) - p_{bar}.\ D_{O2}(pO_{2_g} - pO_{2_b}) \quad [3.6]$$

$$V_g \frac{dpCO2_g}{dt} = \dot{Q}_g \left(pCO_{2_{g,in}} - pCO_{2_g}\right) - p_{bar}.\ D_{CO2}(pCO_{2_g} - pCO_{2_b}) \quad [3.7]$$

ii. Carbon dioxide transfer in blood compartment

Prior to the equation of blood-gas transfer, the volumes and flow for plasma and red blood cell are defined as:

$$V_{rbc} = V_b.hct \quad [3.8]$$

$$V_{pl} = V_b.(1 - hct) \quad [3.9]$$

$$\dot{Q}_{rbc} = \dot{Q}_b.hct \quad [3.10]$$

$$\dot{Q}_{pl} = \dot{Q}_b.(1 - hct) \quad [3.11]$$

Then, the equations for CO_2 transfer are:

(i) For plasma:

$$V_{pl}\,\alpha_{co2}\frac{d\,P_{co2,pl}}{dt} = \dot{Q}_{pl}\left([CO_2]_{pl,in} - [CO_2]_{pl}\right) + D_{CO2,m}\left(P_{CO2,g} - P_{CO2,pl}\right) +$$

$$D_{CO2,rbc}\,(P_{CO2,rbc} - P_{CO2,pl)} + V_{pl}\,.R_{HCO3,pl} \quad [3.12]$$

(ii) For red blood cell:

$$V_{rbc}\,\alpha_{co2}\frac{d\,P_{co2,rbc}}{dt} = \dot{Q}_{rbc}\left([CO_2]_{rbc,in} - [CO_2]_{rbc}\right) + D_{CO2,rbc}\left(P_{CO2,pl} - P_{CO2,rbc}\right) +$$

$$V_{pl}\,.\,R_{HCO3,rbc} - V_{rbc}\frac{d\,[carb]}{dt} \quad [3.13]$$

Where;

$$[CO_2]_{pl} = \alpha_{CO2}\,.P_{CO2,pl} \quad [3.14]$$

$$[CO_2]_{rbc} = \alpha_{CO2}\,.P_{CO2,rbc} \quad [3.15]$$

$$R_{HCO3,pl} = -k_u\alpha_{CO2}\,P_{CO2,pl} + \frac{k_v}{k}[H]_{pl}\,[HCO_3]_{pl} \quad [3.16]$$

$$R_{HCO3,rbc} = cat\,.\,(-k_u\alpha_{CO2}\,P_{CO2,rbc} + \frac{k_v}{k}[H]_{rbc}[HCO_3]_{rbc} \quad [3.17]$$

Equations [3.12] and [3.13] are obtained from assumption that the concentration of CO_2 in both plasma and red blood cell are linked to the partial pressure via the solubility coefficient.

Next, the equations for bicarbonate transfer for plasma ($[HCO_3]_{pl}$) and red blood cell ($[HCO_3]_{rbc}$) are written as:

$$V_{pl}\frac{d[HCO3]_{pl}}{dt} = \dot{Q}_{pl}\left([HCO_3]_{pl,in} - [HCO_3]_{pl}\right) - D_{HCO3,rbc}\left([HCO_3]_{pl} - \frac{[HCO3]_{rbc}}{r}\right) - V_{pl}R_{HCO3,pl} \quad [3.18]$$

$$V_{rbc}\frac{d[HCO3]_{rbc}}{dt} = \dot{Q}_{rbc}\left([HCO_3]_{rbc,in} - [HCO_3]_{rbc}\right) + D_{HCO3,rbc}\left([HCO_3]_{pl} - \frac{[HCO3]_{rbc}}{r}\right) - V_{pl}R_{HCO3,rbc} \quad [3.19]$$

Alphabet '*r*' in equation [3.18] and [3.19], is the result of [HCO_3] diffusion across red blood cell membrane and some complex biochemical effects (Misgeld, 2007). It is defined as:

$$r = (0.058\,pH_{virt} - 0.437)S - 0.529\,pH_{virt} + 4.6 \quad [3.20]$$

Equation [3.20] then influences virtual pH-value, which is the important determinant in pO_2 measurement:

$$pH_{virt} = \log(r[H]_{rbc}) \quad [3.21]$$

The diffusion capacity ($D_{CO2,rbc}$) and ($D_{HCO3,rbc}$) used in equations [3.12], [3.13], [3.18] and [3.19] are estimated from in-vitro measurements (E. Hill et al., 1973b):

$$D_{CO2,rbc} = \frac{0.693\,.\,\alpha_{CO2}}{\tau_{rbc}} \,.\, \frac{V_{rbc}V_{pl}}{V_{rbc}+V_{pl}} \quad [3.22]$$

$$D_{HCO3,rbc} = \frac{0.693}{\tau_{HCO3}} \,.\, \frac{V_{rbc}V_{pl}}{V_{rbc}+V_{pl}} \quad [3.23]$$

Carbamino reaction in equation [3.13] and [3.26] is due to direct bound between part of CO_2 within red blood cell and haemoglobin. The substance that produced from this reaction is called carbamate (*carb*):

$$V_{rbc}\frac{d[carb]}{dt} = \dot{Q}_{rbc}([carb]_{in} - [carb]) + k_a[CO_2]_{rbc}\,.V_{rbc}([Hb] - [carb]).\left(\frac{k_{zo}S}{k_{zo}+[H]_{rbc}} + \frac{k_{zr}(1-S)}{k_{zr}+[H]_{rbc}}\right) - V_{rbc}\,\frac{k_a[carb][H]_{rbc}}{k_c} \quad [3.24]$$

Lastly, exchange of hydrogen ion in plasma ($[H]_{pl}$) and red blood cell ($[H]_{rbc}$) are described by its hydrogen ion concentration:

$$V_{pl}\frac{d[H]_{pl}}{dt} = \dot{Q}_{pl}\left([H]_{pl,in} - [H]_{pl}\right) - V_{pl}\frac{2.303}{\beta_{pl}}[H]_{pl}\,.R_{HCO3,pl} \quad [3.25]$$

$$V_{rbc}\frac{d[H]_{rbc}}{dt} = \dot{Q}_{rbc}\left([H]_{rbc,in} - [H]_{rbc}\right) + V_{rbc}\frac{2.303}{\beta_{rbc}}[H]_{rbc}\,.(-R_{HCO3,rbc} + 1.5\,\frac{dcarb}{dt} - 0.6\,cap\,\frac{dS}{dt}) \quad [3.26]$$

Note that all the initial values, oxygenator parameters, biophysical and chemical parameters mentioned in the equations above are defined in Appendix A until Appendix C. Due to the objectives and scope of this study, only CO_2 transfer will be considered, while the simulation

of O_2 diffusion across hollow fibre membrane can be reviewed elsewhere (Kopp et al., 2016; Walter et al., 2012; Walter et al., 2016; Walter et al., 2010; Walter et al., 2009b; Walter et al., 2010a).

The simulation of gas diffusion in membrane oxygenator (equations [3.2] to [3.26]) was implemented in MATLAB/SIMULINK environment to calculate volume balance for state variables in blood-gas diffusion with respect to time.

In addition to the process simulation, an open loop control study was conducted to determine the controllable factor that influence gas transfer rate in membrane oxygenator. There are many references which stated that pCO_2 is controlled by sweep gas flow rate, while pO_2 is controlled by blood flow rate and oxygen fraction in gas compartment (Estafanous et al., 2001; Gravlee, 2008; Richard et al., 2014). In fact, this determinant factor was also had successfully proven using in both in vitro (Federspiel & Haulert, 1996; Hout et al., 2000a) and in vivo study (Karabulut et al., 2002; Park et al., 2016; Schmidt et al., 2013) or even through simulation via computer-assisted approach (Turri & Yanagihara, 2011a). Thus, the mathematical model used for this present study was simulated using three flow rates of sweep gas, which are 1 L/min, 2 L/min and 4 L/min, while the blood flow rate was kept constant as 2 L/min as shown in Table 3.1. These flow rates are chosen based on the ratio suggested by The Food and Drug Administration (FDA) in their guidance for cardiopulmonary bypass oxygenator (U.S. Food and Drug Administration, 2000).

Table 3.1: Ratio of flow rate.

Sweep gas flow rate, Q_g (L/min)	Blood flow rate, Q_b (L/min)	Q_g/Q_b ratio
1	2	0.5
2	2	1.0
4	2	2.0

Next, a statistical test (one-way ANOVA) was performed using two approaches, which were statistical software (Statistical Package for the Social Sciences or SPSS) and MATLAB. This is to ensure the accuracy and validity of our statistical analysis. ANOVA (analysis of variance) is an extension of t-test, which determine equality between several means by comparing their variance among groups relative to variance within groups (Larson, 2008; Ostertagov & Ostertag, 2013). Using ANOVA, the mean between two or more samples distribution can be determined if it differ significantly from one another with significant level set as α= 0.05 (95% confidential interval) (Manap et al., 2011). Thus, all differences associated with a chance probability of 0.05 or less in this study were considered as statistically significant.

Lastly, upon the proof of strong relationship between the gas flow rate and rate of CO_2 clearance, another test was conducted. In this test, two time periods of t=60 seconds and t= 120 seconds were isolated, where the gas flow was changed markedly. This is to see how the simulated pCO_2 respond accordingly to the change of sweep gas flow rate.

3.2. Result and observations: Modelling and open-loop control

Simulation result of CO_2 transfer across membrane oxygenator is depicted in Figure 3.2. From the figure, it can be seen that Q_g/Q_b= 2 has the highest CO_2 removal rate as compared to the other two.

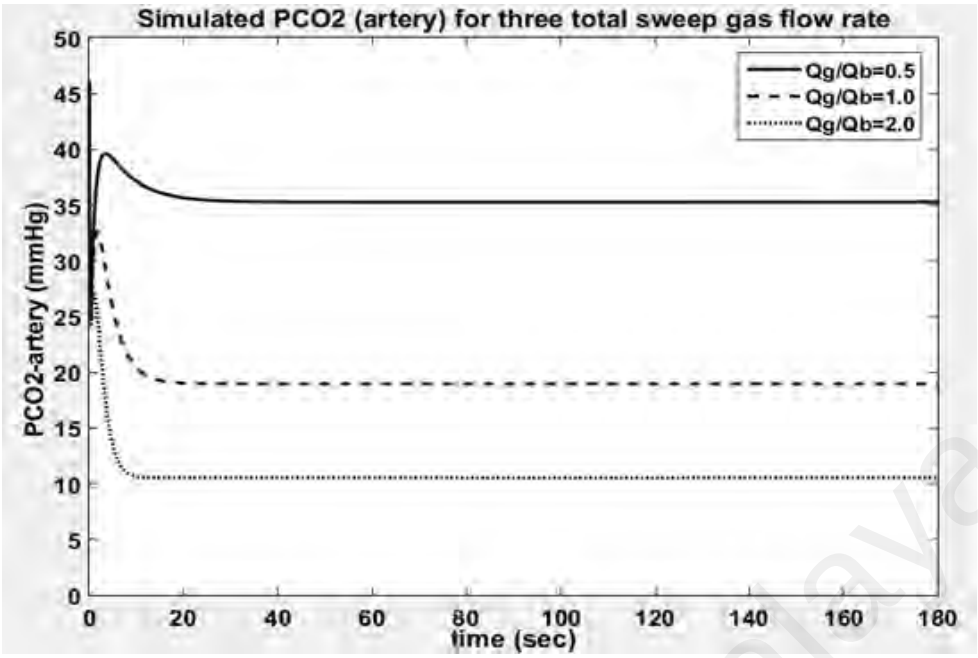

Figure 3.2: Simulated pCO_2 for three total sweep gas flow rates (Q_b= 2 L/min).

The increasing in pCO_2 clearance rate is proportional to the elevation of sweep gas flow rate. This finding agrees with the result reported by previous researchers (Federspiel & Hattler, 1996; Hout et al., 2000a; Karabulut et al., 2002; Turri & Yanagihara, 2011b), which advocated that the sweep gas flow rate has effect on measured pCO_2 under constant rate of blood flow.

Due to the proven relationship between pCO_2 and sweep gas flow rate, statistical analysis was performed in order to provide statistical evidence between these three flow rates. As tabulated in Table 3.2, the mean for calculated pCO_2 of three flow rates showed great deviation between each other with 35.153 mmHg, 20.070 mmHg and 12.052 mmHg for rate ratio (Q_g/Q_b) of 0.5, 1.0 and 2.0, respectively. Results obtained from ANOVA test then proved the significant difference, where *p*-value< 0.001.

Table 3.2: Statistical result for one-way ANOVA (Q_b= 2 L/min).

Q_g/Q_b	Mean ± standard deviation	*p*-Value
0.5	35.153 ± 1.831	< 0.001*
1.0	20.070 ± 3.699	
2.0	12.052 ± 5.329	

* Significant difference (ANOVA, p<0.05)

The present work was then extended to investigate how the simulated pCO_2 in artery respond to the change of sweep gas flow rate at each step change of flow rate. The behaviour of this model is illustrated in Figure 3.3.

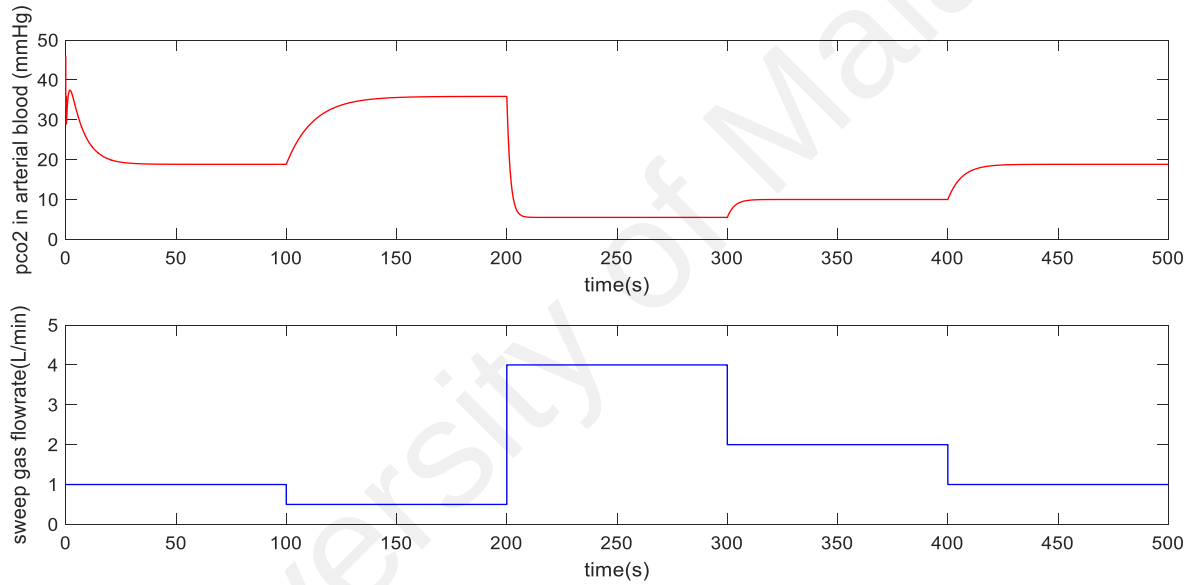

Figure 3.3: Open loop study for step change of sweep gas flowrate (manipulated variable), Q_b= 2 L/min.

Figure 3.3 shows the response of arterial pCO_2 to the step change in sweep gas flow rate, which reflects the relationship between both parameters. The trend of this open loop response is consistent with the reported simulation results by Hexamer et al. (Hexamer & Werner, 2003a). As the flow rate decrease, the CO_2 clearance have increased, and cause the simulated pCO_2 value become lower than before. This can be explained from the theory described by Kolobow et al. (Kolobow et al., 1977). Increasing sweep gas flow rate entering the membrane oxygenator will cause reduction in pCO_2 within the hollow fibre. Hence, the gradient of pCO_2 between

blood and gas phase will elevated. Consequently, the diffusion of CO_2 from blood phase to sweep gas area become greater and increases the CO_2 removal rate.

The continuous removal of CO_2 without any proper control may lead to excessive and unnecessary CO_2 removal, which can produce complications that associated with respiratory alkalosis and acute hypocapnia (Lund & Federspiel, 2013). Hence, this present study develops an automatic controller of CO_2 removal that implemented PID controller to control sweep gas flow rate supplied to membrane oxygenator.

3.3. Discussions

A membrane oxygenator comprised of thousands microporous hollow fibre membranes that allows gas exchange between gas and blood compartment. In most design, sweep gas (commonly O_2) will flows through the inside lumen of the hollow fibre, while blood flows outside the hollow fibre. During extracorporeal circulation, O_2 in sweep gas area will diffuses down its concentration gradient across membrane wall into the blood, while CO_2 will diffuse down its concentration gradient from blood into the sweep gas area, which is then removed when the sweep gas exits the oxygenator (Federspiel & Henchir, 2008). According to Cove et al. (Cove et al., 2012), there are three major factors that influence the amount of gas transfer in membrane oxygenator, which are concentration gradient, contact time between membrane-blood and membrane diffusion characteristics. Adjusting the sweep gas flow rate will affect the concentration gradient of CO_2 in membrane oxygenator. The increment of sweep gas flow rate depreciates CO_2 accumulation along sweep gas pathway (Federspiel & Hattler, 1996). Consequently, the fractional concentration of CO_2 in sweep gas is reduced, while O_2 fractional concentration is elevated. Conversely, increasing in pCO_2 concentration gradient between blood and gas phase then augments CO_2 removal (Scaravilli et al. 2014). This explains why the simulated pCO_2 in arterial blood reduced as the sweep gas flow rate increased. With this

finding, the first hypothesis of this study, which sweep gas flow rate is a major determinant in pCO_2 was validated.

In the aspect of process control, this open loop study shows a clear and important sign of direct-acting controller. From Figure 3.3, when manipulated variable (sweep gas flowrate) was elevated, the decreasing in process variable (pCO_2 in arterial blood) occurred. This is the reverse acting process, which need direct-acting controller. Direct-acting controller in this study means that, when the arterial pCO_2 reading increased above the setpoint, sweep gas flow rate will be also increased in order to bring the pCO_2 reading in arterial blood back accordingly to the setpoint.

Here, the setting of direct parameter will refer to the controller, which the controller output will be increased to correct the increasing process variable (Erickson & Hedrick, 1999). In any control process, direct or reverse direction must be specified carefully prior to the PID implementation, since it represents the relationship between controller output and process variable. It is an extremely important step to do, since the incorrect choice usually will lead to undesired process variable response such as loss of control and runaway processes (Seborg, et al., 2010).

These findings are great indicators for the application of closed-loop control strategy to membrane oxygenator in controlling pCO_2 in blood. According to Chung et al. (Chung et al., 2014), CO_2 is more soluble than O_2, hence it diffuses faster than O_2. Diffusion coefficient for CO_2 in water at 25 ^oC is 1.92×10^{-5} cm^2/s, while 2.10×10^{-5} cm^2/s for O_2 (Cussler, 1997). For solubility coefficient, the CO_2 solubility coefficient is 0.0308 mmol. L^{-1}. $mmHg^{-1}$ at 37 ^oC (Arthurs & Sudhakar, 2005) and O_2 solubility is 0.00139 mmol. L^{-1}. $mmHg^{-1}$ at the same temperature (Valabrègue et al., 2003). Due to this advantage, CO_2 is transfers approximately 20 times more efficiently than O_2 (Chung et al., 2014). Rapid diffusion of CO_2 that leaves blood

will cause hypocapnia (state of reduced CO_2 in blood, where pCO_2 falls below 35 mmHg at sea level) (Solano et al., 2012). To prevent this problem, a good automated controller is needed to ensure pCO_2 do not fall below 35 mmHg. This will be investigated in the next chapter as an extension of the outcome from this chapter.

3.4. Summary

In this chapter, sweep gas flowrate is proven as the determinant factor for pCO_2 level in the arterial blood and also the inversely proportional relationship between manipulated variable (sweep gas flowrate) and process variable (arterial pCO_2). This proven relationship indicates the use of direct-acting controller for closed loop control that will be discussed in the next chapter.

CHAPTER 4: CONTROL OF CARBON DIOXIDE GAS EXCHANGE IN MEMBRANE OXYGENATOR: SIMULATION STUDY

4.0. Introduction

In this chapter, the automatic control process is conducted using three type of controllers, i.e. PID, FLC and Fuzzy-PID to control the arterial pCO_2 according to the desired setpoint in the setpoint tracking and disturbance rejection tasks. Using the same mathematical model developed in Chapter 3, this work is continued with the control process. Finally, the performance evaluation of these three controllers in order to conclude the most suitable controllers for this study.

4.1. Methodology

4.1.1. Closed loop control: PID tuning and automated control

From open-loop study conducted in Manap et al. (Manap et al., 2017), as the sweep gas flowrate increased, the CO_2 clearance have increased, and cause the pCO_2 value become lower than before. An important aspect of process control, open loop study indicates a clear and important sign of direct-acting controller, which the controller output will be increased to correct the increasing process variable (Erickson & Hedrick, 1999).

Hence according to Erickson and Hedrick (Erickson & Hedrick, 1999), error for direct-acting controller was defined as:

$$Error = setpoint - process\ variable \quad [4.1]$$

For this case, the PID have the negative gain. Closed loop control was conducted using PID controller, which involved 2 stages, tuning and automated controlling. In tuning the PID,

Ziegler-Nichols continuous cycling method was implemented for the best PID tuning parameter setting. Ziegler-Nichols method started with the determination of critical value for critical gain (K_{cr}) and critical period (P_{cr}) that produce a continuous oscillation of control loop, according to the tuning procedure described in (Altmann, 2005; Haugen, 2004; Ziegler & Nichols, 1942).

According to Altman (Altmann, 2005), there are few steps must be taken to in order to determine the tuning constant for continuous cycling method:

1. Controller was set in P-control mode, with no integral and derivative control. This is to avoid the influence of controller in the process dynamic assessment
2. Error of the system was defined as Error= SP-PV, where SP is setpoint, PV is process variable, to ensure the P-controller is working accordingly to the change in PV and SP.
3. The controller was left into the automatic mode, since the closed loop situation may lead into a continuous cycle at the critical gain setting.
4. A step change was made to the setpoint only after the process is steady, which only minor dynamic fluctuation visible. This is to evaluate how the PV settles due to the disturbance.
5. Then, the further action was taken based on the observation on process dynamic. There are few guidelines regarding this action. Altman (Altmann, 2005) described that if the oscillation produces settle down quickly or no oscillation at all, then, the value of K_{cr} should be increased. Then, step 4 was repeated by returning the setpoint back to its original value. If the oscillation occurs and the increasing in amplitude can be seen, the exercise is terminated immediately and the value of K_{cr} is reduced, to stabilize the process. The exercise is repeated with careful observation on the high value of K_{cr}.
6. The last step is to find K_{cr} and P_{cr}. Once the continuous cycling of the process was obtained, critical gain, K_{cr} and corresponding period, P_{cr} are experimentally determined

(see Figure 4.1 to 4.3). Ziegler and Nichols suggested the formula shown in Table 4.1 below to set the parameter of K_p, T_i and T_d:

Table 4.1. Ziegler-Nichols tuning rules based on critical gain and critical methods.

Parameters	**Values**
Critical period, P_{cr}	0.12 s
Critical gain, K_{cr}	140
Proportional gain, K_p	$Kp = 0.6 \times Kcr$ $= 84$
Integral time, T_i	$Ti = \frac{Pcr}{2}$ $= 0.06$ s
Derivative time, T_d	Td= P_{cr}/8 = 0.015 s

After tuning process, all of the tuned PID parameters (Kp, Ki and Kd) were used in the PID block in MATLAB/SIMULINK environment for two tasks, which are setpoint tracking (Figure 4.4) and disturbance rejection (Figure 4.5).

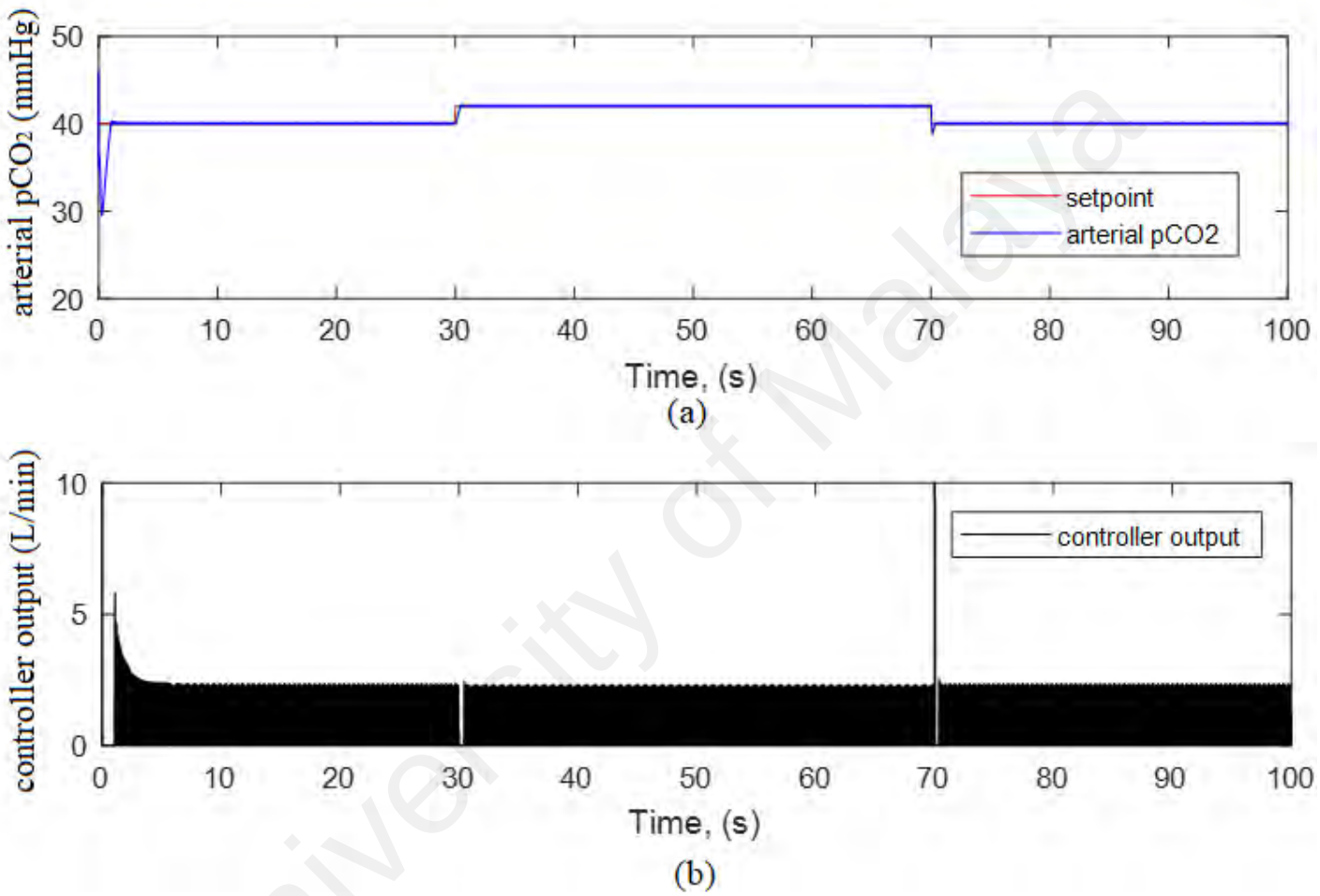

Figure 4.1: The whole simulation on automatic mode at K_{cr}= 140. Figure (a) represents arterial pCO_2 during continuous cycling of the process and Figure (b) represents the controller output given by PID, respectively.

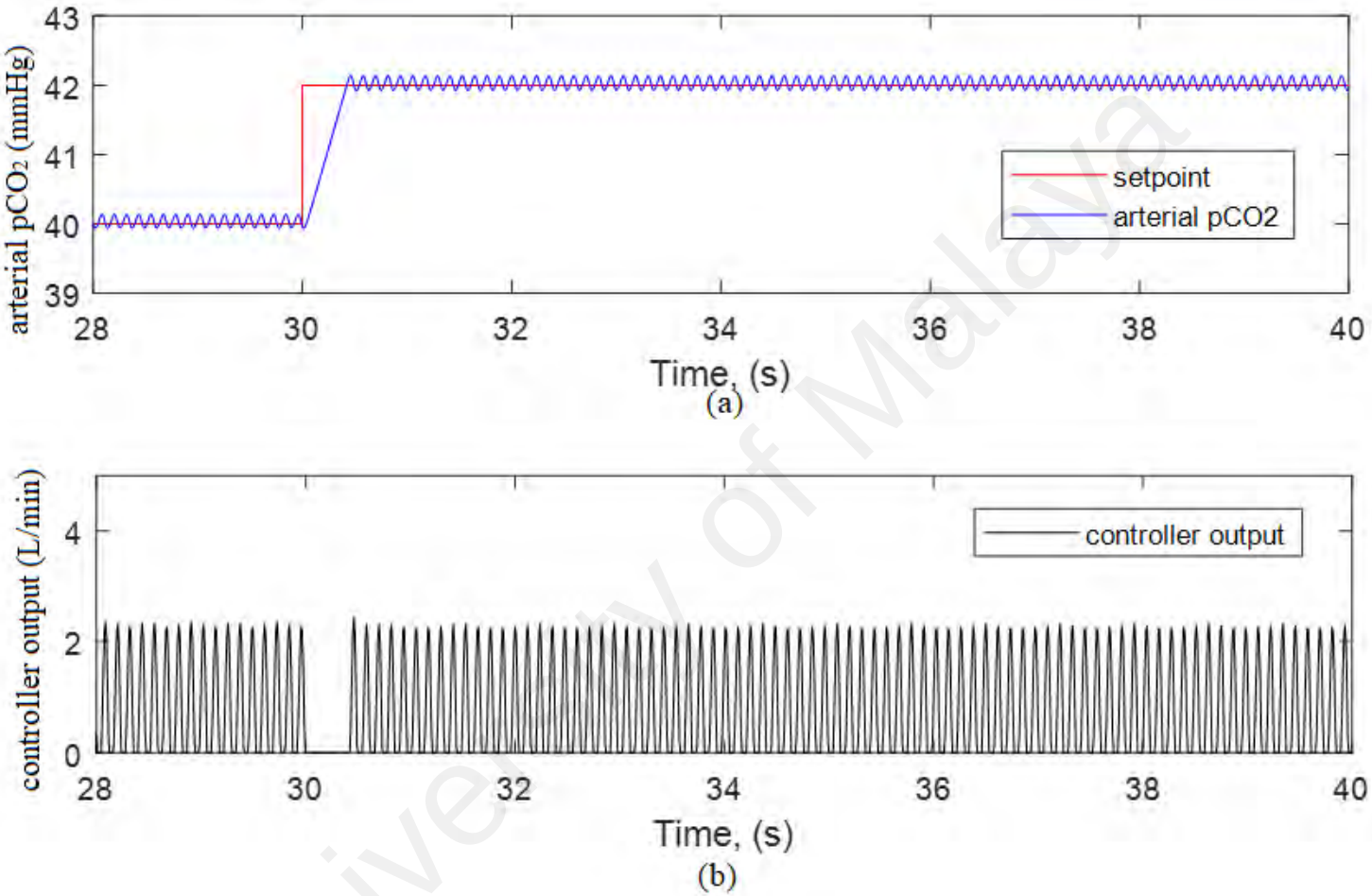

Figure 4.2: The zoomed view of simulation on automatic mode at K_{cr}= 140. Figure (a) represents arterial pCO_2 during continuous cycling of the process and Figure (b) represents the controller output given by PID, respectively.

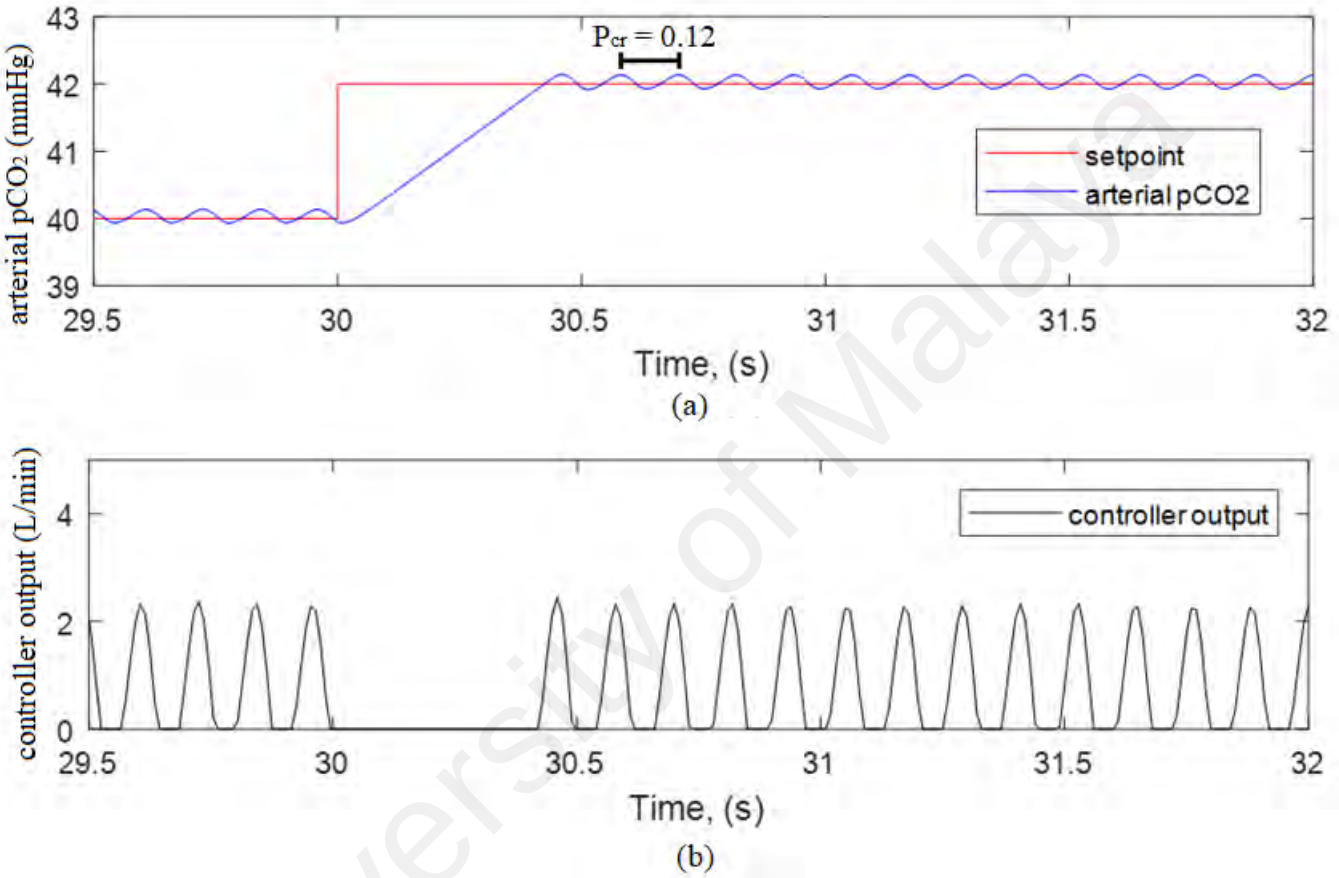

Figure 4.3: P_{cr} during sustained oscillation at K_{cr}=140. Figure (a) represents arterial pCO_2 during continuous cycling of the process and Figure (b) represents the controller output given by PID, respectively.

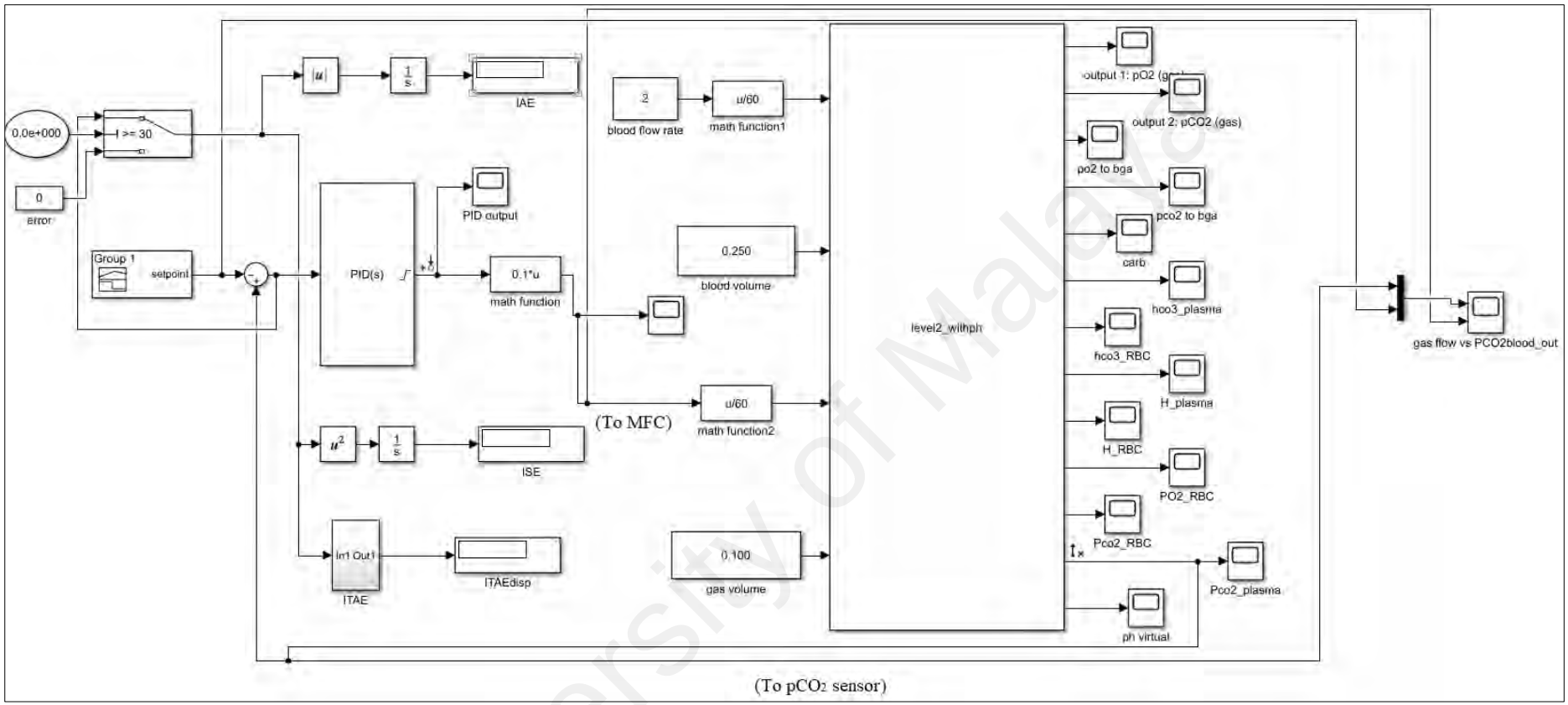

Figure 4.4: MATLAB/SIMULINK interface for setpoint tracking task (PID controller).

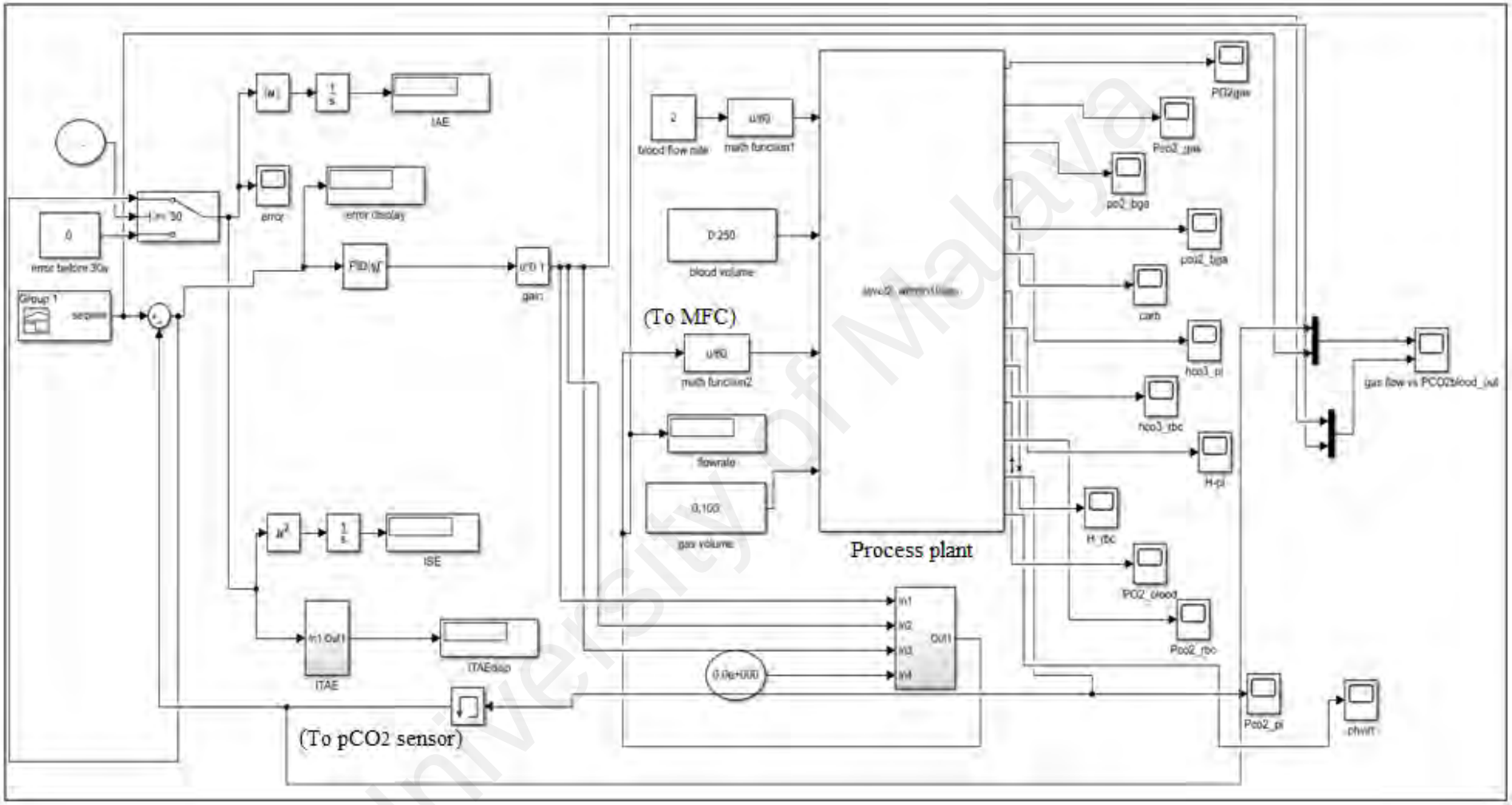

Figure 4.5: MATLAB/SIMULINK interface for disturbance task (PID controller).

4.1.2. Closed loop control: FLC

FLC is known as the good candidate in dealing with degree of vagueness and uncertainty (Ahmadi et al., 2018; Übeyli, 2009), which occurs in this present study. It is a real time expert system that identify the system using its input-output data (Takagi & Sugeno, 1985), which converting a linguistic control action that derived from expert knowledge into automatic control strategy (Tian & Gilbertson, 2004). For FLC used in this study, Takagi- Sugeno fuzzy rules is applied, which involved two input variables (error and change of error) and 1 output variable (controller output). The membership functions of each input variables are designed and shown in Figure 4.6 for both input variable error (a) and rate of change of error (b). The values of linguistic variables for input variable 'error' are composed of linguistic terms LN (Large Negative), SN (Small Negative), ZEN (Zero Negative), ZE (Zero), ZEP (Zero Positive), SP (Small Positive) and LP (large Positive), while N (negative), ZE (Zero) and P (Positive) are determined for input variable 'change of error'. As for output, three constants are identified to determine the controller output (sweep gas flow rate), which are LOW (0.1), MEDIUM (0.8698) and HIGH (1.2).

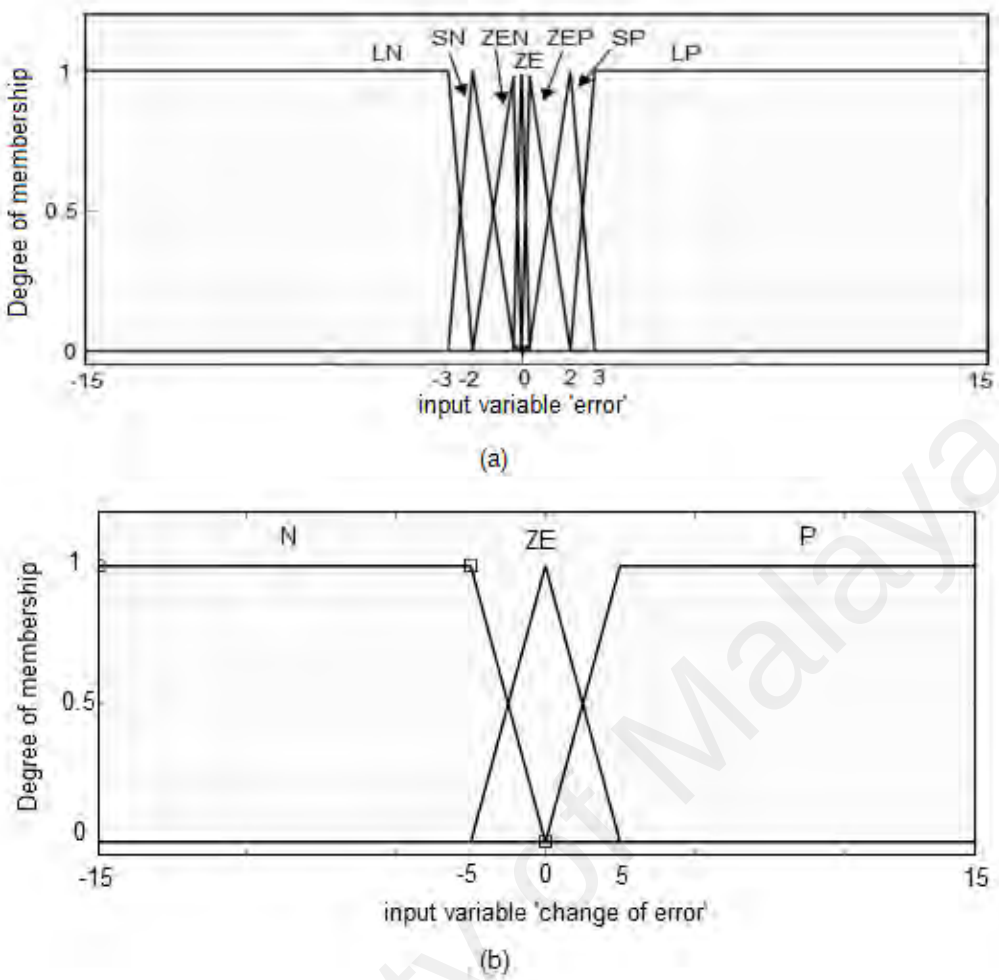

Figure 4.6. (a) Membership functions of error and (b) change of error.

While maintaining pCO_2 according to the setpoint, there are 21 rules are specified as in Table 4.2, which are:

Table 4.2: Rules of fuzzy inference for FLC.

Δe / e	LN	SN	ZEN	ZE	ZEP	SP	LP
N	HIGH	HIGH	HIGH	MEDIUM	LOW	LOW	LOW
ZE	HIGH	HIGH	HIGH	MEDIUM	LOW	LOW	LOW
P	HIGH	HIGH	HIGH	MEDIUM	LOW	LOW	LOW

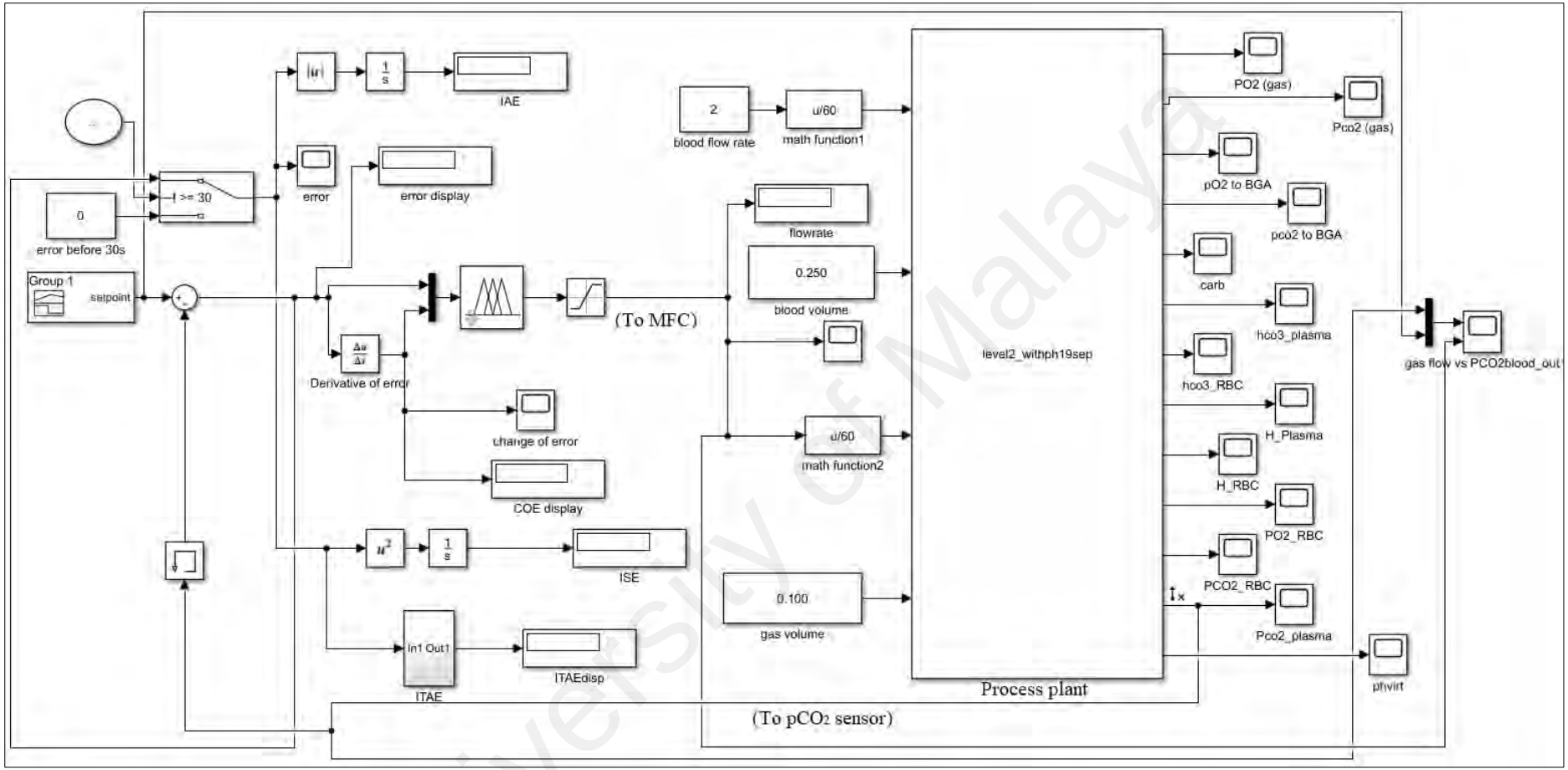

Figure 4.7: MATLAB/SIMULINK interface for setpoint tracking task (FLC).

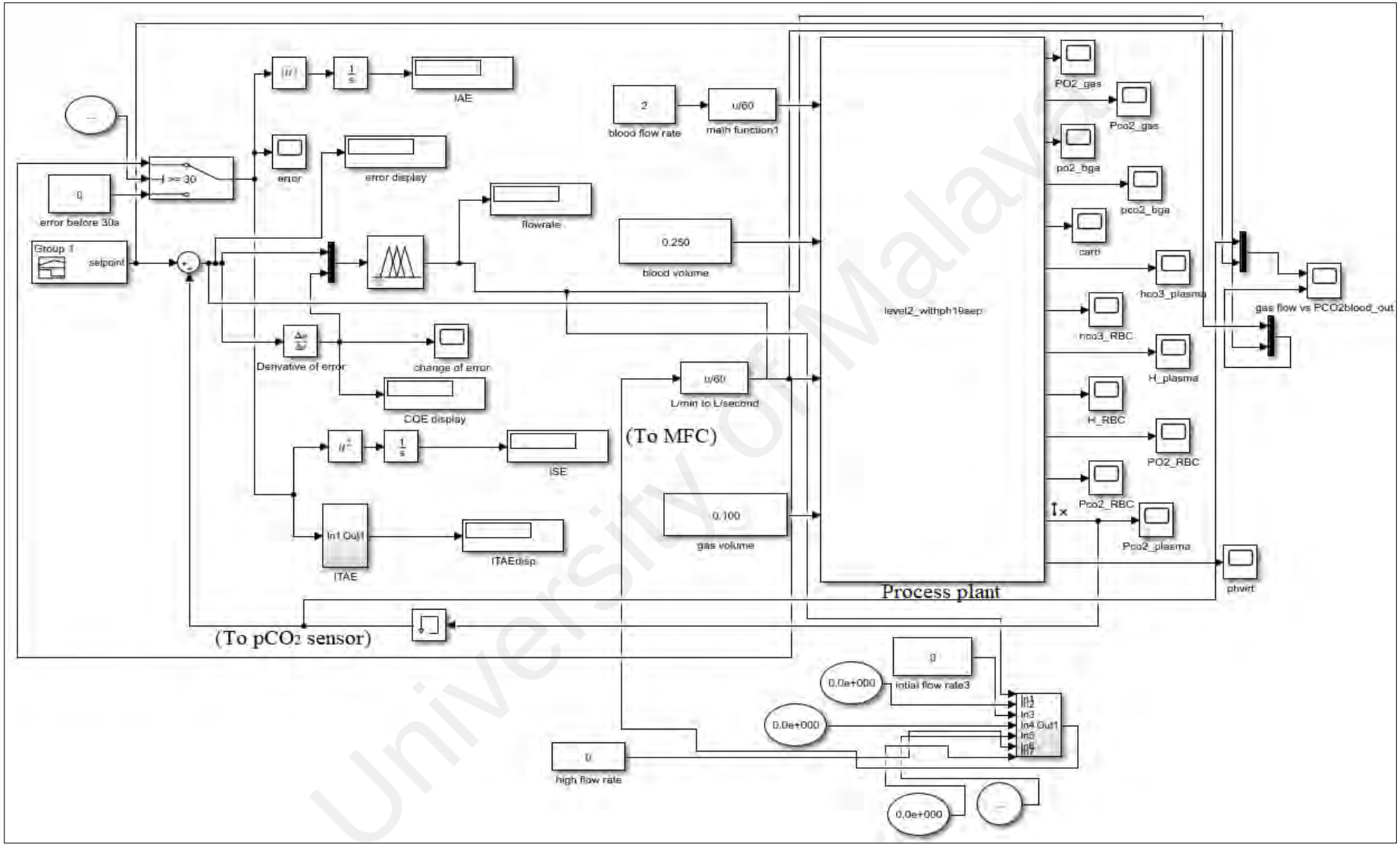

Figure 4.8: MATLAB/SIMULINK interface for disturbance task (FLC).

4.1.3. Closed loop control: Fuzzy-PID

In the Fuzzy-PID, fuzzy logic is applied to tune each parameter in PID, which are the gains for P, I and D. In this controller, gains of the conventional PID are tuned on-line by fuzzy logic controller that based on knowledge and fuzzy inference. The PID gains are acquired online using a fuzzy rule-based computation algorithm. This eliminates the need of manual tuning, calibrations or prior knowledge of plant parameter. Using the gains that are pre-tuned using the fuzzy logic block, the conventional PID controller then generates the control signals to the plant (which referred as controller output). The integration of conventional PID and FLC outputs are then implemented to the process to exploit the beneficial sides of both controllers in controlling the process towards the control objective.

From Figure 4.9, the algorithm can be simplified as follows:

i. Fuzzy controller block calculate error and change of error (de/dt).

ii. Using fuzzy rule based defined in Table 4.3-4.5, determine Kp, Ki and Kd.

iii. Compute controller output, u.

iv. Calculate plant output, pCO_2.

v. Return to step (i).

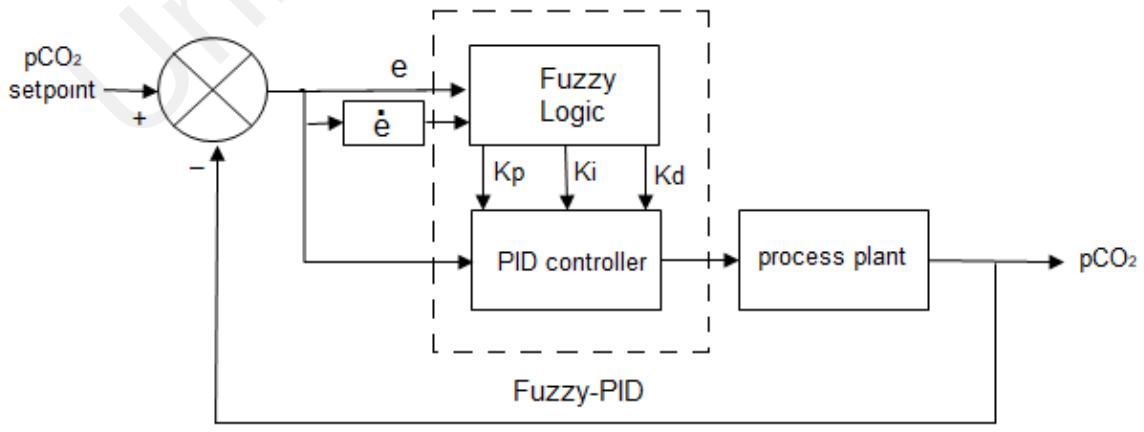

Figure 4.9: Fuzzy-PID structure.

As shown in Figure 4.9, Fuzzy-PID controller that applied in this study consists of both fuzzy controller and conventional PID controller. From this block diagram, fuzzy block is comprised of two inputs and three outputs, where the inputs are error, e and the rate of change of error, ė (Figure 4.10), whist the output are Kp, Ki and Kd values. There are five linguistic terms of the error in pCO_2: LN (Large Negative), SN (Small Negative), ZE (Zero), SP (Small Negative) and LP (Large Positive), followed by N (Negative), ZE (Zero) and P (Positive) for input variable 'change of error' over the interval from -15 to 15.

On the other hand, the linguistics variables for output variables (Kp, Ki and Kd), are assigned as N (Negative), SN (Small Negative), ZE (Zero) and P (Positive) over the normalized interval of [0, 1]. These three gain parameters, Kp, Ki and Kd (Figure 4.11) in PID controller was updated online by fuzzy rules that was designed based on the Fuzzy rules that tabulated in Table 4.3 until 4.5

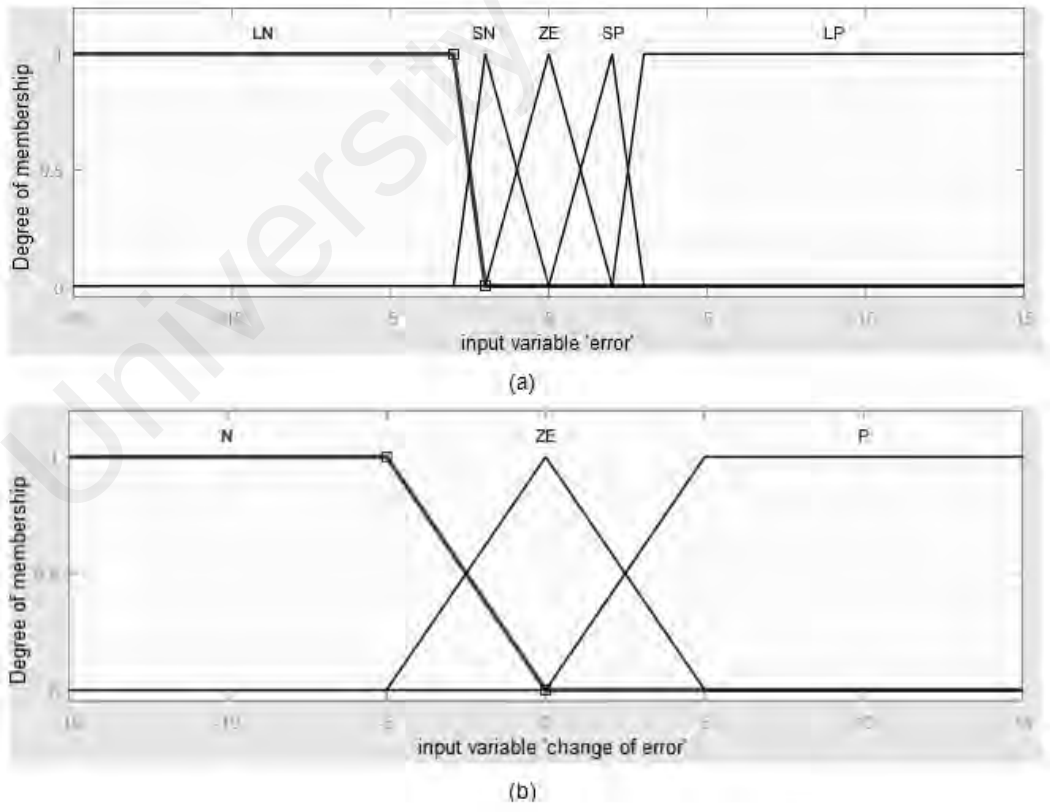

Figure 4.10. (a) Membership functions of error and (b) rate of error.

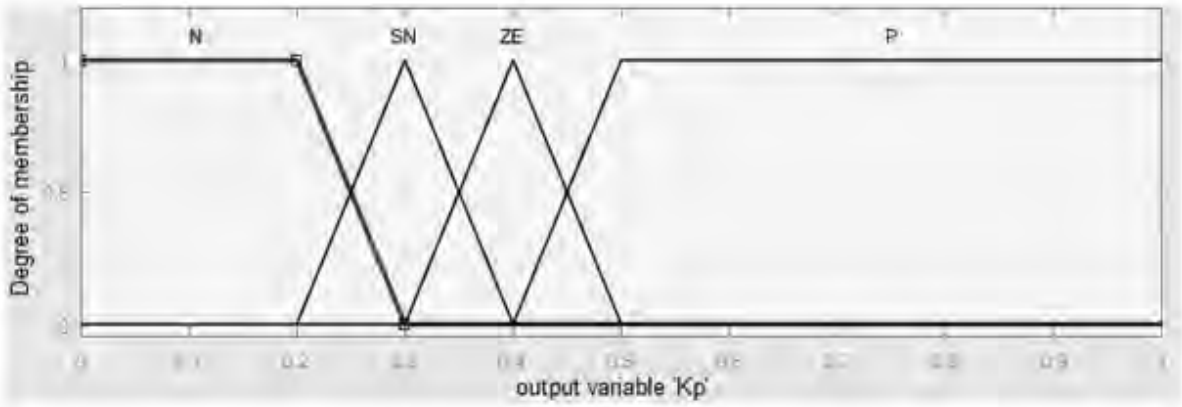

(a)

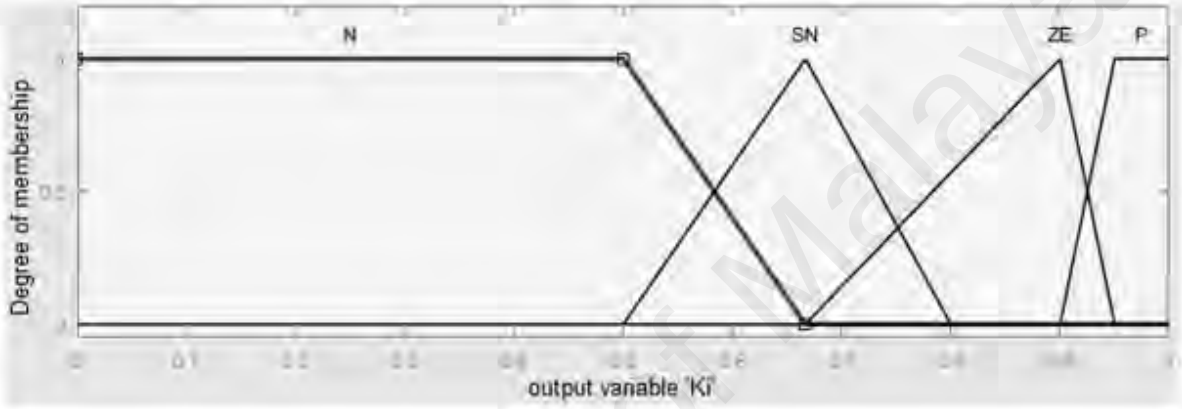

(b)

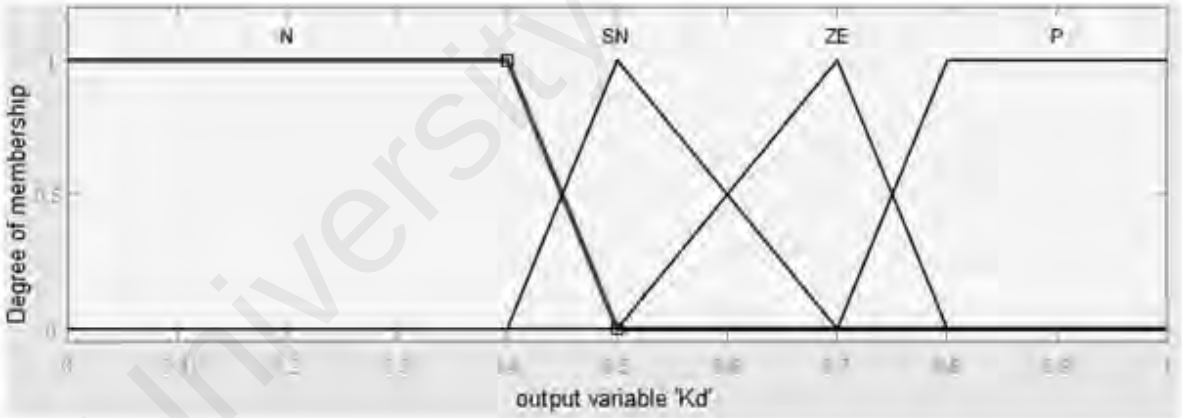

(c)

Figure 4.11. Membership function of (a) Kp, (b) Ki and (c) Kd.

Table 4.3. Rules of fuzzy inference for 'K_p'.

Δe / e	LN	SN	ZE	SP	LP
N	P	ZE	ZE	ZE	P
ZE	ZE	SN	ZE	SN	ZE
P	P	ZE	ZE	ZE	P

Table 4.4. Rules of fuzzy inference for 'K_i'.

Δe / e	LN	SN	ZE	SP	LP
N	P	ZE	ZE	ZE	N
ZE	ZE	SN	ZE	SN	ZE
P	P	ZE	ZE	ZE	N

Table 4.5. Rules of fuzzy inference for 'K_d'.

Δe / e	LN	SN	ZE	SP	LP
N	P	ZE	ZE	ZE	N
ZE	ZE	SN	ZE	SN	ZE
P	P	ZE	ZE	ZE	N

From these gain parameters, the optimum PID controller output (flow rate of sweep gas) is adjusted to produce the best control action to the process plant. The rule of thumb used in tuning K_p, K_i and K_d are based on the input of fuzzy block, where:

1. If $|e|$ is larger, then K_p tuned to larger value while K_d will be decreased in order to make the system responds quickly. To avoid the system from having large overshoot, the integral control will be limited, where K_i usually become zero, K_i=0.

2. If $|e|$ is moderate, then K_p should be decreased, while the attention will be given to K_d to get the small overshoot.

3. If $|e|$ is smaller, both K_p and K_i will be elevated for better steady state performance of this system. In the case of $(\dot{e})$, when $(\dot{e})$ is smaller, K_d will be increased, while K_d is decrease when $(\dot{e})$ is larger. This is to avoid the system from having oscillation near the set point.

For accuracy, value of membership functions, P, I and D were normalized to get the universe of discourse at the interval [0,1] by using the equations:

$$P' = \frac{P - Pmin}{Pmax - Pmin} \quad [4.2]$$

$$I' = \frac{I - Imin}{Imax - Imin} \quad [4.3]$$

$$D' = \frac{D - Dmin}{Dmax - Dmin} \quad [4.4]$$

To get the actual controller output after normalizations to range [0, 1]:

$$Kp = 10\,P' + 80 \quad [4.5]$$

$$Ki = 10\,I' + 10 \quad [4.6]$$

$$Kd = 0.01\,D' + 0.01 \quad [4.7]$$

This membership function is adjusted to the narrower area of membership functions (near the zero region), so that it can produce fine control resolutions.

The simulation was performed in MATLAB/SIMULINK environment. The block diagram of the simulation for setpoint tracking is shown in Figure 4.12, followed by subsystem in Figure 4.13 that consist of equations to get the original controller output prior to PID controller (equation [4.5] to [4.7]). Figure 4.14 is the block diagram for disturbance rejection, followed

by subsystem in Figure 4.15, which consist of equations to get the original controller output (equation [4.5] to [4.7]).

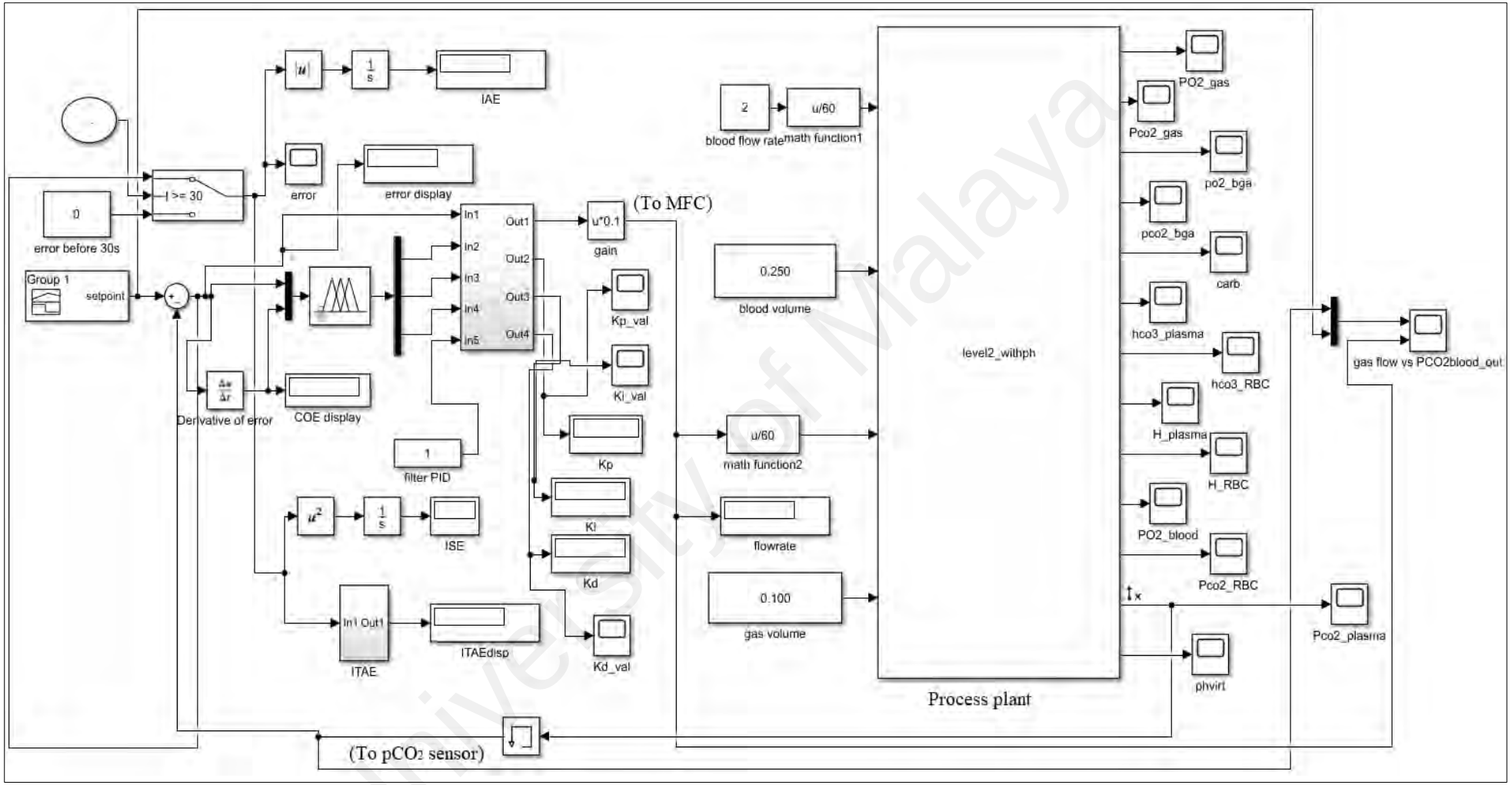

Figure 4.12: MATLAB/SIMULINK interface for setpoint tracking task (Fuzzy-PID).

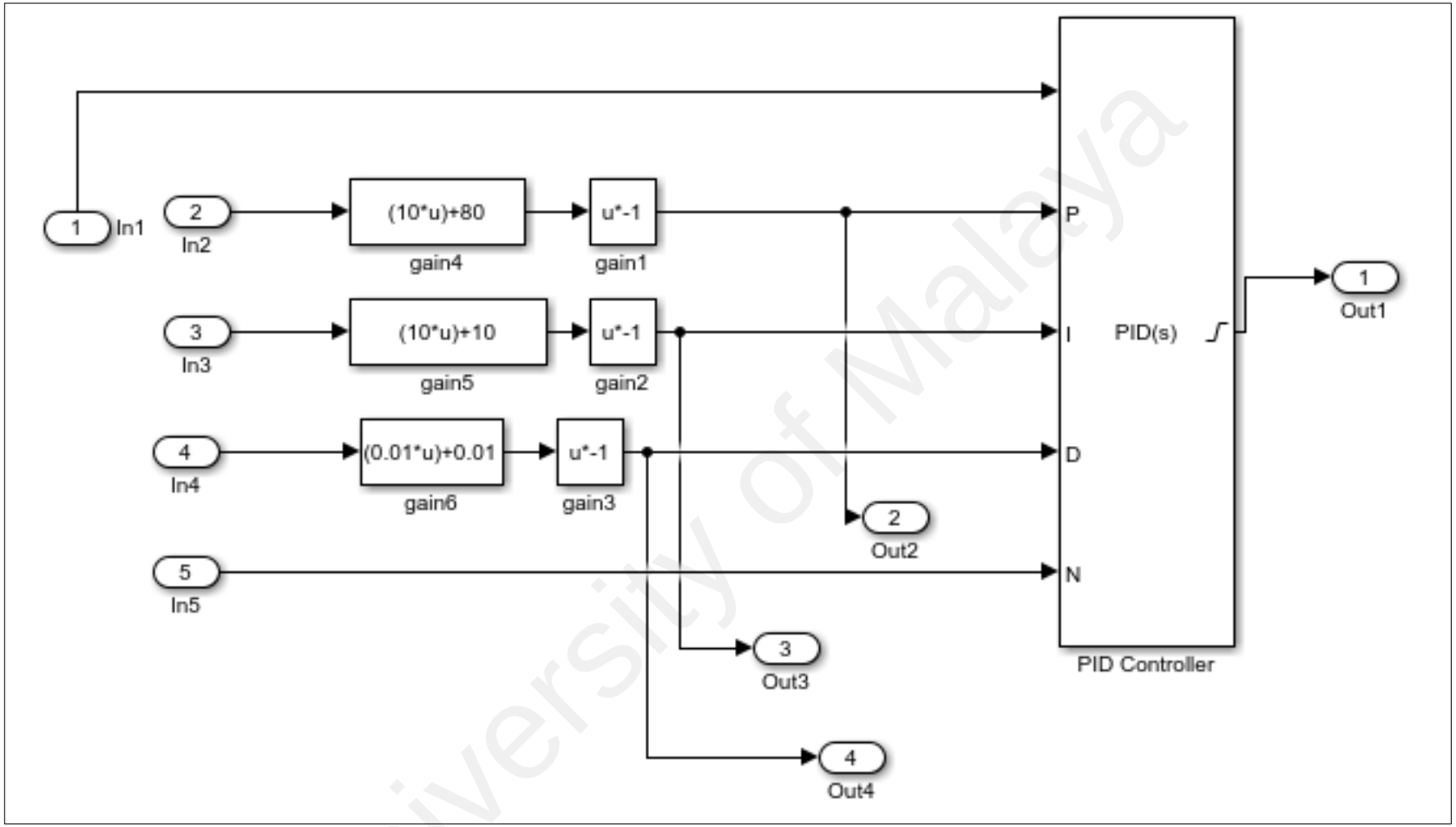

Figure 4.13: Subsystem of MATLAB/SIMULINK interface for setpoint tracking task (Fuzzy-PID).

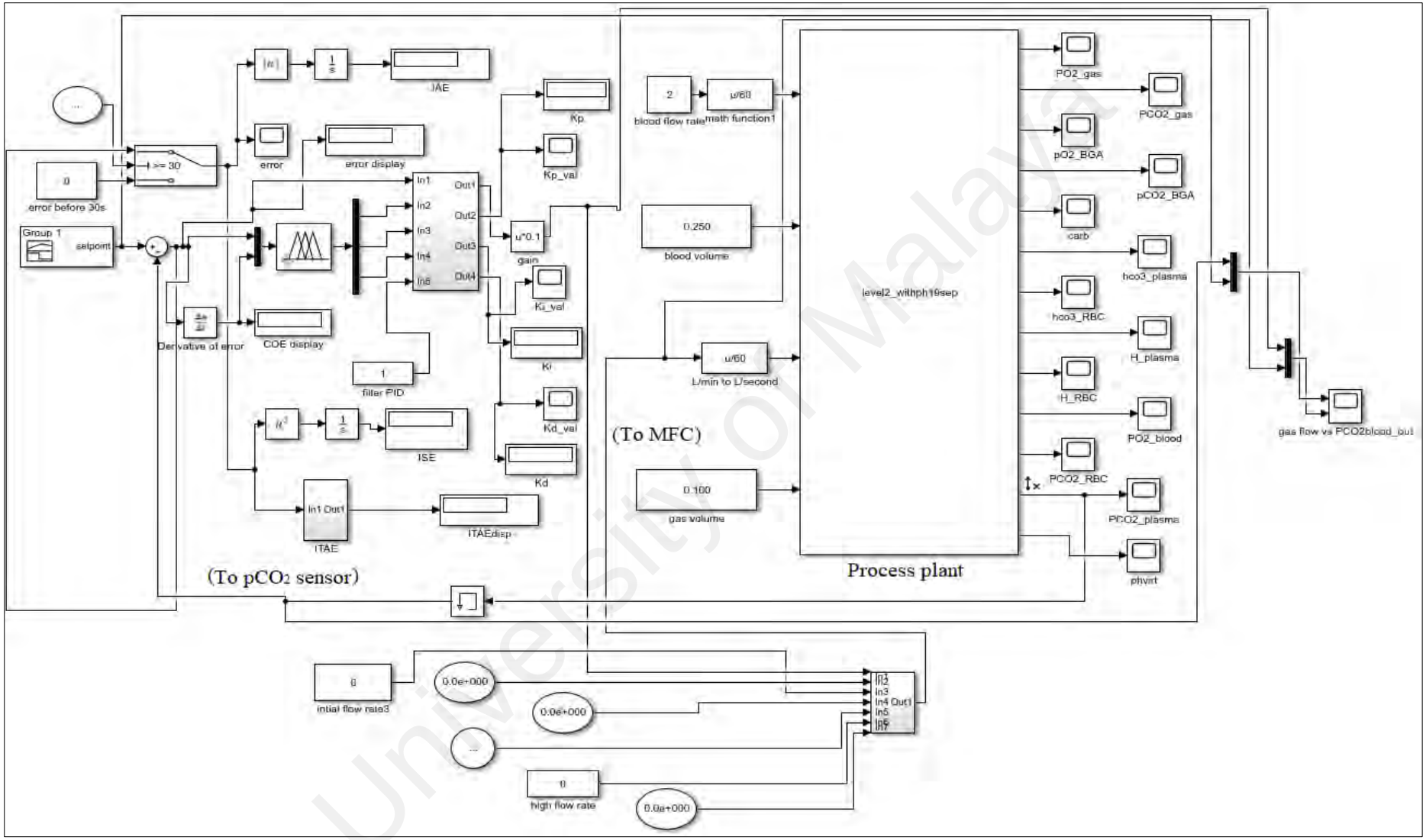

Figure 4.14: MATLAB/SIMULINK interface for disturbance task (Fuzzy-PID).

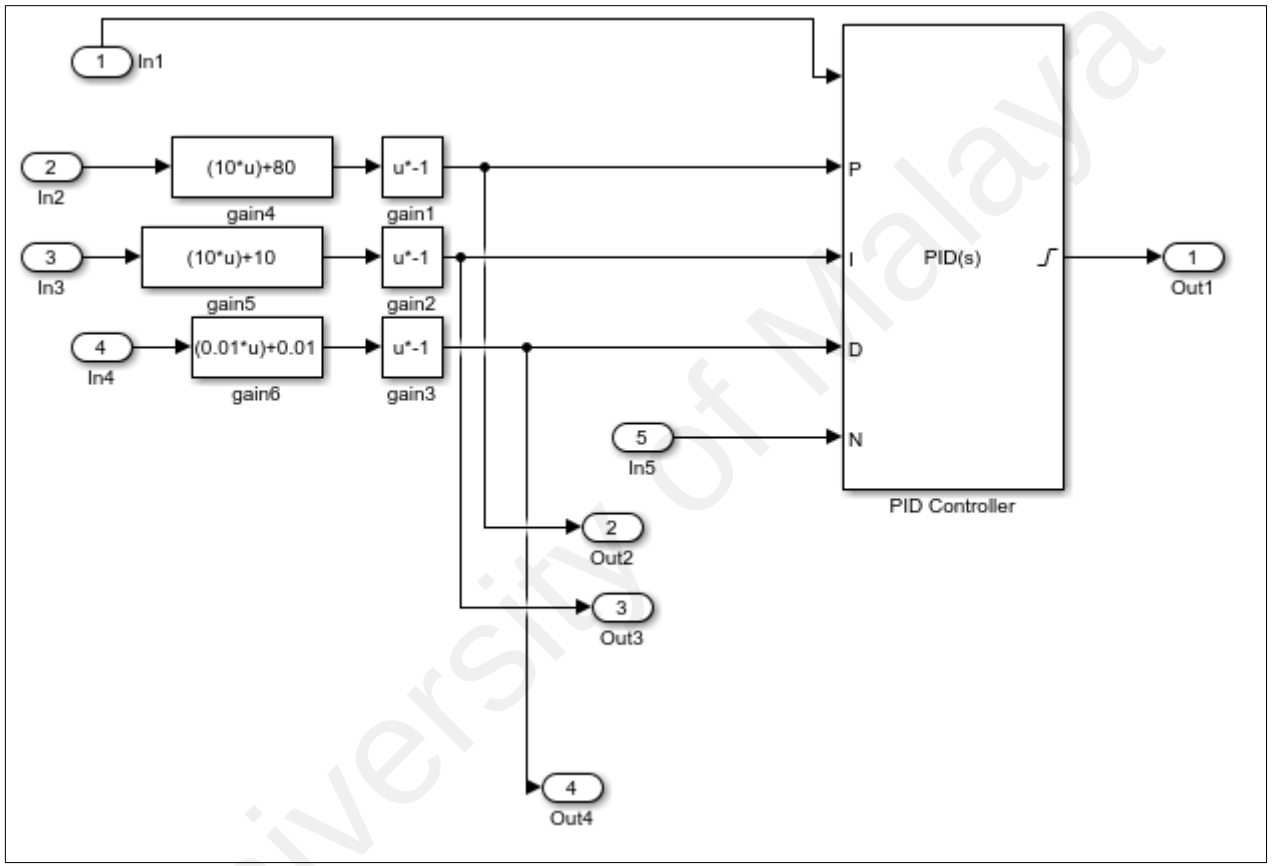

Figure 4.15: Subsystem of MATLAB/SIMULINK interface for disturbance task (Fuzzy-PID).

4.1.4. Closed loop control: Robustness test

In order to further evaluate the robustness of the proposed controllers, they are individually evaluated, subjected to the setpoint tracking and disturbance rejection tests.

4.1.4.1. Setpoint tracking

In common operation of membrane oxygenator, its control loop has a constant setpoint. But, the setpoint may be changed at certain time instance if the operator desire to change the operating condition based on the patient's state. Hence, a good automated control system must have a good setpoint tracking capabilities. For this setpoint tracking task, the setpoint was initially set as 40 mm Hg at t=0. Then it was adjusted to 42 mm Hg from t= 30 s to t=60s. At t= 60.01s, the setpoint was returned back to its initial value, which is 40 mm Hg. This is to see the ability of the controllers to control the process variable accordingly to the desired setpoint in order to minimize the error between arterial pCO_2 and setpoint.

4.1.4.2. Disturbance rejection

Disturbance in this study is defined as a disturbance that enters the control loop at any point in the process and drive the system away from its desired operating point (Astrom & Hagglund, 1995). To assess the ability of the proposed controller in rejecting disturbance, the mass flow controller will be 'switched off' for 1 second at point t=30s and t=60s, which turns the sweep gas flow rate to become 0 L/min for a second. This is to see the effect to the process plant and controller's corrective action if there is no oxygen supplied to the process plant due to system failure, such as black out, which causes the mass flow controller been suddenly switched off. A good controller will act to bring the process variable (arterial pCO_2) back toward the desired setpoint in case of disturbance on the process that cause the deviation.

4.1.4.3. Closed loop control: Performance evaluation

In addition to the graph plotting to evaluate the controllers' performance, accuracy of the entire controllers in completing both tasks described above is calculated. This quantitative analysis involved three performance indices, Integral Absolute Error (IAE), Integral Squared Error (ISE), Integral Time Absolute Error (ITAE) and Mean Squared Error (MSE). The MATLAB/SIMULINK blocks for these indices are shown in Figures 4.16, 4.17 and 4.18 for IAE, ISE and ITAE, respectively:

$$IAE = \int_0^\infty |e(t)|dt \quad [4.8]$$

$$ISE = \int_0^\infty e^2(t)dt \quad [4.9]$$

$$ITAE = \int_0^\infty t|e\,(t)|dt \quad [4.10]$$

$$MSE = \frac{1}{n}\sum_{i=1}^{n} e(t) \quad [4.11]$$

Where:

n= total number of measurements.

e(t)= error (setpoint – measure pco_2 in arterial blood).

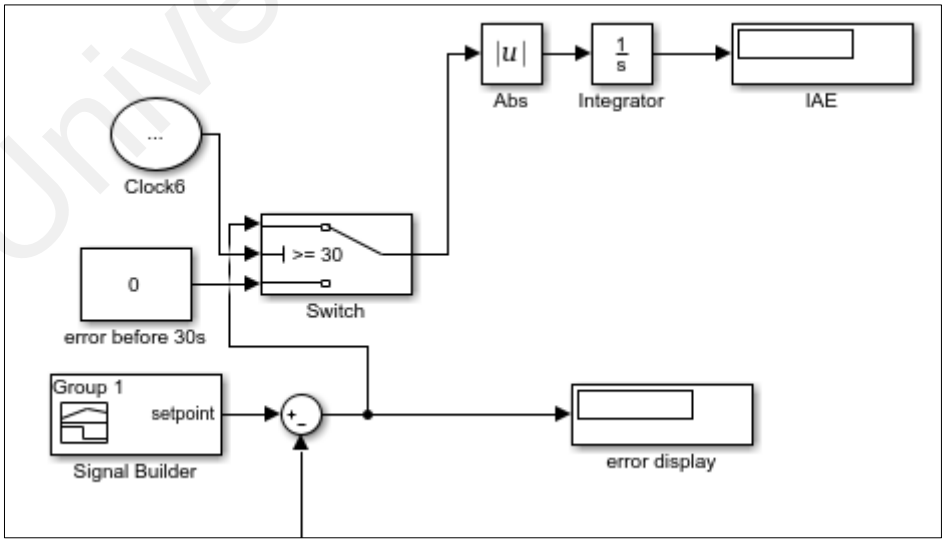

Figure 4.16: MATLAB/SIMULINK blocks for IAE calculation (from equation [4.8]).

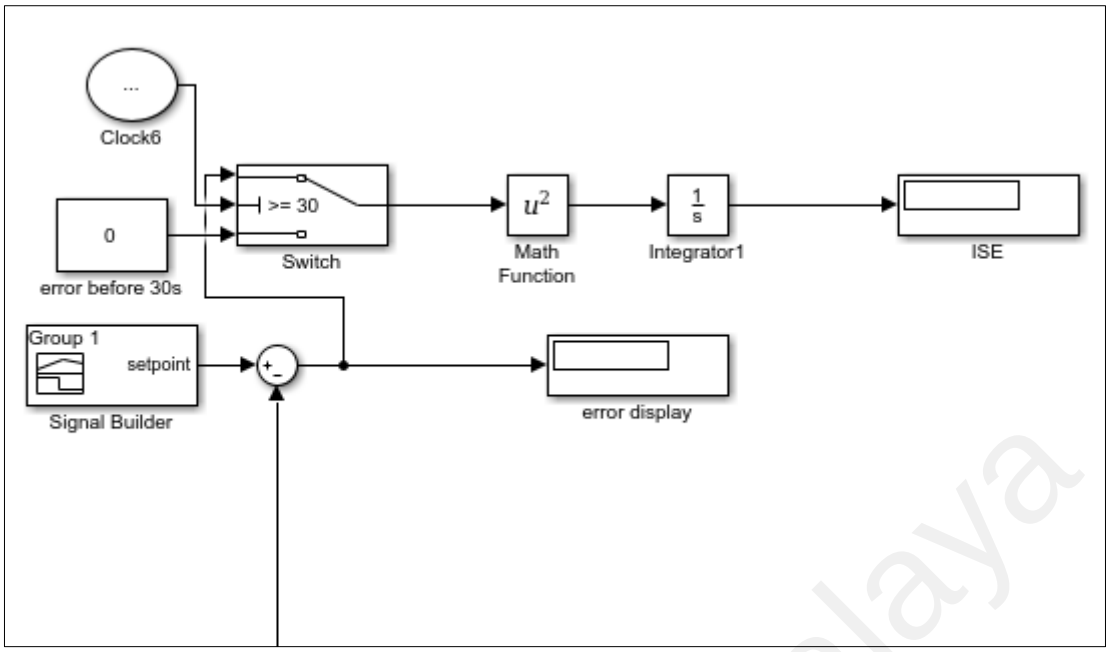

Figure 4.17: MATLAB/SIMULINK blocks for ISE calculation (from equation [4.9]).

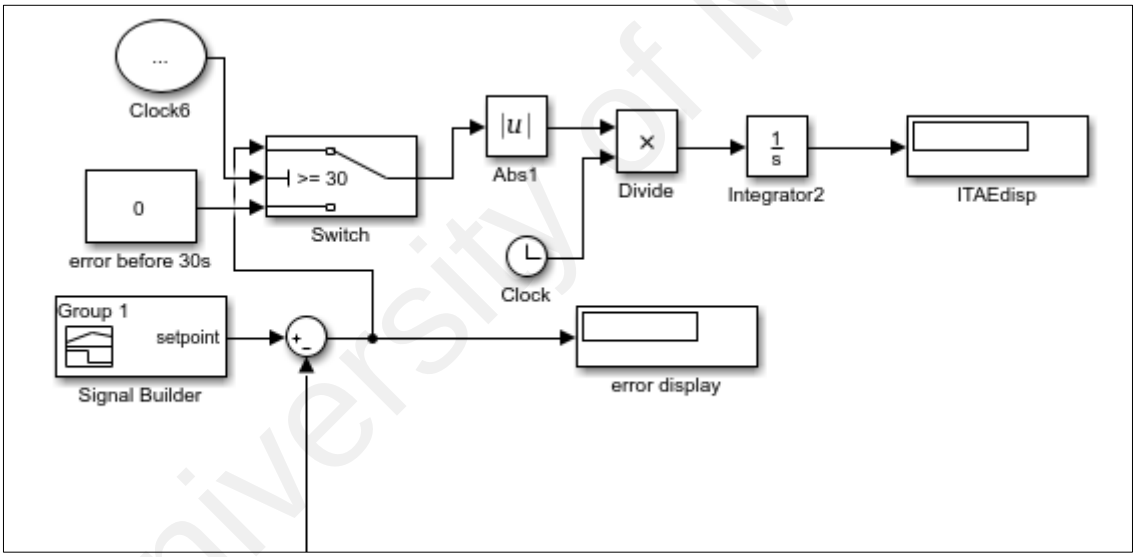

Figure 4.18: MATLAB/SIMULINK blocks for ITAE calculation (from equation [4.10]).

4.2. Result and observation (simulations work)

In this section, the performance of each controller is evaluated in terms of graph plotting and calculation of performance indices namely IAE, ISE and ITAE.

4.2.1. Closed-loop control: Setpoint tracking

4.2.1.1.PID

For PID controller on setpoint tracking, a good control action can be seen from Figure 4.19, where the arterial pCO_2 able to achieve the desired setpoint with some oscillation and overshoot when during setpoint changing at t=30s. At t=30s, setpoint was increased to 42 mmHg. Consequently, overshoot occurred up to 42.08 mmHg (0.08 mmHg above the setpoint), while 0.52s was needed by the PID controller to achieve the setpoint at 42 mmHg.

Similar observation also can be found when the setpoint was adjusted back to its original setpoint, 40 mmHg at t=60s. With the overshoot of 39.03 mmHg (0.07 mmHg below the setpoint), PID controller took 0.65s to achieve the desired point at 40 mmHg. This reflects the ability of PID to control the pCO_2 according to desired setpoint.

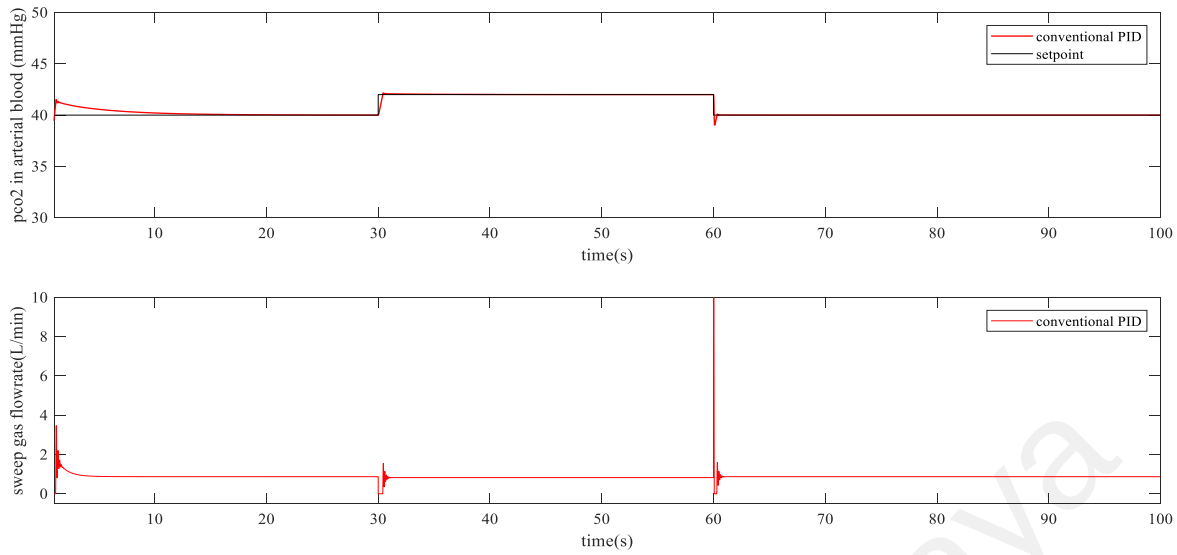

Figure 4.19: Simulated pCO_2 of PID controller for setpoint tracking, (upper part: responses of process variable (simulated pCO_2), lower part: controller output (sweep gas flow rate)).

4.2.1.2. Fuzzy Logic Controller (FLC)

For FLC, a good control effort can be seen from Figure 4.20. When the setpoint was changed to 42 mmHg, the FLC automatically adjusted its manipulated variable by decreasing the sweep gas flow rate to 0.8241 L/min. No overshoot was seen for this controller and it produced sustained error of 0.02 mmHg, which only 0.05% deviated from the setpoint.

At t=60s, when the setpoint was adjusted back to 40 mmHg, FLC once again adjusted the sweep gas flow rate until 0.8698 L/min in order to obtain the desired setpoint. Only at 1.18s of simulation time taken to bring the arterial pCO_2 back to desired setpoint.

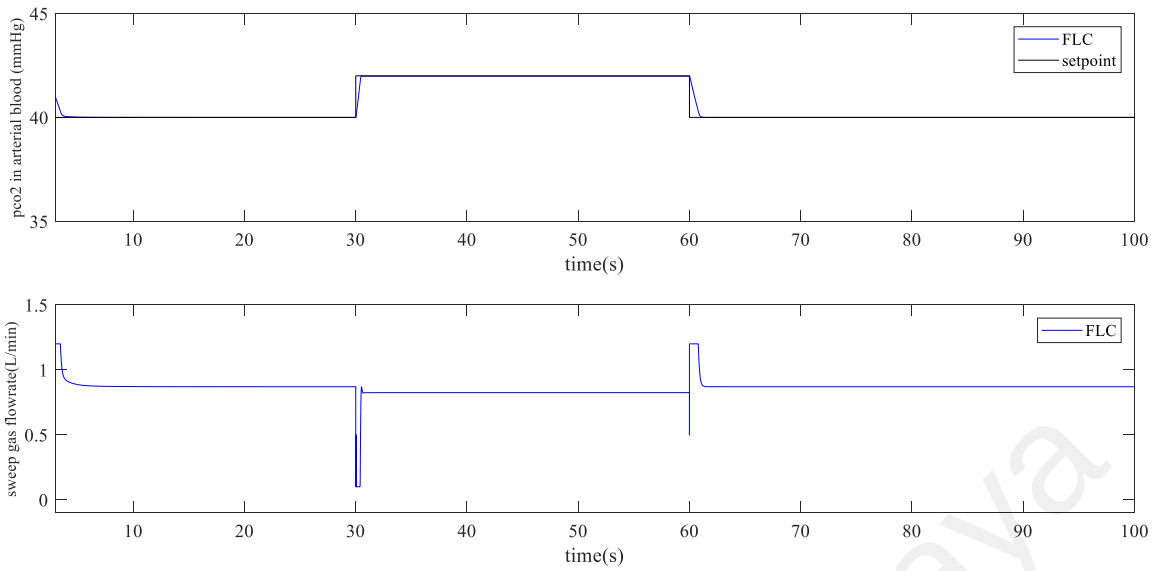

Figure 4.20: Simulated pCO_2 of FLC controller for setpoint tracking, (upper part: response of process variable (simulated pCO_2), lower part: controller output (sweep gas flow rate)).

4.2.1.3. Fuzzy-PID

The best control action for pCO_2 removal was obtained in Figure 4.21, where the Fuzzy-PID was successfully adjusted its sweep gas flowrate according to the setpoint changes. At t=30s, where the setpoint was changed to 42 mmHg, lesser overshoot was seen for this controller, compared to the PID, with 42.019 mmHg, which 0.07 mmHg lesser than PID. In addition, this controller only took 0.41s to control the arterial pCO_2 accordingly to the setpoint (42 mmHg).

At t=60s, when the setpoint was adjusted back to 40 mmHg, Fuzzy-PID controller produce 0.8698 L/min sweep gas flowrate as its controller's output, thus able to obtain the setpoint at 40 mmHg after 0.62s with overshoot that produce 0.51 mmHg of error.

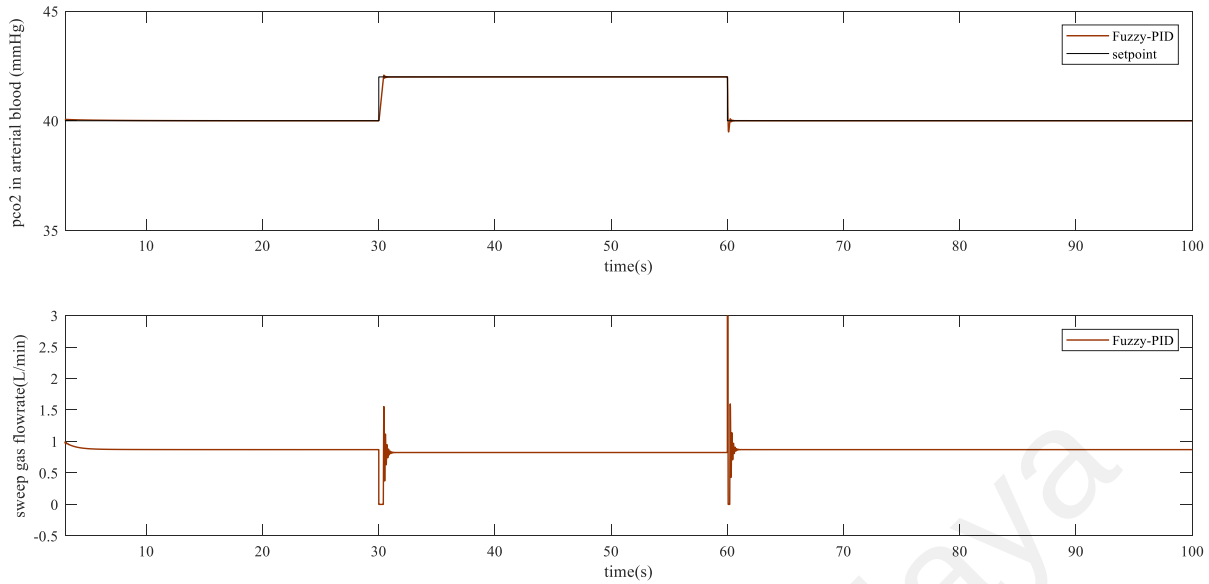

Figure 4.21: Simulated pCO_2 of fuzzy-PID controller for setpoint tracking, (upper part: responses of process variable (simulated pCO_2), lower part: controller output (sweep gas flow rate)).

4.2.1.4. Comparison of simulation between conventional PID, FLC and Fuzzy-PID: setpoint tracking.

Overall, all the controllers able to control the arterial pCO_2 according to the setpoint during setpoint changing. Performance comparison was conducted to find the best controller among this three. Figure 4.22 illustrated the responses of process variable (pCO_2) and controller output (sweep gas flow rate) for different controllers, conventional PID, FLC and Fuzzy-PID.

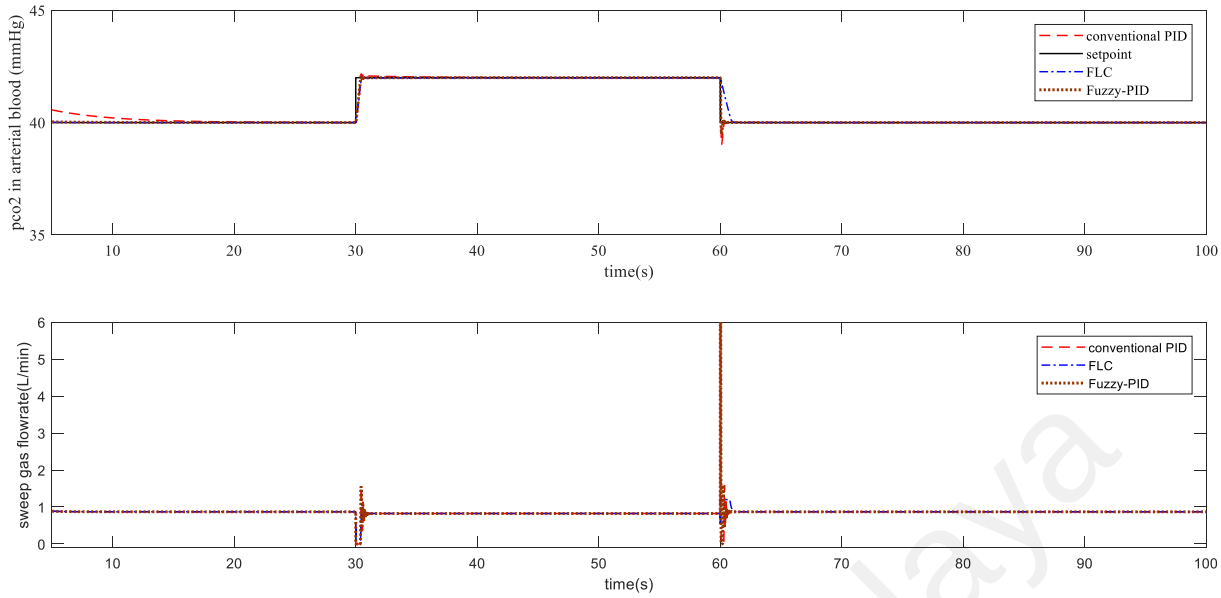

Figure 4.22: Comparison of simulated pCO_2 for different type of controllers for setpoint tracking (upper part: response of process variable (simulated pCO_2), lower part: controller output (sweep gas flow rate)).

For clearer observation, zoomed view of pCO_2 at t=30 s and t=60 s (time where the setpoint change was introduced to the process plant) were also included in Figures 4.23 and 4.24, respectively. From these figures, PID controller had longest settling time, highest oscillation and highest overshoot during tracking the setpoint, as compared to FLC and Fuzzy-PID controllers. Even though FLC had lower oscillation and overshoot than conventional PID, it produced the highest errors, which makes it less preferable as a controller. On the other hand, Fuzzy-PID response was the most stable with fewer oscillation, error and overshoot compared to both PID and FLC. The controller was well-performed, which it successfully followed the setpoint at 40 mm Hg and 42 mm Hg, respectively. These results confirmed that Fuzzy-PID is the best controller compared to conventional PID and FLC in archiving the setpoint. This performance comparison was validated by quantitative analysis on performance indices namely IAE, ISE, ITAE and MSE.

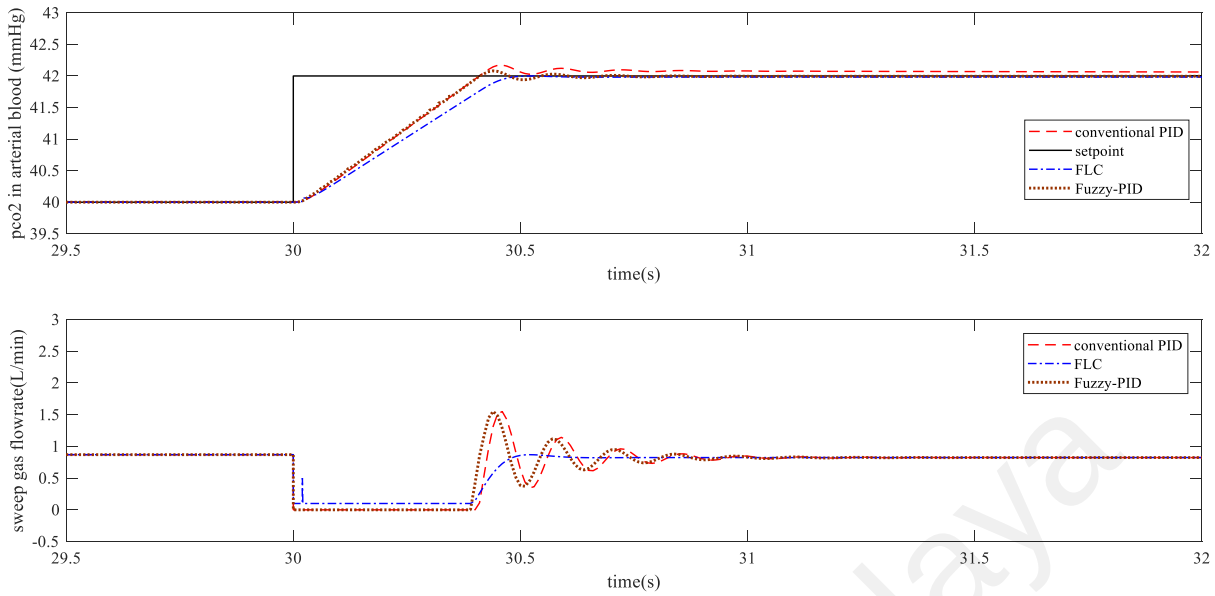

Figure 4.23: Comparison of simulated pCO_2 for different type of controllers for setpoint tracking, zoomed view at t=30s (upper part: response of process variable (simulated pCO_2), lower part: controller output (sweep gas flow rate)).

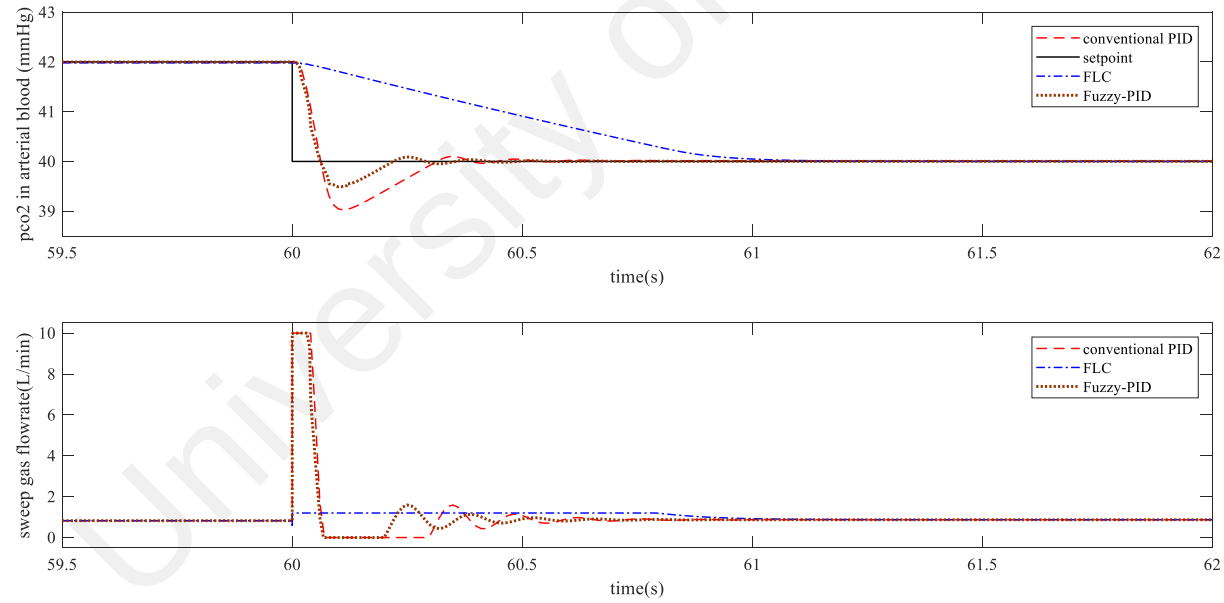

Figure 4.24: Comparison of simulated pCO_2 for different type of controllers for setpoint tracking, closed-up at t=60s (upper part: response of process variable (simulated pCO_2), lower part: controller output (sweep gas flow rate)).

Table 4.6: IAE, ISE, ITAE and MSE for different type of controllers for setpoint tracking task (simulation)

Controllers	IAE	ISE	ITAE	MSE
PID	1.20	0.91	48.10	1.41×10^{-2}
FLC	1.97	1.97	96.19	3.6×10^{-2}
Fuzzy-PID	**0.62**	**0.75**	**23.29**	**1.39×10^{-2}**

Based on the quantitative analysis tabulated in Table 4.6, IAE, ISE, ITAE and MSE for Fuzzy-PID was the lowest among the three controllers, with FLC became the worst controller. Based on these findings, it can be concluded that Fuzzy-PID is the best controller among the controllers studied, with 0.62 IAE, 0.75 ISE, 23.29 ITAE and 1.39×10^{-2} MSE.

4.2.2. Closed-loop control: Disturbance rejection

4.2.2.1. PID

The similar observation on overall controllers' performance was seen for disturbance rejection task. For this task, all the controllers were able to bring the arterial pCO_2 back to the desired setpoint after the introduction of external disturbance to the process plant. Figure 4.25 highlights the control performance of PID when the sweep gas flowrate was shut-off for one second at t=30s and t=60s.

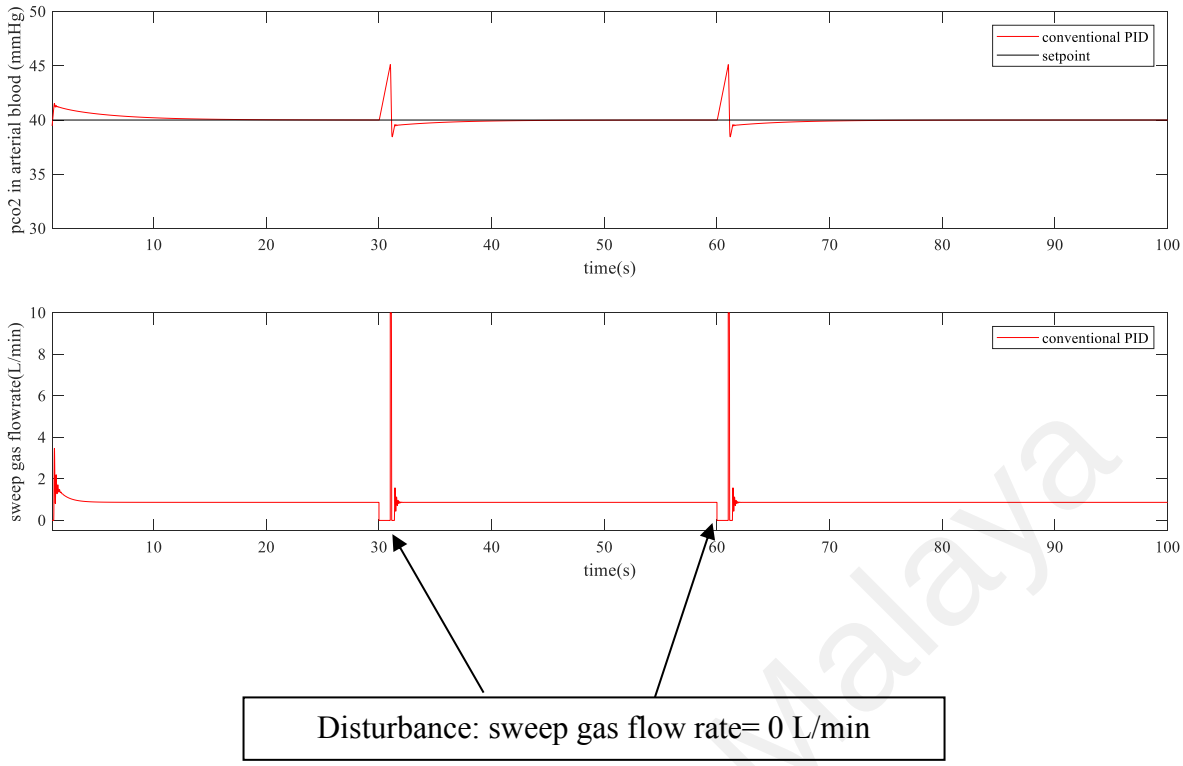

Figure 4.25: Simulated pCO_2 of PID controller for disturbance rejection, (upper part: responses of process variable (simulated pCO_2), lower part: controller output (sweep gas flow rate).

Due to the sudden stop of sweep gas supplied to the process plant, the arterial pCO_2 drastically rose up to 45.117 mmHg, which caused error of 5.117 mmHg, 12.79% higher than the setpoint. The corrective action was taken by this controller, which the maximum sweep gas flowrate (10 L/min) was given to the process plant as the corrective action. After 15 seconds, the PID controller able to bring down the arterial pCO_2 with steady-state error around 0.01-0.02 mmHg. The similar trend was shown by the PID controller at t=60s, when the disturbance was introduced once again to the process plant.

4.2.2.2. Fuzzy Logic Controller (FLC)

Figure 4.26 below is the plotted graph of FLC during the disturbance rejection task. At t=30s, sudden stop of sweep gas supply caused significant affect to the arterial pCO_2, where it increased up to 45.15 mmHg, 12.88% over the desired setpoint, 40 mmHg. Unlike PID which give the maximum flowrate (10 L/min) as its corrective action, controller's output for FLC was 1.2 L/min. This is due to the rule of fuzzy inference for proposed FLC, which 1.2 L/min was set as its highest flowrate (as in Table 4.2). Time taken for this controller to return the arterial pCO_2 back to 40 mmHg was shorter than PID, with only 3.3s needed, which 78% of reduction, compared to PID controller. Unfortunately, the average error for the whole simulation was high for this controller, which was 0.23 mmHg. This occurrence makes FLC less preferable controller compared to the other proposed controllers.

The similar control action was found for FLC during rejecting the second time disturbance at t=60s.

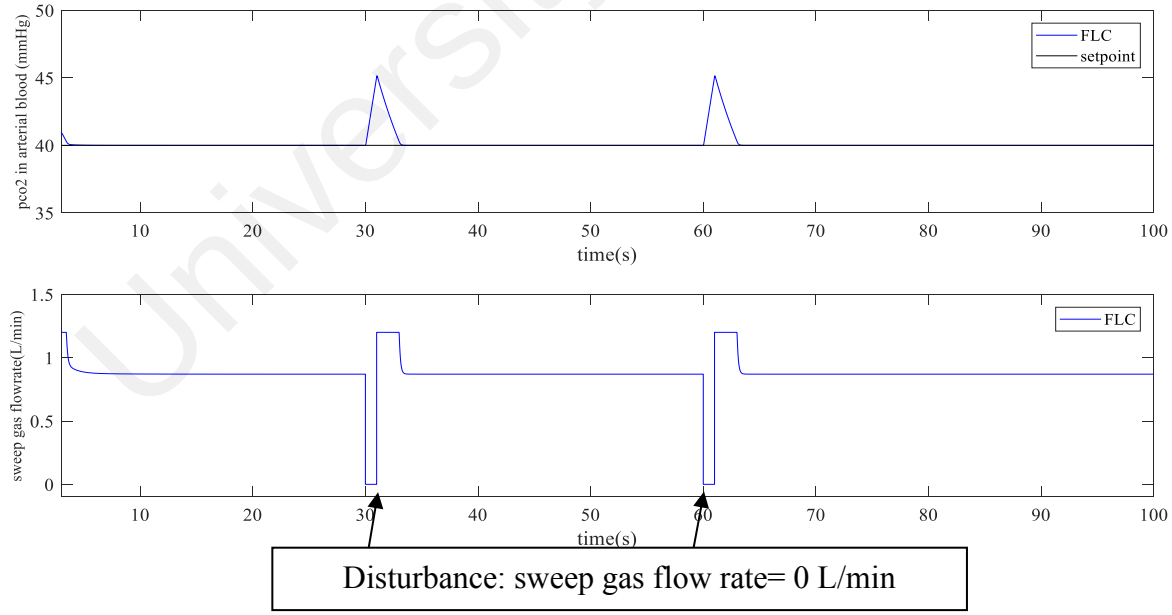

Figure 4.26: Simulated pCO_2 of FLC controller for disturbance rejection (upper part: responses of process variable (simulated pCO_2), lower part: controller output (sweep gas flow rate)).

4.2.2.3. Fuzzy-PID

Response of Fuzzy-PID controllers towards the disturbance introduction to the process plant at t=30s and t=60s was shown in Figure 4.27. The consequence of sudden stop in sweep gas flow was the elevation of arterial pCO_2 up to 45.11 mmHg at both time of event (t=30s and t=60s). To counteract this undesired effect, Fuzzy-PID increased its output to 10 L/min and successfully control the arterial pCO_2 at 40 mmHg after 1.6s. This is very outstanding performance, which reflects its accuracy and effectiveness to control arterial pCO_2 during rejection of the external disturbance to the process plant.

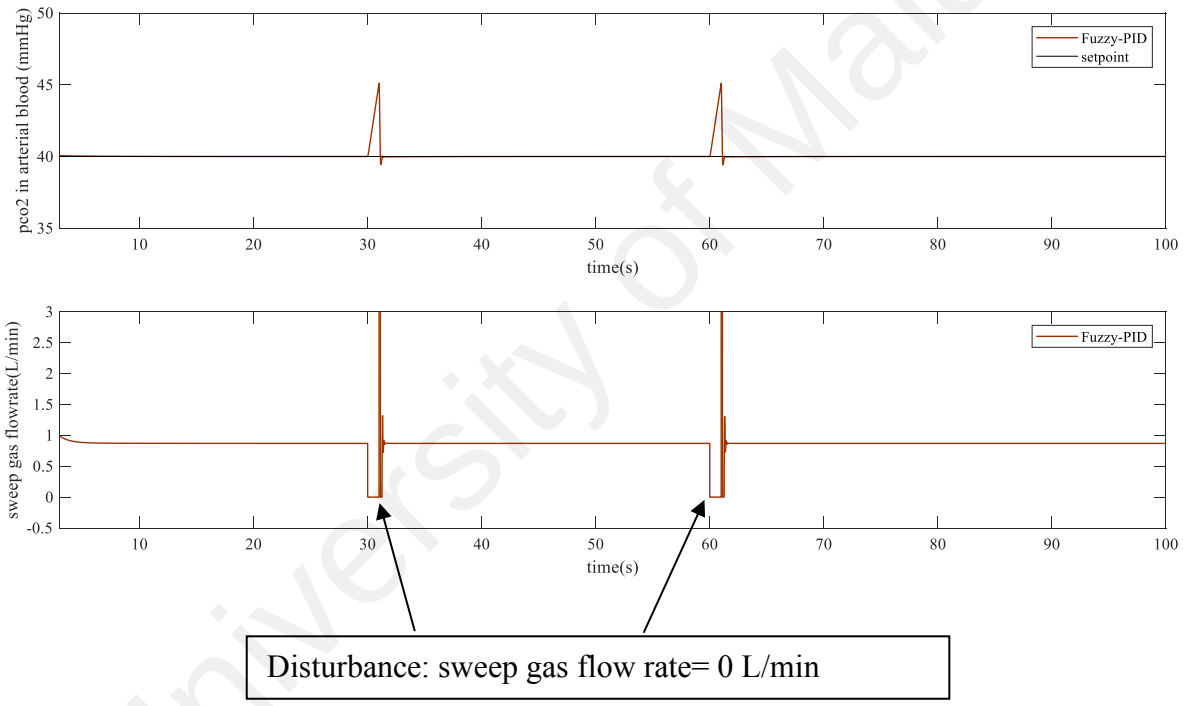

Figure 4.27: Simulated pCO_2 for fuzzy-PID controller for disturbance rejection, (upper part: responses of process variable (simulated pCO_2), lower part: controller output (sweep gas flow rate)).

4.2.2.4. Comparison of simulation between conventional PID, FLC and Fuzzy-PID: Disturbance rejection

Figure 4.28 depicts the effect of disturbance to the controllers and their individual performance to tolerate with the disturbance applied to the process plant. For better analysis, zoomed view of arterial pCO_2 at t=30 s and t=60 s (time where the disturbance was introduced to the process plant) are also included in Figures 4.29 and 4.30, respectively.

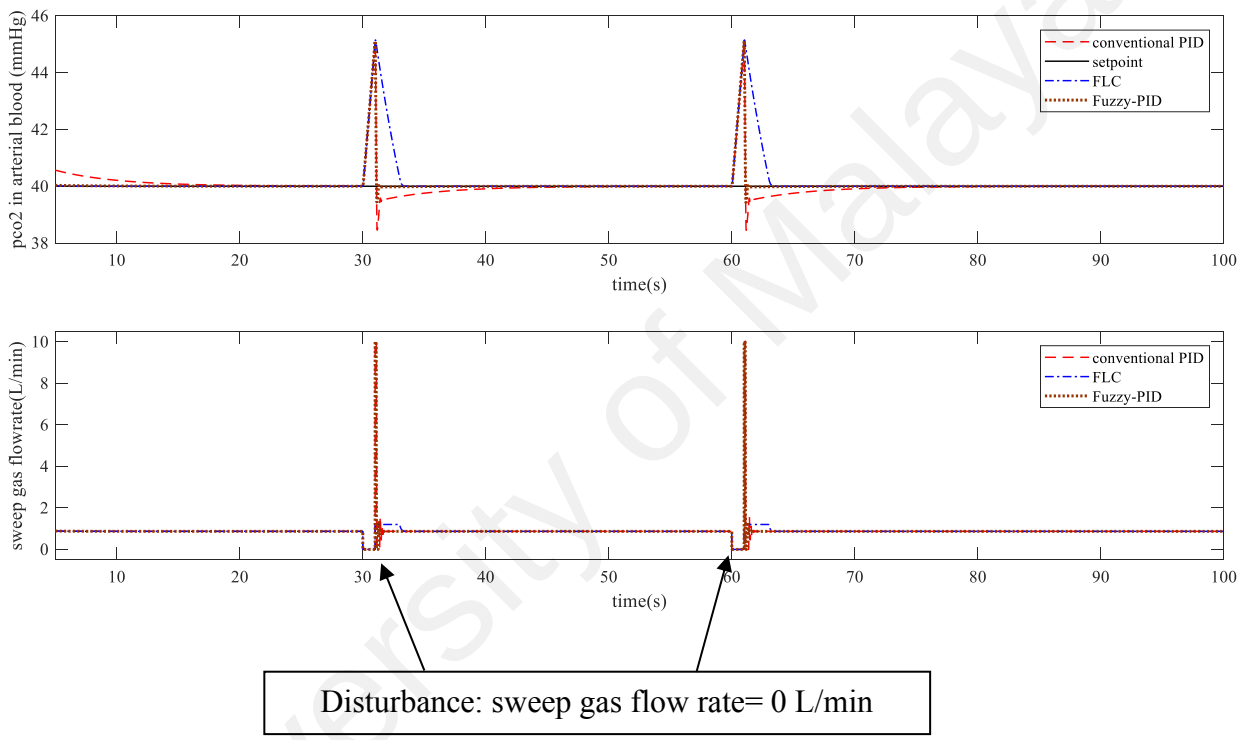

Figure 4.28: Comparison of simulated pCO_2 for different type of controllers for disturbance rejection (upper part: responses of process variable (simulated pCO_2), lower part: controller output (sweep gas flow rate)).

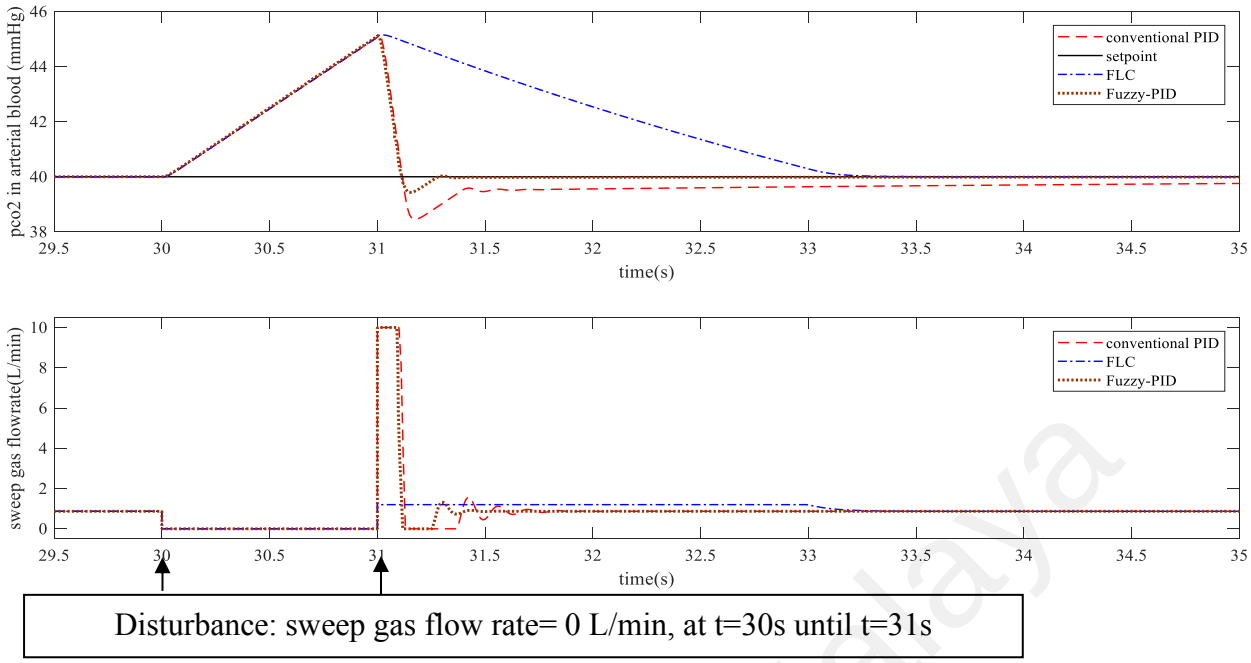

Figure 4.29: Comparison of simulated pCO_2 for different type of controllers for disturbance rejection, zoomed view at t=30s (upper part: responses of process variable (simulated pCO_2), lower part: controller output (sweep gas flow rate)).

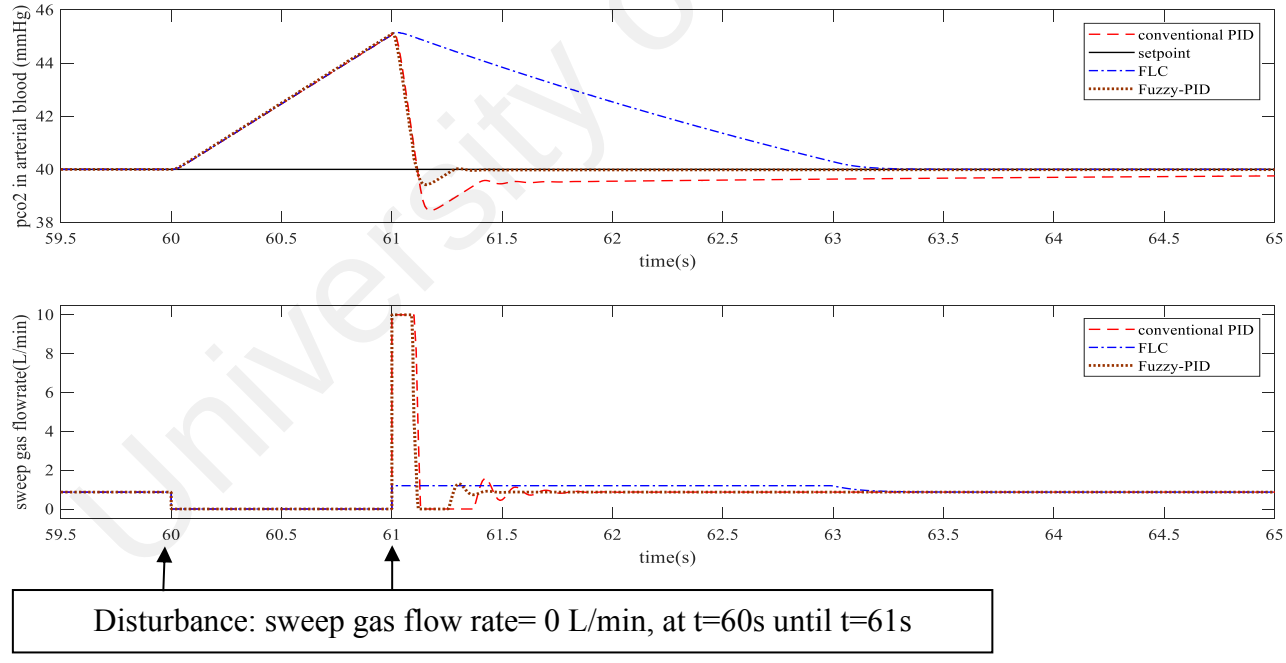

Figure 4.30: Comparison of simulated pCO_2 for different type of controllers for disturbance rejection, zoomed view at t=60s (upper part: responses of process variable (simulated pCO_2), lower part: controller output (sweep gas flow rate)).

Good adaptation of the controllers to disturbance cause process variable (arterial pCO_2) became nearly perfect over the whole simulation period. This indicates the ability of the controller to suit with the applied disturbance, which is the sudden stop of sweep gas supply (sweep gas flowrate= 0 L/min) for 1 second at t=30s and t=60s.

The robustness of controllers was proven by the quantitative analysis in terms of IAE, ISE, ITAE and MSE. These performance indices are tabulated in Table 4.7. Once again, the best control performance is shown by Fuzzy-PID controller, due to its lowest IAE, ISE, ITAE and MSE, with 5.984, 19.49, 274.80 and 0.29, respectively. For IAE, Fuzzy-PID recorded 46.94% lower than PID and 59.45% lower than FLC. For ISE, Fuzzy-PID had 9.90% reduced compared to PID, while 62.77% reduced compared to FLC. On the other hand, for ITAE, Fuzzy-PID obtained 49.53% lessened than PID and 61.71% lessened than FLC. Lastly, for MSE, there was 9.38% of reduction for Fuzzy-PID compared to PID, while 63.29% reduction recorded for Fuzzy-PID against FLC. The trend is similar with set point tracking task, but with higher IAE, ISE, ITAE and MSE. When comparing between these two tasks, it is clearly shown that all the implemented controllers offered better performance and capability to counteract setpoint changing rather than disturbance rejection.

Table 4.7: IAE, ISE, ITAE and MSE for different type of controllers for disturbance rejection task (simulation)

Controllers	IAE	ISE	ITAE	MSE
PID	11.27	21.44	544.50	0.32
FLC	15.48	52.35	717.70	0.79
Fuzzy-PID	**5.98**	**19.49**	**274.80**	**0.29**

4.3. Discussions

This study introduces an alternative method in controlling pCO_2 in hollow fibre membrane oxygenator during extracorporeal life support, which is Fuzzy-PID controller. The results demonstrated three things. Firstly, for any controller, it was proven that CO_2 gas exchange in hollow fibre membrane oxygenator can be automated and controlled by manipulating its sweep gas flow rate.

Second observation is regarding the controllers' performance, which are conventional PID and FLC. Conventional PID has satisfactory performance with some noticeable overshoot and errors in controlling optimum gas exchange during extracorporeal life support, agreed with results that were reported by Dhinakaran and Lincoln (Dhinakaran & Lincon, 2014) and Misgeld et al. (Misgeld et al., 2010).

Compared to previous arterial pCO_2 control of extracorporeal blood-gas exchange, good results were achieved for this study. Misgeld et al. (Misgeld et al., 2008) used the same mathematical model as adopted in this study, but PI controller was employed to control pCO_2 in cardiopulmonary bypass system. From their reported results, during setpoint tracking task, PI controller had successfully maintained the pCO_2 at 38 mmHg with error during overshoot of 2 mmHg. On the other hand, the maximum error for PID controller recorded in this study for setpoint tracking task is only 0.08 mmHg above the setpoint. For disturbance rejection task, change in blood flow was used as the disturbance, and these authors (Misgeld et al., 2008) reported error of 2 mmHg, lower at 60.91% than error obtained by PID controller for this study (5.117 mmHg). This discrepancy may due to the type of the disturbance applied between previous and this study.

In addition, with the benefits of FLC in this context, which ease the integration of knowledge from trained perfusionist to control decision, several researchers (Dhinakaran & Lincon, 2016; Mendoza et al., 2010) had successfully controlled gas exchange in membrane oxygenator within the nominal value, agreeable with findings in this study. Together, these satisfactory performances motivate the integration of both methods in one control system, by the means of Fuzzy-PID.

Next, results also demonstrated that Fuzzy-PID controller became the best and most robust controller for both set point tracking and disturbance rejection tasks. This finding validates the second hypothesis of this study. Robustness in context of this study is defined as the ability of the controller to tolerate with any change in process plant without disturbing the stability of feedback system. Even there is no evidence reported yet for Fuzzy-PID in controlling pCO_2 in hollow fibre membrane oxygenator, it has been successfully applied in different case of nonlinear system (Fereidouni et al., 2015; Kazemian, 2005; Kim & Oh, 2000; Y. Tao et al., 2015) and been advocated as the best controller compared to conventional PID for respective area of studies.

In PID controller, a perfect tuning of PID parameter is very crucial, since the performance of this controller depends heavily on values of P, I and D. This occurrence was explained in detail by Ogata (Ogata, 1997), regarding the effect of proportional, integral and derivative control action. In proportional control alone, there was an offset or steady state error in response to a step input. In order to remove the offset, integral control action is normally introduced. Unfortunately, while removing the offset, an undesirable oscillatory response occurred, which make it insufficient for this case of study. With derivative control action (as in PID), damping was added to the system, thus permits the use of larger value of K_p. This will result in an improvement in steady state accuracy. The advantage of derivative control action is, its

response to rate of change of the actuating error, so that it can initiates a significant correction before the error magnitude becomes too large. With this, derivative control action then anticipated the actuating error, produce an early corrective action and able to improve the stability of the system. Thus, the perfect tuning is intended to be achieved in our proposed Fuzzy-PID controller. Using the fusion of human experience and knowledge, fuzzy logic mechanism is dedicated to measure the error that results from PID controller and alter its gain in order to reduce output errors. Consequently, based on the gain that been tuned by fuzzy logic, PID works accordingly to these three control behaviours (P, I, D) to produce the desired control action.

A conventional PID controller is a simple and reliable, but its parameters (P, I and D) cannot automatically adjust themselves according to the system's changes, since it has no knowledge about the process plant. These parameters have to be manually adjusted in order to improve its performance and will lead to serious error if not being tuned properly. Since PID is a linear and symmetric type of controller, hence its performance is varying in non-linear system (Visek et al., 2014). Unfortunately, CO_2 gas transfer that is simulated in this mathematical modelling is highly non-linear, due to the chemical binding of O_2 and CO_2 that exist within the blood. This constraint motivates the consideration of another controller that can deals with this case study. Since it was proven in the literatures that PID can be very efficient if being tuned properly, the only solution to improve its performance in dealing with non-linear model is to fusion it with another decision-maker controller that is robust in classifying the system's state. This controller is intended to adjust the parameters of PID controller based on the error that is calculated on-line. Thus, fuzzy logic seems to suit this purpose due to its qualities, robustness and good adaptation to non-linearity and disturbance. Furthermore, the suitable of fuzzy logic in dealing with non-linearity of blood's parameter also was proven by Mendoza et al. (Mendoza et al., 2010) and Schreiber et al. (Scheiber et al., 2009) in their respective work. The fusion between

PID and fuzzy logic controllers then is developed and named as 'Fuzzy-PID' in this study, which have self-tuning ability and on-line adaptation to nonlinear, time varying, and uncertain system. In order to highlight its advantages, the performance of this controller then is compared with the conventional and FLC controller, when they are used alone.

In this study, a mathematical modelling of CO_2 gas exchange in membrane oxygenator is developed in simulation manner via MATLAB/SIMULINK environment. A simulation work is an essential during the development of a proposed controller, especially for medical device. There are manifolds advantages of simulation work prior to experimental activity, such as eliminate the risk of failure that might be happened in the experimental setting, allows verification of the controller software and provide experience to the operator on control process. In fact, the capability of stopping a simulation when required by operator without significant effect to the process plant also allows the correction and optimization of the implemented control strategy. These are the reasons why the simulation work was conducted prior to experimental work in this study.

4.4. Summary

To summarize this chapter, it can be said that overall performance of all the proposed controllers are very outstanding, with Fuzzy-PID as the best controller for both setpoint tracking and disturbance rejection. This can be seen from its lowest performance indices and the time taken to achieve the setpoint, which Fuzzy-PID is lower by 21.15% compared to PID and 65.25% lower compared to FLC during setpoint tracking task. For disturbance task, Fuzzy-PID recorded the fastest time to adapt with the disturbance, which 89.33% and 51.52% faster than PID and FLC, respectively. These findings motivate the next steps, which is the implementation of the similar control strategy experimentally, in means of in-vitro gas exchange module bench setup.

CHAPTER 5: CONTROL OF CARBON DIOXIDE GAS EXCHANGE IN MEMBRANE OXYGENATOR: EXPERIMENTAL WORK

5.0. Introduction

In previous chapter (Chapter 3 and Chapter 4), simulation works conducted proved that arterial pCO_2 can be controlled by manipulating gas flowrate that been supplied to the process plant. Overall, all the proposed controllers (PID, FLC and Fuzzy-PID) are able to control CO_2 gas transfer in membrane oxygenator with Fuzzy-PID is the best controller among the three. These findings validate both hypotheses highlighted in this study, thus allow further step of this research, which is the online implementation of proposed automatic control system to the real process plant. Online implementation is important in order to validate the previous simulation results and prove that the proposed strategy is able to work in real implementation. This experimental work will be discussed in details throughout this chapter.

5.1. Design of in-vitro gas exchange module in bench top setup

The automatic control system that developed in this study consists of several important aspects, namely desired setpoint, pCO_2 sensor, actuator (mass flow controller), process plant (membrane oxygenator), and process variable measurement (arterial pCO_2). The diagram of closed-loop feedback system implemented in experimental work of this study is illustrated in Figure 5.1.

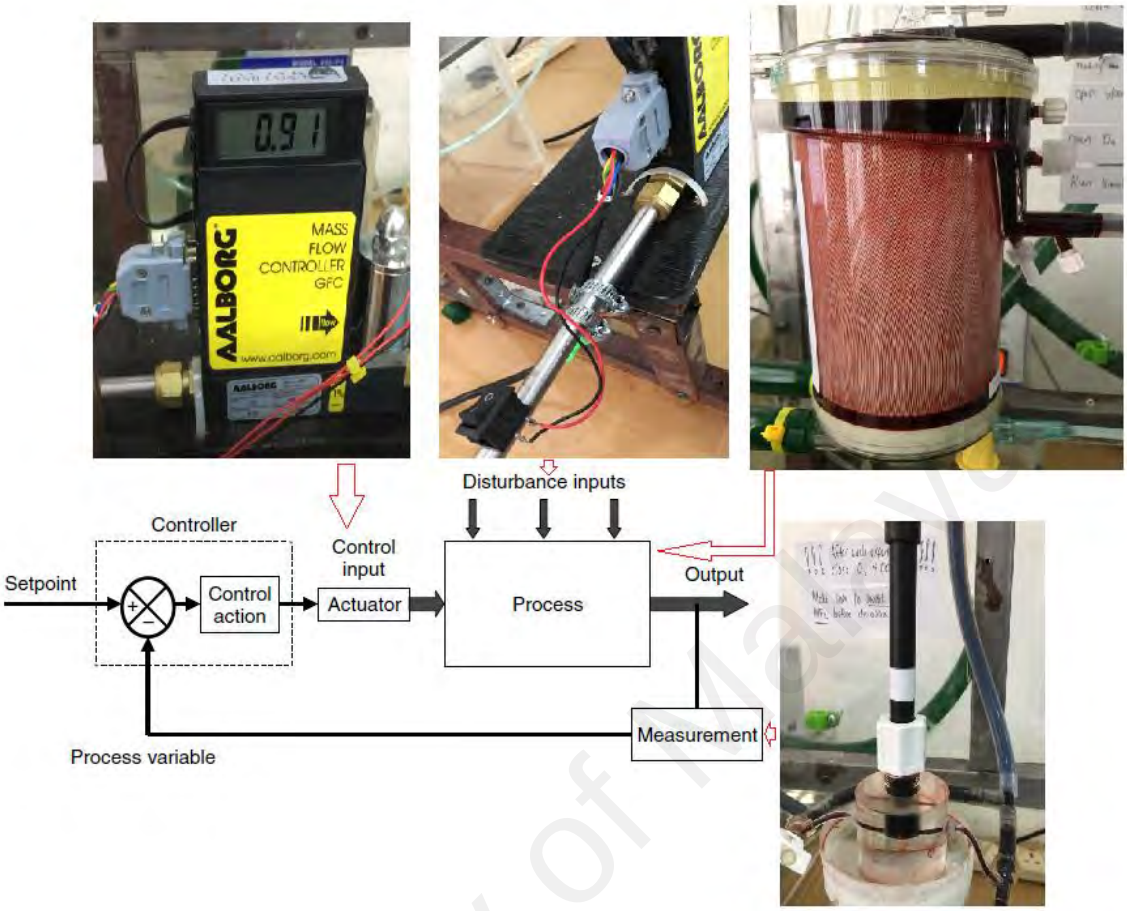

Figure 5.1: Structure of closed loop control system (experimental study).

The schematic design of the in-vitro gas exchange module that been used in experimental work of this study is shown in Figure 5.2 and the actual experimental component arrangement is highlighted in Figure 5.3 The main components for this experimental setup are the membrane oxygenator (process plant), de-oxygenator, DAQ, pCO_2 sensors and Mass Flow Controller (MFC). The details of these components will be described in the next sections.

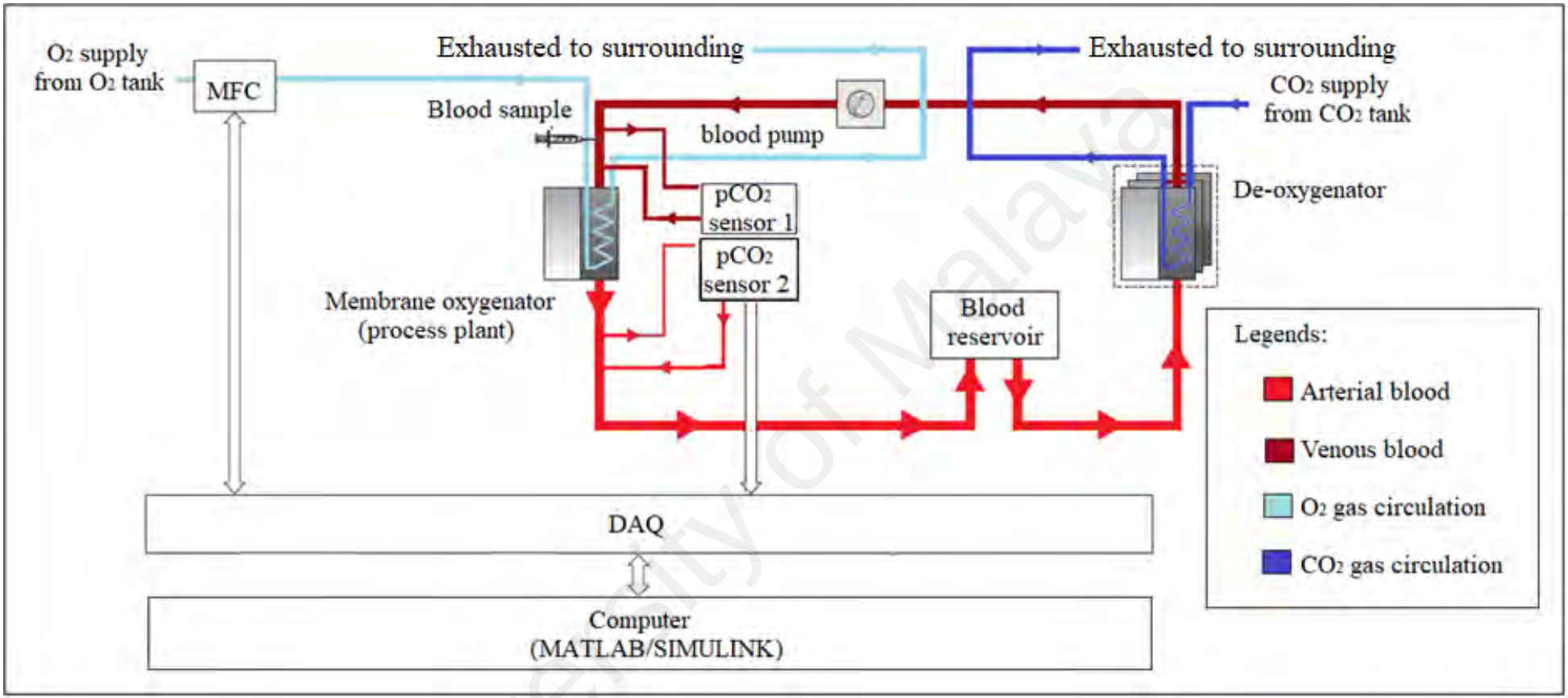

Figure 5.2: Design of in-vitro gas exchange module in bench top setup.

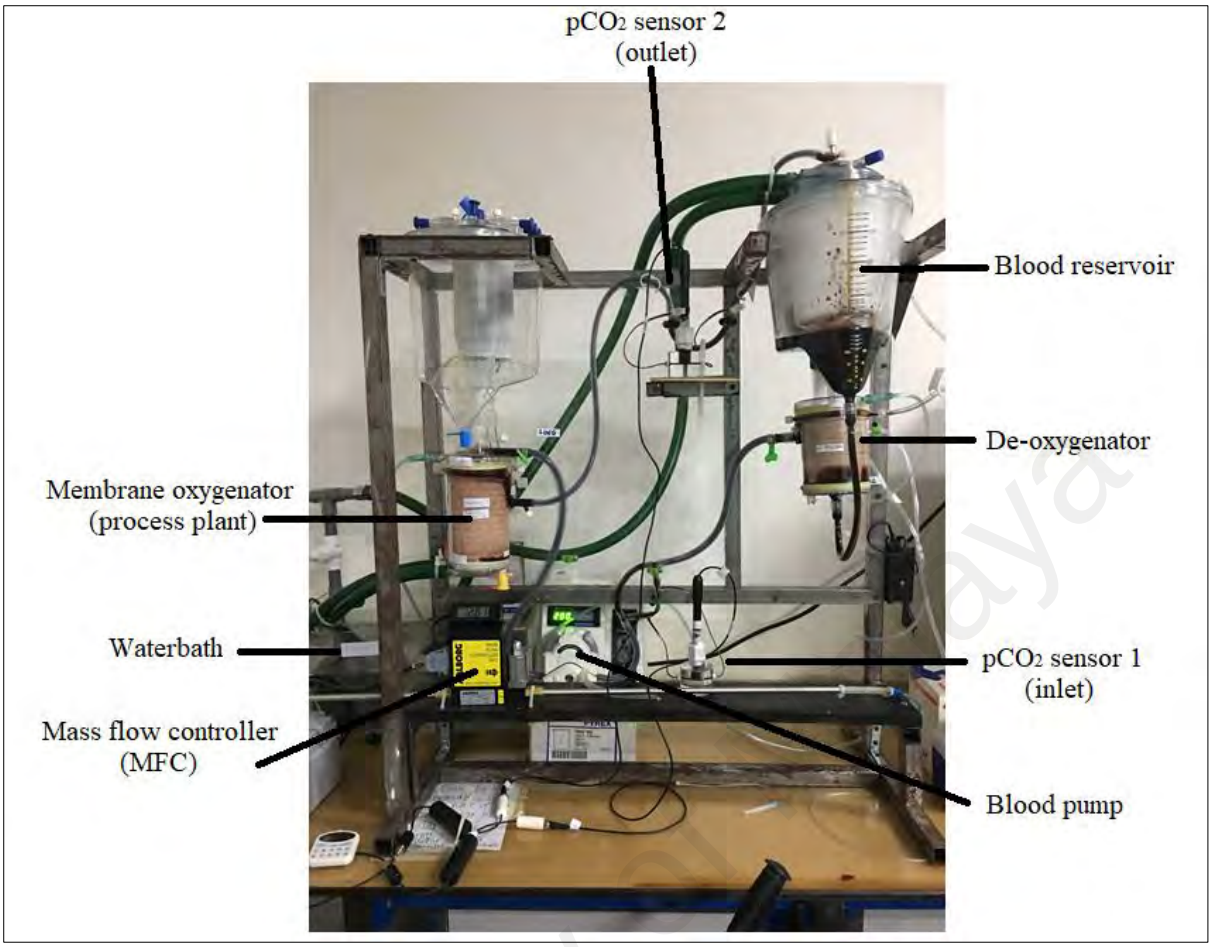

(a)

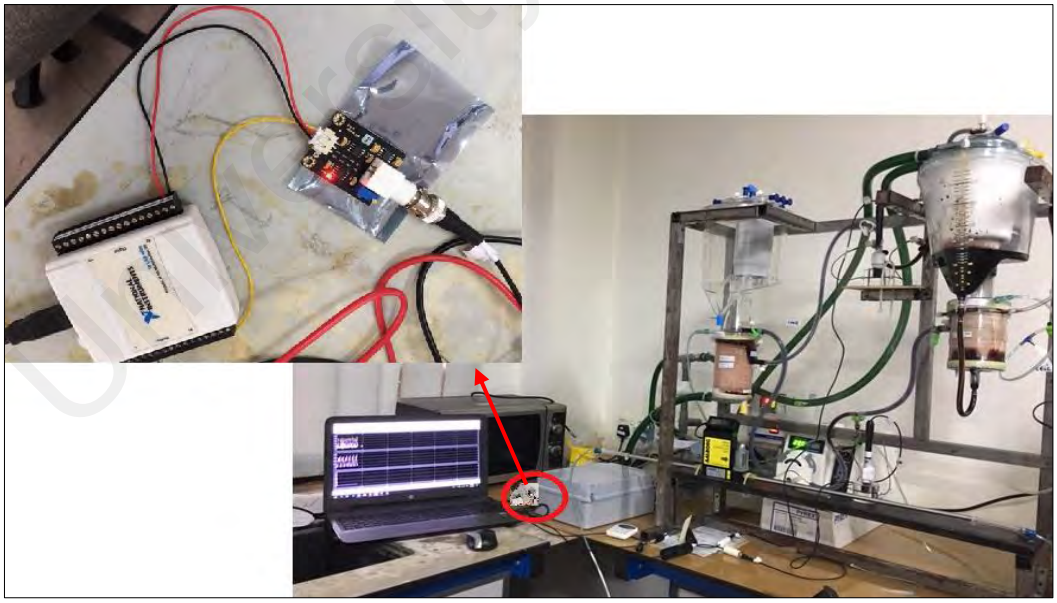

(b)

Figure 5.3: (a) Complete experiment set-up and (b) placement of unit of controllers (DAQ and computer).

5.1.1. Membrane oxygenator (process plant)

Membrane oxygenator for this experimental work functions as the process plant, a place where the gas exchange process occurred (as in Figure 5.4). In this device, CO_2 gas will be removed from the blood, while O_2 will diffuse into the blood by diffusion through a membrane that is permeable to gases. The blood and gas phase are separated by the hydrophobic hollow fibre membrane (in this study, hollow fibre membrane is made of polypropylene), so that there is no direct contact exist between blood and sweep gas flow.

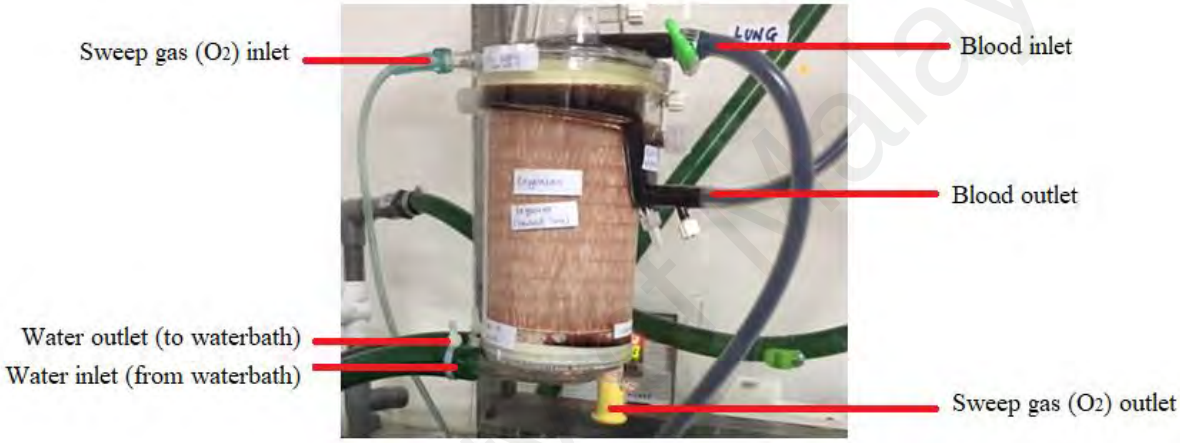

Figure 5.4: Gas exchange process within hollow fibre membrane oxygenator.

In this study, the hollow fibre membrane oxygenator used is Medos Hilite 7000. This membrane oxygenator was selected due to its good performance reported in previous studies by Brendle et al. (Brendle et al., 2017) and Kopp et al. (Kopp et al., 2016). In addition, its effectiveness in CO_2 gas exchange process was tested and validated by Sun et al. (Sun et al., 2018) among four similar different devices (Capiox, Quadrox, Hilite and Novalung, iLA) using 100% of O_2 as ventilating gas.

The arrangement and direction of blood, water and gas can be found in Figure 5.5.

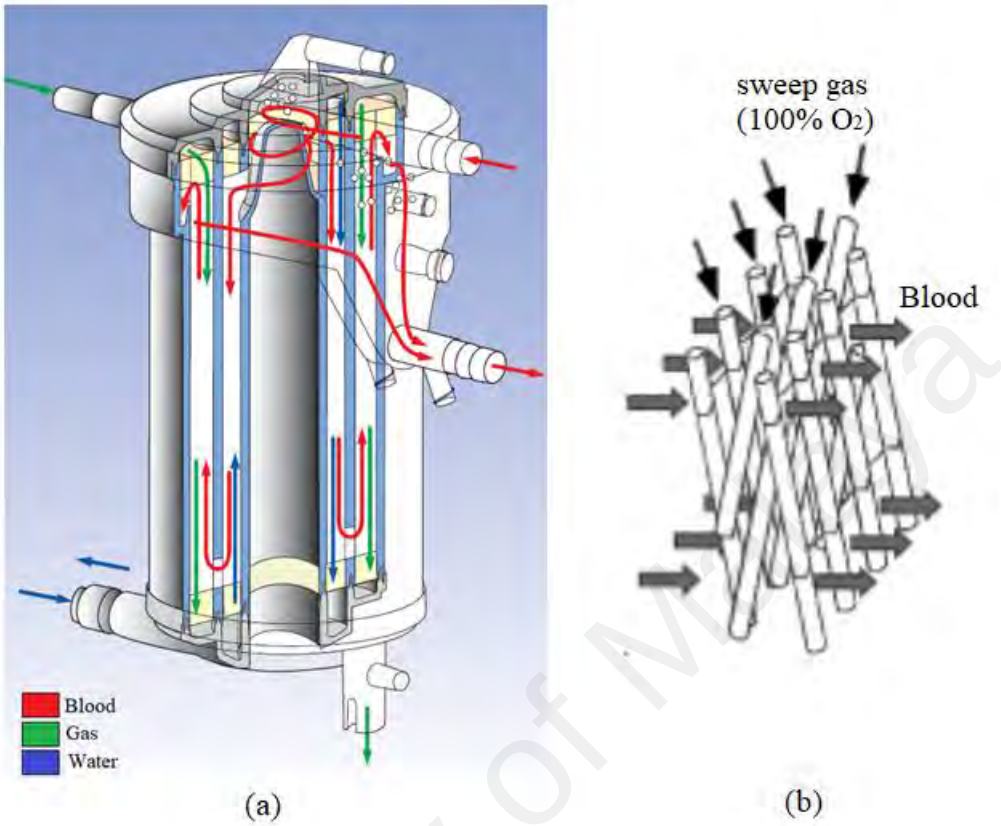

Figure 5.5: (a) Configuration of blood, gas and water direction in Hilite 7000 and (b) counter-current direction inside membrane oxygenator.

From Figure 5.5, sweep gas (100% O_2) and blood flows in counter-current direction inside the membrane oxygenator. This counter-current direction is the main reason why Hilite 7000 is chosen for this study, since the counter-current gas-blood flow allows a constant driving force for gas diffusion, in addition to its longer fibre length. Furthermore, water from water bath, which the temperature is constantly maintained at 37 $^oC\pm$ 2 ^oC enters the membrane oxygenator via the dedicated component for heat exchanger in order to regulate the water temperature at 37^oC. The specifications of this membrane oxygenator are tabulated in Table 5.1.

Table 5.1: Specification of membrane oxygenator used in this study (HILITE 7000).

Components	Specification	Values and units
General	Blood flow rate	1-7 L/min
	Static priming volume	275 ml
	Number of hollow fibres	5000
	Inner/outer module diameter	95/85 mm
	Module length	160 mm
Gas exchanger	Material	Polypropylene
	Type	Microporous Hollow fibre
	Internal diameter/outer diameter	280/380 μm
	Surface	1.9 m^2
Heat exchanger	Material	Polyester
	Type	Hollow fibre
	Surface	0.45 m^2
Port configuration	Blood inlet/outlet	3/8" / 3/8"
	Gas inlet/outlet	1/4" /3/8"
	Water inlet/outlet	3/8", Hansen type coupling

5.1.2. De-oxygenator

In this in-vitro experimental setup, membrane oxygenator (process plant) was coupled to a de-oxygenation device (another membrane oxygenator which functions to de-oxygenate the blood). This device is used to emulate the patient respiration process during the application of ECLS, which involved blood de-oxygenation and carbonation effect of the human body. It was

vented with CO_2 gas and had its own gas supply circulation. The de-oxygenation device was adjusted by flow controller to meet venous pCO_2 conditions, a similar parameter that been used in simulation work, 46 mmHg. This parameter was monitored by the mean of pCO_2 sensor that located at the inlet of the membrane oxygenator (process plant), which was labelled as pCO_2 sensor_1 in previous Figure 5.2.

5.1.3. DAQ device

In this experiment work, DAQ device National Instruments USB 6009 was selected as data acquisition method of the process. This device was used together with Data Acquisition Toolbox, which can be found in MATLAB 2016b or newer. It provides eight single-ended analog input (AI) channels, two analog output (AO) channels, 12 DIO channels, and a 32-bit counter with a full-speed USB interface. The main reason to employ this device in this study is due to its simplicity to be installed, based on its plug-and-play capabilities. This device also is easy to use and user-friendly, since it can incorporate well with MATLAB/SIMULINK. In this experiment setup, 3 analog inputs are acquired (2 from pCO_2 sensors, 1 from MFC) and 1 analog output signal is generated to the MFC, as depicted in Figure 5.8. The output signal from controller that generated to the MFC makes the arrow pointed in to Dev1 (ao1).

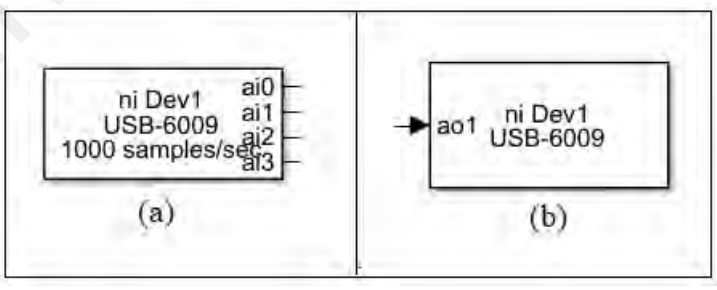

Figure 5.6: Simulink block for (a) analog input and (b) analog output.

During the SIMULINK implementation, Measurement and Automation Explorer (MAX) programme was used to control DAQ device since it is a data acquisition driver. This MAX programme also functions to test the DAQ, reset it and adjust the characteristics of this device

(Benic et al., 2014). The sampling time for DAQ is 1000 samples/sec. Figure 5.9 below shows signal flow chart for feedback control system using DAQ as an interface between computer and hardware (pCO_2 sensors and MFC).

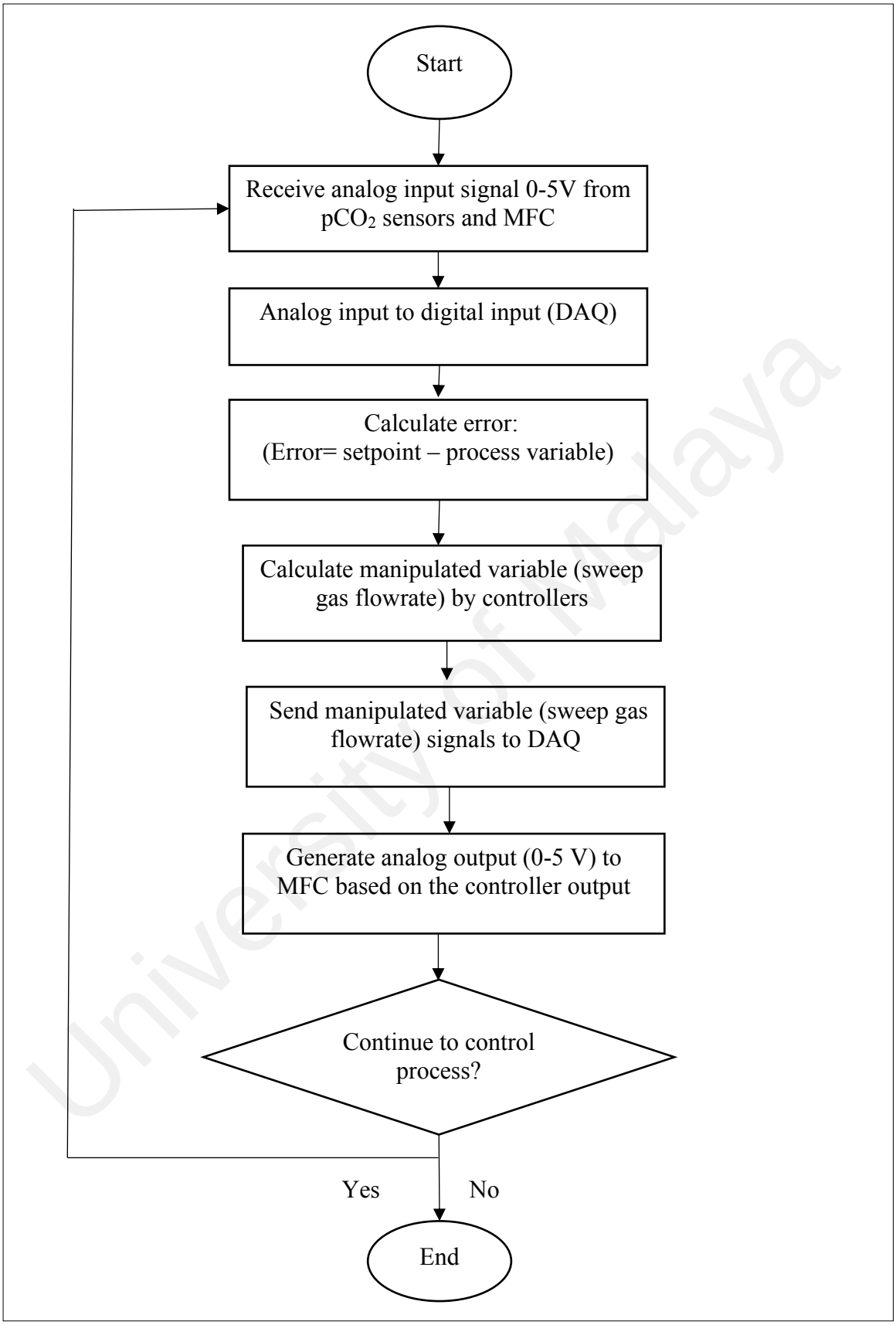

Figure 5.7: Signal flow diagram for feedback control system.

5.1.4. Calibration of sensors and actuator

There are two sensors used in this in-vitro bench setup, which are pCO_2 sensor at the inlet of the process plant (membrane oxygenator) and one actuator to control the sweep gas flowrate (manipulated variable), which is MFC.

5.1.4.1. Calibrating pCO_2 sensor

The pCO_2 sensors (as in Figure 5.8) that been used in this study is Lazar flow-through pCO_2 sensor, Model GS-136-COFT from Lazar Research Laboratories, United States of America.

Figure 5.8: Blood flow-through pCO_2 sensor.

These sensors have been used in many previous studies to determine pCO_2 in blood/aqueous biological sample, as in (Bian & Chang, 2015; Bian et al., 2013; Findlay et al., 2008). The calibration was conducted to determine the relationship between millivolts and $CaCO_3$, since

standard used for this calibration is 1000 ppm as $CaCO_3$. Then, this will be converted into mmHg (pCO_2).

Checking electrode operation method:

1. The electrode was connected to a multimeter.
2. 100 ml of deionised water was placed into a 150 ml beaker. 1ml ISA was added and pH of the water was checked using pH paper (the pH value was maintained between 4.0-4.5. otherwise, ISA was added with 1ml increment until the pH value is between 4.0-4.5).
3. The electrode tip was rinsed and was blotted dry. Then, the tip was immersed into the prepared solution by 1" in depth. To prevent air entrapment on the membrane surface, electrode holder was used to keep the electrode at 20 degree of angle. The multimeter was switched on and left to mV mode.
4. 1 ml if 1000 ppm as CO_2 standard was added into the beaker. The solution was stirred thoroughly, and the potential (E1) was recorded when a stable reading is obtained.
5. 10 ml of the same standard was then pipetted into the same beaker, then stirred thoroughly. The potential (E2) was recorded in mV when the stable reading is achieved.
6. The difference between E1 and E2 (E1-E2) was defined as the slope of the electrode. The normal slope is 56 ± 4mV at 25 ^oC, the slope that beyond this range indicate that the electrode is not functioning well and must be troubleshoot.

Reading the sample with the electrode (millivolts versus concentration):

1. The electrode was connected to DAQ input port.
2. Calibration standards were prepared based on serial dilution method that been described in the next section.

3. Measure 100 ml of 1 ppm standard into 150 ml beaker. 1 ml ISA was added and stirred thoroughly. pH of the standard was checked using pH meter, which must be between 4.0 -4.5.
4. The electrode was rinsed using DI water, blotted dry and was placed into the beaker. When the stable displayed was achieved, the potential reading was recorded (in millivolts) and also the corresponding standard concentration.
5. Repeat steps 3 and 4 with standard solution 10 ppm and 100 ppm (Figure 5.12).
6. Using MATLAB, a calibration curve (semi logarithmic) was prepared by plotting the millivolts values on the linear axis and concentration value standards on the logarithmic axis.

5.1.4.2. Serial dilution of calibration standards:

Since CO_2 standard that been used in this study comes in very concentrated form (1000 ppm as $CaCO_3$), the dilution process was conducted to produce calibration standard of 100 ppm, 10 ppm and 1 ppm. In this case, dilution refers to the process of adding deionized water (act as solvent) to 1000 ppm as $CaCO_3$ standard to decrease its concentration. This was done using volumetric flask (100 mL) for precise dilution process.

In this process, the amount of solution will remain constant, but its final concentration was reduced by adding the deionized water. For this purpose, serial dilutions were performed which involved dilution of standard solution multiple times in a row. Thus, a ten-fold dilutions factor was remained constant to make an exponential decrease in concentration: 1000 ppm, 100 ppm, 10 ppm, 1 ppm.

By using the equations above, a serial dilution of 1000 ppm to 1 ppm was prepared using equation:

$$V_{stock}\ C_{stock} = V_{desired}\ C_{desired} \quad [5.1]$$

V_{stock} is volume of standard being used (to be diluted).

C_{stock} is concentration of standard being used (to be diluted).

$V_{desired}$ is volume of desired calibration standard.

$C_{desired}$ is concentration of desired calibration standard.

The calculations of serial dilution are shown as below:

Using 1000 ppm as $CaCO_3$ to prepare 100 ppm as $CaCO_3$:

Standard to be diluted:		Desired calibration standard:
$V_{stock}\ C_{stock}$	=	$V_{desired}\ C_{desired}$
1000 ppm. x	=	100 ppm. 100 ml
x	=	10 ml

From 100 ppm as $CaCO_3$, the calibration standard was diluted to 10 ppm as $CaCO_3$:

Standard to be diluted:		Desired calibration standard:
$V_{stock}\ C_{stock}$	=	$V_{desired}\ C_{desired}$
100 ppm. x	=	10 ppm. 100 ml
x	=	10 ml

10 ppm as $CaCO_3$ then was diluted further to 1 ppm as $CaCO_3$calibration standard:

Standard to be diluted:		Desired calibration standard:
$V_{stock}\ C_{stock}$	=	$V_{desired}\ C_{desired}$
10 ppm. x	=	1 ppm. 100 ml
x	=	10 ml

The calculation above are summarized in Table 5.2:

Table 5.2: Preparation of standard for different concentration (ppm).

Solutions (standards)	Desired concentration (ppm)	Method of preparation
A	100 ppm standard	10 ml (1000 ppm as $CaCO_3$ standard) was put into a beaker, then deionised water was added until total volume in the beaker become 100 ml.
B	10 ppm standard	10 ml (100 ppm as $CaCO_3$ standard) was put into a beaker, then deionised water was added until total volume in the beaker become 100 ml.
C	1 ppm standard	10 ml (10 ppm as $CaCO_3$ standard) was put into a beaker, then deionised water was added until total volume in the beaker become 100 ml.

There are three main reasons why serial dilutions are selected in this study, despite of direct dilution from 1000 ppm as $CaCO_3$:

1. To reduce error in dilution. Using serial dilution, the measurement of known concentration (1000 ppm) is only one time, while each following calibration standard comes from the previous one. As a result, the absolute size of error in each standard getting smaller and smaller as the concentration drops. For example, if we want to directly dilute 1000 ppm as $CaCO_3$ to 1ppm calibration standard, even an extra volume of 0.01 ml 1000 ppm as $CaCO_3$ (due to error in volume measuring) will cause a significant error to desired calibration standard. On the other hand, when using serial dilution from 10 ppm to 1 ppm, an extra volume of 0.01 ml 10 ppm as $CaCO_3$ (due to error in volume measuring) do not has great effect, compared to direct dilution from 1000 ppm as $CaCO_3$.

2. For faster and easier calibration process

   The calibration standard was prepared in continuation from the previous calibration standard, thus the amount of preparation time can be reduced. Furthermore, the error that introduced with each successive dilution drops will become proportional with solution concentration, thus increasing the accuracy of the prepared calibration standards.

3. To reduce the usage of 1000 ppm standards

   Since only 10 ml of 1000 ppm as $CaCO_3$ was used in serial dilutions, the usage of this standard can be reduced, so that the standard can be used in many times of calibration process.

5.1.5. Configuration of MFC

Mass flow controller that been used in this study is AALBORG GFC17. To configure this:

1. All the power cable was turned off. This is the main precaution to power off the MFC while connecting cable or any wiring activity conducted.
2. The mass flow controller was wired as shown in Figure 5.14:
   i. Pin 8 & 10 was connected to output of DAQ
   ii. Pin 5 & 7 was connected to power supply.
   iii. Pin 3 and 12 was connected for valve off control. This is to close the valve without changing the setpoint. This will be used to create the disturbance to the system during disturbance rejection task. A toggle switch is located between pin 3 and 12, so that the use of this function can be controlled by the user.

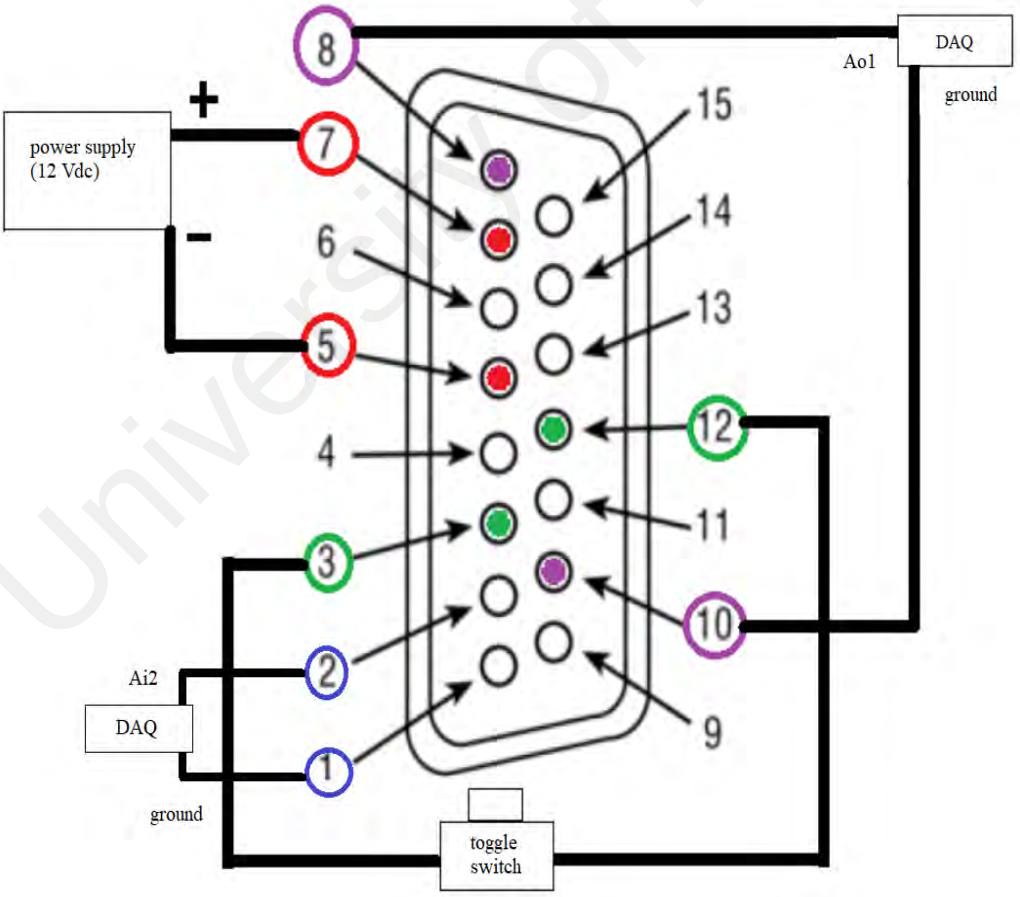

Figure 5.9: Wiring of MFC

3. The mass flow controller that was used is pre-calibrated. Based on the calibration certificate provided by manufacturer. This pre-calibration was made for O_2 gas, since the sweep gas that been supplied to the MFC is 100% O_2. Voltage in Table 5.3 represents the voltage to be supplied to the MFC in to produce the respective gas flowrate.

Table 5.3: The gas flowrate and its respective voltage, according to manufacturer's manual.

Gas flowrate (L/min)	Voltage (volts)
0.000	0.002
2.510	1.253
5.010	2.505
7.510	3.756
10.020	5.009

4. This calibration curve was inserted into the MATLAB (curve fitting tool) to find the mathematical relationships between voltage and flowrate (see Figure 5.15). As the result, the mathematical equation for this calibration curve is:

$$f(x) = 0.4999*x + 0.0006017 \quad [5.2]$$

Where, x is the flowrate and f(x) is the voltage.

5. This mathematical equation was used in the SIMULINK model to convert the flowrate into the voltage. This is the output signal that been transmitted to the MFC from the DAQ.

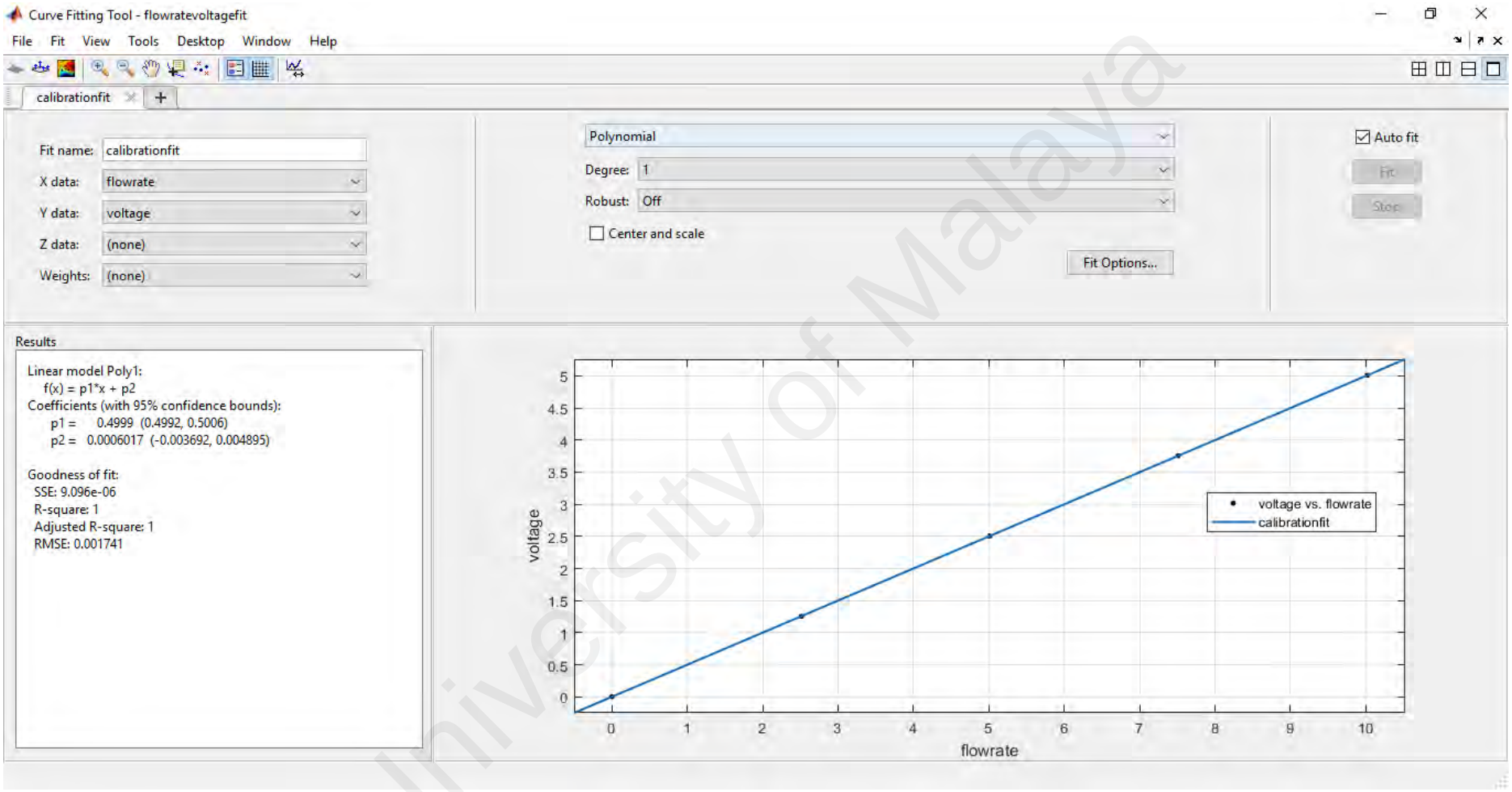

Figure 5.10: Calibration curve for flowrate-voltage relationship for mass flow controller, as specified by manufacturer (Aalborg Inc.).

5.1.6. Water temperature control and sample blood

All in-vitro tests were conducted using fresh bovine blood, and Na-heparin was used as the anticoagulant. To maintain the blood temperature at 37 ± 2°C, water bath was connected to blood reservoirs, which were connected to the heat exchanger. Five minutes after the blood circulation loop was activated, blood temperature was measured. Then the temperature was monitored for every 5 minutes until the end of the experiment (as in Figure 5.11).

Figure 5.11: Blood temperature monitoring.

5.1.7. Signal filtering

For signal filtering, the Butterworth filter is selected and the block diagram for this filter in SIMULINK is displayed in Figure 5.12. There are many selections for this filter, such as filter type, filter order and passband edge frequency (refer to Figure 5.13).

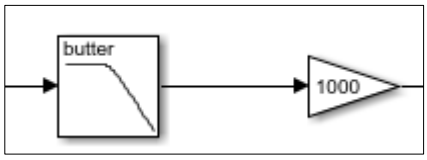

Figure 5.12: Block diagram of butterworth filer in SIMULINK.

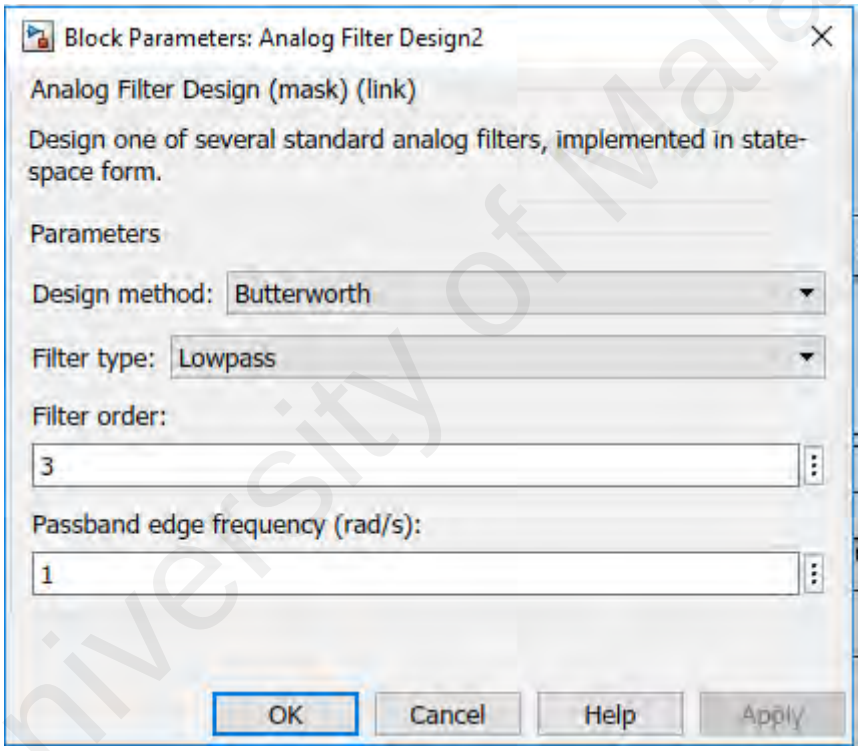

Figure 5.13: Options in Butterworth filter.

The use of filters in controllers is the most common and extensively used throughout a control system. They are used to for difference purpose, such as noise removal, aliasing reduction and resonance calming. In this study, Butterworth low-pass filter is chosen due to its advantage, which it does not have perking. It also known as maximally flat filters, since it has the sharpest roll-off possible without inducing peaking in the Bode plot for any given order (Ellis, 2012).

5.2. Methodology

This section contains the explanation on methodology that were implemented during the experimental work, in three basic aspects, which are open loop control, closed loop control (setpoint tracking) and closed-loop control (disturbance rejection).

5.2.1. Open loop control

An open loop system is also known as non-feedback system, is a type of continuous control system that the input signal has no effect or any influence on the output signal. In this system, the process output is not being measured to be fed back for the comparison with the input. This system is expected to faithfully obey the input command regardless of the final process output result. Since it has no knowledge of the output condition, this system cannot self-correct its error, even though the present result measurement drift or have large deviations from the setpoint. In addition of its inability for self-correct any error, it also cannot compensate for any external disturbances to the system.

In this study, five different sweep gas flow rates are applied for open-loop control. The main intention of this open-loop control is to see how the process output (arterial pCO_2 measurement) responds to the change in sweep gas flow rate. Different sweep gas flow rate used for this open-loop control and its respective output voltage that are generated to MFC are listed in Table 5.4.

Table 5.4. The difference of sweep gas flow rate in open-loop control.

Sweep gas flow rate (L/min)	Voltage (Volt)
1.0	0.5005
0.5	0.2506
4.0	2.0002
2.0	1.0004
1.0	0.5005

5.2.1.1. Measurement of pCO_2 using MATLAB/SIMULINK

By using DAQ USB 6009 device, 4 analog inputs signals were acquired from pCO_2 sensors, MFC and CO_2 analyser, while 1 output signal was generated to MFC. All of these data were analysed and compared with the data obtained from the simulation work, to ensure the agreement between both works in terms of concept of study. The MATLAB/SIMULINK interface for pCO_2 measurement (open loop) can be found in Figure 5.14.

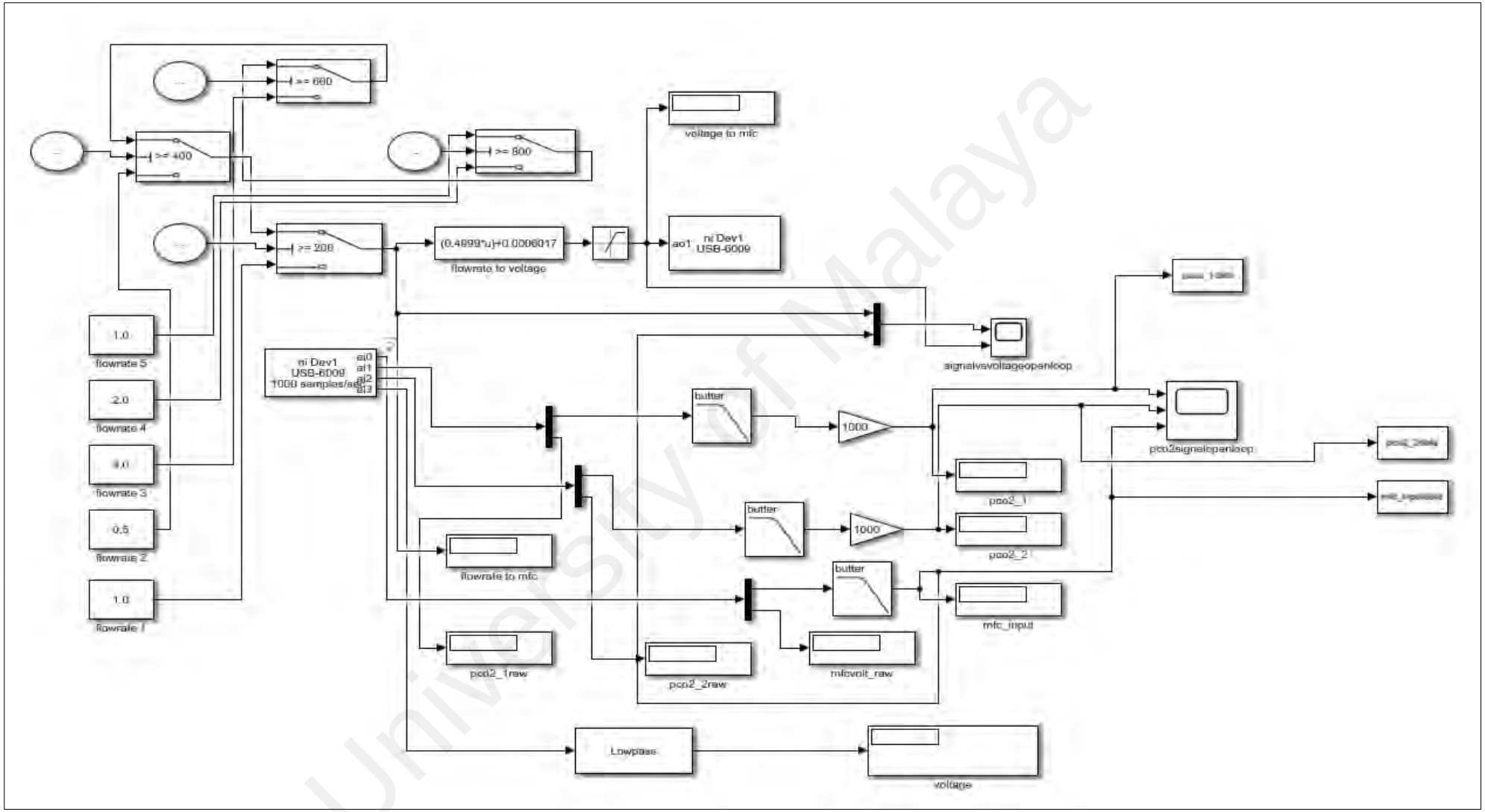

Figure 5.14: Open-loop control in MATLAB/SIMULINK.

5.2.1.2. Measurement of pCO_2 using blood gas analyser (BGA) in Universiti Malaya Medical Centre (commercial BGA).

Five blood samples at different sweep gas flowrate taken were sent to the Department of Pathology, Universiti Malaya Medical Centre (UMMC), in order to measure the arterial pCO_2 using commercial BGA (as implemented in the real patients). This is to ensure that this study is in the real track and the hypothesis was advocated by the same commercial BGA that was implemented to the real patients. The results were presented later in section 5.3.1.2.

5.2.2. Closed loop: setpoint tracking

As conducted in the simulation, setpoint in the experimental work also will be changed at t=300s to 42 mmHg, then adjusted back to 40 mmHg at t=600s.

5.2.3. Closed loop: disturbance rejection

To create a disturbance to process plant, oxygen (sweep gas) supply to the process plant will be sudden shutoff for 1 minute, at time t=300s and t=600s (toggle switch was illustrated in Figure 5.15.

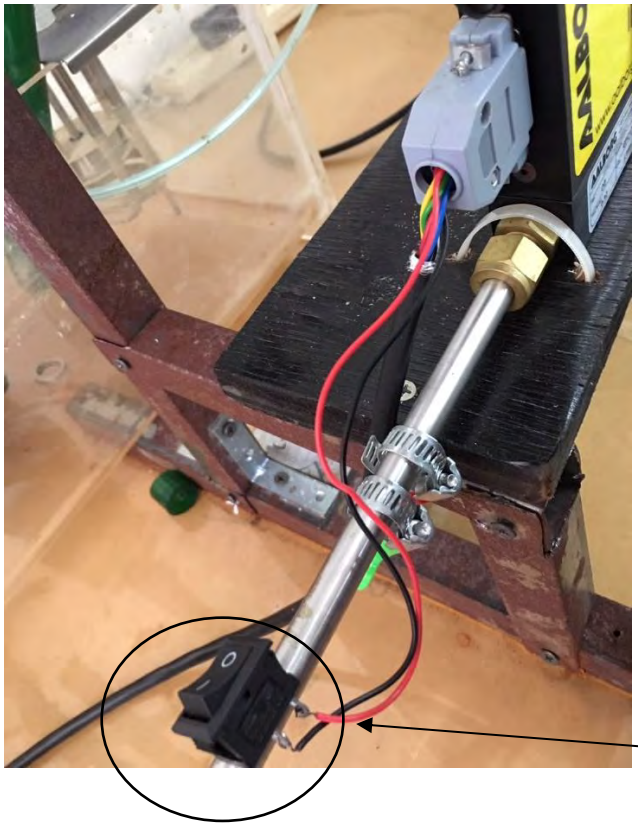

Toggle switch that is connected to mass flow controller, functions to stop the sweep gas supply to process plant, without changing the setpoint. It is used in introducing the disturbance to the process plant.

Figure 5.15: Toggle switch at MFC.

This was accomplished by switching on the toggle switch between pin 3 and 12 (see paragraph 2 (iii) in section 5.1.2.2). Pin 3 and 12 was connected for valve off control, to close the valve without changing the setpoint. A toggle switch is located between pin 3 and 12, so that the use of this function can be controlled by the user. For this task, setpoint was set at 40 mmHg, constant for the whole experiment time, as shown in Figure 5.16.

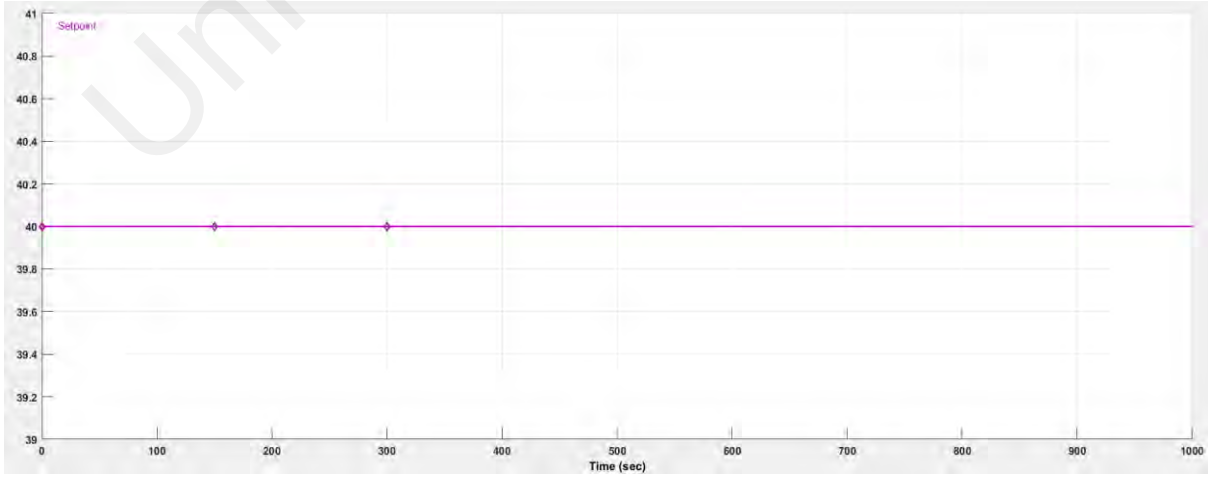

Figure 5.16: Setpoint for disturbance rejection task.

5.2.3.1. PID controller

Figure 5.17 shows the SIMULINK interface of PID controller for setpoint tracking task. For setpoint tracking task, the setpoint will be changed according to section 5.2.2, while for rejection, setpoint will be maintained at 40 mmHg with the external interruption from toggle switch, as described in section 5.2.3. From Figure 5.17, there were four analog input signals were acquired by DAQ and 1 analog output signal was generated to the same DAQ. The signals are in Table 5.5:

Table 5.5: Type of analog input and output for PID controller.

Input/output	Port	Type of analog input signal (volts)
Analog input	A_i0	pCO_2 1 (pre- membrane oxygenator)
	A_i1	pCO_2 2 (post- membrane oxygenator)
	A_i2	Voltage applied to MFC
	A_i3	CO_2 analyser
Output	A_o1	Voltage generated to DAQ as calculated by PID controller

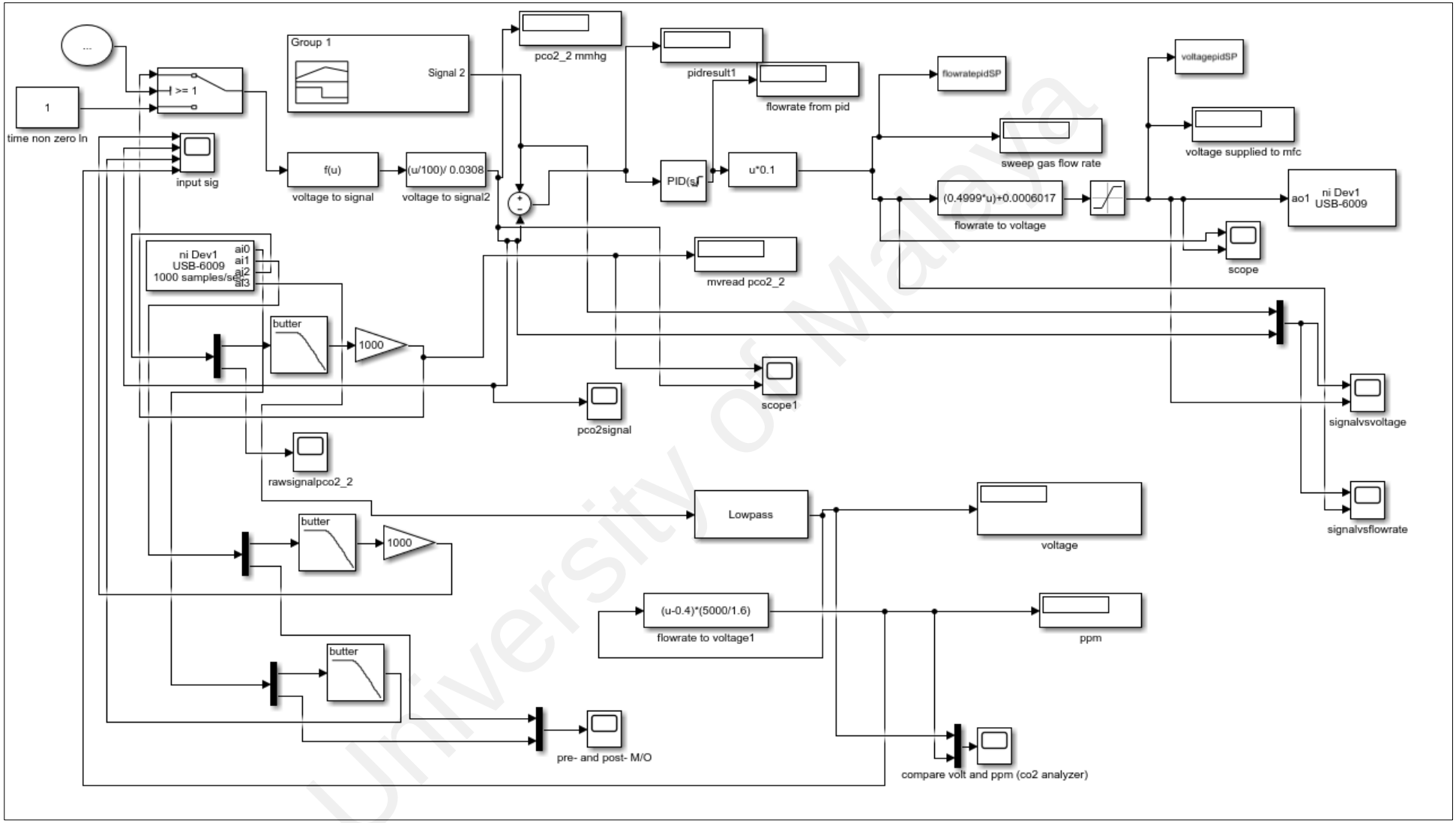

Figure 5.17: SIMULINK interface for PID controller.

Once the proposed system acquires pCO_2 signals from port A_i1, the analog (in volts) signal is converted to mmHg, to find its pCO_2 value. Then, this pCO_2 value is compared with setpoint to find the error, e(t)= setpoint – measured pCO_2. Error then becomes an input for PID controller, which it computes the flowrate that must be applied to process plant. In this study, the PID output is set to 0% to 100% percent, while the allowable range of flowrate to MFC is 0 to 10 L/min. For this reason, the percentage is converted to flowrate with the equation, f(u)= u*0.1. After getting the flowrate, the value is converted to voltage, according to the calibration curve elaborated in 5.1.1.2 (Equation [5.2]). This value then is known as the analog output signal generated to DAQ from port A_o1.

On the other hand, signal that acquired by DAQ from MFC is the real voltage that represents the opening of flowrate valve in MFC. In disturbance task, toggle switch is switch on for 1 minute, which makes the valve opening in MFC shut off for 1 minute. Consequently, sweep gas flowrate will be 0 L/min, no matter how much flowrate that been computed by PID controller during this period of time. This explains why in disturbance task, there are differences in sweep gas flowrate and voltage to MFC (Figure 5.18).

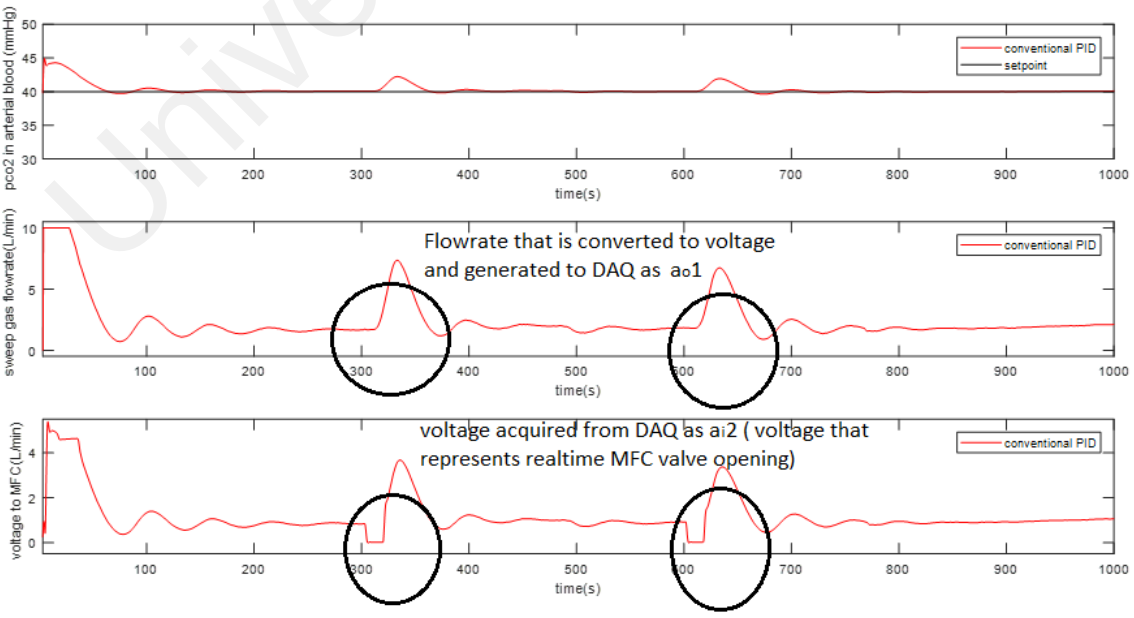

Figure 5.18: Difference between sweep gas flowrate and voltage to MFC.

5.2.3.2. Fuzzy Logic Controller (FLC)

Figure 5.19 shows the SIMULINK interface of FLC controller. For setpoint tracking task, the setpoint will be change according to section 5.2.2, while for rejection, setpoint will be maintained at 40 mmHg with the external interruption from toggle switch, as described in section 5.2.3.

From Figure 5.19, there are four analog input signals were acquired by DAQ and 1 analog output signal were generated to the same DAQ. The signals are in Table 5.6:

Table 5.6: Type of analog input and output for FLC.

Input/output	Port	Type of analog input signal (volts)
Analog input	A_i0	pCO_2 1 (pre- membrane oxygenator)
	A_i1	pCO_2 2 (post- membrane oxygenator)
	A_i2	Voltage applied to MFC
	A_i3	CO_2 analyser
Output	A_o1	Voltage generated to DAQ as calculated by PID controller

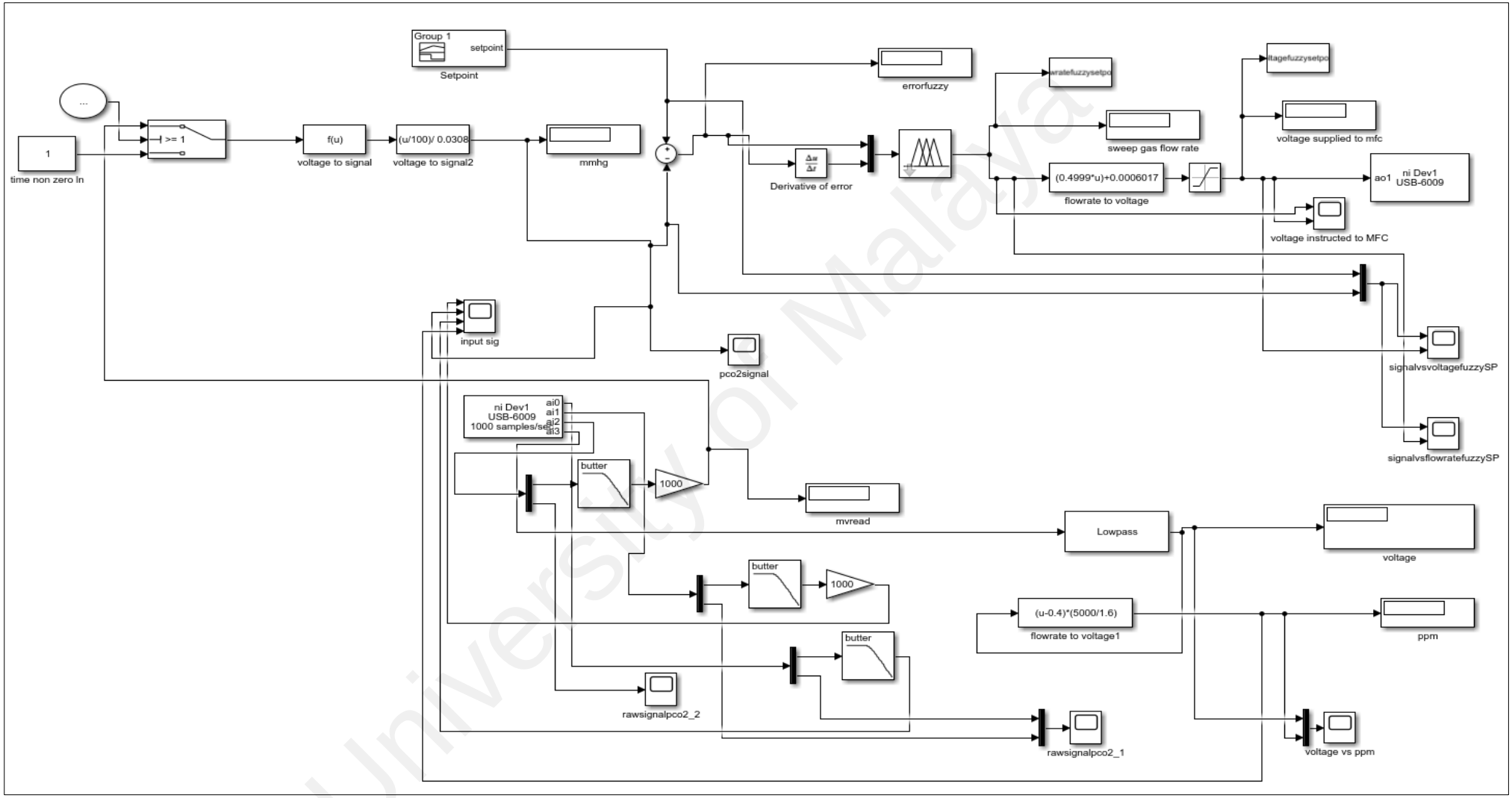

Figure 5.19: SIMULINK interface for FLC controller.

In this proposed automated control system, pCO_2 (post- membrane oxygenator) signal acquired by DAQ from port A_i1 is converted to mmHg before the calculation of the error by comparator. This error and change of error (de/dt) then are directed to fuzzy logic controller with rule viewer block, to compute the best sweep gas flowrate based on the rule determined by the user (Figure 5.20).

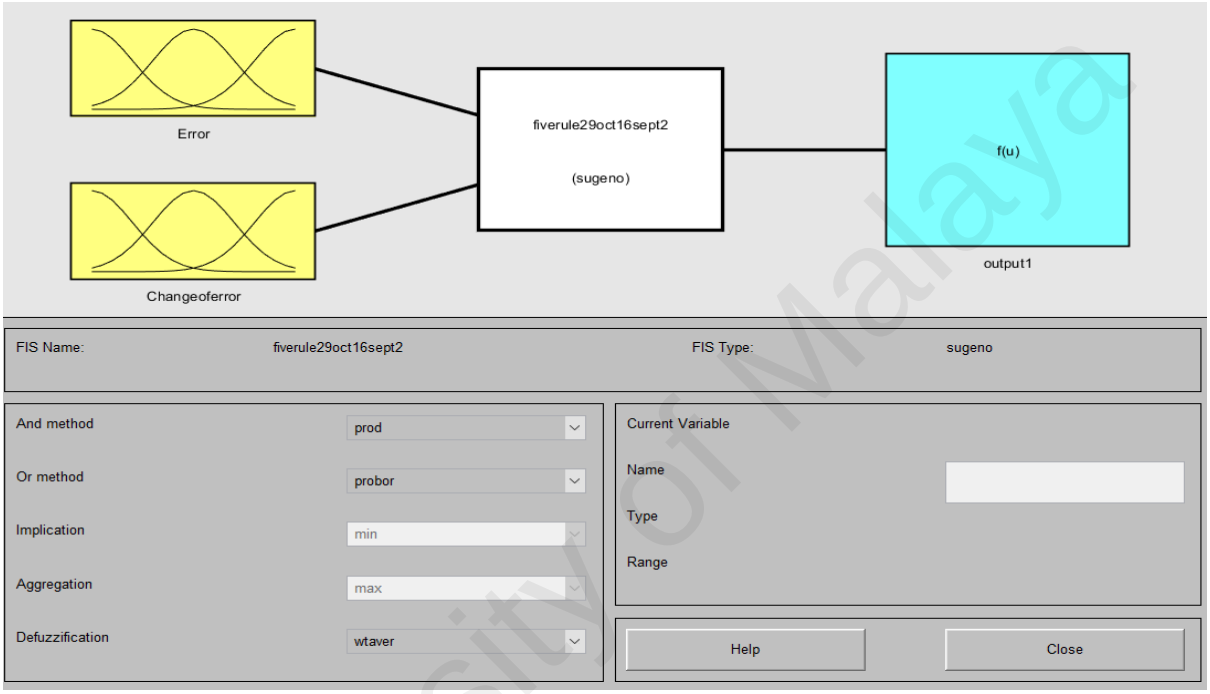

Figure 5.20: Fuzzy logic rule for FLC (experimental work).

For FLC used in this study, Takagi- Sugeno fuzzy rules is applied, which involved two input variables (error and change of error) and 1 output variable (controller output). The membership functions of each input variables are designed and shown in Figures 5.21 and 5.22. From these figures, the values of linguistic variables for input variable 'error' are composed of linguistic terms LN (Large Negative), SN (Small Negative), ZE (Zero), ZEP (Zero Positive), SP (Small Positive) and LP (Large Positive), while N (negative), ZE (Zero) and P (Positive) are determined for input variable 'change of error'. As for output, three constants are identified to

determine the controller output (sweep gas flow rate), which are LOW (0.1), MEDIUM (1.3) and HIGH (5).

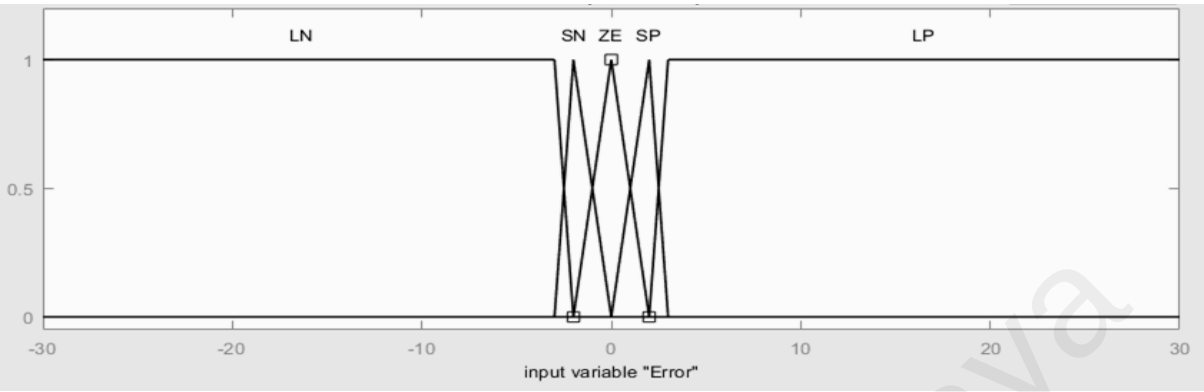

Figure 5.21: Membership function plot for 'error'.

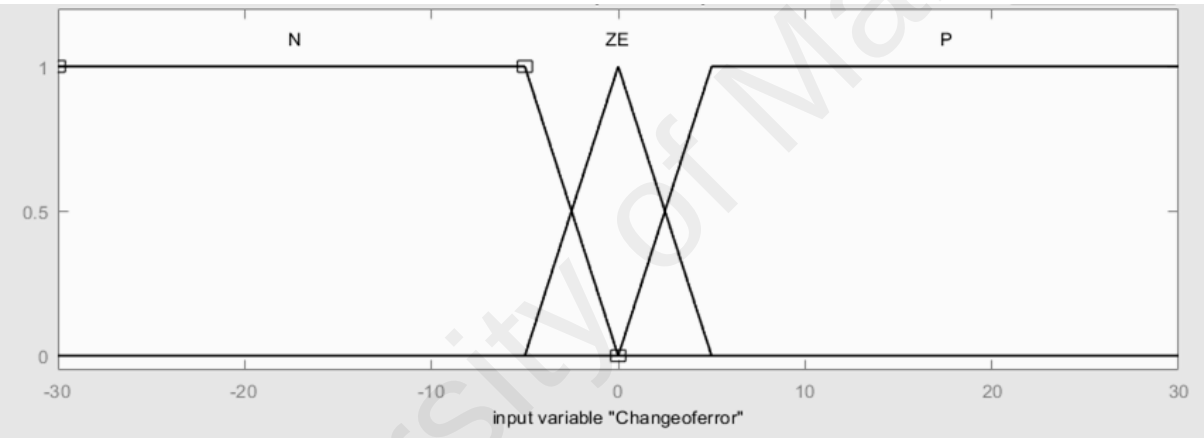

Figure 5.22: Membership function error for 'change of error'.

To maintain pCO_2 according to the setpoint, there are 15 rules are specified as in Table 5.7, which are:

Table 5.7: Rules of fuzzy inference for FLC.

Δe / e	LN	SN	ZE	SP	LP
N	HIGH	MEDIUM	MEDIUM	LOW	LOW
ZE	HIGH	MEDIUM	MEDIUM	LOW	LOW
P	HIGH	MEDIUM	MEDIUM	LOW	LOW

5.2.3.3. Fuzzy-PID controller

Figure 5.23 shows the SIMULINK interface of Fuzzy-PID controller. For setpoint tracking task, the setpoint will be change according to section 5.2.2, while for rejection, setpoint will be maintained at 40 mmHg with the external interruption from toggle switch, as described in section 5.2.3.

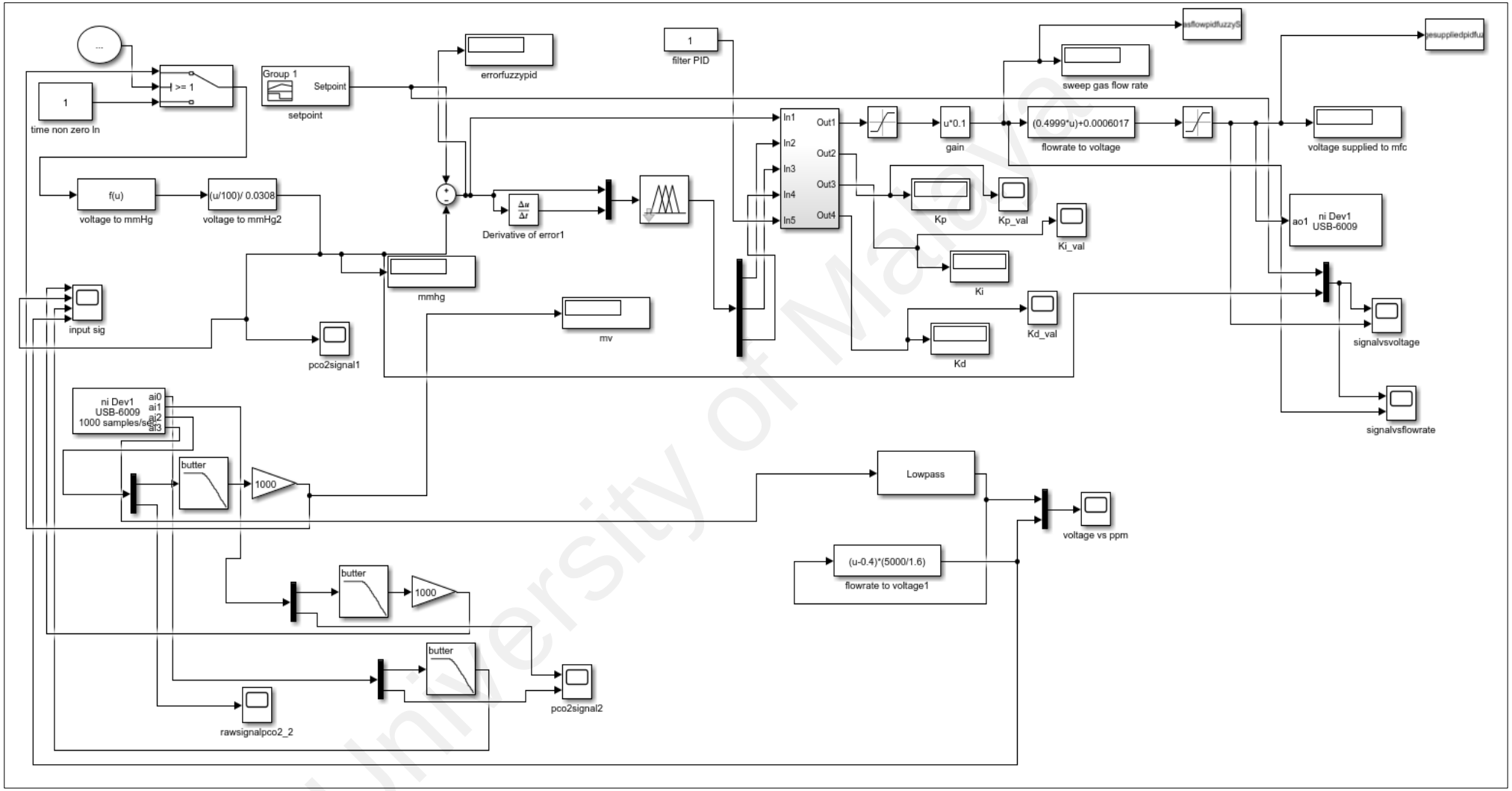

Figure 5.23: SIMULINK interface for Fuzzy-PID controller.

For accuracy, value of membership functions, P, I and D were normalized to get the universe of discourse at the interval [0,1] by using the equations:

$$P' = \frac{P - Pmin}{Pmax - Pmin} \quad [5.3]$$

$$I' = \frac{I - Imin}{Imax - Imin} \quad [5.4]$$

$$D' = \frac{D - Dmin}{Dmax - Dmin} \quad [5.5]$$

To get the original controller output after normalizations to range [0,1], as shown in Figure 5.24:

$$Kp = 5\,P' + 23.3 \quad [5.6]$$

$$Ki = 0.01\,I' + 0.012 \quad [5.7]$$

$$Kd = 1\,D' + 14.1875 \quad [5.8]$$

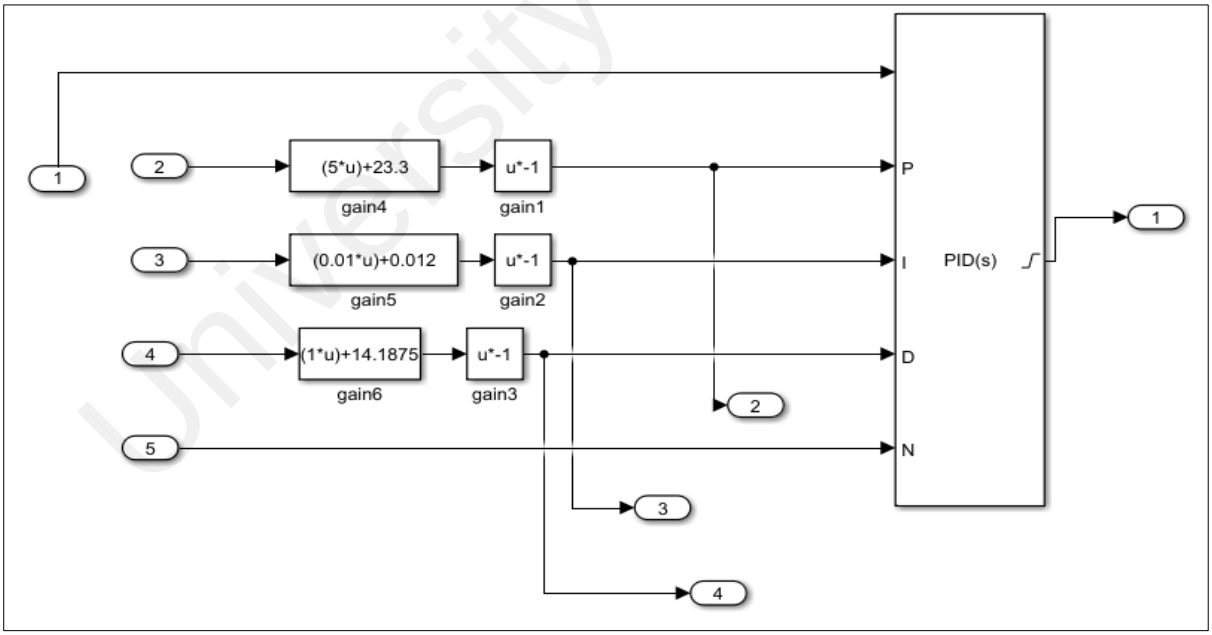

Figure 5.24: Subsystem to convert back PID gain to the original controller output after normalizations to range [0,1].

The application of Fuzzy-PID in this experimental work is similar with the one that used in simulation work. Fuzzy block is comprised of two inputs and three outputs, where the inputs are error, e and the rate of change of error, ė (Figure 5.25). There are five linguistic terms of the error in pCO_2: LN (Large Negative), SN (Small Negative), ZE (Zero), SP (Small Negative) and LP (Large Positive), followed by N (Negative), ZE (Zero) and P (Positive) for input variable 'change of error' over the interval from -15 to 15.

On the other hand, the linguistics variables for output variables (K_p, K_i and K_d), are assigned as N (Negative), SN (Small Negative), ZE (Zero) and P (Positive) over the normalized interval of [0, 1], as in Figure 5.26. These three gain parameters, K_p, K_i and K_d in PID controller was updated online by fuzzy rules that was designed in fuzzy, as tabulated in Table 5.8 until 5.10.

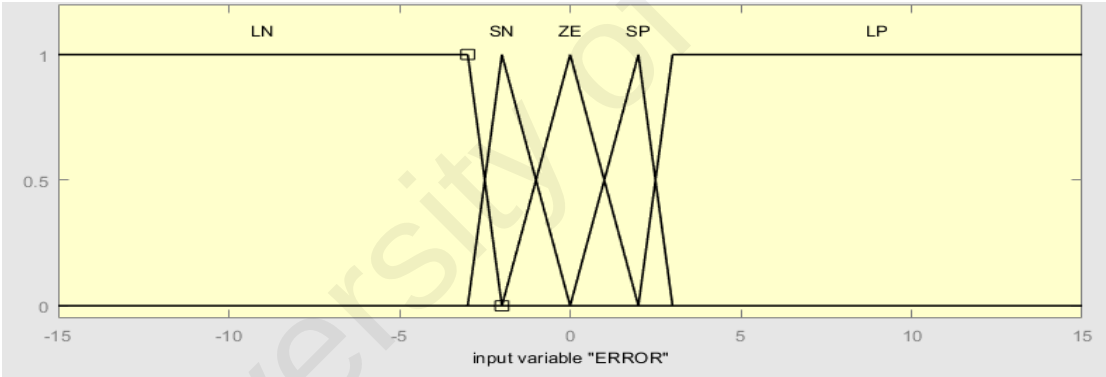

(a)

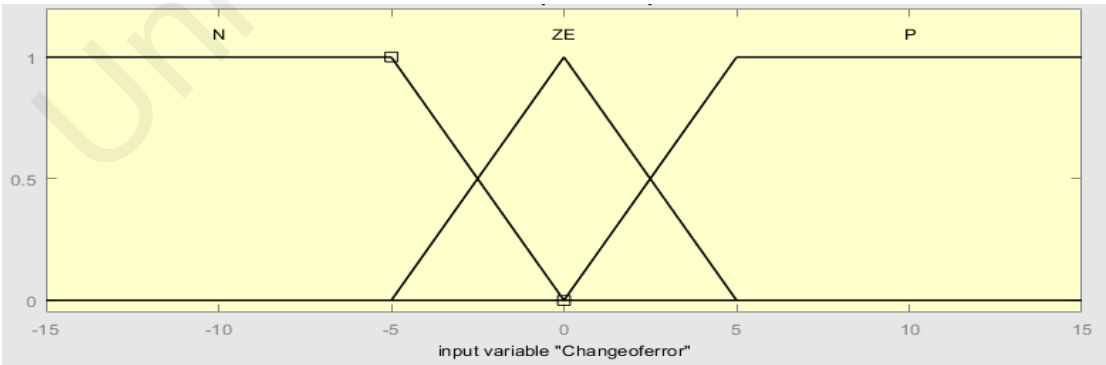

(b)

Figure 5.25: Membership functions of (a) error and (b) rate of change of error.

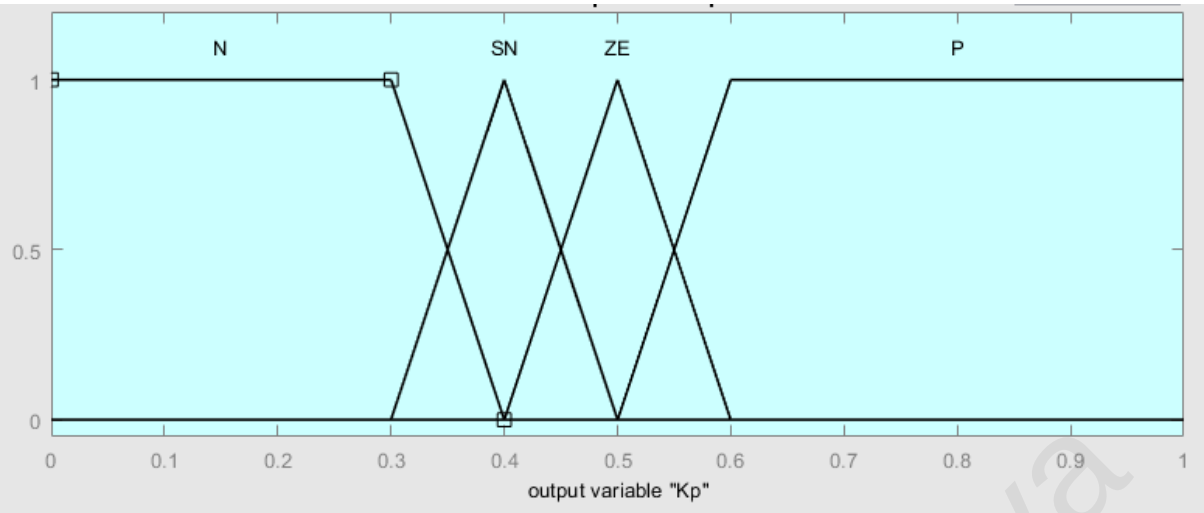

(a)

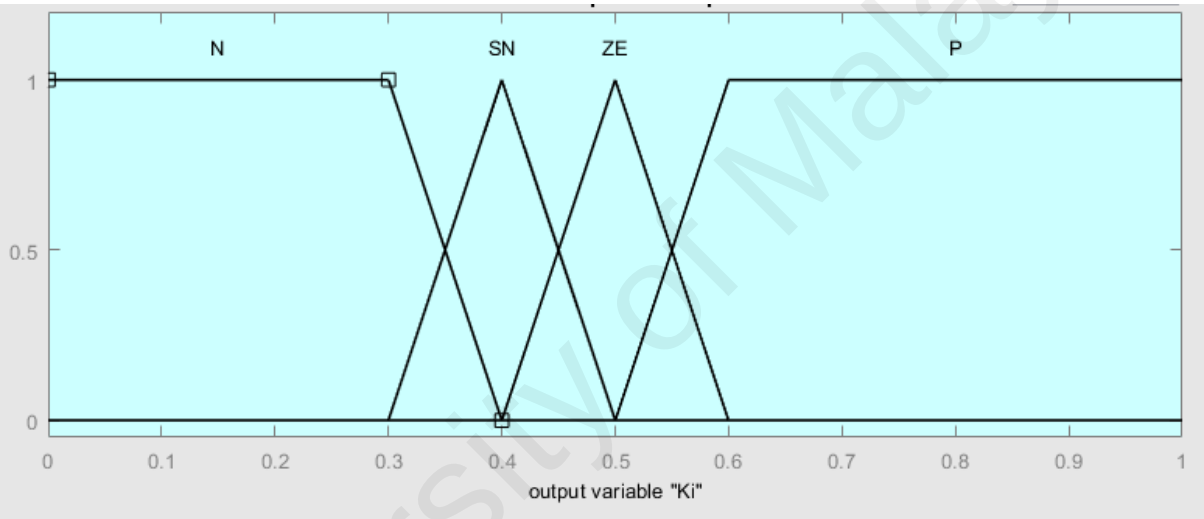

(b)

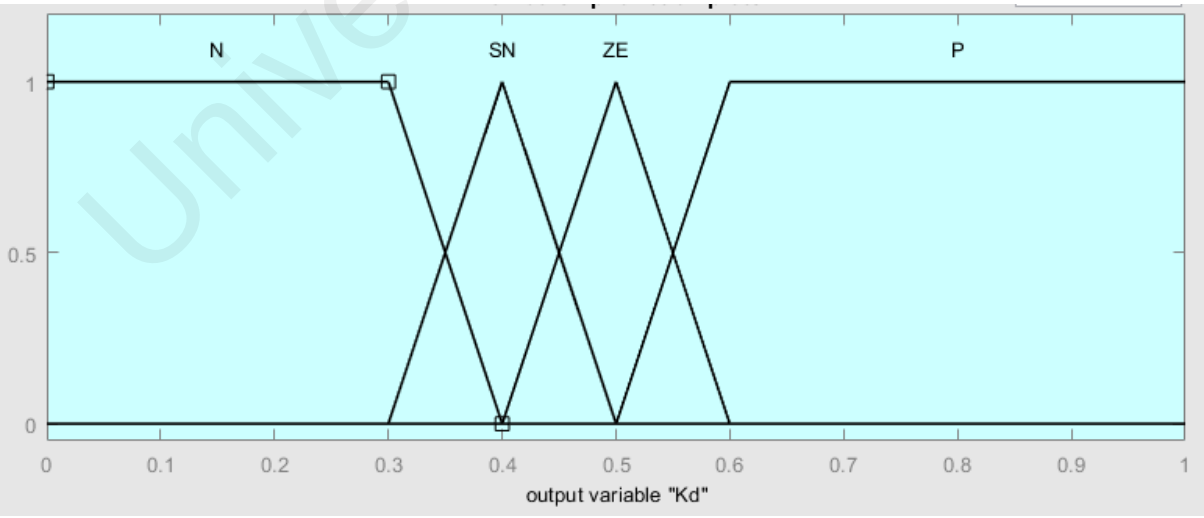

(c)

Figure 5.26: Membership function of (a) K_p, (b) K_i and (c) K_d.

Table 5.8. Rules of fuzzy inference for 'Kp'.

Δe / e	LN	SN	ZE	SP	LP
N	P	ZE	ZE	ZE	P
ZE	ZE	SN	ZE	SN	ZE
P	P	ZE	ZE	ZE	P

Table 5.9. Rules of fuzzy inference for 'Ki'.

Δe / e	LN	SN	ZE	SP	LP
N	P	ZE	ZE	ZE	N
ZE	ZE	SN	ZE	SN	ZE
P	P	ZE	ZE	ZE	N

Table 5.10. Rules of fuzzy inference for 'Kd'.

Δe / e	LN	SN	ZE	SP	LP
N	P	ZE	ZE	ZE	N
ZE	ZE	SN	ZE	SN	ZE
P	P	ZE	ZE	ZE	N

5.2.3.4. Performance comparison of the controllers (experimental)

The performance of the entire controllers will be evaluated based on its ability to track any setpoint change and to reject any disturbance to the process plant. For quantitative analysis, mean squared error (MSE) are calculated for each controller in both tasks. Equation for mean squared error:

$$MSE = \frac{1}{n} \sum_{i=1}^{n} e(t) \qquad [5.9]$$

Where:
n= total number of measurements.

e(t)= error (setpoint – measure pCO_2 in arterial blood).

IAE, ISE and ITAE performance indices are suitable to test control loop in simulation studies as in Chapter 4, but not in the actual plant operation. This is due to the process noise and random noise that occur in actual plant operation, which will produce inaccurate calculation (Shaw, 2003). For these reasons, in experimental work, only MSE was calculated.

5.3. Result and observations (experimental work)

5.3.1. Open loop control:

Results obtained from experimental work for open loop control were compared with results from experimental work for validation. This included both data measured by DAQ device and measurement from commercial BGA used in Universiti Malaya Medical Centre.

5.3.1.1. Data from DAQ device

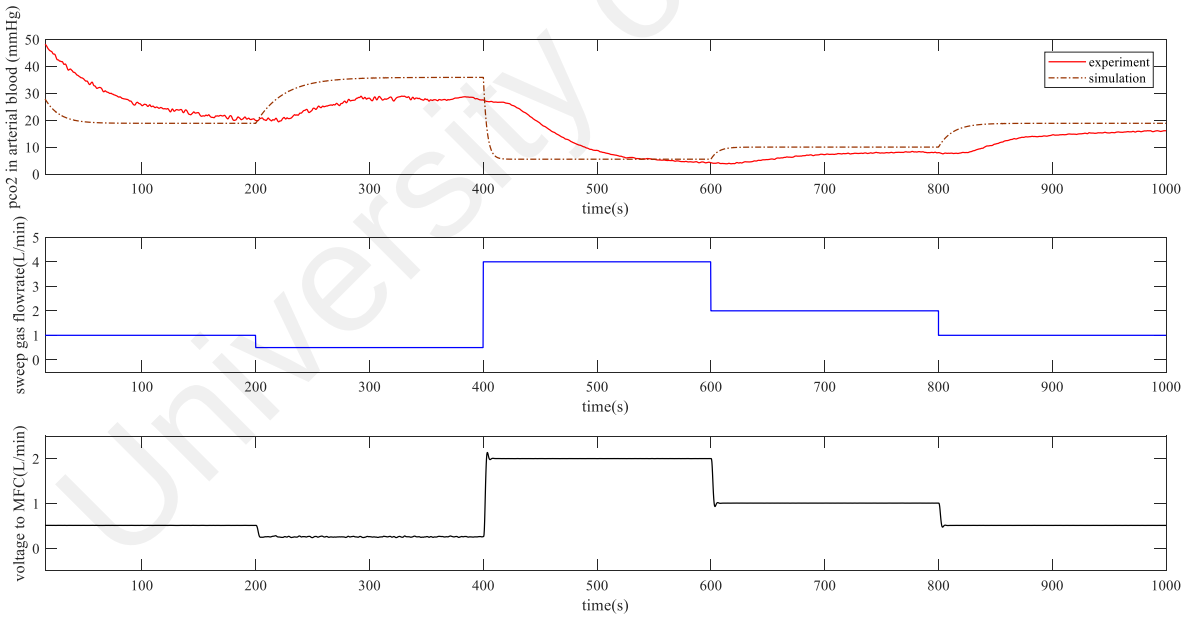

Figure 5.27: Open loop system output (arterial pCO_2) for different input (sweep gas flow rate) applied.

In open-loop control (non-feedback control system), the system only takes input under the consideration without any influence of any feedback or external acting on it to obtain the output.

From Figure 5.27, both simulation (brown line -.-.-.) and experimental (red line ---) showed an agreement for any change in sweep gas flow rate applied to the process plant (membrane oxygenator). From the figure, the system reflected inverse relationship, which the pCO_2 increased as the sweep gas flow rate was decreased and vice versa.

Decreasing in sweep gas flow rate to membrane oxygenator will simultaneously increase pCO_2 inside the hollow fibre unit, hence augmented the partial pressure gradient that exist between blood phase and gas phase. This difference then consequently reduces the CO_2 removal from blood to gas phase, cause high pCO_2 measurement in arterial blood.

This type of response needs direct-acting controller for closed loop control system, which was implemented in next section of this study. In direct-acting controller, when the pCO_2 falls below the setpoint, the controller will reduce the sweep gas supply to membrane oxygenator, so that the CO_2 removal rate can be reduced to increase the arterial pCO_2.

5.3.1.2. Results obtained from commercial BGA used in UMMC for real patients.

Table 5.11 tabulates measurements of arterial pCO_2 according to the different sweep gas flowrate. These results are the measurement of arterial pCO_2 which were measured by the commercial BGA that been used in UMMC for arterial blood gas test.

Table 5.11: Results of arterial pCO_2 from 5 samples with different sweep gas flow rate measured by commercial BGA in UMMC.

Sweep gas flowrate (L/min)	pCO_2 (mmHg)
1.0	26
0.5	45
4.0	14
2.0	20
1.0	26

There are two findings from Table 5.11. Firstly, these results advocated the hypothesis of this study, which the pCO_2 in blood is determined by sweep gas flowrate. It indicates that this study is in the right track. Secondly, at 1 L/min, arterial pCO_2 is 26 mmHg. It changed according to the change of sweep gas flowrate, which pCO_2 will decreased as the sweep gas flowrate increased. At the end of the experiment, when the sweep gas flowrate was adjusted back to 1 L/min, arterial pCO_2 also returned to its initial measurement, which is 26 L/min. This validates the hypothesis of this study, and the effectiveness of membrane oxygenator that was applied in this experimental work. In short, from both measurement from DAQ using MATLAB/SIMULINK and direct measurement using commercial BGA, it can be said that the experimental results agreed with the simulation results, which validates the first hypothesis of this study.

5.3.2. Closed-loop control: Setpoint tracking

5.3.2.1. PID

Firstly, in the real experiment using bovine blood, the same simulation gain was used, which are:

Kp= 84

Ti= 0.06

Td= 0.015

Figure 5.34 shows the measured arterial pCO_2 when being controlled by PID with the gains that are similar with the tuned gain in simulation work. Clearly, the PID controller was unable to control the pCO_2 accordingly to the desired setpoint. The PID only gives the output either 0% (0 L/min in sweep gas flow rate) or 100% (10 L/min) for any change in pCO_2. This observation indicates that a new tune of PID gain is necessary for experimental work in order to produces a good PID controller.

The plotted graph for pCO_2 which controlled by PID was illustrated in Figure 5.28 below:

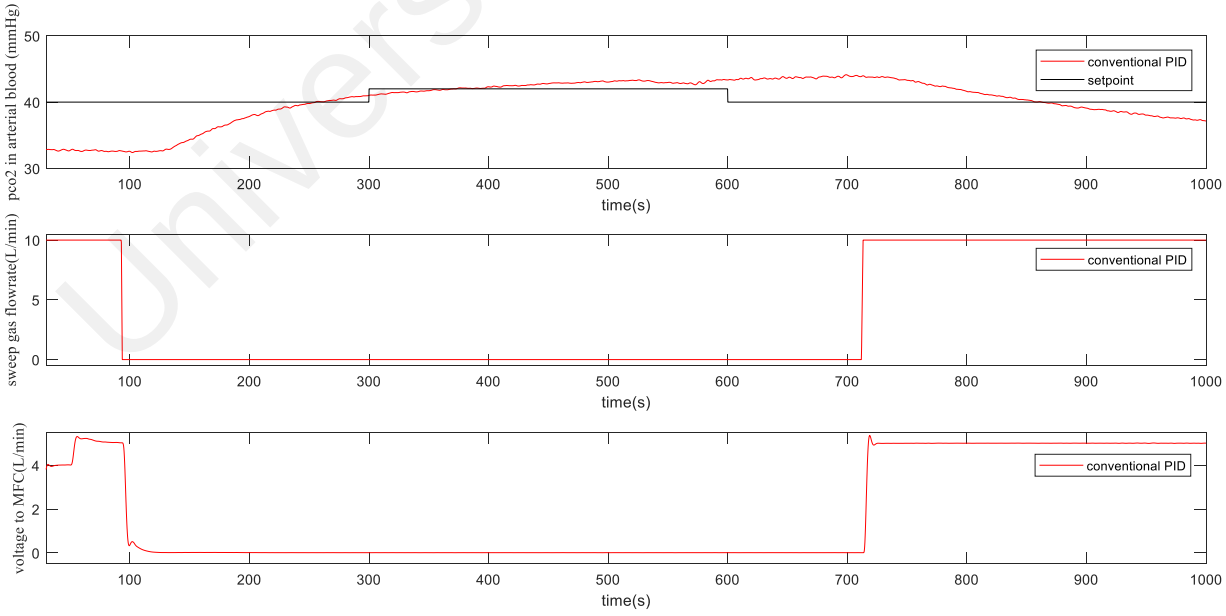

Figure 5.28: Measured arterial pCO_2, its respective sweep gas flowrate and voltage supplied to MFC for PID controller (setpoint tracking).

5.3.2.2. Fuzzy Logic Controller (FLC)

Rules that were implemented for this in-vitro experiment can be found in section 3.1.3, since the similar rule was used as in simulation study. From Figure 5.29, when pCO_2 approaching the setpoint, the FLC tuned the sweep gas flow rate to 0.8698, according the fuzzy rules. A good control action can be seen for this controller. When comparing the performance between FLC and PID, FLC performed better than PID, which only produce on-off control due to inaccurate PID parameter.

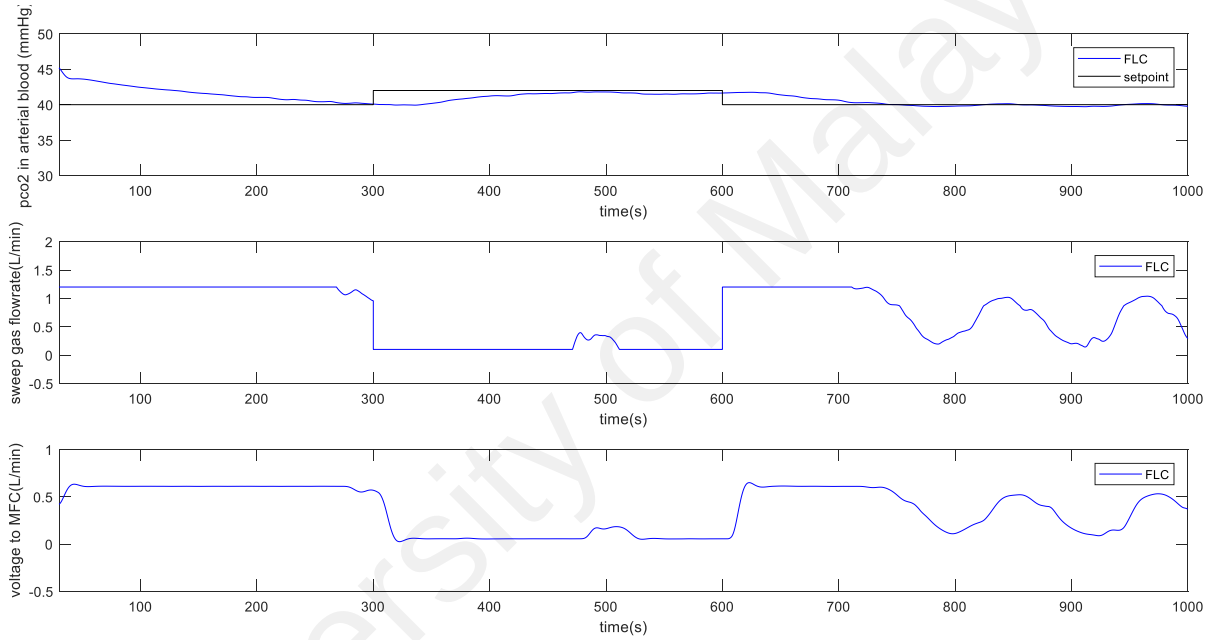

Figure 5.29: Measured arterial pCO_2, its respective sweep gas flowrate and voltage supplied to MFC for FLC controller (setpoint tracking).

5.3.2.3. Fuzzy-PID

Figure 5.30 is the plotted graph of Fuzzy-PID in controlling arterial pCO_2 for setpoint tracking task. Fuzzy rule and PID gains that were implemented for this experiment can be found in section 3.1.4, since it used the similar rule as in simulation study. Even though the similar PID gains (P, I and D) were used in PID part, Fuzzy-PID controller reflected good learning ability and adaptability to the error.

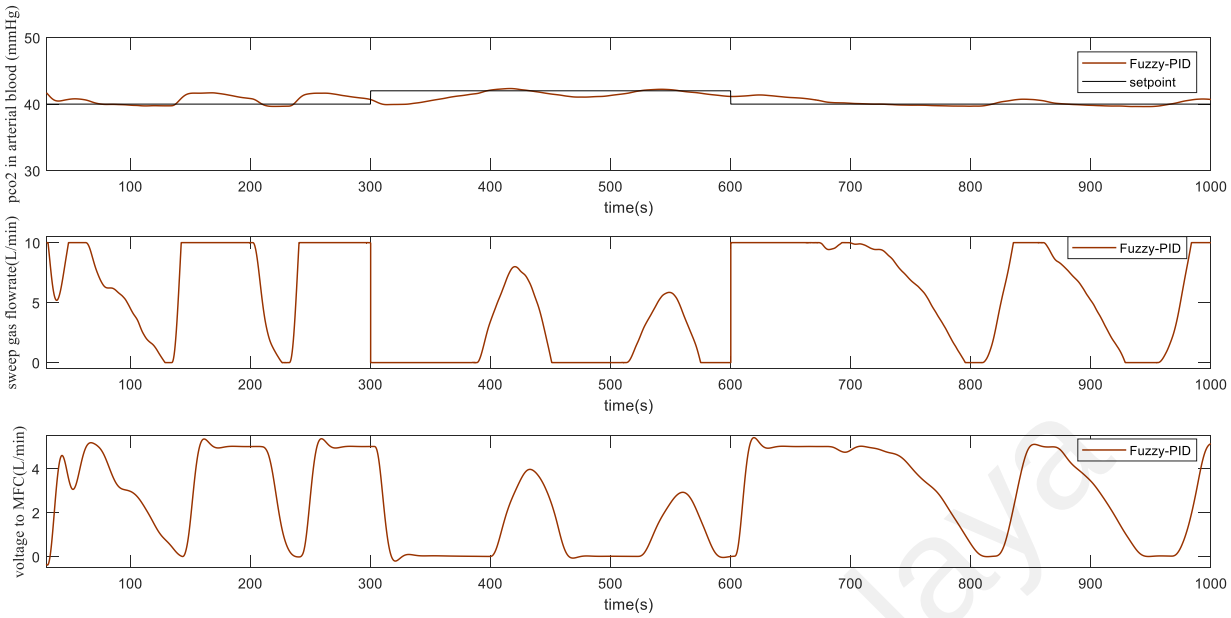

Figure 5.30: Measured arterial pCO_2, its respective sweep gas flowrate and voltage supplied to MFC for Fuzzy-PID controller (setpoint tracking).

Comparison of experimental results between conventional PID, FLC and Fuzzy-PID: Setpoint tracking

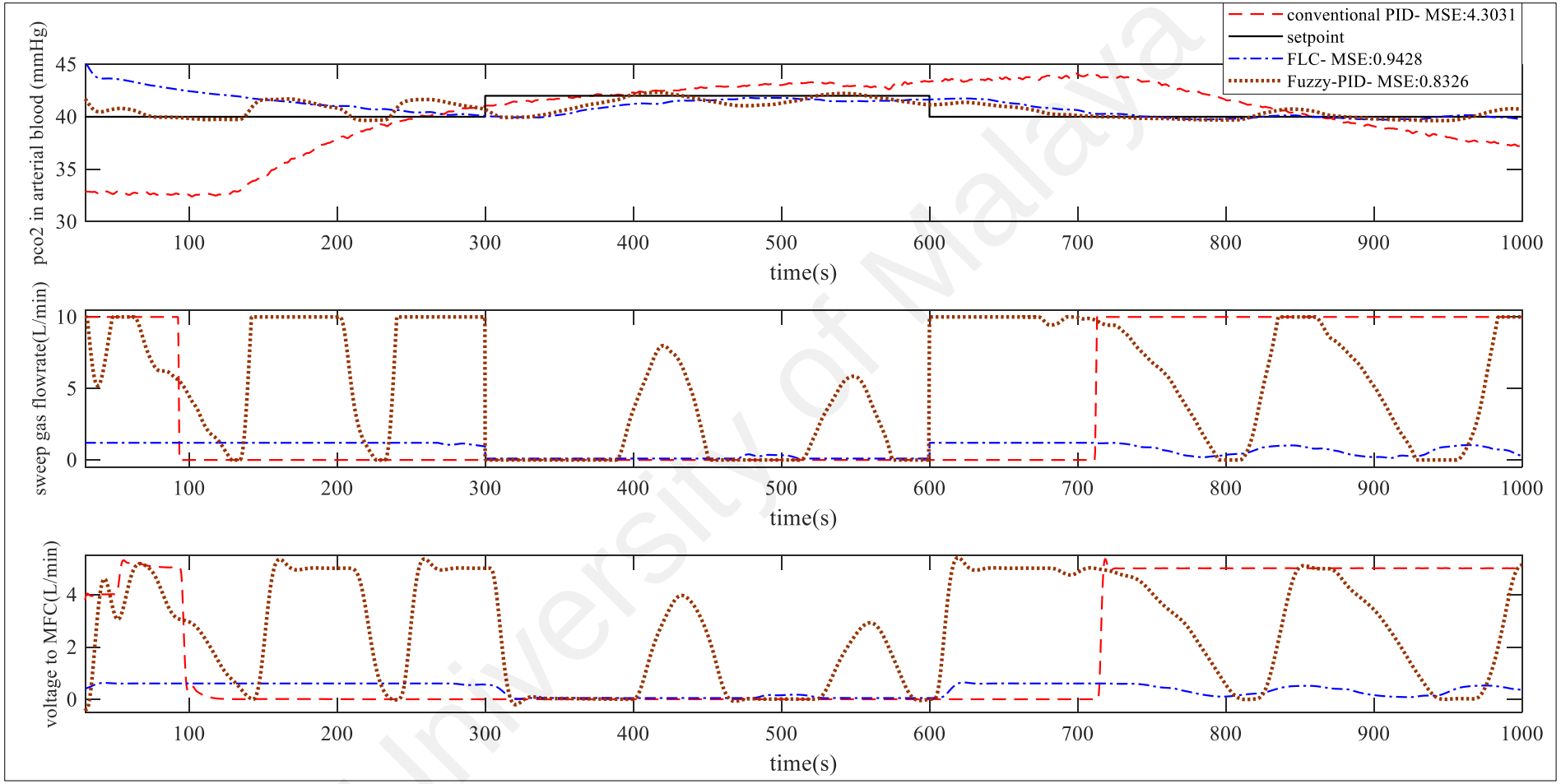

Figure 5.31: Performance comparison for all three controllers (PID, FLC and Fuzzy-PID) for setpoint tracking task (experimental), using similar controller's parameter/gain with simulation.

From Figure 5.31, all of the three controllers were unable to efficiently control the process plant to achieve the desired setpoint, with PID controller become the worst controller. This occurrence also highlights the advantages of FLC compared to conventional PID. Unlike conventional PID which have the tuned gain (P, I, and D), FLC works based on predicate logic and probability-based method (Zadeh, 1983). With this feature, FLC have ability on parameter adaptation, since it will update its parameter in each control cycles, based on the feedback obtained from the sensors (arterial pCO_2).

When comparing the calculated MSE, Fuzzy-PID had the lowest MSE compared to conventional PID and FLC. Even the system was oscillated during the whole experiment time, the error for this controller still the lowest, due to its online adaptation ability that inherited from FLC part.

From the current findings, it is proven that, PID can be a good controller when being tuned properly, while FLC have advantage in adapting its parameter based on the error obtained in each cycle. With the fusion of these controllers (PID+FLC) as fuzzy-PID, both beneficial advantages can be obtained for better automated control performance on the process plant.

5.3.3. Closed-loop control: Disturbance rejection

5.3.3.1. PID

Using the same gains as in the simulation, measurement of arterial pCO_2 in experimental work was inconsistent, due to the poor control of PID controller, as seen in Figure 5.32. This poor control ability indicates the importance of proper tuning of PID gains during its operation on the process plant.

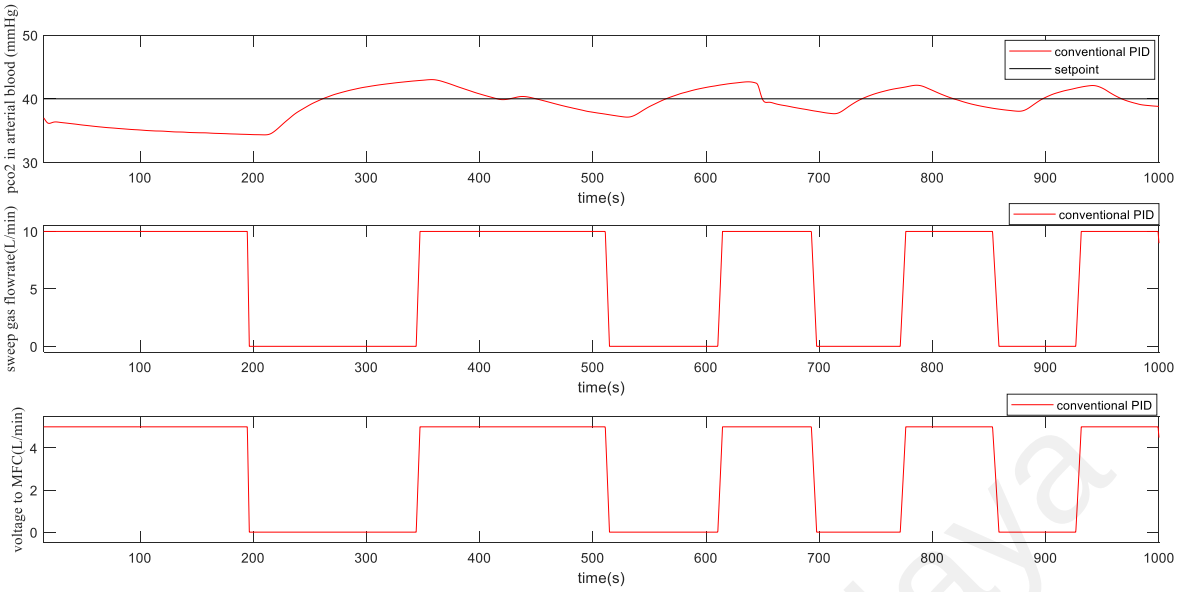

Figure 5.32: Measured arterial pCO_2, its respective sweep gas flowrate and voltage supplied to MFC for PID controller (disturbance rejection task).

5.3.3.2. Fuzzy Logic Controller (FLC)

From Figure 5.33, better control performance can be seen for FLC controller, compared to PID. This achievement was similar with its performance in setpoint tracking task, which due to the flexibility of FLC.

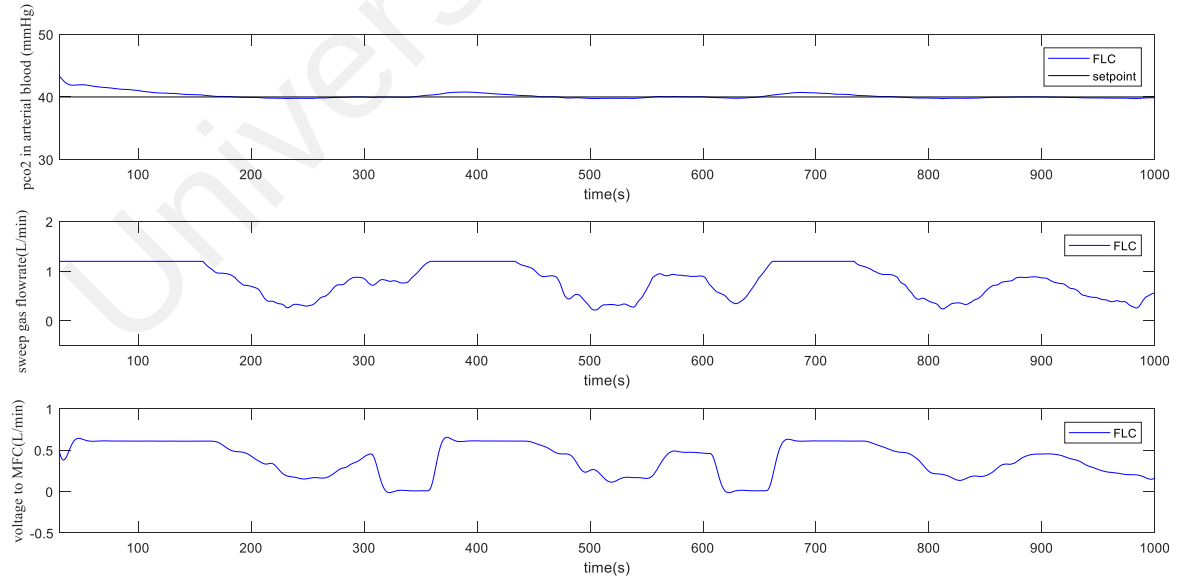

Figure 5.33: Measured arterial pCO_2, its respective sweep gas flowrate and voltage supplied to MFC for FLC controller (disturbance rejection task).

5.3.3.3. Fuzzy-PID

Figure 5.34 shows unsatisfactory performance of Fuzzy-PID using the same PID parameters tuned in simulation work. Unlike PID which only give two outputs (0 L/min or 10 L/min), Fuzzy-PID was able to control the arterial pCO_2 according to the setpoint in rejecting the disturbance due to the interference of fuzzy logic block. This somehow shows the significance of fuzzy logic rules in this controller. In short, Fuzzy-PID can perform better than PID alone, even in the case of inappropriate PID gains applied to the system.

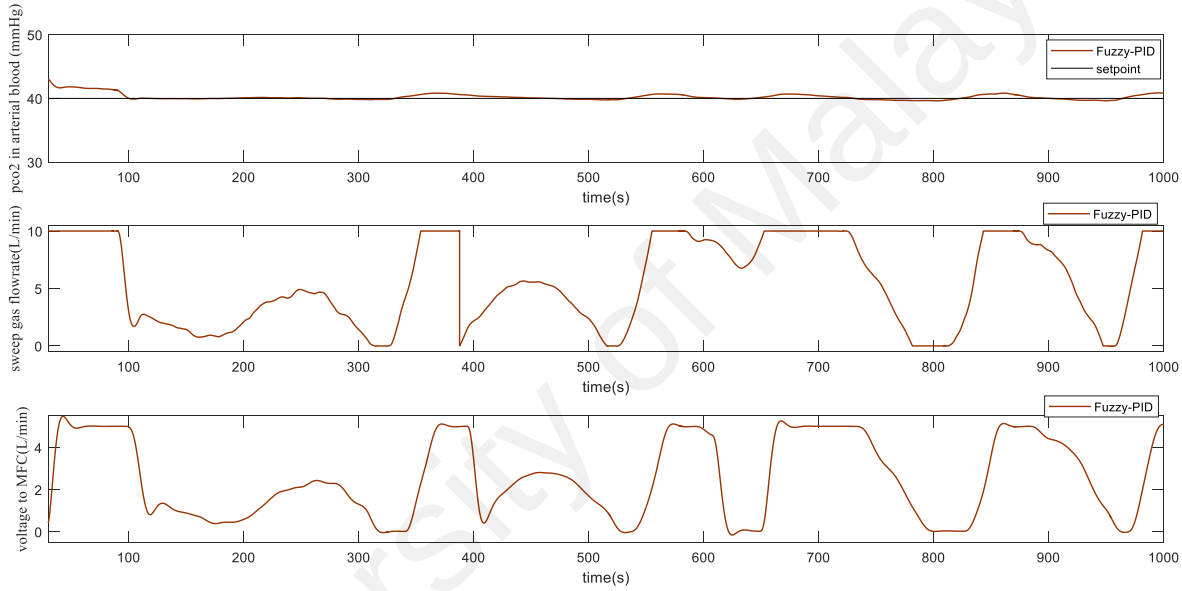

Figure 5.34: Measured arterial pCO_2, its respective sweep gas flowrate and voltage supplied to MFC for Fuzzy-PID controller (disturbance rejection task).

5.3.3.4.Comparison of experimental results between conventional PID, FLC and Fuzzy-PID: Disturbance rejection

Figure 5.35 depicts the performance comparison for all three controllers (PID, FLC and Fuzzy-PID) for disturbance rejection task using similar PID gain and fuzzy rules tuned in simulation work. Here, it can be seen that, PID become the worst controller, which only give two output decision of mass flow controller, which either 0 L/min or 10 L/min. In fact, there was no improvement made as the corrective action by this controller.

On the other hand, FLC seems to be the best controller in this case with 0.1853 MSE, since it has the advantage to handle vague data. In addition to its simplicity during design process, this controller allows a straightforward implementation of expert knowledge (Scheiber et al., 2009). Thus, inappropriate tuning parameters did not affect the FLC performance much during controlling pCO_2 when a disturbance was applied to the process plant.

Fuzzy-PID then implies a better control action compared to PID controller. From the figure, MSE for Fuzzy-PID is 0.3569, compared to 2.5287 for PID alone (less by 85.87%). This clearly indicates the improvement of fuzzy logic rules to this controller.

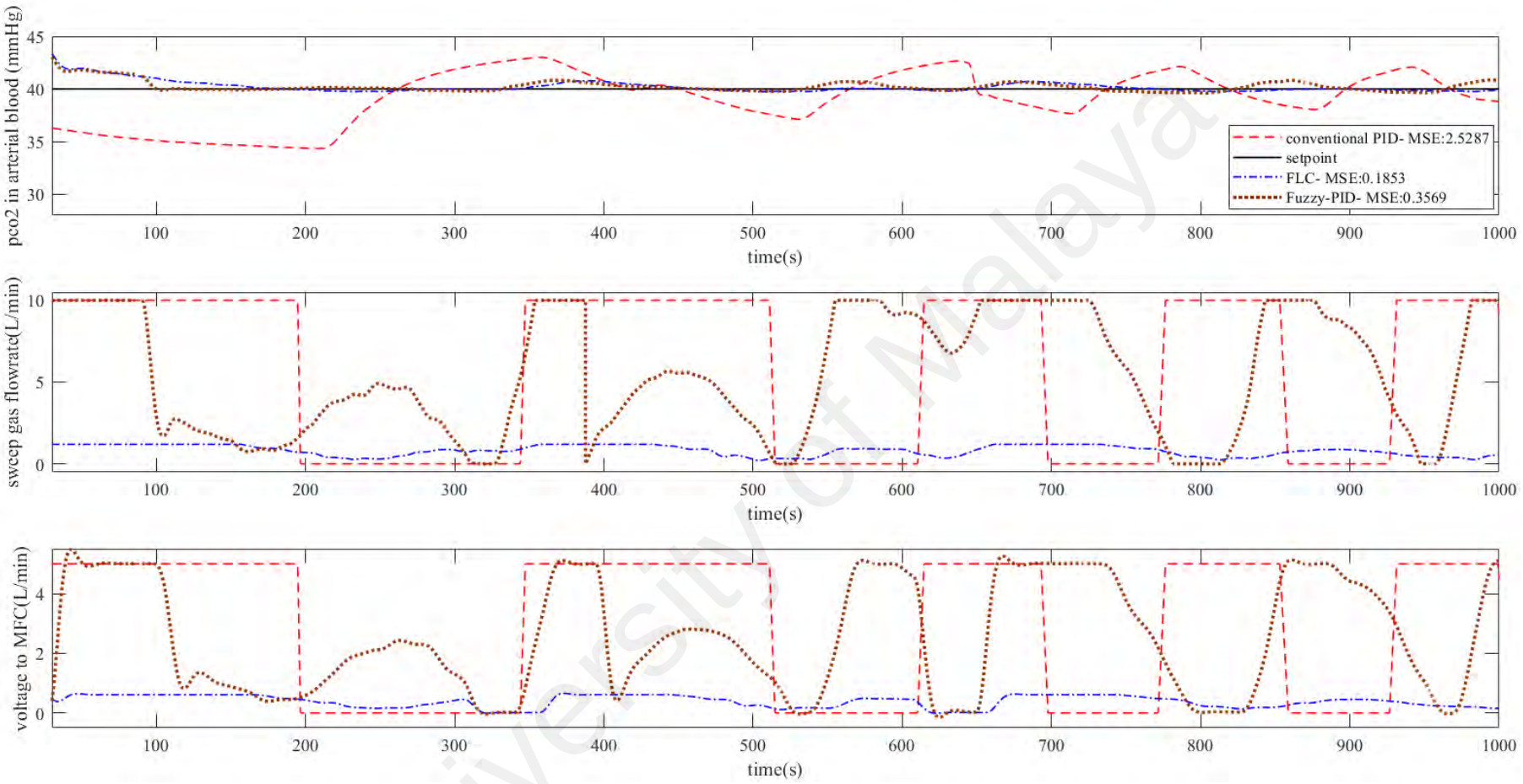

Figure 5.35: Performance comparison for all three controllers (PID, FLC and Fuzzy-PID for disturbance rejection task-experimental, similar controller's parameter/gain with simulation).

5.3.4. New tuned of PID parameter and fuzzy logic rule from experiment

It was found that the controller has unsatisfactorily performance in controlling pCO_2 value in arterial blood experimentally. This was due to the difference in time domain between simulation and experimental study. For example, one cycle of oscillation (peak-to-peak) for simulation is 0.12s, while time taken in experiment for one cycle is around 120s. This surely will affect the τ_i and τ_d parameter. The observed differences also probably due to the assumptions and defined parameters used in both mathematical modelling and experimental works. Hence, the entire controller has to be re-tuned to produce the most optimum control action to the system. Further, these newly tuned parameter and fuzzy rule will be implemented to the simulation study to see the control ability of the controllers.

The re-tune of PID parameter was conducted with similar procedures of Ziegler-Nichols continuous cycling method explained in section 3.1.2. PID controller was set at K_{cr}=43, to find the new K_p, τ_i and τ_d using Ziegler-Nichols continuous cycling method. Result of sustained oscillation on automatic mode was illustrated in Figure 5.36, and the newly tuned PID parameters were tabulated in Table 5.12.

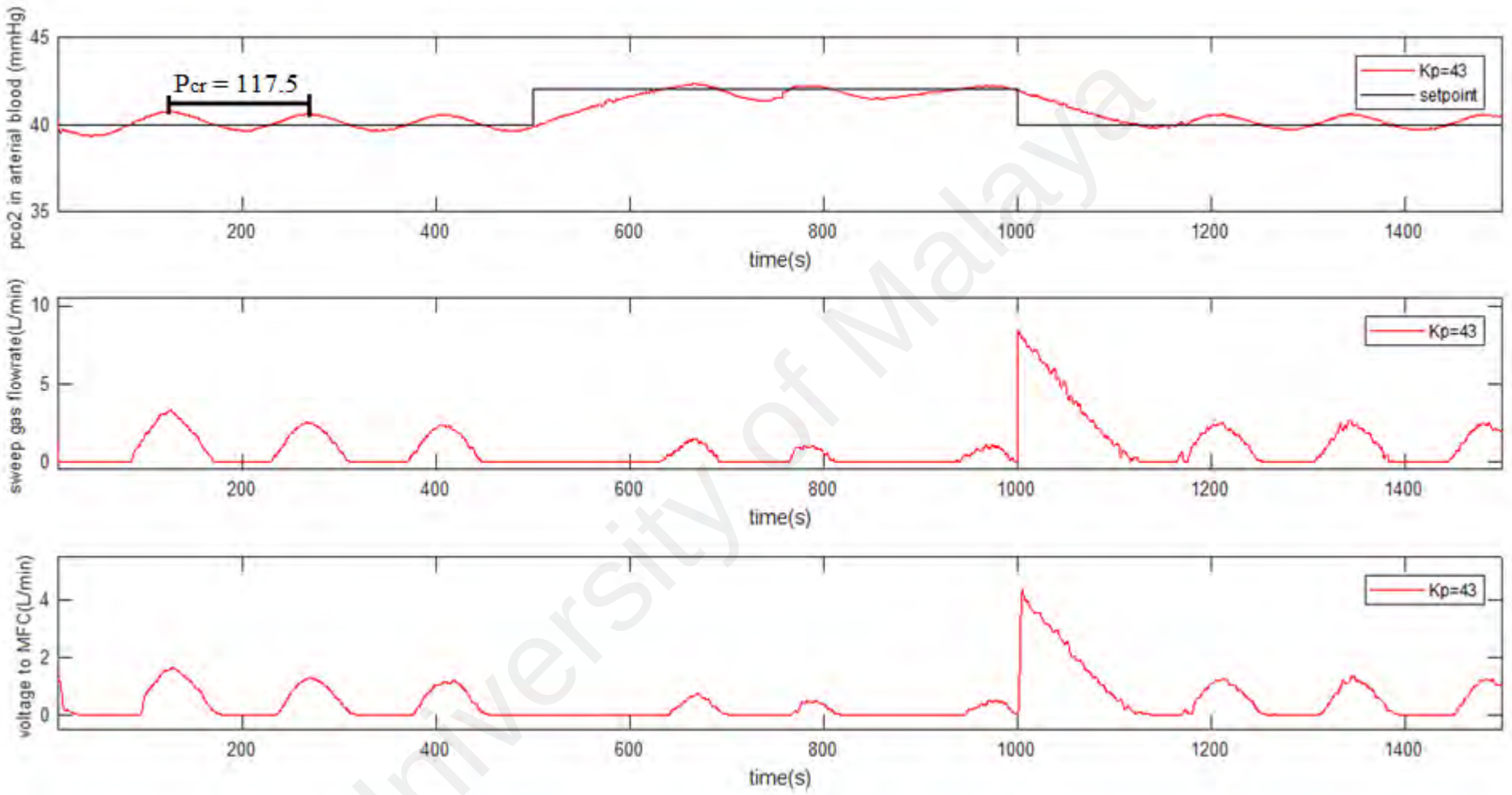

Figure 5.36: Measurement of arterial pCO_2 on automatic mode at K_{cr}= 43.

Table 5.12. Ziegler-Nichols tuning rules based on critical gain and critical methods.

Parameters	Values
Critical period, P_{cr}	P_{cr}= 117.5 s
Critical gain, K_{cr}	43
Proportional gain, K_p	$Kp = 0.6 \times Kcr$ $= 25.8$
Integral time, T_i	$Ti = \frac{Pcr}{2}$ $= 58.750$ s
Derivative time, T_d	Td= P_{cr}/8 = 14.688 s

5.3.4.1. Closed loop control (experimental): Setpoint tracking

5.3.4.1.1. PID

Figure 5.37 shows the arterial pCO_2 measured by pCO_2 sensors in respect to the change in setpoint. When changing from 40 mmHg to 42 mmHg at t=300s, PID controller took around 70 seconds to regulate the effect of setpoint changing. This controller able to increase the pCO_2 to 42 mmHg with offset around 0.6 mmHg. At t=600s, the setpoint was adjusted back to 40 mmHg. Here, the PID controller increased its sweep gas flow rate to around 2.6 L/min in order to adapt with the setpoint changes. After around 150s, the error was constant at approximately 0.4 mmHg, which is small and promising.

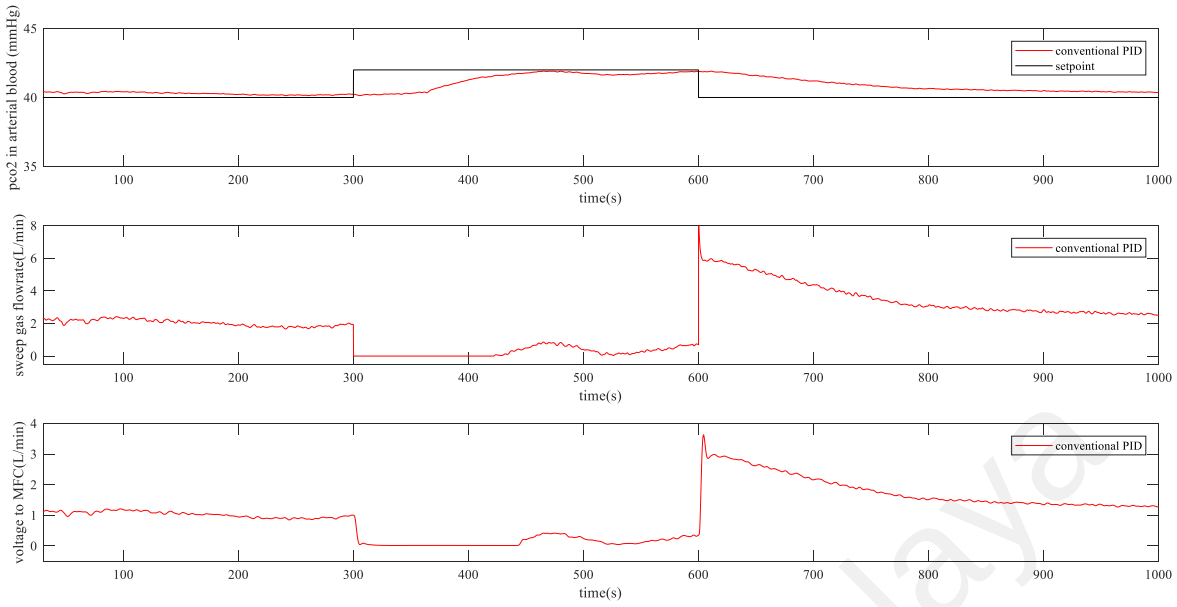

Figure 5.37: Measured arterial pCO_2, its respective sweep gas flowrate and voltage supplied to MFC for PID controller (setpoint tracking task).

5.3.4.1.2. Fuzzy Logic Controller (FLC)

For FLC controller, to produce 40 mmHg of pCO_2, the FLC set the sweep gas flowrate at 1.3 L/min at the beginning of the control process, before the setpoint was changed to 42 mmHg at t=300s. As seen from Figure 5.38, the controller reduced the sweep gas flow rate to around 0.6 L/min to achieve the desired setpoint. The arterial pCO_2 was unable to rise to 42 mmHg, and been constant around 40.86 mmHg with sustained error of 1.14 mmHg. Again, when the setpoint was adjusted back to 40 mmHg, flowrate of 1.3 L/min was applied once again, which reduced the arterial pCO_2 to 40.3 mmHg with the sustained error of 0.37 mmHg after 150s.

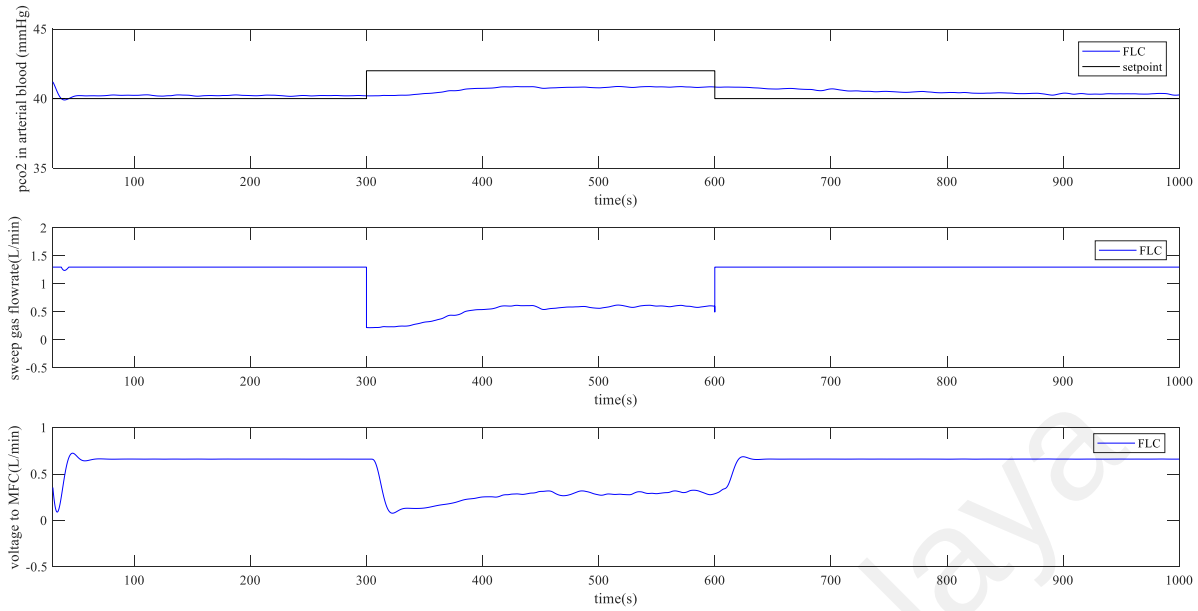

Figure 5.38: Measured arterial pCO_2, its respective sweep gas flowrate and voltage supplied to MFC for FLC controller (setpoint tracking task).

5.3.4.1.3. Fuzzy-PID

Figure 5.39 depicts the response of arterial pCO_2 on setpoint changing. As we can see from the figure, the accuracy for this controller is higher compared to the previous results for PID and FLC. This controller took only approximately 87 s to achieve the first setpoint change (42 mmHg) and 170s to return to its initial setpoint, 40 mmHg. Towards the end of the experiment, the sustained error obtained was very small, which only 0.07 mmHg (arterial pCO_2 measurement of 40.07 mmHg) with controller output (sweep gas flowrate) around 2.0-2.1 L/min.

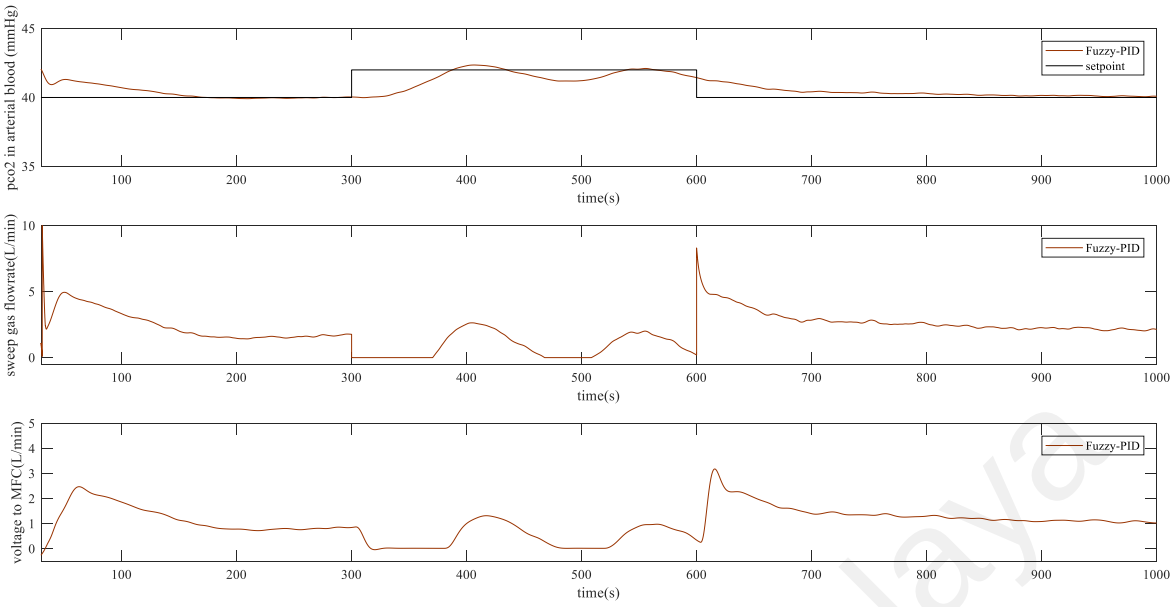

Figure 5.39: Measured arterial pCO_2, its respective sweep gas flowrate and voltage supplied to MFC for Fuzzy-PID controller (setpoint tracking task).

5.3.4.1.4. Comparison of all controllers for setpoint tracking

Performance between the controllers for setpoint tracking task was compared quantitatively by MSE. As stated in Figure 5.40, MSE for PID is 0.9238, 0.9186 for FLC and Fuzzy-PID recorded the lowest MSE with 0.4800. Here, Fuzzy-PID have 48.04% reduction in MSE compared to PID and 47.75% lower MSE than FLC. These MSE reduction indicate that the smallest average error calculated when Fuzzy-PID was used to control the CO_2 gas transfer within membrane oxygenator.

In short, it can be said that Fuzzy-PID controller provides an excellent set-point response, while PID have significant overshoots and longer settling times. As for FLC, even though the response is more stable with no overshoot at all, its large error makes it less suitable as a controller for this task.

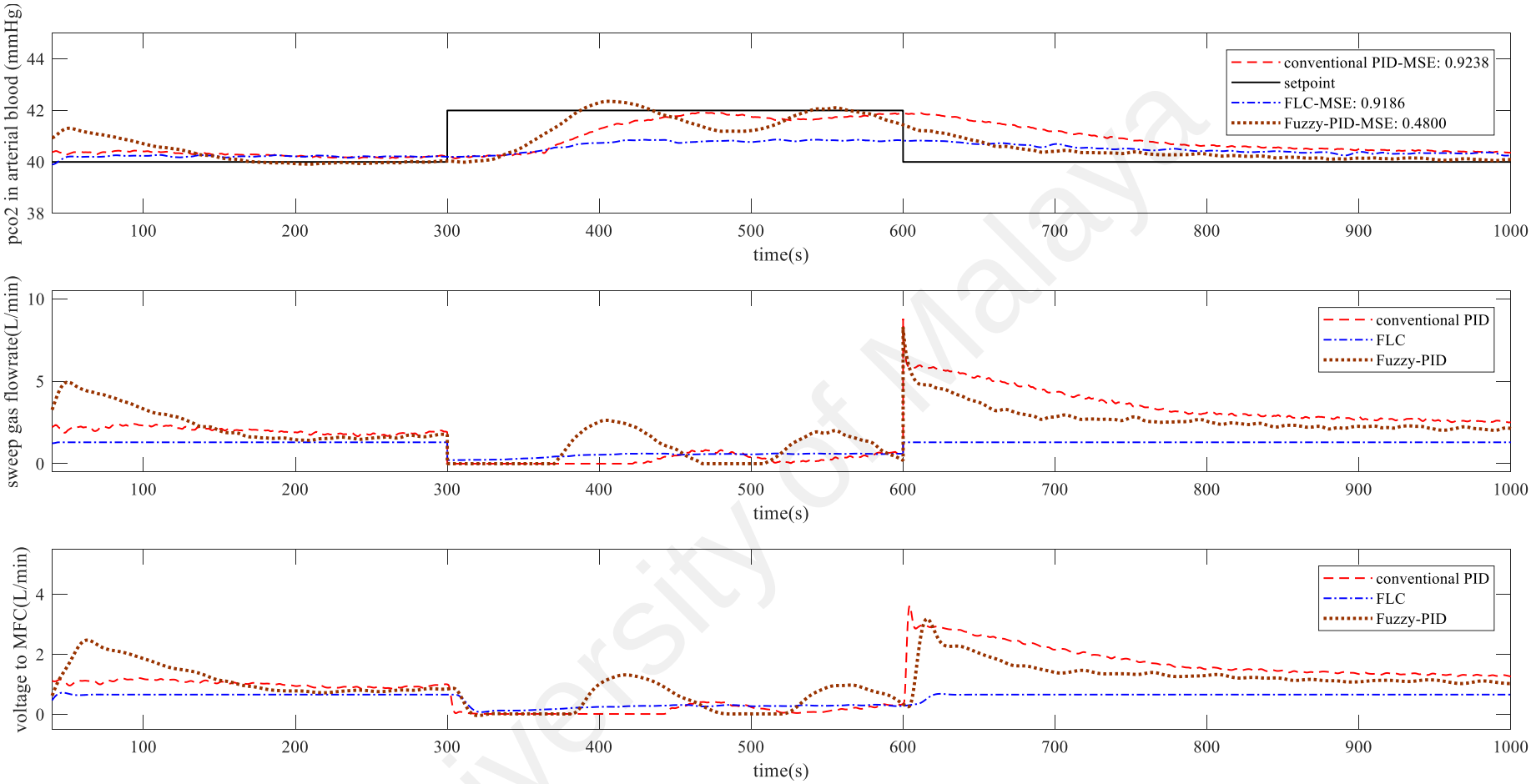

Figure 5.40: Performance comparison for all three controllers (PID, FLC and Fuzzy-PID for setpoint tracking task-experimental, newly-tuned controller's parameter/gain).

5.3.4.2. Closed loop control (experimental): Disturbance rejection

5.3.4.2.1. PID

Disturbance in this study is the sudden shut-off of MFC (sweep gas flowrate= 0 L/min). This disturbance was applied at t=300s and t=600s. Response of PID controller to this disturbance is shown in Figure 5.41.

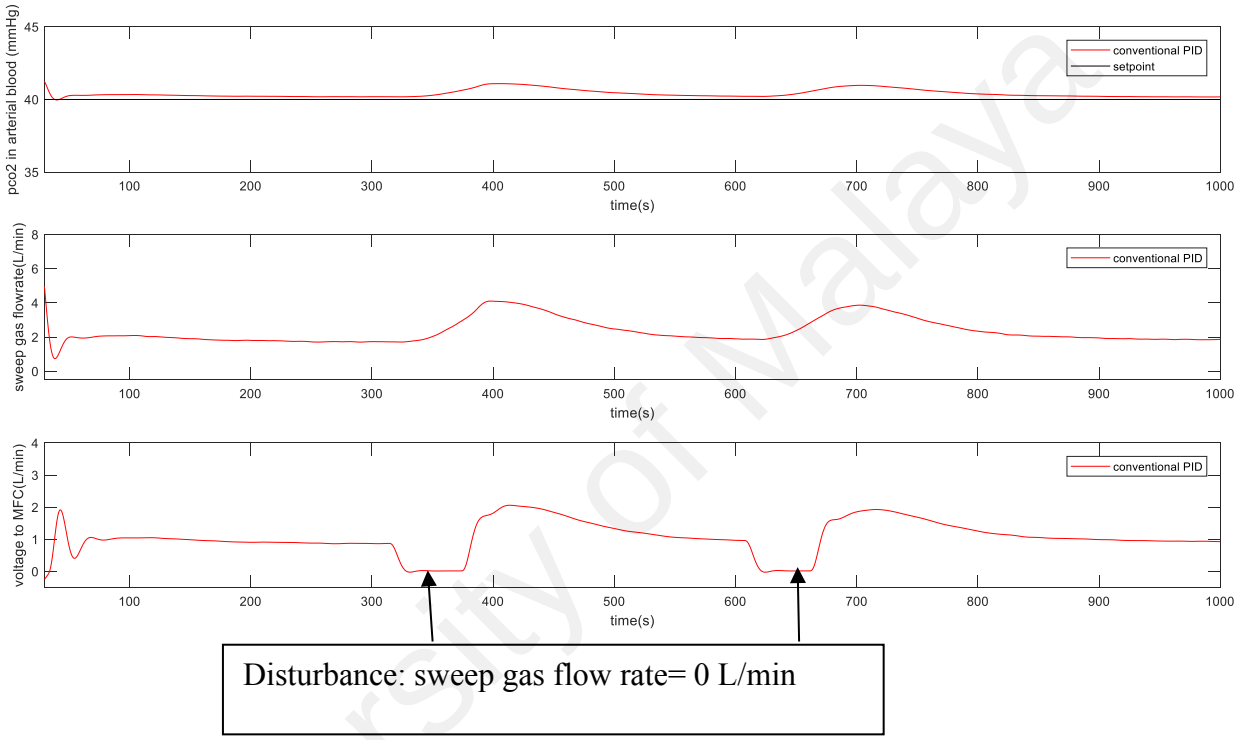

Figure 5.41: Measured arterial pCO_2, its respective sweep gas flowrate and voltage supplied to MFC for PID controller (disturbance rejection task).

Prior to the disturbance, PID controller managed to maintain the arterial pCO_2 according to the setpoint (40 mmHg) with only small error occurred, around 0.19 mmHg. After the sudden shut-off of MFC for 1 minute at t=300, without the sweep gas, arterial pCO_2 rose at 2.73%, up to 41.09 mmHg after 95s. With the continuation of sweep gas after 1 minute of shut-off, the controller simultaneously increased the flowrate up to 4.1 L/min to compensate with the arterial pCO_2 that exceeded the desired setpoint. This high flowrate seems to be effective, since it successfully brought the pCO_2 back to around 40.21 mmHg after 200s. The similar observation

can be seen for disturbance at t=600s. These good responses proved the ability of PID controller in controlling arterial pCO_2 towards the setpoint, but the time taken is quite high, thus a better controller for this task is needed.

5.3.4.2.2. Fuzzy Logic Controller (FLC)

Figure 5.42 illustrates the measurement of arterial pCO_2 with the respective sweep gas flowrate and voltage that been supplied to MFC. Surprisingly, the FLC only gave the constant flowrate at 1.3 L/min for the whole experiment. Unlike PID controller, FLC only gave 1.3 L/min for the whole experiment. This constant sweep gas flowrate also able to bring the pCO_2 according to the setpoint, but the time taken was longer (around 210s for both events of disturbance). Furthermore, sustained error of 0.6 mmHg was measured.

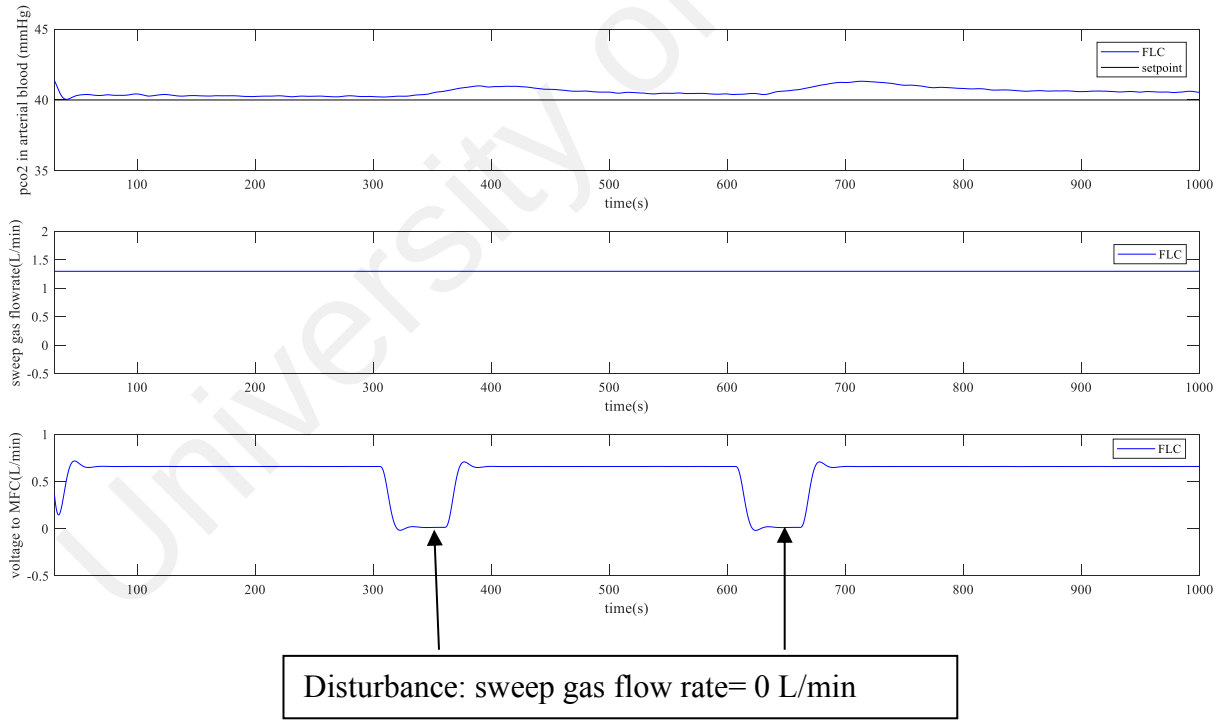

Figure 5.42: Measured arterial pCO_2, its respective sweep gas flowrate and voltage supplied to MFC for FLC controller (disturbance rejection task).

5.3.4.2.3. Fuzzy-PID

Figure 5.43 shows the Fuzzy-PID controller's response over the introduction of the disturbance, which is very outstanding. At time t=300s, disturbance was applied to the process plant, and the controller was expected to adapt with this disturbance. In this scenario, the controller augmented sweep gas flowrate from 0 L/min to 4.4 L/min over a period of 150s, with the peak pCO_2 of 41 mmHg. Consequently, the system able to maintain relative stability around the setpoint with only small offset was recorded, which is 0.2 mmHg. The similar observations also seen at t=600s.

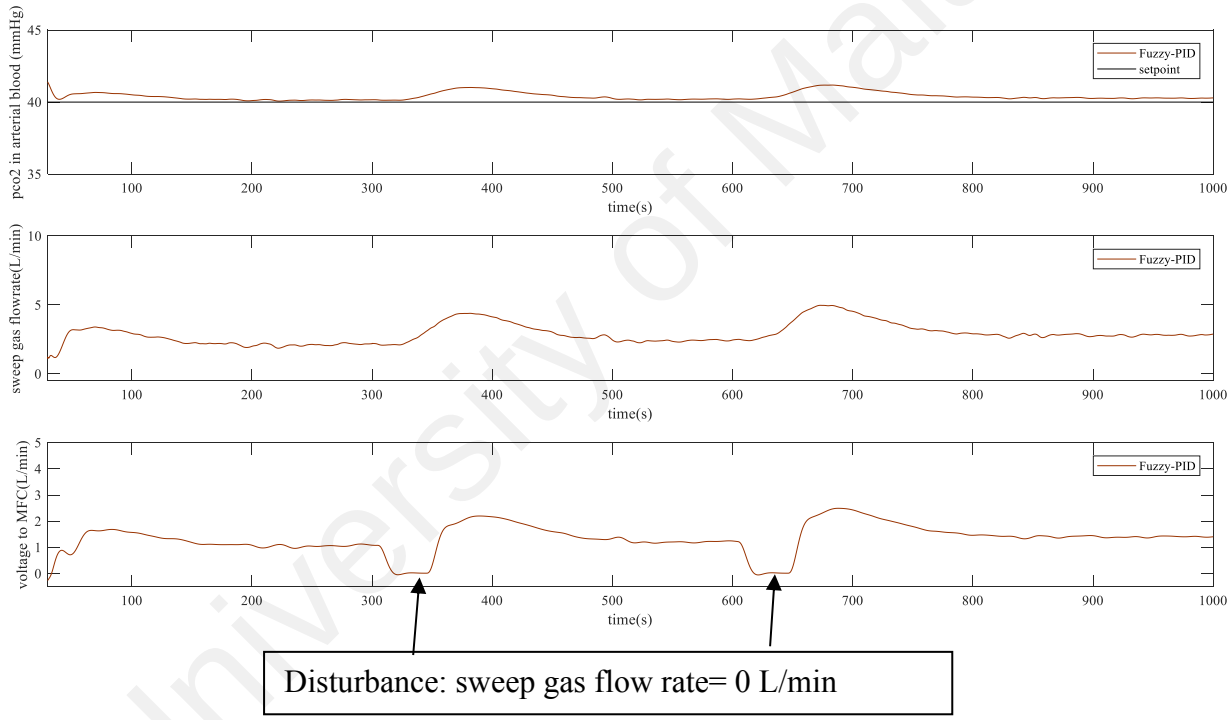

Figure 5.43: Measured arterial pCO_2, its respective sweep gas flowrate and voltage supplied to MFC for Fuzzy-PID controller (disturbance rejection task).

5.3.4.2.4. Comparison of all controllers for disturbance rejection

The responses of the three proposed controllers to this disturbance were depicted in Figure 5.50. A significant reduced in steady state error for Fuzzy-PID can be seen by quantitative fact of MSE, which is the smallest compared to the PID and FLC. When compared quantitatively

by means of MSE calculation, Fuzzy-PID recorded the lowest MSE with 0.2842, whereas 0.2913 and 0.5413 calculated for PID and FLC, respectively. This means that Fuzzy-PID able to reduce the MSE by 0.02% from PID and 47.5% from FLC. Here, it can be concluded that among the three controllers, Fuzzy-PID gave the most outstanding control performance with the lowest overshoot, less oscillation compared to PID, a better disturbance response with a smaller maximum deviation of the desired setpoint and better disturbance rejection in view of their smaller settling times. All of these indicate a good control response of Fuzzy-PID controller to achieve the setpoint while maintaining the hemodynamic stabilization.

From the graph presented in Figure 5.44, a similar trend of disturbance rejection was found. After a sudden stop of sweep gas, the controllers increased the sweep gas flowrate up to 4 L/min for PID, 4.4 L/min for Fuzzy-PID, while FLC maintained its flowrate at 1.3 L/min to compensate with the increase in arterial pCO_2. By this strategy, all the controllers managed to bring the measure pCO_2 back to the setpoint after some period of time, with Fuzzy-PID as the fastest controller to reject this disturbance. The differences among these three controllers are the percentage of offset, overshoot and settling time.

Here, it can be concluded that among this three controllers, Fuzzy-PID have the most outstanding control performance with the lowest overshoot, less oscillation compared to PID, better disturbance rejection response with a smaller maximum deviation of the desired setpoint (4.76% lower in offset than PID and 66.67% lower than FLC) and much better disturbance rejection in view of their smaller settling times (reduction of 25% compared to PID and 28.57% compared to FLC). A decreased steady state error for Fuzzy-PID also can be concluded by quantitative fact of MSE, which is the smallest compared to the PID and FLC. A good control response of Fuzzy-PID controller makes it rapidly achieves the setpoint while maintaining the hemodynamic stabilization.

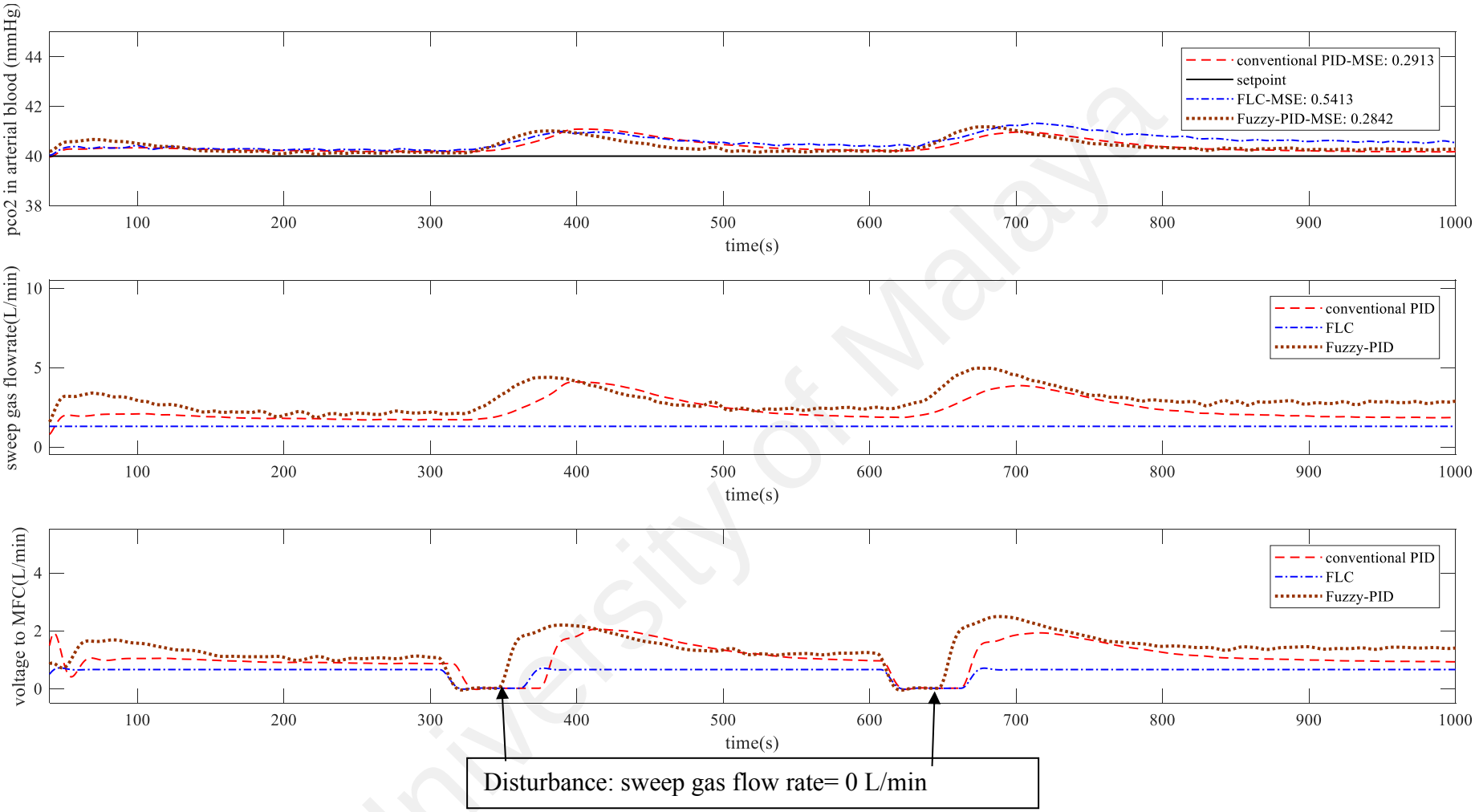

Figure 5.44: Performance comparison for all three controllers (PID, FLC and Fuzzy-PID for disturbance rejection task-experimental, newly-tuned controller's parameter/gain).

5.3.5. Simulation of closed loop control using experimental parameter

The new PID gains and fuzzy rules were successfully control pCO_2 in in-vitro CO_2 gas exchange module. Hence, the same PID parameter and fuzzy rule were implemented in simulation model, to ensure that it works well too in simulation.

5.3.5.1. Closed loop control (simulation): setpoint tracking

5.3.5.1.1. PID

The same gain (newly-tuned based on the experimental process) was implemented to the mathematical model for simulation. A satisfactory result was obtained, which the sustained error was recorded at around 0.33 mmHg. The PID controller was able to control the CO_2 process, unlike the on-off control action previously.

i. PID with K_p= 25.8, K_i= 0.017, K_d= 14.6875.

From Figure 5.45, a good control to the process variable (arterial pCO_2) can be seen for PID controller. There was small offset, but overall, this controller managed to bring the arterial pCO_2 around the desired setpoint.

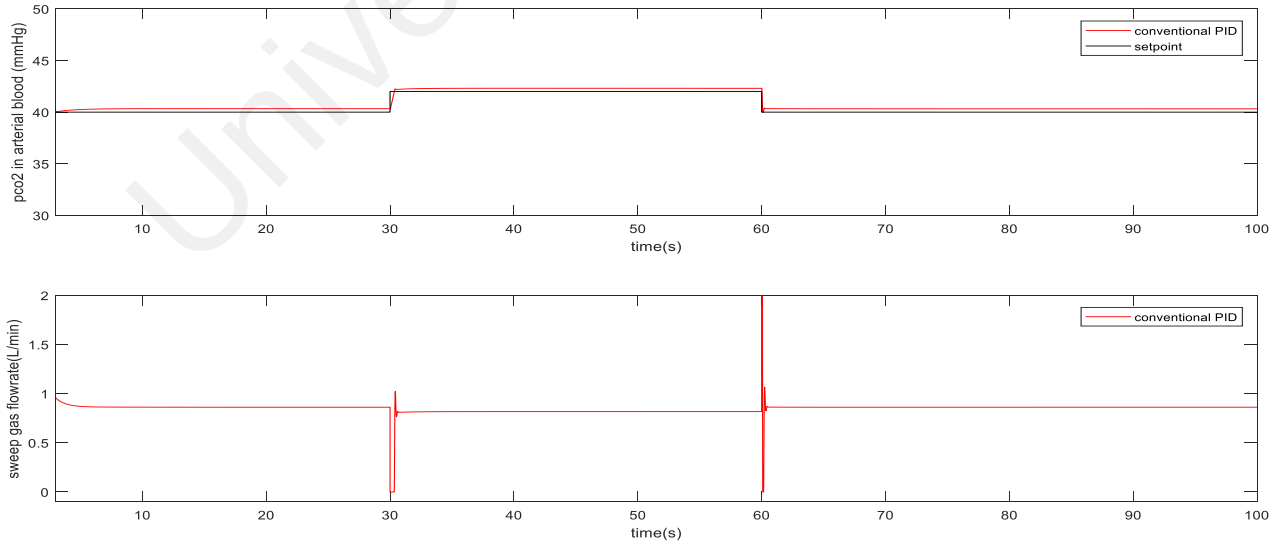

Figure 5.45: Simulated arterial pCO_2 and its respective sweep gas flowrate for PID controller (setpoint tracking task).

5.3.5.1.2. Fuzzy Logic Controller (FLC)

In contrast, FLC response to the setpoint changes (as in Figure 5.46) contains larger offset. Arterial pCO_2 simulated was smaller than the desired point for the whole simulation time. Even though there was no overshoot and oscillation, but the larger error makes it less efficient, compared to the other controllers.

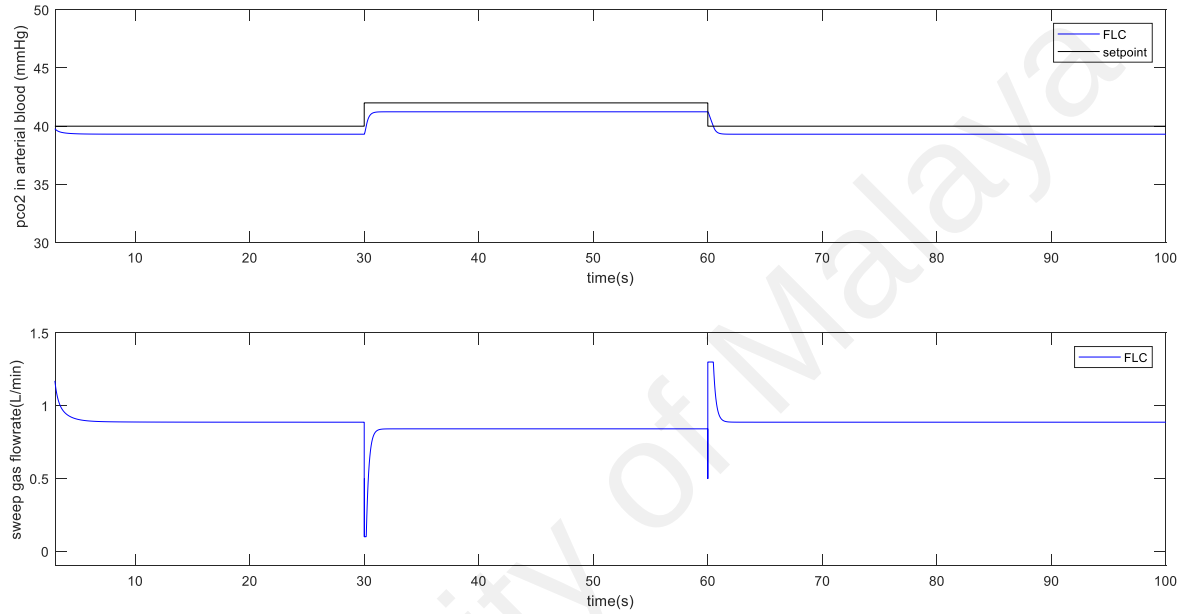

Figure 5.46: Simulated arterial pCO_2 and its respective sweep gas for FLC controller (setpoint tracking task).

5.3.5.1.3. Fuzzy-PID

For Fuzzy-PID controller in Figure 5.47, offset was very small, despite of its good control ability to maintain the arterial pCO_2 according to the desired setpoint.

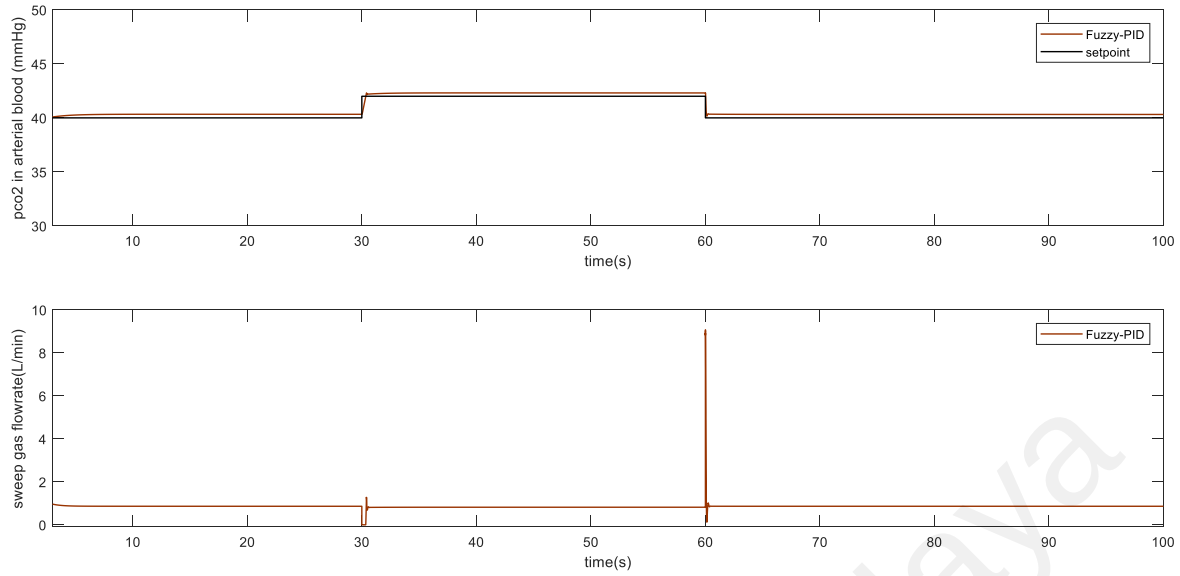

Figure 5.47: Simulated arterial pCO_2 and its respective sweep gas flowrate for Fuzzy-PID controller (setpoint tracking task).

5.3.5.1.4. Performance comparison for all controllers (simulations)

In this section, the response of the controllers with their respective sweep gas flowrate were plotted in Figure 5.48. Clearly, the worst controller among these three was FLC, while PID and Fuzzy-PID showed the comparable performance.

i. Whole simulation

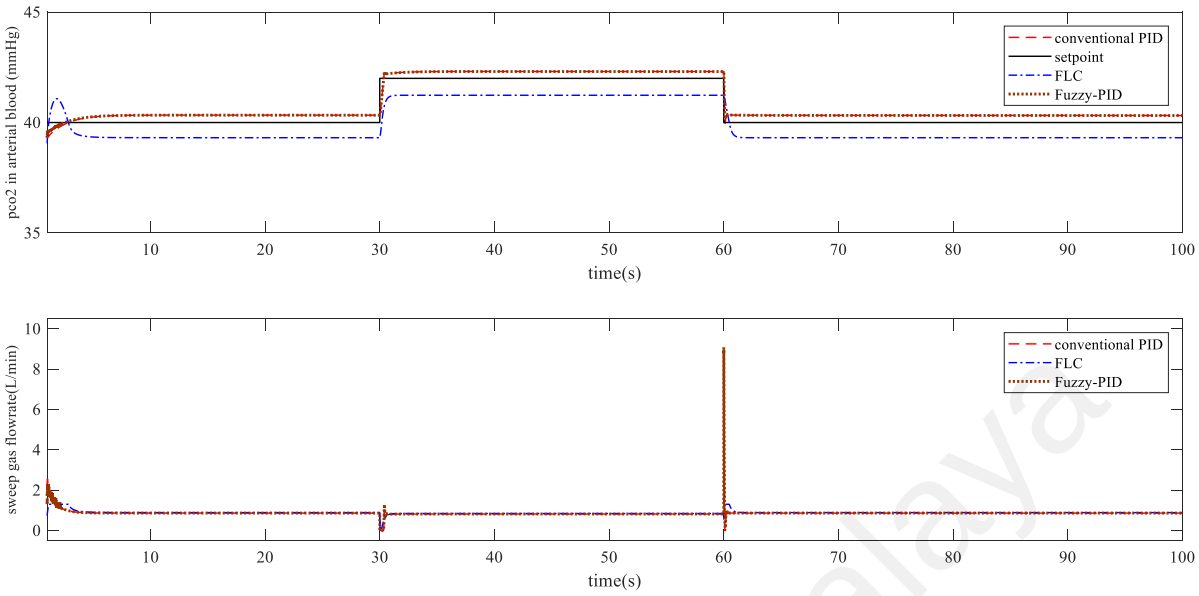

Figure 5.48: Comparison of whole simulation time for simulated arterial pCO_2 and its respective sweep gas flowrate (setpoint tracking task).

For clearer observation, zoomed view at t=30s was presented in Figure 5.49 and Figure 5.50 at t=60s. This is the moment when the setpoint was changed. From these figures, Fuzzy-PID showed fast response with lesser oscillation compared to PID. This good performance was validated quantitatively by the calculation of performance indices tabulated in Table 5.13. From this table, FLC become the worst controller in setpoint tracking task with 50.90 IAE, 37.96 ISE, 3243 ITAE and 0.5506 MSE, while Fuzzy-PID become the best controller in similar task with 22.22 IAE, 7.423 ISE, 1448 ITAE and 0.1099 MSE, which is better compared to PID, which recorded 22.35, 7.561, 1459 and 0.1192 for IAE, ISE, ITAE and MSE, respectively.

ii. At t=30s

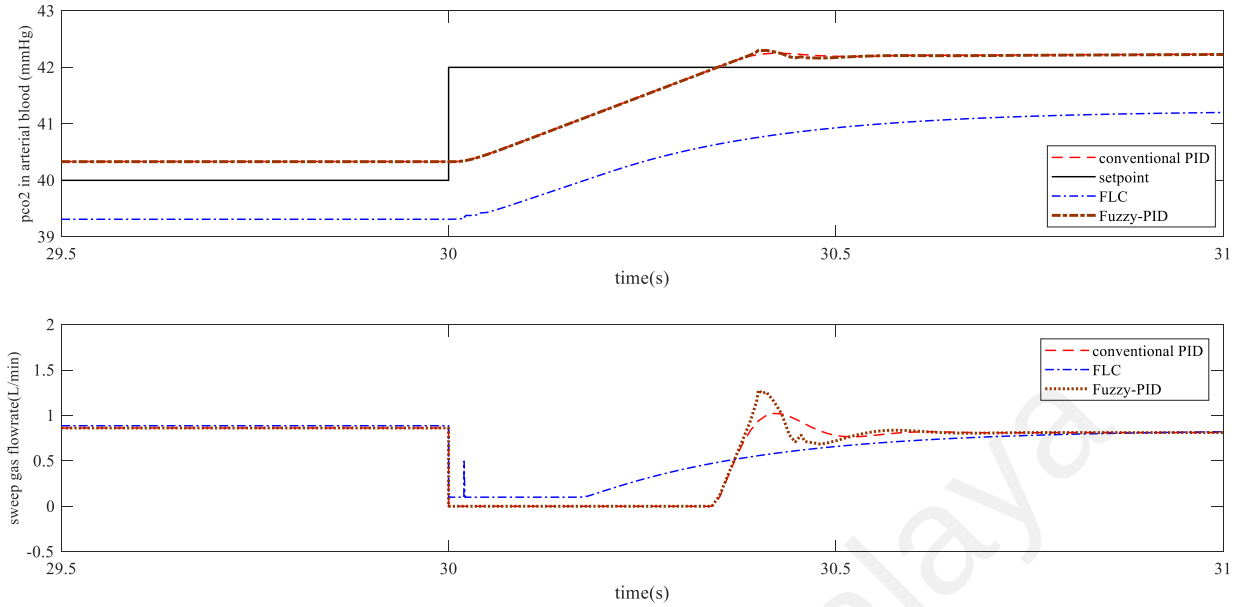

Figure 5.49: Comparison of simulation at t=30s for simulated arterial pCO_2 and its respective sweep gas flowrate (setpoint tracking task).

iii. At t=60s

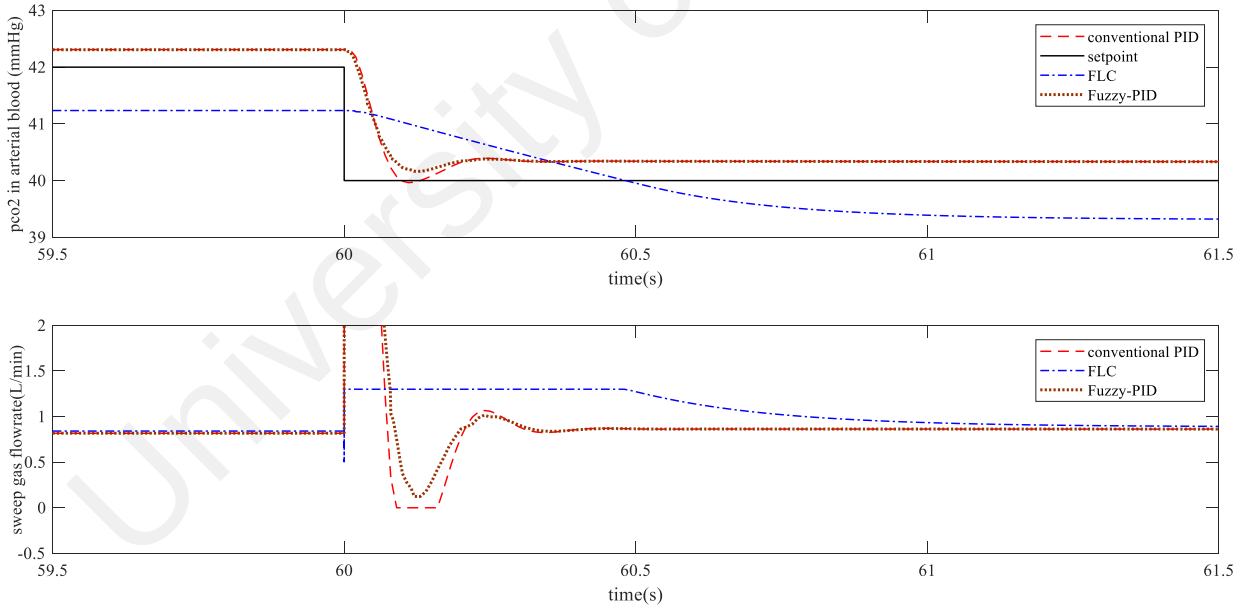

Figure 5.50: Comparison of simulation at t=60s for simulated arterial pCO_2, and its respective sweep gas flowrate (setpoint tracking task).

Table 5.13: Comparison of IAE, ISE, ITAE and MSE for three controllers during setpoint tracking task (simulation).

Controllers	IAE	ISE	ITAE	MSE
PID	22.35	7.561	1459	0.1192
FLC	50.90	37.96	3243	0.5506
Fuzzy-PID	**22.22**	**7.423**	**1448**	**0.1099**

5.3.5.2. Closed loop control (simulation): Disturbance rejection

5.3.5.2.1. PID

Figure 5.51 represents arterial pCO_2 and its respective sweep gas flowrate in rejecting disturbance. In conjunction to the sudden stop of sweep gas flowrate to the process plant (membrane oxygenator), arterial pCO_2 increased to 45 mmHg, since there was no sweep gas supplied to remove CO_2. As a counteract response, PID increased the flowrate to 10 L/min, and successfully brought the pCO_2 back to the desired setpoint, 40 mmHg. Small sustained error was seen with good control action shown by this controller.

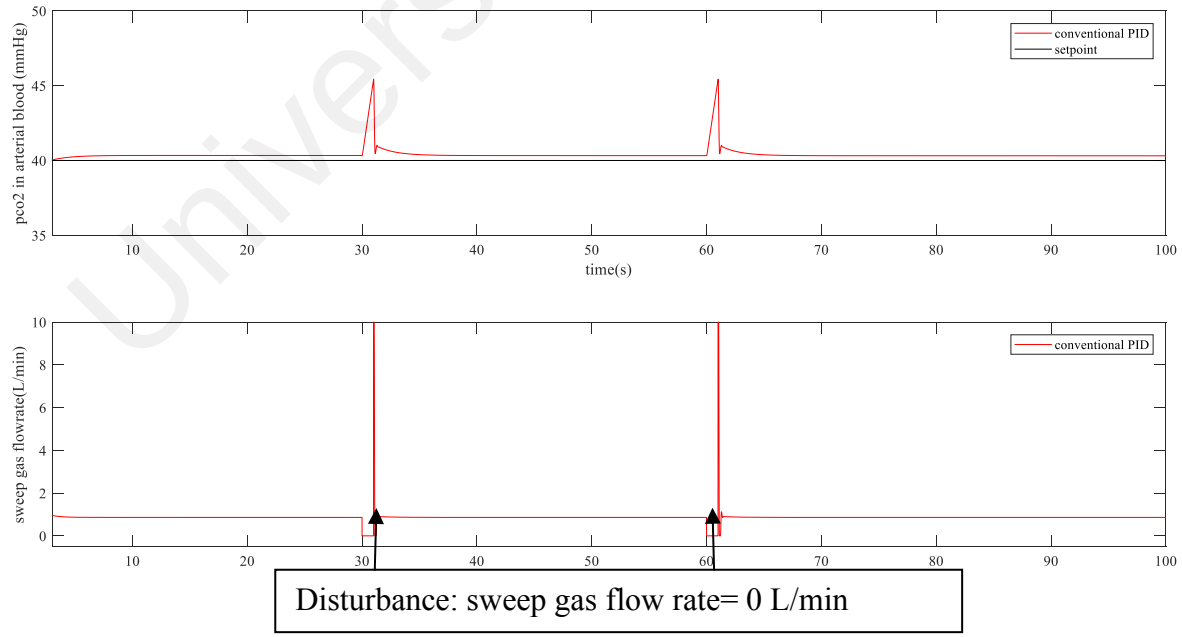

Figure 5.51: Simulated arterial pCO_2 and its respective sweep gas flowrate for PID controller (disturbance rejection task).

5.3.5.2.2. Fuzzy Logic Controller (FLC)

FLC response against disturbance is illustrated in Figure 5.52. Sustained error was observed and the accuracy of this controller to maintain the desired setpoint is unsatisfactory.

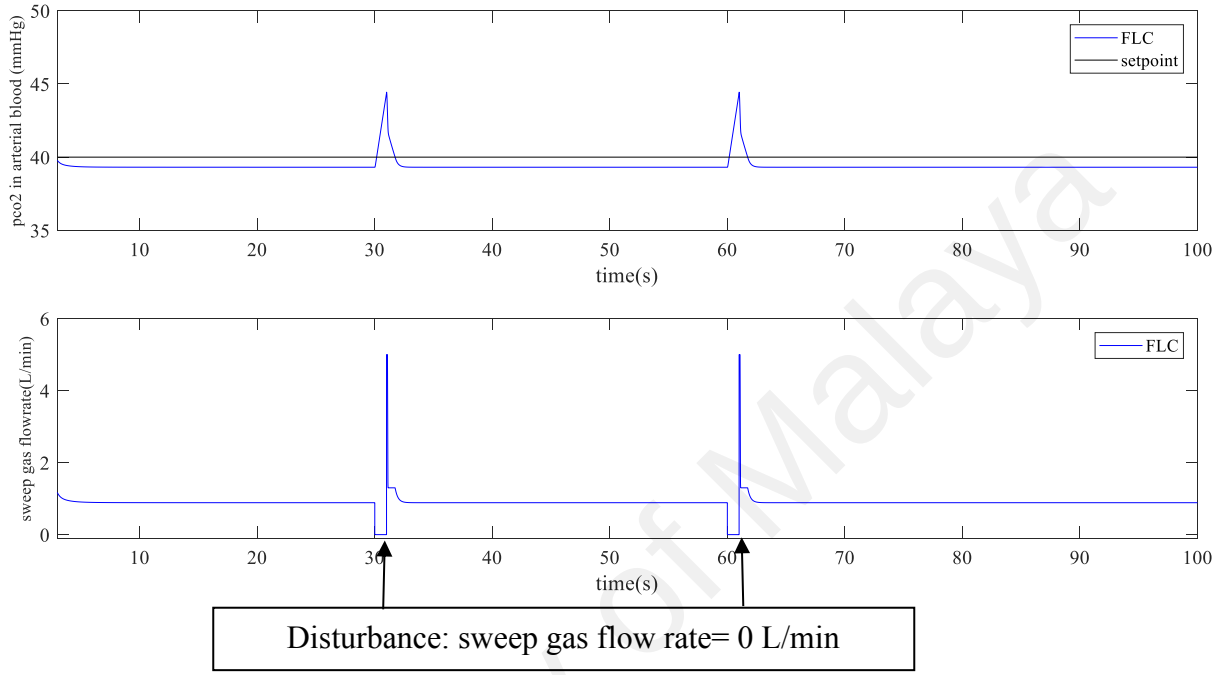

Figure 5.52: Simulated arterial pCO_2 and its respective sweep gas flowrate for FLC controller (disturbance rejection task).

5.3.5.2.3. Fuzzy-PID

Graph in Figure 5.53 shows response of Fuzzy-PID controller in the similar task as PID and FLC. From this figure, good control action was shown by this controller, compared to FLC controller, by appropriately adjusted the sweep gas flowrate in response to progressive increase in arterial pCO_2. Fuzzy-PID was able to adapt with the sudden stop of flowrate to the membrane oxygenator and able to bring the arterial pCO_2 back to the desired setpoint with small sustained error.

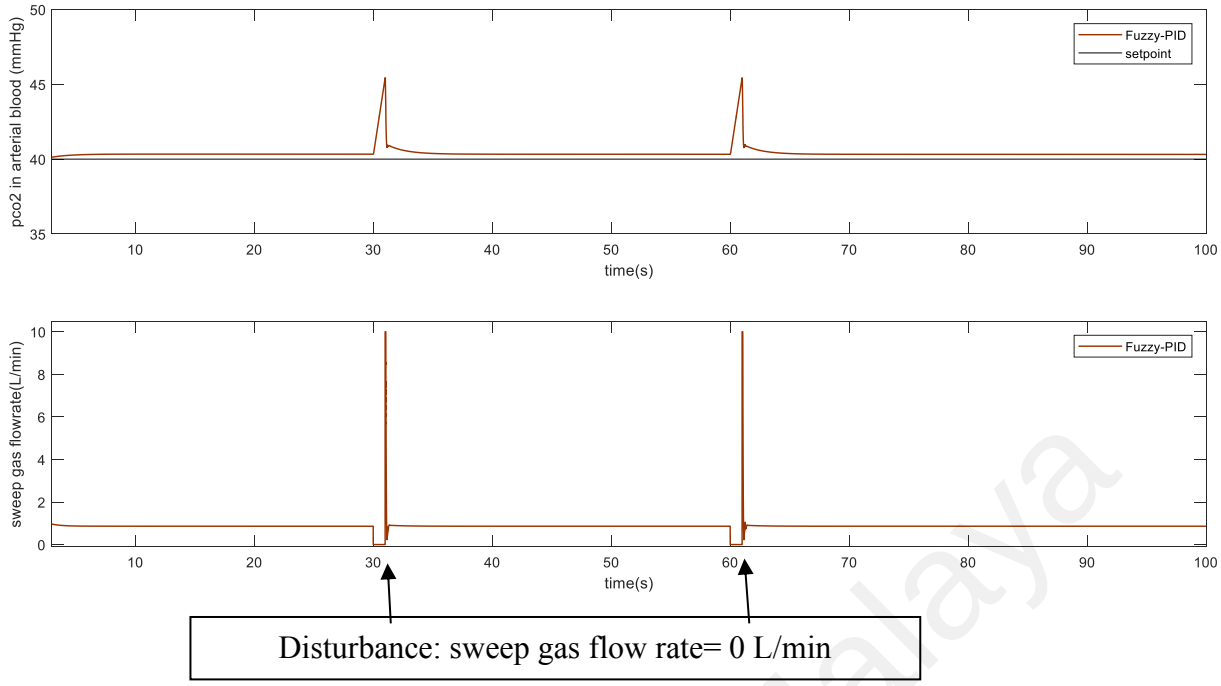

Figure 5.53: Simulated arterial pCO_2 and its respective sweep gas flowrate for Fuzzy-PID controller (disturbance rejection task).

5.3.5.2.4. Performance comparison for all controller (simulation)

Figure 5.54 depicted the entire control performance for all the three controllers evaluated in this study, which are PID, FLC and Fuzzy-PID. The worst control action was produced by FLC controller, with the best recorded by Fuzzy-PID.

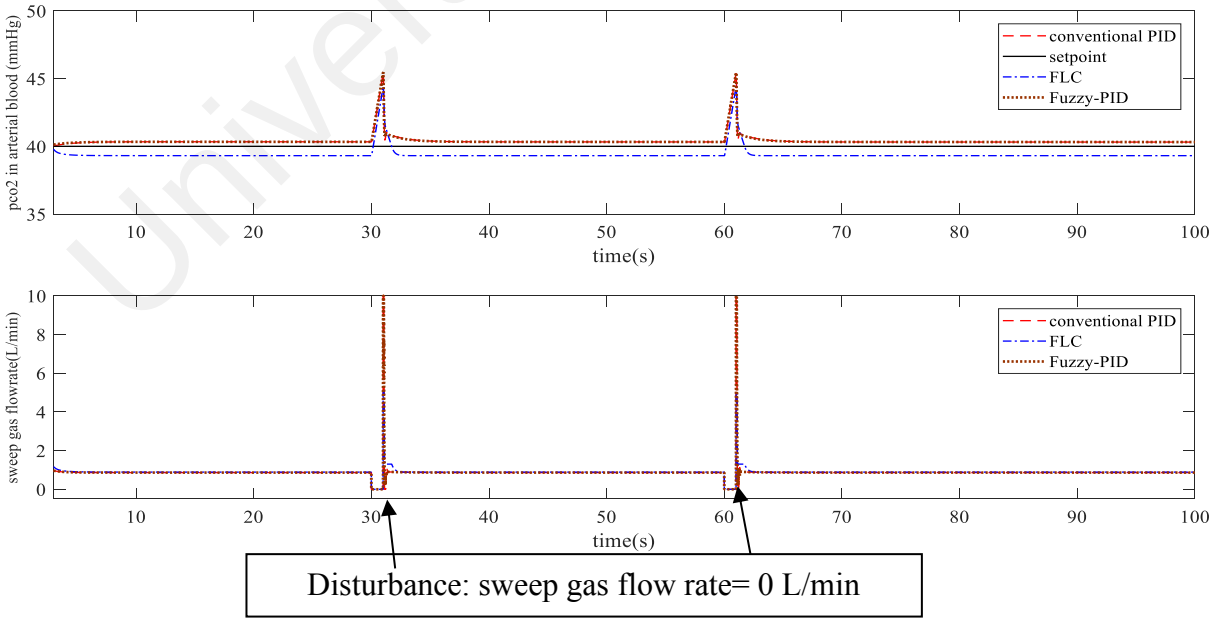

Figure 5.54: Comparison of whole simulation time for simulated arterial pCO_2 and its respective sweep gas flowrate (disturbance rejection task).

The zoomed view graph was also plotted in Figure 5.55 (at t=30s) and Figure 5.56 (at t=60s). From these figures, all the three controllers able to reject the disturbance by increasing the flowrate to reduce the arterial pCO_2, that exceeded the desired setpoint, due to the sudden stop of sweep gas supply to membrane oxygenator at both event of disturbance (t=30s and t=60s).

From the figure, it was seen that Fuzzy-PID is the best controller for this task, and this qualitative analysis later was proven by the calculation of performance indices in terms of IAE, ISE and ITAE, as tabulated in Table 5.14. The best controller is Fuzzy-PID with 30.19 IAE, 32.29 ISE, 1851 ITAE and 0.4697, followed by PID which recorded 30.30 IAE, 32.58 ISE, 1881 ITAE and 0.4790 MSE. Among the three controllers, FLC become the least efficient controller with 51.16 IAE, 46.24 ISE, 3269 ITAE and 0.6982 MSE.

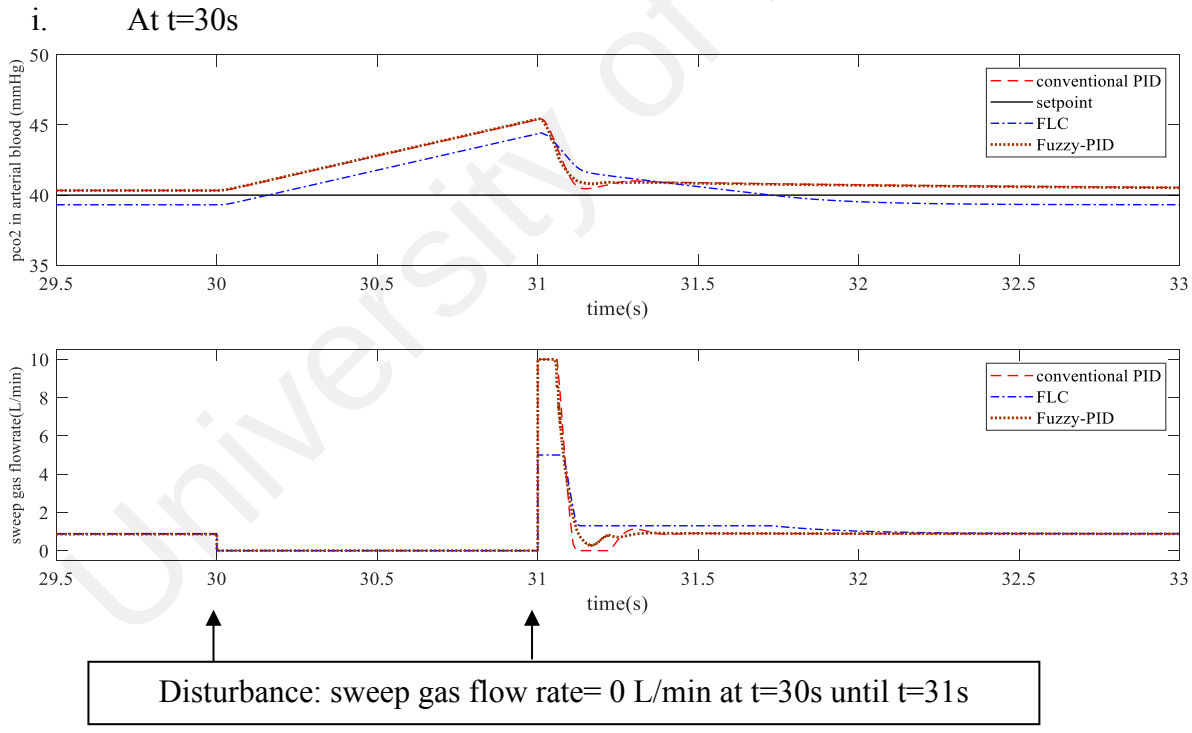

Figure 5.55: Comparison of simulation at t=30s for simulated arterial pCO_2 and its respective sweep gas flowrate (disturbance rejection task).

ii. At t=60s

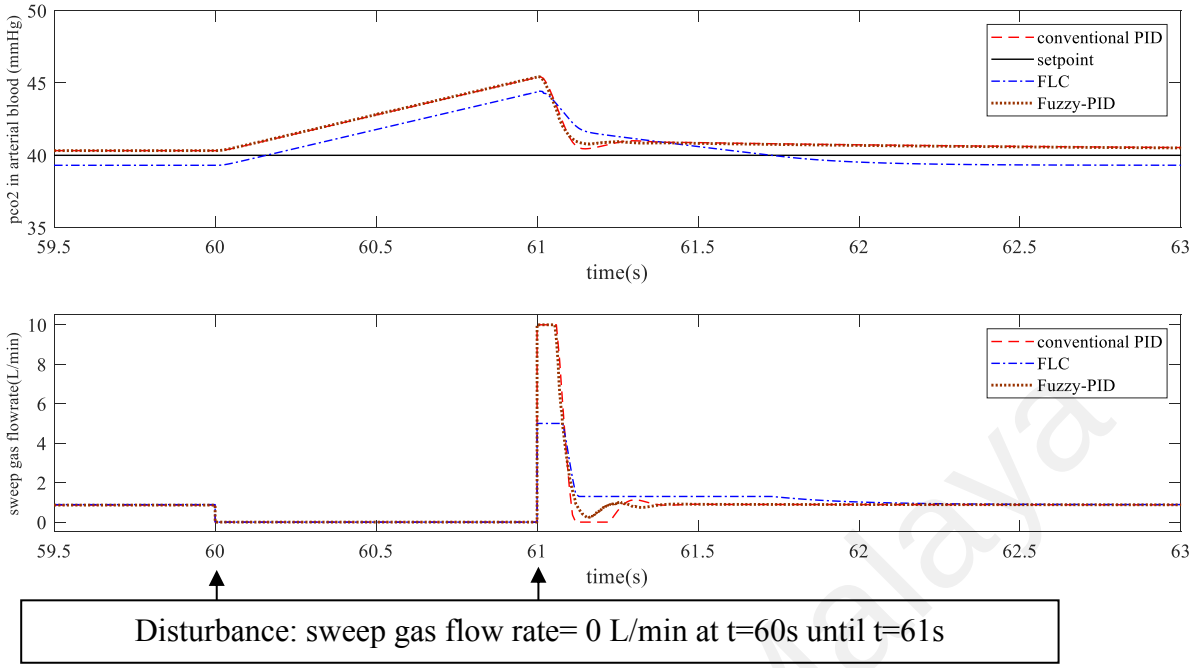

Figure 5.56: Comparison of simulation at t=60s for simulated arterial pCO_2 and its respective sweep gas flowrate (disturbance rejection task).

Table 5.14: Comparison of IAE, ISE, ITAE and MSE for three controllers during disturbance rejection task (simulation).

Controllers	IAE	ISE	ITAE	MSE
PID	30.30	32.58	1881	0.4760
FLC	51.16	46.24	3269	0.6982
Fuzzy-PID	**30.19**	**32.29**	**1851**	**0.4697**

5.4. Discussion (experimental work)

For open-loop control, the process variable (pCO_2) changed in according to the changed of the manipulated variable (sweep gas flowrate) by inverse relationship. The behaviour of this system was agreed with the previous study conducted by Fedespiel and Hattler (Federspiel & Hattler, 1996), Hout et al. (Hout et al., 2000a) and Sun et al. (Sun et al., 2018) using in-vitro model. Decreasing in sweep gas flow rate to membrane oxygenator will simultaneously increase pCO_2 inside the hollow fibre unit, hence reduce the partial pressure gradient that exist

between blood phase and gas phase. The difference then consequently lessens the CO_2 removal from blood to gas phase, cause high pCO_2 measurement in arterial blood. This finding then confirms the first hypothesis of this study.

Following the open loop study, closed loop study was conducted to evaluate the ability of the proposed controller to control CO_2 gas transfer in membrane oxygenator by manipulating its sweep gas flowrate, experimentally. Through this experimental work, CO_2 gas exchange module that developed in this study demonstrated the ability to maintain optimum CO_2 gas exchange in membrane oxygenator in both setpoint and disturbance rejection task.

At first, the experimental work was conducted using the similar PID parameters and FLC rules determined in simulation work, but the results obtained were unsatisfactory. PID and Fuzzy-PID were unable to control the process, while FLC showed a good control action. This is due to the characteristic of FLC itself, which has good control in dealing with nonlinear system, since it uses the human operator knowledge (Gouda et al., 2000).

However, the control profiles are similar between both simulation and experimental findings, which is the inverse relationship exist between manipulated variable (sweep gas flowrate) and process variable (arterial pCO_2). The controllers also exhibit direct-control action, where the controllers increase its sweep gas flowrate as the arterial pCO_2 exceeds the desired setpoint, and vice versa.

The inability to control of PID and Fuzzy-PID controllers indicate that the PID parameters that been tuned previously in simulation work is not suitable to be implemented in experimental work setting. This is most probably due to:

1. The exchange and transport of O_2 and CO_2 in blood are complex biological process, since it deals with nonlinearities, time delay, uncertainties and time varying parameters (Misgeld et al., 2010). This will produce some difficulty to develop a suitable model for feedback control.

2. There is difference in time taken to complete one cycle of control process. For example, during tuning process, only 0.12s is needed to complete one cycle of simulation, while 117.5s is taken to complete one cycle of process control in experimental measurement.

3. There is long transport delay (around 100s) exist during experimental measurement, while no transport delay is considered in simulation.

4. Difference in assumption used. For example, venous pCO_2 is assumed to be constant at 46 mmHg for the whole simulation, while during experiment, venous pCO_2 is quite changing and have to monitored closely from pCO_2 (inlet) measurement. Also, in mathematical modelling (refer Chapter 3), perfect mixing is assumed for gas compartment with no volume loss ($Q_{in}=Q_{out}$), which is quite impossible to be achieved in the real situation.

Due to these reasons, new tuning process of PID gain parameters was performed, using the same tuning method as in simulation work (Ziegler-Nichols continuous cycling method).

In closed-loop control using newly tuned PID gains, all the three proposed controllers, PID, FLC and Fuzzy-PID were able to maintain arterial pCO_2 according to desired setpoint, with Fuzzy-PID outshines the other two controllers. These findings validate the second hypothesis of this study.

Since Fuzzy-PID is a new strategy for automatic controller in membrane oxygenator, which is the novelty element of this study, thus performance comparison is only available for PID and FLC. Walter et al. (Walter et al., 2009b) in their in-vitro test stand used smith predictor with internal PI control and recorded nearly 35 mmHg – 45 mmHg of pCO_2 measurement with 40 mmHg as their setpoint. In 2016, Kopp et al. (Kopp et al., 2016) implemented PI controller with gain scheduling for their in-vivo experiment to set sweep gas flowrate in control CO_2, and reported pCO_2 reading between 30.9 mmHg to 42.7 on blood gas analysis. For PID controller used in this study, pCO_2 reading was between 39.63 mmHg to 42.23 mmHg by taking up the setpoint as 40 mmHg (in both setpoint tracking and disturbance rejection task). Smaller deviation from setpoint that obtained in this study proved that the proposed PID has better control ability than the literatures.

The performance of FLC in rejecting disturbance is also competitive with the findings reported in previous study. Conway et al. (Conway et al., 2019) in their in-vivo experiment revealed the average error of 1.10 mmHg during controlling pCO_2 at 40 mmHg within membrane oxygenator when implemented FLC in their auto regulatory ECMO system. Conversely, in this study, the average error for setpoint tracking task is 0.76 mmHg, which is lower by 30.91%.

In this experimental work, the blood flowrate that been used is 2 L/min, which can be considered as low. It is chosen due to the diffusion capacity of CO_2, which is far higher than O_2 (Karagiannidis et al., 2019), since Krogh's diffusion constant is about 20 times higher for CO_2 than for O_2 (Piiper et al., 1980). This characteristic facilitates the process of CO_2 removal, thus lower blood flowrate is required for this process, compared to oxygenation. But how low the blood flowrate should be the to be considered. Strassmann et al (Strassmann et al., 2019) in their reported study also concluded that influence of sweep gas flowrate on CO_2 removal capacity in $ECCO_2R$ system only considerable in the case with larger membrane lung surface

(0.8 m^2) and blood flow rates of 900 mL/min and above are applied. Thus, in this study, blood flowrate of 2 L/min with 1.9 m^2 membrane oxygenator surface seems fits these requirements to produce the credible results.

In addition to blood flowrate, ventilation gas that supplied to membrane oxygenator also worth further discussion. In this study, 100% of O_2 gas was supplied to the membrane oxygenator, since Karangiannidis et al. (Karagiannidis et al., 2019) proved that CO_2 removal capacity is not related to O_2 content of sweep gas. For example, ambient air (21% O_2) has no significant effect to CO_2 removal capacity, compared to when using 100% of O_2. The similar O_2 content (100%) also was used by Sun et al. (Sun et al., 2018) during their work during evaluating CO_2 clearance in different membrane oxygenator on single pass in-vitro bench model.

Since the closed-loop control of ECMO and CPB systems has been proposed over the past decade, there are numerous reporting progress was published previously. In contrast, the CO_2 gas control in $ECCO_2R$ system is very rare. The scope of this study is only focus on the pCO_2 control rate in membrane oxygenator, which intended for the use in $ECCO_2R$ system, rather than ECMO and CPB.

This proof-of-concept study also has several limitations, including the use of heparinised bovine blood, compared with the human blood during the real application in clinical practice on real patients. There are a lot of similarities between various elements between human and bovine blood. Various studies have been conducted on the comparison of bovine blood with human blood and advocated similarity of both type of bloods in different aspects, such as blood rheology (Amin & Sirs, 1985), similarity of blood groups between J substance of cattle and A substance of human (Stone, 1962) and blood absorption coefficients (Hayes et al., 2008). Table 5.15 lists the comparison between human and bovine blood for several blood's characteristics.

From this table, both types of blood have not much differing, thus the use of bovine blood to substitute the human blood in in-vitro gas exchange module developed in this study is well-acceptable.

Table 5.15: Characteristics of blood in human and bovine.

Characteristics	Human blood	Bovine blood
Diameter of erythrocytes	7.5-8.7 µm (Applegate, 2006; Diez-Silva et al., 2010)	4.7-5.5 µm (Adili, et al., 2016)
Content of erythrocytes in peripheral venous blood, million per cubic millimetre ($10^6/mm^3$)	4.3- 5.8 (Christman, 1996)	6- 10.5 (Christman, 1996)
HCT (%)	37- 52 (Lewis, 1996)	34 (Lewis, 1996)
Haemoglobin (g/dL)	12- 18 (Lewis, 1996)	12.3 (Lewis, 1996)
Total CO_2 content in blood (mEq/L)	23 to 30 (Centor, 1990)	30 (Lewis, 1996)

5.5. Summary

From this chapter, control responses of the three controllers (PID, FLC and Fuzzy-PID) were demonstrated experimentally. The controllers that implemented in this study showed improvement compared to the literatures, as tabulated in Table 5.16. Briefly speaking, all the controllers showed a good control and able to bring the arterial pCO_2 to the desired setpoint without causing large error, and the best controllers in this experimental part is Fuzzy-PID,

followed by PID and lastly FLC. This achievement was proven qualitative (from plotted graph) and quantitatively by calculation of MSE value.

Table 5.16: Performance comparison with the previous studies.

Controller	Results from previous studies	Improvement of this study
Smith predictor with internal PI control (Walter et al., 2009b)	pCO_2 reading was between 35 mmHg – 45 mmHg, with error of 5 mmHg (setpoint was 40 mmHg).	Error obtained for PID controller in this study was 0.37 mmHg- 2.23 mmHg, which lower by 55.4% compared to Walter et al.
PI controller with gain scheduling (Kopp et al., 2016)	pCO_2 reading reported between 30.9 mmHg to 42.7 mmHg (setpoint was 40 mmHg) measured by blood gas analysis, which produced the error between 2.7 mmHg- 9.1 mmHg.	Error obtained for PID controller in this study was 0.37 mmHg-2.23 mmHg, which reduced by 75.50%, compared to Kopp et al..
FLC (Conway et al., 2019)	Average error of 1.10 mmHg, where the setpoint was 40 mmHg.	Error obtained for FLC in this study was 0.76 mmHg, which lower by 30.91% from error reported by Conway et al..

CHAPTER 6: CONCLUSION AND FUTURE RECOMMENDATIONS

The therapeutic options for patients with respiratory deficiency continue to evolved, especially in providing an automatically adapting in extracorporeal life support system. In this in-vitro gas exchange module in benchtop setup, a satisfactory management of automatic control for CO_2 removal system was demonstrated, with Fuzzy-PID outshines the performance of other controllers, such as PID and FLC. From both simulation and experimental work, all the 5 objectives of this study are achieved.

In Chapter 3, a complete mathematical modelling of CO_2 gas exchange was successfully demonstrated using mathematical model introduced by Hexamer and Werner in 2003. This modelling was simulated in MATLAB/SIMULINK environment with the use of level-2 s-function block. The findings showed the inverse relationships between sweep gas flowrate and simulated arterial pCO_2, where the pCO_2 decreased with the rise of the sweep gas flowrate. This verifies the first hypothesis of this study. From these findings, objective 1 of this study was achieved.

The second objective of this study was accomplished in Chapter 4. Simulation work on the automatic control of CO_2 gas transfer in membrane oxygenator using PID, FLC and Fuzzy-PID was successfully performed and elaborated in Chapter 4. The results satisfy the second hypothesis of this study, where all the three controllers have great ability to control arterial pCO_2 level in membrane oxygenator in both setpoint tracking and disturbance rejection task. Among these three, Fuzzy-PID became the best controller with lowest sustained error, less overshoot, fastest response to the changes of setpoint and in rejecting disturbance.

As for third objective, which is to develop an in-vitro gas exchange module, an experimental setup was developed in Chapter 5, which involved three main components, namely membrane oxygenator, pump and blood circuit. In order to produce an automatic control system, 2 pCO_2 sensors and 1 MFC as actuator to control the sweep gas flow rate (manipulated variable) were used. All the details regarding the involved component also described thoroughly in Chapter 5. This information can be used for the other researcher in developing the similar in-vitro gas exchange system.

As a continuation step, the same control strategy that implemented in simulation work (Chapter 4) was conducted experimentally in Chapter 5. When the same PID parameter gain and FLC rules were used in experimental work, it did not produce satisfactory results. All the three controllers were unable to control the CO_2 gas transfer efficiently, leading to the significant drift in control process. This is most probably due to difference in assumption and parameter set between simulation and experimental setting. Thus, a new tuning of PID parameter and fuzzy logic rule was conducted. As the results, with these new PID parameters and fuzzy logic rule, satisfactory control ability was achieved for all controllers, with Fuzzy-PID became the best controller for both setpoint tracking and disturbance rejection task. From Chapter 5, it can be concluded that all the controllers with new PID tuning parameter and fuzzy logic rule able to control arterial pCO_2 according to the desired setpoint with Fuzzy-PID outshines the others controllers. Since this experimental work has high repeatability value, the same strategy can be used in evaluating the other type of controller in the same field of study.

To complete objective 5, the comparison of the performance between these three controllers were reported in Chapter 5 for both qualitative and quantitative method. In aspect of qualitative analysis, plotted graph of simulated arterial pCO_2 and measured arterial pCO_2 in experimental work were compared to determine the best controller, followed by the quantitative analysis by

the calculation of four performance indices, IAE, ISE, ITAE and MSE (for simulation data) and MSE for experimental data. Similar observations were found for both simulation and experimental work, which Fuzzy-PID became the best controller compared to PID and FLC. Once again, the same profile and agreeable findings were observed for both simulation and experimental data. Results obtained from this objective can be used as a reference in the future to the other researchers, since it advocated and proved the efficiency of Fuzzy-PID in maintaining desired setpoint to achieve an optimum control performance of membrane oxygenator for CO_2 removal in $ECCO_2R$ system.

From the achievement of all the five objectives above, it can be concluded that this in-vitro study had successfully provide an encouraging basis for future automatic control system in membrane oxygenator for CO_2 transfer during extracorporeal life support, especially in $ECCO_2R$ system.

The ultimate goal of innovations in medical device is to provide therapeutic advantage to the patients, with highest level of safety level. To fulfil this goal, this study must undergo further validation and tests prior to pursuing with clinical implementation. Thus, it is recommended to extend this in-vitro bench study to in-vivo experiment, which started with small number of animals, followed with larger number of animals and clinical application on human.

REFERENCES

(NICE), N. I. f. H. a. C. E. (2011). International procedure overview of extracorporeal membrane carbon dioxide removal. London: National Institute for Health and Clinical Excellent.

Adili, N., Melizi, M., & Belabbas, H. (2016). Species determination using the red blood cells morphometry in domestic animals. *Veterinary world, 9*(9), 960-963. doi:10.14202/vetworld.2016.960-963

Ahmadi, H., Gholamzadeh, M., Shahmoradi, L., Nilashi, M., & Rashvand, P. (2018). Diseases diagnosis using fuzzy logic methods: A systematic and meta-analysis review. *Computer Methods and Programs in Biomedicine, 161*, 145-172. doi:https://doi.org/10.1016/j.cmpb.2018.04.013

Altmann, W. (2005). *Practical Process Control for Engineers and Technicians*: Elsevier Science.

Ambrosino, N., Foglio, K., Rubini, F., Clini, E., Nava, S., & Vitacca, M. (1995). Non-invasive mechanical ventilation in acute respiratory failure due to chronic obstructive pulmonary disease: correlates for success. *Thorax, 50*(7), 755-757.

Amin, T. M., & Sirs, J. A. (1985). The blood rheology of man and various animal species. *Quarterly Journal of Experimental Physiology, 70*(1), 37-49. doi:doi:10.1113/expphysiol.1985.sp002895

Applegate, E. (2006). *The anatomy and physiology learning system. Third edition*. USA: Elseview.

Arazawa, D. T., Kimmel, J. D., Finn, M. C., & Federspiel, W. J. (2015). Acidic sweep gas with carbonic anhydrase coated hollow fiber membranes synergistically accelerates CO2 removal from blood. *Acta Biomater, 25*, 143-149. doi:10.1016/j.actbio.2015.07.007

Arazawa, D. T., Oh, H. I., Ye, S. H., Johnson, C. A., Jr., Woolley, J. R., Wagner, W. R., & Federspiel, W. J. (2012). Immobilized Carbonic Anhydrase on Hollow Fiber Membranes Accelerates CO(2) Removal from Blood. *J Memb Sci, 404-404*, 25-31. doi:10.1016/j.memsci.2012.02.006

Arthurs, G., & Sudhakar, M. (2005). Carbon dioxide transport. *Continuing Education in Anaesthesia, Critical Care & Pain, 5*(6), 207-210. doi:10.1093/bjaceaccp/mki050

Astrom, K., & Hagglund, T. (1995). *PID Controllers - Theory, Design, and Tuning (2nd Edition)*. United States of America: Instrument Society of America.

Aubron, C., Cheng, A. C., Pilcher, D., Leong, T., Magrin, G., Cooper, D. J., . . . Pellegrino, V. (2013). Factors associated with outcomes of patients on extracorporeal membrane oxygenation support: a 5-year cohort study. *Crit Care, 17*(2), R73. doi:10.1186/cc12681

Baker, A., Richardson, D., & Craig, G. (2012). Extracorporeal carbon dioxide removal (ECCO2R) in respiratory failure: An overview, and where next? . *Journal of the Intensive Care Society, 12*(3), 232-237.

Bao, L. H., Goldman, S. L., & Trachtenberg, M. C. (2004). *CO2 transfer across a liquid membrane facilitated by carbonic anhydrase.* Paper presented at the AIChE Annual Meeting Austin, Texas.

Bartlett, R. H., Gazzaniga, A. B., Jefferies, M. R., Huxtable, R. F., Haiduc, N. J., & Fong, S. W. (1976). Extracorporeal membrane oxygenation (ECMO) cardiopulmonary support in infancy. *Trans Am Soc Artif Intern Organs, 22*, 80-93.

Batchinsky, A. I., Jordan, B. S., Regn, D., Necsoiu, C., Federspiel, W., Morris, M., & Cancio, L. C. (2010). *Veno-venous extracorporeal CO2 removal: Can we reduce dependence*

on mechanical ventilation during en-route care? . Paper presented at the RTO Human Factors and Medicine Panel (HFM) Symposium, Essen, Germany.

Bein, T., Weber, F., Philipp, A., Prasser, C., Pfeifer, M., Schmid, F. X., . . . Schlitt, H. J. (2006). A new pumpless extracorporeal interventional lung assist in critical hypoxemia/hypercapnia. *Crit Care Med, 34*(5), 1372-1377. doi:10.1097/01.ccm.0000215111.85483.bd

Benic, H., Fruk, M., & Vujisic, G. (2014, 26-30 May 2014). *Acquisition card NI USB-6009 in automatic control laboratory exercises.* Paper presented at the 2014 37th International Convention on Information and Communication Technology, Electronics and Microelectronics (MIPRO).

Berg, J. M., Tymoczko, J. L., & Stryer, L. (2002). *Biochemistry: 5th edition*. New York: W H Freeman.

Bermudez, C. A., Rocha, R. V., Zaldonis, D., Bhama, J. K., Crespo, M. M., Shigemura, N., . . . Toyoda, Y. (2011). Extracorporeal membrane oxygenation as a bridge to lung transplant: midterm outcomes. *Ann Thorac Surg, 92*(4), 1226-1231; discussion 1231-1222. doi:10.1016/j.athoracsur.2011.04.122

Bian, Y., & Chang, T. M. (2015). A novel nanobiotherapeutic poly-[hemoglobin-superoxide dismutase-catalase-carbonic anhydrase] with no cardiac toxicity for the resuscitation of a rat model with 90 minutes of sustained severe hemorrhagic shock with loss of 2/3 blood volume. *Artif Cells Nanomed Biotechnol, 43*(1), 1-9. doi:10.3109/21691401.2014.964554

Bian, Y., Wei, G., & Chang, T. M. (2013). Lowering of elevated tissue PCO2 in a hemorrhagic shock rat model after reinfusion of a novel nanobiotechnological polyhemoglobin-superoxide dismutase-catalase-carbonic anhydrase that is an oxygen and a carbon dioxide carrier with enhanced antioxidant properties. *Artif Cells Nanomed Biotechnol, 41*(1), 60-68. doi:10.3109/10731199.2013.745291

Bittner, H. B., Lehmann, S., Rastan, A., Garbade, J., Binner, C., Mohr, F. W., & Barten, M. J. (2012). Outcome of extracorporeal membrane oxygenation as a bridge to lung transplantation and graft recovery. *Ann Thorac Surg, 94*(3), 942-949; author reply 949-950. doi:10.1016/j.athoracsur.2012.05.006

Bonin, F., Sommerwerck, U., Lund, L. W., & Teschler, H. (2013). Avoidance of intubation during acute exacerbation of chronic obstructive pulmonary disease for a lung transplant candidate using extracorporeal carbon dioxide removal with the Hemolung. *J Thorac Cardiovasc Surg, 145*(5), e43-44. doi:10.1016/j.jtcvs.2013.01.040

Boschetti, F., Mantero, S., Miglietta, F., Costantino, M. L., Montevecchi, F. M., & Fumero, R. (2002). An approach to computer automation of the extracorporeal circulation. *Computers in Biology and Medicine, 32*(2), 73-83. doi:https://doi.org/10.1016/S0010-4825(01)00037-3

Brendle, C., Hackmack, K. F., Kühn, J., Wardeh, M. N., Janisch, T., Kopp, R., . . . Misgeld, B. J. (2017). Closed-loop control of extracorporeal oxygen and carbon dioxide gas transfer. *Control Engineering Practice, 59*, 173-182. doi:https://doi.org/10.1016/j.conengprac.2016.09.016

Brendle, C., Hackmack, K. F., Kühn, J., Wardeh, M. N., Janisch, T., Kopp, R., . . . Walter, M. (2017). Continuous gas transfer monitoring during extracorporeal membrane oxygenation. *Biomedical Signal Processing and Control, 31*, 321-330. doi:https://doi.org/10.1016/j.bspc.2016.08.023

Brodie, D. (2018). The Evolution of Extracorporeal Membrane Oxygenation for Adult Respiratory Failure. *Ann Am Thorac Soc, 15*(Supplement_1), S57-S60. doi:10.1513/AnnalsATS.201705-386KV

Broun, G., Selegny, E., Minh, C. T., & Thomas, D. (1970). Facilitated transport of CO2 across a membrane bearing carbonic anhydrase. *FEBS Letters, 7*(3), 223-226. doi:http://dx.doi.org/10.1016/0014-5793(70)80166-1

Burki, N. K., Mani, R. K., Herth, F. J., Schmidt, W., Teschler, H., Bonin, F., . . . Moerer, O. (2013). A novel extracorporeal CO(2) removal system: results of a pilot study of hypercapnic respiratory failure in patients with COPD. *Chest, 143*(3), 678-686. doi:10.1378/chest.12-0228

Carroll, R. H., Barber, T. A., & Reed, B. W. (1992). Liquid membrane modules with minimal effective membrane thickness and methods of making the same: Google Patents.

Centor, R. M. (1990). *Clinical methods: The history, physical, and laboratory examinations. 3rd edition.* Boston: Butterworths.

Chan, K. K., Lee, K. L., Lam, P. K., Law, K. I., Joynt, G. M., & Yan, W. W. (2010). Hong Kong's experience on the use of extracorporeal membrane oxygenation for the treatment of influenza A (H1N1). *Hong Kong Med J, 16*(6), 447-454.

Chauhan, S., & Subin, S. (2011). Extracorporeal membrane oxygenation, an anesthesiologist's perspective: physiology and principles. Part 1. *Ann Card Anaesth, 14*(3), 218-229. doi:10.4103/0971-9784.84030

Chegwidden, W. R., Carter, N. D., & Edwards, Y. H. (2013). *The Carbonic Anhydrases: New Horizons*: Birkhäuser Basel.

Chen, N., Zhou, M., Dong, X., Qu, J., Gong, F., Han, Y., . . . Zhang, L. (2020). Epidemiological and clinical characteristics of 99 cases of 2019 novel coronavirus pneumonia in Wuhan, China: a descriptive study. *Lancet (London, England), 395*(10223), 507-513. doi:10.1016/S0140-6736(20)30211-7

Chen, Y. C., Tsai, F. C., Fang, J. T., & Yang, C. W. (2014). Acute kidney injury in adults receiving extracorporeal membrane oxygenation. *J Formos Med Assoc, 113*(11), 778-785. doi:10.1016/j.jfma.2014.04.006

Chiu, L. C., Tsai, F. C., Hu, H. C., Chang, C. H., Hung, C. Y., Lee, C. S., . . . Kao, K. C. (2015). Survival predictors in acute respiratory distress syndrome with extracorporeal membrane oxygenation. *Ann Thorac Surg, 99*(1), 243-250. doi:10.1016/j.athoracsur.2014.07.064

Christman, D. V. (1996). A study to compare and contrast animal blood to human blood product. *IABPA News, 12*(2), 10-25.

Chung, M., Shiloh, A. L., & Carlese, A. (2014). Monitoring of the Adult Patient on Venoarterial Extracorporeal Membrane Oxygenation. *The Scientific World Journal, 2014*, 10. doi:10.1155/2014/393258

Confalonieri, M., Parigi, P., Scartabellati, A., Aiolfi, S., Scorsetti, S., Nava, S., & Gandola, L. (1996). Noninvasive mechanical ventilation improves the immediate and long-term outcome of COPD patients with acute respiratory failure. *Eur Respir J, 9*(3), 422-430.

Conway, R. G., Berk, Z. B., Zhang, J., Li, T., Tran, D., Wu, Z. J., & Griffith, B. P. (2019). Evaluation of an Auto-Regulatory ECMO System for Total Respiratory Support in an Acute Ovine Model. *Artif Organs*. doi:10.1111/aor.13618

Cove, M. E., MacLaren, G., Federspiel, W. J., & Kellum, J. A. (2012). Bench to bedside review: Extracorporeal carbon dioxide removal, past present and future. *Crit Care, 16*(5), 232. doi:10.1186/cc11356

Cowan, R. M., Ge, J. J., Qin, Y. J., McGregor, M. L., & Trachtenberg, M. C. (2003). CO2 capture by means of an enzyme-based reactor. *Ann N Y Acad Sci, 984*, 453-469.

Cussler, E. L. (1997). *Diffusion: Mass Transfer in Fluid Systems (2nd ed.)*. New York: Cambridge University Press.

Del Sorbo, L., Cypel, M., & Fan, E. (2014). Extracorporeal life support for adults with severe acute respiratory failure. *Lancet Respir Med, 2*(2), 154-164. doi:10.1016/S2213-2600(13)70197-8

Dhinakaran, M., & Lincon, S. A. (2014). Perfusion system controller strategies during and ECMO support. *International Journal on Soft Computing (IJSC), 5*(3), 13-22.

Dhinakaran, M., & Lincon, S. A. (2014). A study and development of auto tuning control in a perfusion system for extracorporeal membrane oxygenator. *International Journal of Computer Applications, 106*(16), 21-26.

Dhinakaran, M., & Lincon, S. A. (2016). A novel fuzzy based internal model controller design of a perfusion system for CPB surgery conditions. *ARPN Journal of Engineering and Applied Sciences, 11*(2), 1154-1157.

Diez-Silva, M., Dao, M., Han, J., Lim, C.-T., & Suresh, S. (2010). Shape and Biomechanical Characteristics of Human Red Blood Cells in Health and Disease. *MRS bulletin, 35*(5), 382-388. doi:10.1557/mrs2010.571

Drolet, P., Girard, M., Poirier, J., & Grenier, Y. (2000). Facilitating submental endotracheal intubation with an endotracheal tube exchanger. *Anesth Analg, 90*(1), 222-223.

Duncan, B. (2001). *Mechanical Support for Cardiac and Respiratory Failure in Pediatric Patients*. United States of America: CRC Press.

Elliot, S. C., Paramasivam, K., Oram, J., Bodenham, A. R., Howell, S. J., & Mallick, A. (2007). Pumpless extracorporeal carbon dioxide removal for life-threatening asthma. *Crit Care Med, 35*(3), 945-948. doi:10.1097/01.ccm.0000257462.04514.15

Ellis, G. (2012). *Control System Design Guide: Using Your Computer to Understand and Diagnose Feedback Controllers*. United States of America: Butterworth-Heinemann.

Erickson, K. T., & Hedrick, J. L. (1999). *Plant-Wide Process Control*. Canada: John Wiley and Sons, Inc.

Estafanous, F. G., Barash, P. G., & Reves, J. G. (2001). *Cardiac Anesthesia: Principles and Clinical Practice*. USA: Lippincott Williams & Wilkins.

Extracorporeal Life Support Organization (ELSO). (2013). General Guidelines for all ECLS Cases. Retrieved from Retrieved from https://www.elso.org/Portals/0/IGD/Archive/FileManager/929122ae88cusersshyerdocumentselsoguidelinesgeneralalleclsversion1.3.pdf

Federspiel, W. J., & Hattler, B. G. (1996). Sweep gas flowrate and CO2 exchange in artificial lungs. *Artif Organs, 20*(9), 1050-1052.

Federspiel, W. J., & Haulert, B. G. (1996). Sweep Gas Flowrate and C02 Exchange in Artificial Lungs. *Artif Organs, 20*(9), 1050-1052. doi:10.1111/j.1525-1594.1996.tb04593.x

Federspiel, W. J., & Henchir, K. A. (2008). Lung, Artificial: Basic principles and current applications *Encyclopedia of Biomaterials and Biomedical Engineering, Second Edition (Online Version)* (pp. 1661-1672): CRC Press.

Federspiel, W. J., Hout, M. S., Hewitt, T. J., Lund, L. W., Heinrich, S. A., Litwak, P., . . . Hattler, B. G. (1997). Development of a low flow resistance intravenous oxygenator. *Asaio j, 43*(5), M725-730.

Federspiel, W. J., & Svitek, R. G. (2004). Lung, artificial: Current research and future directions. *Encyclopedia of Biomaterials and Biomedical Engineering, 2*, 922-931.

Fereidouni, A., Masoum, M. A. S., & Moghbel, M. (2015). A new adaptive configuration of PID type fuzzy logic controller. *ISA Transactions, 56*, 222-240. doi:https://doi.org/10.1016/j.isatra.2014.11.010

Fica, M., Suarez, F., Aparicio, R., & Suarez, C. (2012). Single site venovenous extracorporeal membrane oxygenation as an alternative to invasive ventilation in post-pneumonectomy fistula with acute respiratory failure. *Eur J Cardiothorac Surg, 41*(4), 950-952. doi:10.1093/ejcts/ezr103

Findlay, H., Kendall, M., Spicer, J., Turley, C., & Widdicombe, S. (2008). Novel microcosm system for investigating the effects of elevated carbon dioxide and temperature on intertidal organisms. *Aquatic Biology - AQUAT BIOL, 3*, 51-62. doi:10.3354/ab00061

Finney, S. J. (2014). Extracorporeal support for patients with acute respiratory distress syndrome. *Eur Respir Rev, 23*(133), 379-389. doi:10.1183/09059180.00005514

Fuehner, T., Kuehn, C., Hadem, J., Wiesner, O., Gottlieb, J., Tudorache, I., . . . Warnecke, G. (2012). Extracorporeal membrane oxygenation in awake patients as bridge to lung transplantation. *Am J Respir Crit Care Med, 185*(7), 763-768. doi:10.1164/rccm.201109-1599OC

Geers, C., & Gros, G. (2000). Carbon dioxide transport and carbonic anhydrase in blood and muscle. *Physiol Rev, 80*(2), 681-715.

Gilmour, K. M. (2010). Perspectives on carbonic anhydrase. *Comp Biochem Physiol A Mol Integr Physiol, 157*(3), 193-197. doi:10.1016/j.cbpa.2010.06.161

Gouda, M. M., Danaher, S., & Underwood, C. P. (2000). Fuzzy Logic Control Versus Conventional PID Control for Controlling Indoor Temperature of a Building Space. *IFAC Proceedings Volumes, 33*(24), 249-254. doi:https://doi.org/10.1016/S1474-6670(17)36900-8

Gramaticopolo, S., Chronopoulos, A., Piccinni, P., Nalesso, F., Brendolan, A., Zanella, M., . . . Ronco, C. (2010). Extracorporeal CO2 removal--a way to achieve ultraprotective mechanical ventilation and lung support: the missing piece of multiple organ support therapy. *Contrib Nephrol, 165*, 174-184. doi:10.1159/000313757

Gravlee, G. P. (2008). *Cardiopulmonary Bypass: Principles and Practice*. USA: Lippincott Williams & Wilkins.

Guan, W. J., Ni, Z. Y., Hu, Y., Liang, W. H., Ou, C. Q., He, J. X., . . . Zhong, N. S. (2020). Clinical Characteristics of Coronavirus Disease 2019 in China. *N Engl J Med, 382*(18), 1708-1720. doi:10.1056/NEJMoa2002032

Hatzakis, G., Olivenstein, R., & Bates, J. H. T. (2001). Fuzzy Logic and Mechanical Ventilation of COPD Patients. *Proceedings of the AMIA Symposium*, 923.

Hatzakis, G. E., & Davis, G. M. (2002). Fuzzy logic controller for weaning neonates from mechanical ventilation. *Proceedings of the AMIA Symposium*, 315-319.

Haugen, F. (2004). *PID Control*: Tapir Academic Press.

Hayes, M., Vanzant, E., Stombaugh, T., & Gates, R. (2008, Aug 31 2008 -Sep 4 2008). *Comparison of Bovine Blood Absorption Coefficients to Human Curves*. Paper presented at the 8th International Livestock Environment Symposium, ILES VIII, Brazil.

Hervey-Jumper, S. L., Annich, G. M., Yancon, A. R., Garton, H. J., Muraszko, K. M., & Maher, C. O. (2011). Neurological complications of extracorporeal membrane oxygenation in children. *J Neurosurg Pediatr, 7*(4), 338-344. doi:10.3171/2011.1.peds10443

Hexamer, M., Misgeld, B. J., Prenger-Berninghoff, A., Schutt, U., Knobl, H. J., Korfer, R., & Werner, J. (2004). Automatic control of the extra-corporal bypass: system analysis, modelling and evaluation of different control modes. *Biomed Tech (Berl), 49*(11), 316-321. doi:10.1515/bmt.2004.059

Hexamer, M., Misgeld, B. J., Prenger-Berninghoff, A., Schütt, U., Knobl, H. J., Körfer, R., & Werner, J. (2004). Automatic Control of the Extra-Corporal Bypass: System Analysis, Modelling and Evaluation of Different Control Modes / Automatische Regelung der extrakorporalen Zirkulation: Analyse, Modelbildung und Evaluation von Regelstrategien *Biomedizinische Technik/Biomedical Engineering* (Vol. 49, pp. 316).

Hexamer, M., & Werner, J. (2003a). *A mathematical model for the gas tranfer in an oxygenator*. Paper presented at the IFAC Conference on Modelling and Control in Biomedical System, Melbourne, Australia.

Hexamer, M., & Werner, J. (2003b). *A mathematical model for the gas transfer in an oxygenator*. Paper presented at the Modelling and control in biomedical systems, Melbourne.

Hill, E., Power, G., & Longo, L. (1973a). A mathematical model of carbon dioxide transfer in the placenta and its interaction with oxygen. *American Journal of Physiology -- Legacy Content, 224*(2), 283-299.

Hill, E., Power, G., & Longo, L. (1973b). Mathematical simulation of pulmonary O 2 and CO 2 exchange. *American Journal of Physiology -- Legacy Content, 224*(4), 904-917.

Hill, J. D., O'Brien, T. G., Murray, J. J., Dontigny, L., Bramson, M. L., Osborn, J. J., & Gerbode, F. (1972). Prolonged extracorporeal oxygenation for acute post-traumatic respiratory failure (shock-lung syndrome). Use of the Bramson membrane lung. *N Engl J Med, 286*(12), 629-634. doi:10.1056/NEJM197203232861204

Hormes, M., Borchardt, R., Mager, I., Rode, T. S., Behr, M., & Steinseifer, U. (2011). A validated CFD model to predict O(2) and CO(2) transfer within hollow fiber membrane oxygenators. *Int J Artif Organs, 34*(3), 317-325.

Hout, M. S., Hattler, B. G., & Federspiel, W. J. (2000a). Validation of a model for flow-dependent carbon dioxide exchange in artificial lungs. *Artif Organs, 24*(2), 114-118.

Hout, M. S., Hattler, B. G., & Federspiel, W. J. (2000b). Validation of a model for flow-dependent carbon dioxide exchange in artificial lungs. *Artif Organs, 24*(2), 114-118.

Huang, C., Wang, Y., Li, X., Ren, L., Zhao, J., Hu, Y., . . . Cao, B. (2020). Clinical features of patients infected with 2019 novel coronavirus in Wuhan, China. *The Lancet, 395*(10223), 497-506. doi:https://doi.org/10.1016/S0140-6736(20)30183-5

Iacovazzi, M., Oreste, N., Sardelli, P., Barrettara, B., & Grasso, S. (2012). Extracorporeal carbon dioxyde removal for additional pulmonary resection after pneumonectomy. *Minerva Anestesiol, 78*(3), 381-384.

Jacobs, J. P., Stammers, A. H., St Louis, J., Hayanga, J. W. A., Firstenberg, M. S., Mongero, L. B., . . . Slepian, M. J. (2020). Extracorporeal Membrane Oxygenation in the Treatment of Severe Pulmonary and Cardiac Compromise in Coronavirus Disease 2019: Experience with 32 Patients. *Asaio j, 66*(7), 722-730. doi:10.1097/mat.0000000000001185

Javidfar, J., Brodie, D., Iribarne, A., Jurado, J., Lavelle, M., Brenner, K., . . . Bacchetta, M. (2012). Extracorporeal membrane oxygenation as a bridge to lung transplantation and recovery. *J Thorac Cardiovasc Surg, 144*(3), 716-721. doi:10.1016/j.jtcvs.2012.05.040

Kaar, J. L., Oh, H.-I., Russell, A. J., & Federspiel, W. J. (2007). Towards Improved Artificial Lungs Through Biocatalysis. *Biomaterials, 28*(20), 3131-3139. doi:10.1016/j.biomaterials.2007.03.021

Kanbar, B., & Ozdemir, E. (2010). Thermal stability of carbonic anhydrase immobilized within polyurethane foam. *Biotechnol Prog, 26*(5), 1474-1480. doi:10.1002/btpr.452

Karabulut, H., Toraman, F., Tarcan, S., Demirhisar, O., & Alhan, C. (2002). Adjustment of sweep gas flow during cardiopulmonary bypass. *Perfusion, 17*(5), 353-356.

Karagiannidis, C., Hesselmann, F., & Fan, E. (2019). Physiological and Technical Considerations of Extracorporeal CO2 Removal. *Critical Care, 23*(1), 6.

Kazemian, H. B. (2005). Developments of fuzzy PID controllers. *Expert Systems, 22*(5), 254-264. doi:doi:10.1111/j.1468-0394.2005.00316.x

Kim, J. H., & Oh, S. J. (2000). A fuzzy PID controller for nonlinear and uncertain systems. *Soft Computing, 4*(2), 123-129. doi:10.1007/s005000000039

Kimmel, J. D., Arazawa, D. T., Ye, S. H., Shankarraman, V., Wagner, W. R., & Federspiel, W. J. (2013). Carbonic anhydrase immobilized on hollow fiber membranes using glutaraldehyde activated chitosan for artificial lung applications. *J Mater Sci Mater Med, 24*(11), 2611-2621. doi:10.1007/s10856-013-5006-2

Klee, H., & Allen, R. (2007). *Simulation of Dynamic Systems with MATLAB and Simulink (Second Edition)*. United States of America: CRC Press, Inc.

Kluge, S., Braune, S. A., Engel, M., Nierhaus, A., Frings, D., Ebelt, H., . . . Rousseau, S. (2012). Avoiding invasive mechanical ventilation by extracorporeal carbon dioxide removal in patients failing noninvasive ventilation. *Intensive Care Med, 38*(10), 1632-1639. doi:10.1007/s00134-012-2649-2

Kolobow, T., Gattinoni, L., Tomlinson, T., White, D., Pierce, J., & Iapichino, G. (1977). The carbon dioxide membrane lung (CDML): a new concept. *Trans Am Soc Artif Intern Organs, 23*, 17-21.

Kopp, R., Bensberg, R., Stollenwerk, A., Arens, J., Grottke, O., Walter, M., & Rossaint, R. (2016). Automatic Control of Veno-Venous Extracorporeal Lung Assist. *Artif Organs, 40*(10), 992-998. doi:10.1111/aor.12664

Larson, M. G. (2008). Analysis of Variance. *Circulation, 117*(1), 115-121.

Lewis, J. H. (1996). *Comparative hemostasis in vertebrates*. New York, USA: Springer Science+ Business Media.

Li, X., Guo, Z., Li, B., Zhang, X., Tian, R., Wu, W., . . . Huang, J. (2020). Extracorporeal Membrane Oxygenation for Coronavirus Disease 2019 in Shanghai, China. *Asaio j, 66*(5), 475-481. doi:10.1097/MAT.0000000000001172

Linden, V. B., Lidegran, M. K., Frisen, G., Dahlgren, P., Frenckner, B. P., & Larsen, F. (2009). ECMO in ARDS: a long-term follow-up study regarding pulmonary morphology and function and health-related quality of life. *Acta Anaesthesiol Scand, 53*(4), 489-495. doi:10.1111/j.1399-6576.2008.01808.x

Lobaz, S., & Carey, M. (2011). Rescue of acute refractory hypercapnia and acidosis secondary to life-threatening asthma with extracorporeal Carbon Dioxide removal (ECCO2R) *Journal of Intensive Care Society, 12*(2), 140-142.

Luksza, A. R., Smith, P., Coakley, J., Gordan, I. J., & Atherton, S. T. (1986). Acute severe asthma treated by mechanical ventilation: 10 years' experience from a district general hospital. *Thorax, 41*(6), 459-463.

Lund, L. W., & Federspiel, W. J. (2013). Removing extra CO in COPD patients. *Curr Respir Care Rep, 2*, 131-138. doi:10.1007/s13665-013-0057-x

Manap, H. H., & Abdul Wahab, A. K. (2016). Extracorporeal carbon dioxide removal (ECCO2R) in respiratory deficiency and current investigations on its improvement: a review. *Journal of Artificial Organs*, 1-10. doi:10.1007/s10047-016-0905-x

Manap, H. H., Abdul Wahab, A. K., & Mohamed Zuki, F. (2017). Mathematical Modelling of Carbon Dioxide Exchange in Hollow Fiber Membrane Oxygenator. *IOP Conference Series: Materials Science and Engineering, 210*(1), 012003.

Manap, H. H., Md Tahir, N., & Yassin, A. I. M. (2011, 14-17 Dec. 2011). *Statistical analysis of parkinson disease gait classification using Artificial Neural Network.* Paper presented at the 2011 IEEE International Symposium on Signal Processing and Information Technology (ISSPIT).

Matheis, G. (2003). New technologies for respiratory assist. *Perfusion, 18*(4), 245-251.

Matsuda, N., & Sakai, K. (2000). Blood flow and oxygen transfer rate of an outside blood flow membrane oxygenator. *J Memb Sci, 170*(2), 153-158. doi:Doi 10.1016/S0376-7388(00)00331-8

Mendoza, G. A., Baumgartner, B., Schreiber, U., Eichhorn, S., Krane, M., Bauernschmitt, R., & Knoll, A. (2010). *Design of a fuzzy controller for the automation of an extracorporeal support system with the use of a simulation environment*. Paper presented at the Conf Proc IEEE Eng Med Biol Soc.

Mihelc, K. M., Frankowski, B. J., Lieber, S. C., Moore, N. D., Hattler, B. G., & Federspiel, W. J. (2009). Evaluation of a respiratory assist catheter that uses an impeller within a

hollow fiber membrane bundle. *Asaio j, 55*(6), 569-574. doi:10.1097/MAT.0b013e3181bc2655

Misgeld, B. J. (2007). *Automatic control of the heart-lung mechine.* (Dissertation), Ruhr-University Bochum, Germany. Retrieved from http://www-brs.ub.ruhr-uni-bochum.de/netahtml/HSS/Diss/MisgeldBernoJohannesEngelbert/diss.pdf

Misgeld, B. J., Leonhardt, S., & Hexamer, M. (2012, 3-5 Oct. 2012). *Multivariable control design for artificial blood-gas exchange with heart-lung machine support.* Paper presented at the 2012 IEEE International Conference on Control Applications.

Misgeld, B. J., Werner, J., & Hexamer, M. (2005). Robust and self-tuning blood flow control during extracorporeal circulation in the presence of system parameter uncertainties. *Med Biol Eng Comput, 43*(5), 589-598.

Misgeld, B. J., Werner, J., & Hexamer, M. (2008). *Nonlinear robust blood gas control by state linearisation for the cardiopulmonary bypass*.

Misgeld, B. J., Werner, J., & Hexamer, M. (2010). Simultaneous automatic control of oxygen and carbon dioxide blood gases during cardiopulmonary bypass. *Artif Organs, 34*(6), 503-512. doi:10.1111/j.1525-1594.2009.00890.x

Mockros, L. F., & Leonard, R. (1985). Compact cross-flow tubular oxygenators. *Trans Am Soc Artif Intern Organs, 31*, 628-633.

Molnar, C., & Gair, J. (2013). *Concepts of Biology—1st Canadian Edition*. Canada: BCcampus and Camosun College.

Mortensen, J. D. (1992). Intravascular oxygenator: a new alternative method for augmenting blood gas transfer in patients with acute respiratory failure. *Artif Organs, 16*(1), 75-82.

Muller, T., Philipp, A., Luchner, A., Karagiannidis, C., Bein, T., Hilker, M., . . . Lubnow, M. (2009). A new miniaturized system for extracorporeal membrane oxygenation in adult respiratory failure. *Crit Care, 13*(6), R205. doi:10.1186/cc8213

Nemoto, T., Hatzakis, G. E., Thorpe, C. W., Olivenstein, R., Dial, S., & Bates, J. H. T. (1999). Automatic Control of Pressure Support Mechanical Ventilation Using Fuzzy Logic. *American Journal of Respiratory and Critical Care Medicine, 160*(2), 550-556. doi:10.1164/ajrccm.160.2.9809013

Ogata, K. (1997). *Modern control engineering (Third edition)*. United States of America: Prentice Hall International, Inc.

Oh, H. I., Ye, S. H., Johnson, C. A., Jr., Woolley, J. R., Federspiel, W. J., & Wagner, W. R. (2010). Hemocompatibility assessment of carbonic anhydrase modified hollow fiber membranes for artificial lungs. *Artif Organs, 34*(5), 439-442. doi:10.1111/j.1525-1594.2009.00882.x

Ostertagov¨¢, E., & Ostertag, O. (2013). Methodology and Application of Oneway ANOVA. *American Journal of Mechanical Engineering, 1*(7), 256-261.

Pappalardo, F., Pieri, M., Greco, T., Patroniti, N., Pesenti, A., Arcadipane, A., . . . Italian, E. (2013). Predicting mortality risk in patients undergoing venovenous ECMO for ARDS due to influenza A (H1N1) pneumonia: the ECMOnet score. *Intensive Care Med, 39*(2), 275-281. doi:10.1007/s00134-012-2747-1

Park, M., Mendes, P. V., Costa, E. L. V., Barbosa, E. V. S., Hirota, A. S., & Azevedo, L. C. P. (2016). Factors associated with blood oxygen partial pressure and carbon dioxide partial pressure regulation during respiratory extracorporeal membrane oxygenation support: data from a swine model. *Revista Brasileira de Terapia Intensiva, 28*, 11-18.

Pego-Fernandes, P. M., Hajjar, L. A., Galas, F. R., Samano, M. N., Ribeiro, A. K., Park, M., . . . Jatene, F. B. (2012). Respiratory failure after lung transplantation: extra-corporeal membrane oxygenation as a rescue treatment. *Clinics (Sao Paulo), 67*(12), 1529-1532.

Piiper, J., Meyer, M., & Scheid, P. (1980, 1980//). *Diffusion Limitation in Alveolar-Capillary CO2 Transfer in Human Lungs: Experimental Evidence from Rebreathing*

Equilibration. Paper presented at the Biophysics and Physiology of Carbon Dioxide, Berlin, Heidelberg.

Plant, P. K., Owen, J. L., & Elliott, M. W. (2000). Early use of non-invasive ventilation for acute exacerbations of chronic obstructive pulmonary disease on general respiratory wards: a multicentre randomised controlled trial. *Lancet, 355*(9219), 1931-1935.

Punjabi, P. P., & Taylor, K. M. (2013). The science and practice of cardiopulmonary bypass: From cross circulation to ECMO and SIRS. *Global Cardiology Science and Practice, 2013*(3), 249-260.

Rhoades, R., & Bell, D. R. (2009). *Medical Physiology: Principles for Clinical Medicine*: Lippincott Williams & Wilkins.

Richard, C., Argaud, L., Blet, A., Boulain, T., Contentin, L., Dechartres, A., . . . Tamion, F. (2014). Extracorporeal life support for patients with acute respiratory distress syndrome: report of a Consensus Conference. *Ann Intensive Care, 4*, 15. doi:10.1186/2110-5820-4-15

Roch, A., Hraiech, S., Masson, E., Grisoli, D., Forel, J. M., Boucekine, M., . . . Papazian, L. (2014). Outcome of acute respiratory distress syndrome patients treated with extracorporeal membrane oxygenation and brought to a referral center. *Intensive Care Med, 40*(1), 74-83. doi:10.1007/s00134-013-3135-1

Sahoo, P. C., Jang, Y.-N., & Lee, S.-W. (2012). Immobilization of carbonic anhydrase and an artificial Zn(II) complex on a magnetic support for biomimetic carbon dioxide sequestration. *Journal of Molecular Catalysis B: Enzymatic, 82*, 37-45. doi:http://dx.doi.org/10.1016/j.molcatb.2012.05.020

Salley, S. O., Song, J. Y., Whittlesey, G. C., & Klein, M. D. (1990). Immobilized carbonic anhydrase in a membrane lung for enhanced CO2 removal. *ASAIO Trans, 36*(3), M486-490.

Scaravilli, V., Kreyer, S., Linden, K., Belenkiy, S., Jordan, B., Pesenti, A., . . . Batchinsky, A. I. (2014). Modular extracorporeal life support: effects of ultrafiltrate recirculation on the performance of an extracorporeal carbon dioxide removal device. *Asaio j, 60*(3), 335-341. doi:10.1097/mat.0000000000000070

Scaravilli, V., Zanella, A., Sangalli, F., & Patroniti, N. (2014). Basic aspect of physiology during ECMO support. In F. Sangalli, A. Pesenti, & N. Patroniti (Eds.), *ECMO-Extracorporeal Life Support in Adults*. Italy: Springer-Verlag.

Scheiber, U., Garcia, A. M., Eichhorn, S., Baumgartner, B., Krane, M., Bauernschmitt, R., & Knoll, A. (2009). *A simple fuzzy controller for extra-corporeal circulation system-limitation and potentials.* Paper presented at the 5th Russian Bavarian Congress Proceedings, Rusia.

Schmidt, M., Tachon, G., Devilliers, C., Muller, G., Hekimian, G., Bréchot, N., . . . Combes, A. (2013). Blood oxygenation and decarboxylation determinants during venovenous ECMO for respiratory failure in adults. *Intensive Care Med, 39*(5), 838-846. doi:10.1007/s00134-012-2785-8

Seborg, D. E., Mellichamp, D. A., Edgar, T. F., & Doyle, F. J. (2010). *Process Dynamics and Control 3rd Edition*. United States of America: John Wiley & Sons.

Serpa Neto, A., Filho, R. R., Rocha, L. L., & Schultz, M. J. (2014). Recent advances in mechanical ventilation in patients without acute respiratory distress syndrome. *F1000Prime Rep, 6*, 115. doi:10.12703/P6-115

Shaw, J. A. (2003). *The PID Control Algorithm: How it works, how to tune it, and how to use it (Second Edition)*

Singh, V., Khatana, S., & Gupta, P. (2013). Blood gas analysis for bedside diagnosis. *National journal of maxillofacial surgery, 4*(2), 136-141. doi:10.4103/0975-5950.127641

Skinner, S. C., Hirschl, R. B., & Bartlett, R. H. (2006). Extracorporeal life support. *Seminars in Pediatric Surgery, 15*(4), 242-250. doi:https://doi.org/10.1053/j.sempedsurg.2006.07.003

Solano C, M. E., Castillo B, I., & Niño de Mejía, M. C. (2012). Hypocapnia in Neuroanesthesia: Current Situation. *Colombian Journal of Anesthesiology, 40*(2), 137-144. doi:http://dx.doi.org/10.1016/S2256-2087(12)70029-9

Stone, W. H. (1962). The Relation of Human and Cattle Blood Groups. *Transfusion, 2*(3), 172-177. doi:doi:10.1111/j.1537-2995.1962.tb00217.x

Strassmann, S., Merten, M., Schäfer, S., de Moll, J., Brodie, D., Larsson, A., . . . Karagiannidis, C. (2019). Impact of sweep gas flow on extracorporeal CO2 removal (ECCO2R). *Intensive Care Medicine Experimental, 7*(1), 17. doi:10.1186/s40635-019-0244-3

Sun, L., Kaesler, A., Fernando, P., Thompson, A. J., Toomasian, J. M., & Bartlett, R. H. (2018). CO(2) clearance by membrane lungs. *Perfusion, 33*(4), 249-253. doi:10.1177/0267659117736379

Supuran, C. T., & De Simone, G. (2015). *Carbonic Anhydrases as Biocatalysts: From Theory to Medical and Industrial Applications*: Elsevier Science.

Svitek, R. G., & Federspiel, W. J. (2008). A mathematical model to predict CO2 removal in hollow fiber membrane oxygenators. *Ann Biomed Eng, 36*(6), 992-1003. doi:10.1007/s10439-008-9482-3

Tabesh, H., Amoabediny, G., Poorkhalil, A., Khachab, A., Kashefi, A., & Mottaghy, K. (2012). A theoretical model for evaluation of the design of a hollow-fiber membrane oxygenator. *J Artif Organs, 15*(4), 347-356. doi:10.1007/s10047-012-0655-3

Takagi, T., & Sugeno, M. (1985). *Fuzzy Identification of Systems and Its Applications to Modeling and Control*. Paper presented at the IEEE Transactions on Systems, Man, and Cybernatics.

Tao, W., Schroeder, T., Bidani, A., Cardenas, V. J., Jr., Nguyen, P. D., Bradford, D. W., . . . Zwischenberger, J. B. (1994). Improved gas exchange performance of the intravascular oxygenator by active blood mixing. *Asaio j, 40*(3), M527-532.

Tao, Y., Zheng, J., Yuanchang, L., Wang, T., Xiong, H., He, G., & Xu, D. (2015). Fuzzy PID control method of deburring industrial robots. *Journal of Intelligent & Fuzzy Systems, 29*(6), 2447-2455. doi:10.3233/IFS-151945

Taskin, M. E., Fraser, K. H., Zhang, T., Griffith, B. P., & Wu, Z. J. (2010). Micro-scale Modeling of Flow and Oxygen Transfer in Hollow Fiber Membrane Bundle. *J Memb Sci, 362*(1-2), 172-183. doi:10.1016/j.memsci.2010.06.034

Tehrani, F. T. (2012). A closed-loop system for control of the fraction of inspired oxygen and the positive end-expiratory pressure in mechanical ventilation. *Computers in Biology and Medicine, 42*(11), 1150-1156. doi:10.1016/j.compbiomed.2012.09.007

Terragni, P. P., Del Sorbo, L., Mascia, L., Urbino, R., Martin, E. L., Birocco, A., . . . Ranieri, V. M. (2009). Tidal volume lower than 6 ml/kg enhances lung protection: role of extracorporeal carbon dioxide removal. *Anesthesiology, 111*(4), 826-835. doi:10.1097/ALN.0b013e3181b764d2

Tian, L., & Gilbertson, L. G. (2004). The study of control methods for the robotic testing system for human musculoskeletal joints. *Computer Methods and Programs in Biomedicine, 74*(3), 211-220. doi:https://doi.org/10.1016/j.cmpb.2003.07.003

Tomii, K., Seo, R., Tachikawa, R., Harada, Y., Murase, K., Kaji, R., . . . Ishihara, K. (2009). Impact of noninvasive ventilation (NIV) trial for various types of acute respiratory failure in the emergency department; decreased mortality and use of the ICU. *Respir Med, 103*(1), 67-73. doi:10.1016/j.rmed.2008.08.001

Toomasian, J. M., Schreiner, R. J., Meyer, D. E., Schmidt, M. E., Hagan, S. E., Griffith, G. W., . . . Cook, K. E. (2005). A polymethylpentene fiber gas exchanger for long-term extracorporeal life support. *Asaio j, 51*(4), 390-397.

Toyoda, Y., Bhama, J. K., Shigemura, N., Zaldonis, D., Pilewski, J., Crespo, M., & Bermudez, C. (2013). Efficacy of extracorporeal membrane oxygenation as a bridge to lung transplantation. *J Thorac Cardiovasc Surg, 145*(4), 1065-1070; discussion 1070-1061. doi:10.1016/j.jtcvs.2012.12.067

Trachtenberg, M. C., Cowan, R. M., Smith, D. A., Horazak, D. A., Jensen, M. D., Laumb, J. D., . . . Wu, X. (2009). Membrane-based, enzyme-facilitated, efficient carbon dioxide capture. *Energy Procedia, 1*(1), 353-360. doi:http://dx.doi.org/10.1016/j.egypro.2009.01.048

Turri, F., & Yanagihara, J. I. (2011a). Computer-Assisted Numerical Analysis for Oxygen and Carbon Dioxide Mass Transfer in Blood Oxygenators. *Artif Organs, 35*(6), 579-592. doi:10.1111/j.1525-1594.2010.01150.x

Turri, F., & Yanagihara, J. I. (2011b). Computer-assisted numerical analysis for oxygen and carbon dioxide mass transfer in blood oxygenators. *Artif Organs, 35*(6), 579-592. doi:10.1111/j.1525-1594.2010.01150.x

U.S. Food and Drug Administration. (2000). Guidance for Cardiopulmonary Bypass Oxygenators 510(k) Submissions; Final Guidance for Industry and FDA Staff. Retrieved from http://www.fda.gov/RegulatoryInformation/Guidances/ucm073668.htm

Übeyli, E. D. (2009). Adaptive neuro-fuzzy inference system for classification of ECG signals using Lyapunov exponents. *Computer Methods and Programs in Biomedicine, 93*(3), 313-321. doi:https://doi.org/10.1016/j.cmpb.2008.10.012

Uchikawa, J., & Zeebe, R. E. (2012). The effect of carbonic anhydrase on the kinetics and equilibrium of the oxygen isotope exchange in the CO2–H2O system: Implications for δ18O vital effects in biogenic carbonates. *Geochimica et Cosmochimica Acta, 95*, 15-34. doi:http://dx.doi.org/10.1016/j.gca.2012.07.022

Valabrègue, R., Aubert, A., Burger, J., Bittoun, J., & Costalat, R. (2003). Relation between cerebral blood flow and metabolism explained by a model of oxygen exchange *Journal of Cerebral Blood Flow & Metabolism, 23*(5), 536-545.

Vaslef, S. N., Mockros, L. F., Anderson, R. W., & Leonard, R. J. (1994). Use of a mathematical model to predict oxygen transfer rates in hollow fiber membrane oxygenators. *Asaio j, 40*(4), 990-996.

Vaslef, S. N., Mockros, L. F., Cook, K. E., Leonard, R. J., Sung, J. C., & Anderson, R. W. (1994). Computer-assisted design of an implantable, intrathoracic artificial lung. *Artif Organs, 18*(11), 813-817.

Vinoba, M., Bhagiyalakshmi, M., Jeong, S. K., Yoon, Y. I., & Nam, S. C. (2012). Immobilization of carbonic anhydrase on spherical SBA-15 for hydration and sequestration of CO2. *Colloids Surf B Biointerfaces, 90*, 91-96. doi:10.1016/j.colsurfb.2011.10.001

Visek, E., Mazzarella, L., & Motta, M. (2014). Performance analysis of a solar cooling system using self tuning fuzzy-PID control with TRNSYS. *Energy Procedia, 57*, 2609-2618. doi:10.1016/j.egypro.2014.10.272

Walles, T. (2007). Clinical experience with the iLA Membrane Ventilator pumpless extracorporeal lung-assist device. *Expert Rev Med Devices, 4*(3), 297-305. doi:10.1586/17434440.4.3.297

Walter, M., Brendle, C., Bensberg, R., Kopp, R., Arens, J., Stollenwerk, A., & Leonhardt, S. (2012). Closed Loop Physiological ECMO Control. In Á. Jobbágy (Ed.), *5th European Conference of the International Federation for Medical and Biological Engineering:*

14–18 September 2011, Budapest, Hungary (pp. 319-322). Berlin, Heidelberg: Springer Berlin Heidelberg.

Walter, M., Brendle, C., Kühn, J., Janisch, T., Kopp, R., Stollenwerk, A., & Leonhardt, S. (2016). *Assistive Control of Extracorporeal Oxygenation Systems*. Paper presented at the 12th German Russian Conference on Biomedical Engineering, Suzdal, Russia.

Walter, M., Stollenwerk, A., Wartzek, T., Arens, J., Kopp, R., & Leonhardt, S. (2010). Automatisierung und Fehlerdiagnose bei der extrakorporalen Membranoxygenierung (Automation and Fault Supervision for Extracorporeal Membrane Oxygenation Systems). *Automatisierungstechnik, 58*, 277-285.

Walter, M., Wartzek, T., Kopp, R., Stollenwerk, A., Kashefi, A., & Leonhardt, S. (2009a, 23-26 Aug. 2009). *Automation of long term extracorporeal oxygenation systems.* Paper presented at the Control Conference (ECC), 2009 European.

Walter, M., Wartzek, T., Kopp, R., Stollenwerk, A., Kashefi, A., & Leonhardt, S. (2009b, 23-26 Aug. 2009). *Automation of long term extracorporeal oxygenation systems.* Paper presented at the 2009 European Control Conference (ECC).

Walter, M., Weyer, S., Stollenwerk, A., Kopp, R., Arens, J., & Leonhardt, S. (2010a, Aug. 31 2010-Sept. 4 2010). *A physiological model for extracorporeal oxygenation controller design.* Paper presented at the 2010 Annual International Conference of the IEEE Engineering in Medicine and Biology.

Walter, M., Weyer, S., Stollenwerk, A., Kopp, R., Arens, J., & Leonhardt, S. (2010b). A physiological model for extracorporeal oxygenation controller design. *Conf Proc IEEE Eng Med Biol Soc, 2010*, 434-437. doi:10.1109/iembs.2010.5627416

Wang, D., Hu, B., Hu, C., Zhu, F., Liu, X., Zhang, J., . . . Peng, Z. (2020). Clinical Characteristics of 138 Hospitalized Patients With 2019 Novel Coronavirus-Infected Pneumonia in Wuhan, China. *JAMA, 323*(11), 1061-1069. doi:10.1001/jama.2020.1585

Wearden, P. D., Federspiel, W. J., Morley, S. W., Rosenberg, M., Bieniek, P. D., Lund, L. W., & Ochs, B. D. (2012). Respiratory dialysis with an active-mixing extracorporeal carbon dioxide removal system in a chronic sheep study. *Intensive Care Med, 38*(10), 1705-1711. doi:10.1007/s00134-012-2651-8

Weissman, M. H., & Mockros, L. F. (1967). Oxygen transfer to blood flowing in round tubes. *Journal of the Engineering Mechanics Division, 93*(6), 225-244.

Weissman, M. H., & Mockros, L. F. (1969). Oxygen and carbon dioxide transfer in membrane oxygenators. *Medical and Biological Engineering, 7*(2), 169-184.

Wickramasinghe, S. R., Han, B., Garcia, J. D., & Specht, R. (2005). Microporous membrane blood oxygenator. *AiChE Journal, 51*(2), 656-670.

Yang, X., Yu, Y., Xu, J., Shu, H., Xia, J. a., Liu, H., . . . Shang, Y. (2020). Clinical course and outcomes of critically ill patients with SARS-CoV-2 pneumonia in Wuhan, China: a single-centered, retrospective, observational study. *Lancet Respir Med, 8*(5), 475-481. doi:10.1016/S2213-2600(20)30079-5

Yong, J. K. J., Stevens, G. W., Caruso, F., & Kentish, S. E. (2015). The use of carbonic anhydrase to accelerate carbon dioxide capture processes. *Journal of Chemical Technology & Biotechnology, 90*(1), 3-10. doi:10.1002/jctb.4502

Zadeh, L. A. (1983). The role of fuzzy logic in the management of uncertainty in expert systems. *Fuzzy Sets and Systems, 11*(1), 199-227. doi:https://doi.org/10.1016/S0165-0114(83)80081-5

Zanella, A., Castagna, L., Abd El Aziz El Sayed Deab, S., Scaravilli, V., Ferlicca, D., Magni, F., . . . Pesenti, A. (2016). Extracorporeal CO2 Removal by Respiratory Electrodialysis: An In Vitro Study. *Asaio j, 62*(2), 143-149. doi:10.1097/mat.0000000000000316

Zanella, A., Castagna, L., Salerno, D., Scaravilli, V., Abd El Aziz El Sayed Deab, S., Magni, F., . . . Pesenti, A. (2015). Respiratory Electrodialysis. A Novel, Highly Efficient Extracorporeal CO2 Removal Technique. *Am J Respir Crit Care Med, 192*(6), 719-726. doi:10.1164/rccm.201502-0289OC

Zanella, A., Mangili, P., Giani, M., Redaelli, S., Scaravilli, V., Castagna, L., . . . Pesenti, A. (2014). Extracorporeal carbon dioxide removal through ventilation of acidified dialysate: an experimental study. *J Heart Lung Transplant, 33*(5), 536-541. doi:10.1016/j.healun.2013.12.006

Zanella, A., Mangili, P., Redaelli, S., Scaravilli, V., Giani, M., Ferlicca, D., . . . Pesenti, A. (2014). Regional blood acidification enhances extracorporeal carbon dioxide removal: a 48-hour animal study. *Anesthesiology, 120*(2), 416-424. doi:10.1097/aln.0000000000000099

Zanella, A., Patroniti, N., Isgro, S., Albertini, M., Costanzi, M., Pirrone, F., . . . Pesenti, A. (2009). Blood acidification enhances carbon dioxide removal of membrane lung: an experimental study. *Intensive Care Med, 35*(8), 1484-1487. doi:10.1007/s00134-009-1513-5

Zhan, W.-Q., Li, M.-D., Xu, M., & Lu, Y.-B. (2020). Successful treatment of COVID-19 using extracorporeal membrane oxygenation, a case report. *Eur Rev Med Pharmacol Sci, 24*(6), 3385-3389.

Zhang, Y.-T., Zhang, L., Chen, H.-L., & Zhang, H.-M. (2010). Selective separation of low concentration CO2 using hydrogel immobilized CA enzyme based hollow fiber membrane reactors. *Chemical Engineering Science, 65*(10), 3199-3207. doi:http://dx.doi.org/10.1016/j.ces.2010.02.010

Zhou, F., Yu, T., Du, R., Fan, G., Liu, Y., Liu, Z., . . . Cao, B. (2020). Clinical course and risk factors for mortality of adult inpatients with COVID-19 in Wuhan, China: a retrospective cohort study. *Lancet (London, England), 395*(10229), 1054-1062. doi:10.1016/S0140-6736(20)30566-3

Ziegler, J. G., & Nichols, N. B. (1942). Optimum Settings for Automatic Controllers. *Transactions of ASME, 64*, 759-768.

Zimmerman, J. L., Dellinger, R. P., Shah, A. N., & Taylor, R. W. (1993). Endotracheal intubation and mechanical ventilation in severe asthma. *Crit Care Med, 21*(11), 1727-1730.

Zimmermann, M., Philipp, A., Schmid, F. X., Dorlac, W., Arlt, M., & Bein, T. (2007). From Baghdad to Germany: use of a new pumpless extracorporeal lung assist system in two severely injured US soldiers. *Asaio j, 53*(3), e4-6. doi:10.1097/MAT.0b013e3180574b37

List of Publications and Papers Presented

1. Hany Hazfiza Manap, Ahmad Khairi Abdul Wahab, Extracorporeal Carbon Dioxide Removal (ECCO2R) in Respiratory Deficiency and Current Investigation on Carbonic Anhydrase Immobilization: A Review, Submitted to Journal of Artificial Organs, Published Online on 18 May 2016; JCR 2014, Q3: Engineering, Biomedical; DOI: 10.1007/s10047-016-0905-x) (*ISI-Indexed*).

2. Hany Hazfiza Manap, A.K. Abdul Wahab, and Fathiah Mohamed Zuki. Control for Carbon Dioxide Exchange Process in a Membrane Oxygenator Using Online Self-Tuning Fuzzy-PID Controller, Biomedical Signal Processing and Control (ISI-cited), accepted for publication on 24/10/2020.

3. Hany Hazfiza Manap, A.K. Abdul Wahab, and Fathiah Mohamed Zuki. Fuzzy Logic Based Control Strategies for Carbon Dioxide Gas Transfer In Hollow Fiber Membrane Oxygenator: In-Vitro Study, submitted to Artificial Organs (ISI-cited) on 23/9/2020. Current status: Under Review

4. Hany Hazfiza Manap, Ahmad Khairi Abdul Wahab, and Fathiah Mohamed Zaki, Optimal Control of Carbon Dioxide Exchange Process in a Membrane Oxygenator Using Particle Swarm Optimization Approach, 26th Regional Symposium on Chemical Engineering, 29 Oct 2019- 1 Nov 2019, Kuala Lumpur, Malaysia. (*SCOPUS-Indexed*).

5. Hany Hazfiza Manap, Ahmad Khairi Abdul Wahab, and Fathiah Mohamed Zaki, Mathematical modelling of carbon dioxide exchange in hollow fiber membrane oxygenator. IOP Conference Series: International Technical Postgraduate Conference, Vol. 210, Paper 012003, 5-6 April 2017, University of Malaya, Kuala Lumpur, Malaysia (ISI-Indexed).